

This is to certify that the
dissertation entitled

TITANIUM-CATALYZED ADDITIONS OF SUBSTITUTED
HYDRAZINES TO ALKYNES: CATALYST DESIGN,
MECHANISTIC STUDIES, AND APPLICATIONS IN
HETEROCYCLE SYNTHESIS

presented by

SANJUKTA BANERJEE

has been accepted towards fulfillment
of the requirements for the

Ph. D. degree in CHEMISTRY



Major Professor's Signature



Date

TITANIUM-CATALYZED ADDITIONS OF SUBSTITUTED HYDRAZINES TO
ALKYNES: CATALYST DESIGN, MECHANISTIC STUDIES, AND
APPLICATIONS IN HETEROCYCLE SYNTHESIS

VOLUME I

By

Sanjukta Banerjee

A DISSERTATION

Submitted to
Michigan State University
in partial fulfillment of the requirements
for the degree of

DOCTOR OF PHILOSOPHY

Chemistry

2008

ABSTRACT

TITANIUM-CATALYZED ADDITIONS OF SUBSTITUTED HYDRAZINES TO ALKYNES: CATALYST DESIGN, MECHANISTIC STUDIES, AND APPLICATIONS IN HETEROCYCLE SYNTHESIS

By

SANJUKTA BANERJEE

The primary focus of this thesis is the development of hydrohydrazination reactions for alkynes and their applications towards the synthesis of heterocycles. Hydrohydrazination is the formal addition of a hydrazine to an unsaturated C–C bond resulting in hydrazone or substituted hydrazine. Hydrohydrazination reactions are closely related to hydroamination. In hydroamination, amines (instead of hydrazines) are added across the C–C unsaturation. While hydrohydrazination of alkyne has been developed only recently, hydroamination has been known since 1950's and studied extensively. To cover sufficient background information for hydrohydrazination, hydroamination reactions are discussed in the first chapter.

In 2002, our group first discovered the hydrohydrazination of alkynes with 1,1-disubstituted hydrazines leading to the synthesis of *N*-protected indoles. Here, we have developed a new pyrrole-based titanium catalyst that is found to be active for the monosubstituted hydrazines. In addition, this catalyst is also active for both terminal and internal alkynes. The design of the catalyst, substrate scope, and applications to different heterocycles synthesis including compounds containing *NH*-indoles are discussed in the second chapter.

Iminohydrazination is the conversion of an alkyne to an α,β -unsaturated β -aminohydrazone, making both C–C and C–N bonds in a single step. This is a new multicomponent reaction (MCR) between an alkyne, 1,1-disubstituted hydrazine, and isonitrile in the presence of a catalyst. The design of new Ti-based catalysts, the scope of the iminohydrazination reaction, mechanistic investigation, and applications towards the synthesis of pyrazoles are discussed in the third chapter.

Vanadium(V) hydrazido complexes have been found in the active sites of different nitrogenase enzymes. The metal in these complexes is believed to be simultaneously coordinated to different donating centers such as N, O, and S. To understand the structures and functions of the active sites, different vanadium hydrazido complexes have been synthesized as model compounds. Interesting structural feature involving contributions from both hydrazido and isodiazene resonance forms has been observed in one of the model compounds. The synthesis of different vanadium(V) hydrazido complexes and important structural aspects are discussed in the fourth chapter.

Copyright by
Sanjukta Banerjee
2008

To my mother, Dr. Shyamali Banerjee

ACKNOWLEDGMENTS

First of all, I would like to thank Michigan State University for the support during my years as graduate student at MSU. I also want to thank the people in the Chemistry department for their help and generous support.

I consider myself very fortunate to have Prof. Aaron L. Odom as my Ph. D. mentor. He was never tired of discussing science and always listened to my questions with deep interest (even the silliest one!). He helped me a lot to learn many aspects of inorganic and organometallic chemistry and to develop the analytical skills necessary to survive in an experimental lab. I am also indebted to him for doing the hard work of correcting and proofreading this thesis. “Thank you” Aaron for your guidance, patience, and understanding. “Sandy” has thoroughly enjoyed her experience working with you.

I express my gratitude to Prof. Mitch Smith, Prof. Robert E. Maleczka, and Prof. Babak Borhan for serving on my committee and for all their suggestions.

Thanks to Dr. Daniel Holmes and Mr. Kermit Johnson for their assistance in NMR, and especially for allowing me to reserve extended time slots to perform the kinetic experiments. A special thank is due Dr. Richard Staples in the crystallography division. I am thankful to Bob Rasico, Melissa Parsons, and Bill Flick for their help in the general maintenance of the lab. I also want to thank Scott Bankroft in the glass blowing shop, Tom Geissenger and Diane Karsten in the stockroom, Glenn Wesley and Tom Bartlett in

the machine shop, and Scott Sanderson and Dave Cedarstaff in the electronics shop. Karen Maki, Beth McGaw, Cindy Sanford in the Business office and Nan Murray, Wendy Tsuji, Steve Poilios, Debbie Roper, Lisa Dillingham in the Graduate office were always very supportive and I thank them all.

In the process of working on one of my projects, and also in writing this thesis, I have received generous assistance from my colleague Dr. Eyal Bernea. He deserves a special thank you. I am also grateful to all the previous and present Odom group members: Yahong, Jim, Bala, Kapil, Supriyo, Doug, Steve, Sameer, and Kevin(s) for their support. I also want to mention all the undergraduates with whom I've worked in this lab. I've really enjoyed my experience working with all of you.

I acknowledge my family for support and inspiration. Especially, my mother and sister Aparajita for all of your loving support. I also like to thank all my friends in and outside East Lansing. Finally, the patience, inspiration, and encouragement of my husband, Ujjal, have been crucial to complete this thesis.

Sanjukta Banerjee
East Lansing, Michigan

TABLE OF CONTENTS

List of Tables	xi
List of Figures	xv
List of Schemes.....	xviii
List of Abbreviations	xxi
Hydroamination of alkynes.....	1
1.1 Introduction	1
1.2 Hydroamination with alkali and alkaline earth metals.....	4
1.3 Hydroamination with transition metals (Group 3 and 5)	6
1.4 Hydroamination with late transition metals	8
1.5 Hydroamination with lanthanides and actinides	13
1.6 Hydroamination with Group 4 metal complexes	17
1.6.1 Hydroamination of alkynes with Zirconium	17
1.6.2 Hydroamination of alkynes with Titanium.....	19
1.6.3 Research in the Odom group	25
1.7 Concluding Remarks	29
1.8 References	30
Hydrohydrazination of alkynes with monosubstituted hydrazines	34
2.1 Introduction	34
2.1.1 Hydrohydrazination with Titanium	35
2.1.2 Hydrohydrazination with Cobalt	41
2.1.3 Hydrohydrazination with Manganese.....	45

2.1.4 Hydrohydrazination with Palladium.....	46
2.1.5 Hydrohydrazination with Zinc.....	46
2.2 Synthesis of <i>NH</i> -indoles.....	50
2.3 Aim of the current project.....	51
2.4 Results and Discussion.....	52
2.5 Concluding Remarks.....	66
2.6 Experimental.....	67
2.7 References.....	87

Iminohydrazination of alkynes: scope, mechanistic investigation, and applications towards pyrazole synthesis..... 91

3.1 Introduction.....	91
3.2 Results and Discussion.....	94
3.2.1 Iminohydrazination Results.....	94
3.3 Mechanistic Investigation.....	101
3.3.1 Pathway via 1,2-insertion.....	101
3.3.2 [2 + 2]-cycloaddition mechanism.....	102
3.3.3 Kinetic studies.....	109
3.3.4 Overall mechanism for Iminohydrazination reaction.....	118
3.3.5 Experimental observations on regioselectivities.....	118
3.4 Applications of the Iminohydrazination reaction towards the synthesis of pyrazoles.....	122
3.4.1 Background information.....	122
3.4.2 Results and Discussion.....	123
3.5 Multicomponent Coupling Reactions of alkynes, monosubstituted hydrazines, and isonitriles.....	130
3.6 Concluding Remarks.....	136
3.7 Experimental.....	137
3.8 References.....	166

Synthesis of Vanadium(V) hydrazido(2-) thiolate imine alkoxide complexes..... 169

4.1 Introduction.....	169
4.2 Hydrazido versus isodiazene bonding in $MNNR_2$ complexes.....	171

4.3	Vanadium(V) hydrazido(2-) complexes	173
4.4	Titanium hydrazido(2-) complexes	177
4.5	Aim of the current project	183
4.6	Results and Discussion	184
4.7	Concluding Remarks	189
4.8	Experimental	190
4.9	References	201

Appendix

A	Crystallographic information	205
B	Kinetic reaction plots	303
C	^1H and ^{13}C NMR spectra	312

LIST OF TABLES

Table 2.1	Hydrohydrazination of alkynes with phenylhydrazine	58
Table 2.2	Hydrohydrazination with substituted phenylhydrazines	62
Table 2.3	Hydrohydrazination with diynes and enyne	65
Table 3.1	Examples of alkyne Iminohydrazination	98
Table 3.2	Rate Constants and conditions for kinetic experiments	114
Table 3.3	Observed rate constant vs catalyst concentration	117
Table 3.4	Iminohydrazination of phenylacetylene by different catalysts	120
Table 3.5	Effect of <i>p</i> -substituents on arylhydrazine on pyrazole formation.....	128
Table A1.1	Crystal data of H ₂ enp (4).....	205
Table A1.2	Atomic coordinates ($\times 10^4$) and equivalent isotropic displacement parameters ($\text{\AA}^2 \times 10^3$) for H ₂ enp. U(eq) is defined as one third of the trace of the orthogonalized U ^{ij} tensor.....	206
Table A1.3	Bond lengths (Å) and angles (°) for H ₂ enp	207
Table A1.4	Anisotropic displacement parameters ($\text{\AA}^2 \times 10^3$) for H ₂ enp. The anisotropic displacement factor exponent takes the form: -2 pi ² [h ² a* ² U ¹¹ +...+ 2 h k a* b* U ¹²]	211
Table A1.5	Hydrogen coordinates ($\times 10^4$) and isotropic displacement parameters ($\text{\AA}^2 \times 10^3$) for H ₂ enp	212
Table A1.6	Torsion angles (°) for H ₂ enp.....	213
Table A1.7	Hydrogen bonds (Å) and angles (°) for H ₂ enp	214

Table A2.1	Crystal data for Ti(bap)(NMe ₂) ₃ (28).....	215
Table A2.2	Atomic coordinates ($\times 10^4$) and equivalent isotropic displacement parameters ($\text{\AA}^2 \times 10^3$) for Ti(bap)(NMe ₂) ₃ . U(eq) is defined as one third of the trace of the orthogonalized U ^{ij} tensor	216
Table A2.3	Bond lengths (\AA) and angles ($^\circ$) for Ti(bap)(NMe ₂) ₃	217
Table A2.4	Anisotropic displacement parameters ($\text{\AA}^2 \times 10^3$) for Ti(bap)(NMe ₂) ₃ . The anisotropic displacement factor exponent takes the form: $-2 \pi^2 [h^2 a^{*2} U^{11} + \dots + 2 h k a^* b^* U^{12}]$	219
Table A2.5	Hydrogen coordinates ($\times 10^4$) and isotropic displacement parameters ($\text{\AA}^2 \times 10^3$) for Ti(bap)(NMe ₂) ₃	220
Table A3.1	Crystal data for Ti(NNMe ₂)(dap)(nacnac) (36).....	222
Table A3.2	Atomic coordinates ($\times 10^4$) and equivalent isotropic displacement parameters ($\text{\AA}^2 \times 10^3$) for Ti(NNMe ₂)(dap)(nacnac). U(eq) is defined as one third of the trace of the orthogonalized U ^{ij} tensor	223
Table A3.3	Bond lengths (\AA) and angles ($^\circ$) for Ti(NNMe ₂)(dap)(nacnac).....	224
Table A3.4	Anisotropic displacement parameters ($\text{\AA}^2 \times 10^3$) for Ti(NNMe ₂)(dap)(nacnac). The anisotropic displacement factor exponent takes the form: $-2 \pi^2 [h^2 a^{*2} U^{11} + \dots + 2 h k a^* b^* U^{12}]$	227
Table A3.5	Hydrogen coordinates ($\times 10^4$) and isotropic displacement parameters ($\text{\AA}^2 \times 10^3$) for Ti(NNMe ₂)(dap)(nacnac)	228
Table A4.1	Crystal data for Ti ₂ (dap) ₃ (NNMe ₂) ₂ (NHNMe ₂) (37).....	231
Table A4.2	Atomic coordinates ($\times 10^4$) and equivalent isotropic displacement parameters ($\text{\AA}^2 \times 10^3$) for Ti ₂ (dap) ₃ (NNMe ₂) ₂ (NHNMe ₂). U(eq) is defined as one third of the trace of the orthogonalized U ^{ij} tensor	232
Table A4.3	Bond lengths (\AA) and angles ($^\circ$) for Ti ₂ (dap) ₃ (NNMe ₂) ₂ (NHNMe ₂)..	233

P

P

P

T

T

T

T

T

P

P

Table A4.4	Anisotropic displacement parameters ($\text{\AA}^2 \times 10^3$) for $\text{Ti}_2(\text{dap})_3(\text{NNMe}_2)_2(\text{NHNMe}_2)$. The anisotropic displacement factor exponent takes the form: $-2 \pi^2 [h^2 a^{*2} U^{11} + \dots + 2 h k a^* b^* U^{12}] \dots$	245
Table A4.5	Hydrogen coordinates ($\times 10^4$) and isotropic displacement parameters ($\text{\AA}^2 \times 10^3$) for $\text{Ti}_2(\text{dap})_3(\text{NNMe}_2)_2(\text{NHNMe}_2)$	247
Table A4.6	Torsion angles ($^\circ$) for $\text{Ti}_2(\text{dap})_3(\text{NNMe}_2)_2(\text{NHNMe}_2)$	249
Table A5.1	Crystal data for 3-mesitylpyrrole (43)	259
Table A5.2	Atomic coordinates ($\times 10^4$) and equivalent isotropic displacement parameters ($\text{\AA}^2 \times 10^3$) for 3-mesitylpyrrole. $U(\text{eq})$ is defined as one third of the trace of the orthogonalized U^{ij} tensor	260
Table A5.3	Bond lengths (\AA) and angles ($^\circ$) for 3-mesitylpyrrole	261
Table A5.4	Anisotropic displacement parameters ($\text{\AA}^2 \times 10^3$) for 3-mesitylpyrrole. The anisotropic displacement factor exponent takes the form: $-2 \pi^2 [h^2 a^{*2} U^{11} + \dots + 2 h k a^* b^* U^{12}] \dots$	263
Table A5.5	Hydrogen coordinates ($\times 10^4$) and isotropic displacement parameters ($\text{\AA}^2 \times 10^3$) for 3-mesitylpyrrole	264
Table A5.6	Torsion angles ($^\circ$) for 3-mesitylpyrrole	265
Table A6.1	Crystal data for $\text{Ti}(\text{dap}^{3\text{-mes}})_2(\text{NMe}_2)_2$ (45)	266
Table A6.2	Atomic coordinates ($\times 10^4$) and equivalent isotropic displacement parameters ($\text{\AA}^2 \times 10^3$) for H_2enp . $U(\text{eq})$ is defined as one third of the trace of the orthogonalized U^{ij} tensor.....	267
Table A6.3	Bond lengths (\AA) and angles ($^\circ$) for $\text{Ti}(\text{dap}^{3\text{-mes}})_2(\text{NMe}_2)_2$	269
Table A6.4	Anisotropic displacement parameters ($\text{\AA}^2 \times 10^3$) for $\text{Ti}(\text{dap}^{3\text{-mes}})_2(\text{NMe}_2)_2$. The anisotropic displacement factor exponent takes the form: $-2 \pi^2 [h^2 a^{*2} U^{11} + \dots + 2 h k a^* b^* U^{12}] \dots$	279

Table A6.5	Hydrogen coordinates ($\times 10^4$) and isotropic displacement parameters ($\text{\AA}^2 \times 10^3$) for $\text{Ti}(\text{dap}^{3\text{-mes}})_2(\text{NMe}_2)_2$	281
Table A6.6	Torsion angles ($^\circ$) for $\text{Ti}(\text{dap}^{3\text{-mes}})_2(\text{NMe}_2)_2$	283
Table A7.1	Crystal data of $\text{V}(\text{NNMe}_2)(\text{TIP})(\text{dmpe})(\text{I})$ (49).....	288
Table A7.2	Atomic coordinates ($\times 10^4$) and equivalent isotropic displacement parameters ($\text{\AA}^2 \times 10^3$) for $\text{V}(\text{NNMe}_2)(\text{TIP})(\text{dmpe})(\text{I})$. $U(\text{eq})$ is defined as one third of the trace of the orthogonalized U^{ij} tensor	289
Table A7.3	Bond lengths (\AA) and angles ($^\circ$) for $\text{V}(\text{NNMe}_2)(\text{TIP})(\text{dmpe})(\text{I})$	290
Table A7.4	Anisotropic displacement parameters ($\text{\AA}^2 \times 10^3$) for $\text{V}(\text{NNMe}_2)(\text{TIP})(\text{dmpe})(\text{I})$. The anisotropic displacement factor exponent takes the form: $-2 \pi^2 [h^2 a^{*2} U^{11} + \dots + 2 h k a^* b^* U^{12}]$...	296
Table A7.5	Hydrogen coordinates ($\times 10^4$) and isotropic displacement parameters ($\text{\AA}^2 \times 10^3$) for $\text{V}(\text{NNMe}_2)(\text{TIP})(\text{dmpe})(\text{I})$	297
Table A7.6	Torsion angles ($^\circ$) for $\text{V}(\text{NNMe}_2)(\text{TIP})(\text{dmpe})(\text{I})$	299

LIST OF FIGURES

“Images in this dissertation are presented in color”

Figure 1.1	Scandium-based metal complexes for intramolecular hydroamination ...	6
Figure 1.2	Tantalum catalysts (neutral and cationic) for intramolecular hydroamination	7
Figure 2.1	ORTEP representation (50% probability level) of H ₂ enp (4)	53
Figure 2.2	Synthesis of Ti(enp)(NMe ₂) ₂ (5) and comparison with Ti(dap) ₂ (NMe ₂) ₂ (1)	54
Figure 3.1	Solid-state structure of Ti(NMe ₂) ₃ (bap) (28) from X-ray diffraction....	97
Figure 3.2	Structure of hydrazido(2-) complex 36 from X-ray diffraction.....	105
Figure 3.3	Possible resonance forms of 36 . (For simplicity, the other ligands are not shown).....	106
Figure 3.4	ORTEP representation of Ti ₂ (dap) ₃ (μ ₂ :η ¹ , η ² -NNMe ₂) ₂ (μ ₁ :η ¹ -NHNMe ₂) (37) at 50% probability level	108
Figure 3.5	Representative plot for the catalysis with Ti(dap) ₂ (NMe ₂) ₂ (1)	110
Figure 3.6	Representative plot for the catalysis with 36	112
Figure 3.7	Representative plot for reaction of 36 with 1,1-dimethylhydrazine.....	113
Figure 3.8	Representative plot for the catalysis with 10 mol% of 36 and Hdap ...	115
Figure 3.9	Dependence of <i>k</i> _{obs} on catalyst concentration	117
Figure 3.10	ORTEP representation of 3-mesitylpyrrole (43)	132
Figure 3.11	ORTEP representation of Ti(dap ^{3-mes}) ₂ (NMe ₂) ₂ (45)	134
Figure 4.1	Hydrazido(2-) vs isodiazene resonance forms	171

Figure 4.2	ORTEP representation of the cationic part in 49	187
Figure 4.3	(a) Hydrazido(2-) vs isodiazene resonance forms in vanadium complex. (b) Structure of 52	188
Figure B1.1	Kinetic plot for Run 1 with 10% Ti(dap) ₂ (NMe ₂) ₂ (1).	303
Figure B1.2	Kinetic plot for Run 2 with 10% Ti(dap) ₂ (NMe ₂) ₂ (1).	304
Figure B1.3	Kinetic plot for Run 3 with 10% Ti(dap) ₂ (NMe ₂) ₂ (1).	304
Figure B2.1	Kinetic plot for run 1 with 10% 36	305
Figure B2.2	Kinetic plot for run 2 with 10% 36	305
Figure B2.3	Kinetic plot for run 3 with 10% 36	306
Figure B3.1	Kinetic plot for run 1 with 36 + 10 Me ₂ NNH ₂ reaction.....	306
Figure B3.2	Kinetic plot for run 2 with 36 + 10 Me ₂ NNH ₂ reaction.....	307
Figure B3.3	Kinetic plot for run 3 with 36 + 10 Me ₂ NNH ₂ reaction.....	307
Figure B4.1	Kinetic plot for run 1 with 10% 36 + 10% Hdap reaction	308
Figure B4.2	Kinetic plot for run 2 with 10% 36 + 10% Hdap reaction	308
Figure B4.3	Kinetic plot for run 3 with 10% 36 + 10% Hdap reaction	309
Figure B5.1	Kinetic plot for run 1 with 10% 37	309
Figure B6.1	Kinetic plot with 15% Ti(dap) ₂ (NMe ₂) ₂	310
Figure B6.2	Kinetic plot with 5% Ti(dap) ₂ (NMe ₂) ₂	310
Figure B6.3	Kinetic plot with 2.5% Ti(dap) ₂ (NMe ₂) ₂	311
Figure C.1	¹ H and ¹³ C NMR spectra of compound 2	312
Figure C.2	¹ H and ¹³ C NMR spectra of compound 4	313

Figure C.3	^1H and ^{13}C NMR spectra of compound 5	314
Figure C.4	^1H and ^{13}C NMR spectra of compound 7	315
Figure C.5	^1H and ^{13}C NMR spectra of compound 13 and 14	316
Figure C.6	^1H and ^{13}C NMR spectra of compound 15	317
Figure C.7	^1H and ^{13}C NMR spectra of compound 17	318
Figure C.8	^1H and ^{13}C NMR spectra of compound 20	319
Figure C.9	^1H and ^{13}C NMR spectra of compound 21	320
Figure C.10	^1H and ^{13}C NMR spectra of compound 24	321
Figure C.11	^1H and ^{13}C NMR spectra of compound 25	322
Figure C.12	^1H and ^{13}C NMR spectra of compound 35	323
Figure C.13	^1H and ^{13}C NMR spectra of compound 38	324
Figure C.14	^1H and ^{13}C NMR spectra of compound 39	325
Figure C.15	^1H and ^{13}C NMR spectra of compound 40	326
Figure C.16	^1H and ^{13}C NMR spectra of compound 41	327
Figure C.17	^1H and ^{13}C NMR spectra of compound 42	328
Figure C.18	^1H and ^{13}C NMR spectra of compound 44	329
Figure C.19	^1H and ^{13}C NMR spectra of compound 45	330
Figure C.20	^1H and ^{13}C NMR spectra of compound 46	331

LIST OF SCHEMES

Scheme 1.1	Hydroamination of alkenes and alkynes generating amines.....	2
Scheme 1.2	Thermodynamics for addition of ammonia and ethylamine to ethylene ..	3
Scheme 1.3	Indole synthesis via hydroamination of vinylarenes by alkali metals	4
Scheme 1.4	Mechanistic pathway for hydroamination of alkynes by lanthanides.....	14
Scheme 1.5	Intermolecular hydroamination with actinides	15
Scheme 1.6	Mechanistic pathway of hydroamination of alkynes by actinides.....	16
Scheme 1.7	Mechanistic pathway for catalytic hydroamination of alkynes	18
Scheme 1.8	Synthesis of first titanium-based hydroamination catalyst	20
Scheme 1.9	Synthesis of (\pm)-monomorine	21
Scheme 1.10	Intermolecular hydroamination of alkyne with Cp_2TiMe_2	22
Scheme 1.11	Synthesis of α -amino esters via hydroamination pathway	25
Scheme 1.12	Synthesis of $\text{Ti}(\text{dpma})(\text{NMe}_2)_2$	27
Scheme 1.13	Proposed mechanistic pathway for hydroamination of alkyne.....	27
Scheme 1.14	Synthesis of $\text{Ti}(\text{dpm})(\text{NMe}_2)_2$	28
Scheme 2.1	Titanium-catalyzed hydrohydrazination of alkynes and synthesis of <i>N</i> -substituted indole	35
Scheme 2.2	Proposed mechanistic pathway for the hydrohydrazination reaction using 1,1-disubstituted hydrazines.....	37
Scheme 2.3	Cp-based titanium-catalyzed hydrohydrazination of alkynes and synthesis of substituted <i>N</i> -methylindoles.....	38
Scheme 2.4	Cp-based titanium-catalyzed hydrohydrazination of alkynes and synthesis of substituted <i>N</i> -methyltryptamines	38

Scheme 2.5	Synthesis of tryptamine derivatives by aryloxo-based Ti-catalyst	40
Scheme 2.6	Proposed mechanism for Co-catalyzed hydrohydrazination of olefin....	42
Scheme 2.7	Synthesis of <i>NH</i> -indole by zinc salts	47
Scheme 2.8	Synthesis of pyrazoline and pyrazole by Zn(OTf) ₂ -catalyzed hydrohydrazination	48
Scheme 2.9	Synthesis of pyridazinones via hydrohydrazination using ZnCl ₂	49
Scheme 2.10	Synthesis of H ₂ enp (4).....	53
Scheme 2.11	Reaction of 2-hexyne with phenylhydrazine catalyzed by 5	56
Scheme 2.12	Hydrohydrazination of 5-chloropent-1-yne with phenylhydrazine	61
Scheme 2.13	Possible pathways to 24 and 25	64
Scheme 3.1	Ugi 4-component reaction	92
Scheme 3.2	Possible 1,2-insertion pathway for the iminohydrazination reaction ...	101
Scheme 3.3	Possible mechanistic pathway of iminohydrazination by 1 for Entry 1 in Table 3.1	103
Scheme 3.4	Synthesis of pyrazole from 4-amino-1-azabutadienes	122
Scheme 3.5	Synthesis of <i>N</i> -phenyl-5- <i>n</i> -butylpyrazole and <i>N</i> -phenyl-3- <i>n</i> -butylpyrazole.....	124
Scheme 3.6	Possible mechanistic pathways for the pyrazole formation.....	125
Scheme 3.7	Synthesis of 3-mesitylpyrrole (43)	131
Scheme 4.1	Synthesis of a vanadium hydrazido(2-) complex with O(SCH ₂ CH ₂) ₂ ²⁻ as co-ligand	175
Scheme 4.2	Synthesis of titanium hydrazido(2-) complexes.....	180
Scheme 4.3	Synthesis of titanium-hydrazido(2-) complexes with different <i>fac</i> -N ₃ donor ligands	181
Scheme 4.4	Synthesis of titanium hydrazido(2-) complexes from imido complexes	182

Scheme 4.5	Synthesis of V(NNMe ₂)(OAr)(TIP) (46) (Ar = 2,6-Pr ⁱ ₂ C ₆ H ₃)	184
Scheme 4.6	Synthesis of cationic hydrazido(2-) complexes	186

LIST OF ABBREVIATIONS

bap	<i>bis</i> -2,5-(<i>N,N</i> -dimethylaminomethyl)pyrrolyl
BOC	<i>tert</i> -butyloxycarbonyl
bpy	2,2'-bipyridine
Bu ^t -bpy	4,4'-di- <i>tert</i> -butyl-2,2'-bipyridine
COD	cyclooctadiene
dap	2-((dimethylamino)methyl)pyrrolyl
DEAD	di- <i>tert</i> -butylazodicarboxylate
DIPP	di- <i>iso</i> -propylphenyloxide
DMAP	<i>N,N</i> -dimethylaminopyridine
dpm	Dipivaloylmethanato
H ₂ dpm	5,5-dimethyldipyrrolylmethane
dpma	<i>N,N</i> -di(pyrrolyl- α -methyl)- <i>N</i> -methylamine
dppf	1,1'- <i>bis</i> (diphenylphosphino)ferrocene
GC/FID	Gas Chromatography Flame Ionization Detector
GCMS	Gas Chromatography Mass Spectroscopy
H ₂ enp	<i>N</i> ¹ , <i>N</i> ² -bis((1 <i>H</i> -pyrrol-2-yl)methyl)- <i>N</i> ¹ , <i>N</i> ² -dimethylethane-1,2-diamine
LLCT	Ligand to ligand charge transfer
Nacnac	[N(Bu ^t)CHCHC(Bu ⁿ)N(NMe ₂)- <i>k</i> ² N]
RT	room temperature
TBS	<i>tert</i> -butyldimethylsilyl
triphos	1,1,1- <i>tris</i> (diphenylphosphinomethyl)ethane
Tosyl	<i>p</i> -tolylsulfonyl

CHAPTER 1

Hydroamination of alkynes

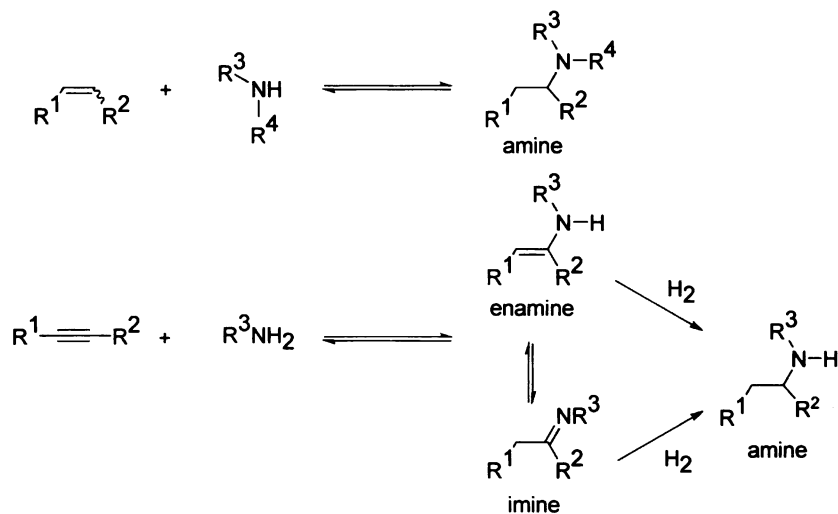
The primary focus of this thesis is the development of hydrohydrazination reactions for alkynes and their applications towards the synthesis of heterocycles. Hydrohydrazination is the formal addition of hydrazine to unsaturated C–C bonds resulting in hydrazones or substituted hydrazines. The first example of hydrohydrazination was reported in 2002 by our group; since, it has been explored by us and other research groups. On the other hand, hydroamination, where amines (instead of hydrazines) are added across the C–C unsaturation, has been more extensively studied since its discovery in the 1950's. Because hydroamination reactions are closely related to hydrohydrazination, and more prominent in the literature, they will be discussed as an introduction in this chapter. Hydrohydrazination of alkynes and its synthetic applications will be discussed in subsequent chapters.

1.1 Introduction

Hydroamination is the formal addition of an N–H bond across C–C unsaturation resulting in nitrogen-containing products such as amines, imines, or enamines (Scheme 1.1).¹ These molecules are important building blocks of different biologically active

compounds (e.g. alkaloids, amino acids, vitamins), fine chemicals, and pharmaceuticals. Hydroamination is an efficient way to synthesize amines, imines, or enamines with 100% atom economy. While hydroamination of alkenes generates amines, alkynes produce imines and enamines, which can also be reduced to amines if desired. Therefore, hydroamination provides an efficient route to synthesize amines, which are produced in several million tons per year industrially.² In addition to this, 80% of the pharmaceutical products are composed of C–N bonds.

Scheme 1.1 Hydroamination of alkenes and alkynes generating amines

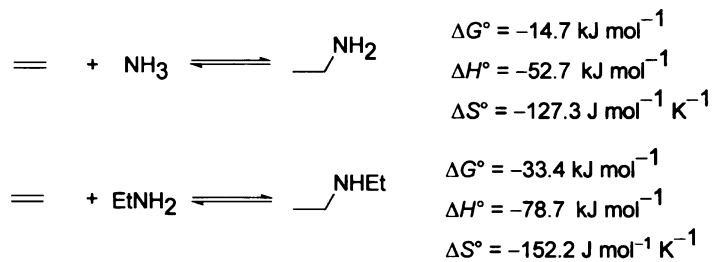


However, hydroamination usually has a high activation energy, primarily due to repulsion between the lone pair on nitrogen and π -electrons of the C–C unsaturated bond. In addition to that, since the uncatalyzed reactions exhibit a negative entropy change,

increasing the temperature makes the forward reaction thermodynamically less favorable (Scheme 1.2). To overcome all these barriers, a suitable catalyst design is necessary.¹

As illustrated in Scheme 1.2, the addition of ammonia or simple amines to ethylene is slightly exothermic or thermoneutral.³ Semiempirical calculations have shown that the addition of ammonia to acetylene is even more exothermic than ethylene by approximately 63 kJ mol^{-1} .¹ As a consequence, while hydroamination of alkynes have been extensively explored, that of unactivated alkenes is still a challenge.

Scheme 1.2 Thermodynamics for addition of ammonia and ethylamine to ethylene



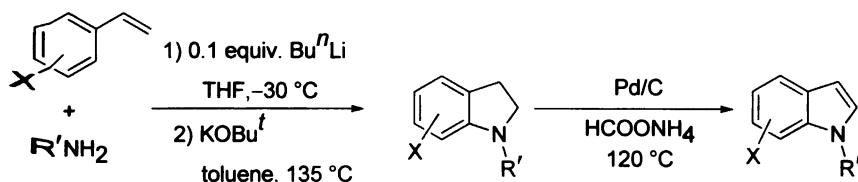
Over the last few decades, extensive research efforts have been directed towards the hydroamination reaction. Hydroamination of alkynes is known with different metals spanning the periodic table from alkali metals to transition and f-block metals. In the following sections, intermolecular hydroamination (mainly) with some of the representative metals will be discussed with an emphasis on Group 4 metal catalysis.

1.2 Hydroamination with alkali and alkaline earth metals

The first well-recognized example of alkali metal catalyzed hydroamination was reported in 1954 by Howk et al.⁴ They demonstrated that ammonia adds to ethylene in the presence of metallic sodium at about 200 °C and 1000 bar in an inert medium forming ethyl-, diethyl-, and triethylamine in 70% total yield. Alkali metal hydrides such as NaH and LiH have also been found to be equally active. Aniline is converted to *N*-ethylaniline by Na or NaNH₂ at 250–300 °C and 50–200 bar. It is interesting to note that a few late alkali metal amides such as rubidium and cesium amides catalyze the amination of ethylene at considerably milder conditions (80–110 °C and 90–120 bar) in moderate yields.^{5,6} Since milder conditions are used in the case of alkali metal amides, mono-alkylated amines are formed selectively.

Apart from the inorganic salts of alkali metals, organic salts have also been found to be active for hydroamination of alkynes with amines. For example, BuⁿLi⁷ and KOBu^t⁸ serve as active precatalysts for the addition of amines to alkenes (ethylene or styrene). Beller has expanded this protocol towards the synthesis of indoles by hydroamination of styrene derivatives followed by oxidation (Scheme 1.3).⁹

Scheme 1.3 Indole synthesis via hydroamination of vinylarenes by alkali metals



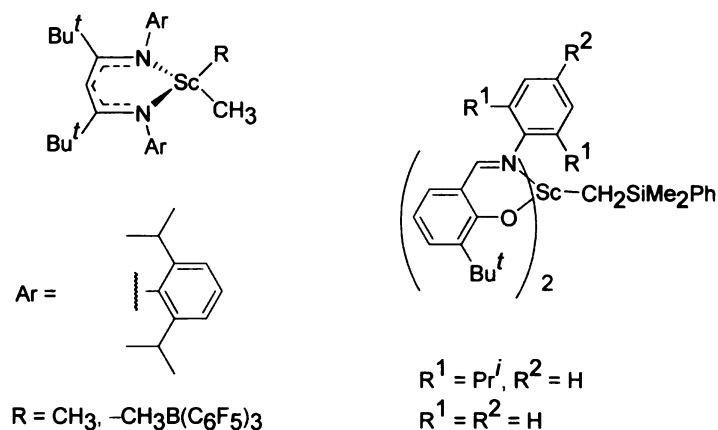
Knochel has shown that CsOH·H₂O is an effective precatalyst for the addition of secondary aromatic or heterocyclic amines to phenylacetylene in NMP (N-methylpiperidine) leading to enamines.¹⁰

There are only a few examples in the literature of hydroamination catalyzed by alkaline earth metals. Hill first reported Ca-catalyzed intramolecular hydroamination of aminoalkene. A β-diketiminato-based Ca complex, [$\{HC-(C(Me)_2N-2,6-Pr^i_2C_6H_3)_2\}Ca\{N(SiMe_3)_2\} \cdot (THF)\}$], was used as the catalyst.¹¹ More recently, Roesky et al. has reported a different complex with Group 2 metals (M = Ca, Ba, Sr), [$\{(Pri)_2ATI\}M\{N(SiMe_3)_2\}(THF)_2\}$], where (Pri)₂ATI = *N*-isopropyl-2-(isopropylamino)troponimate.^{12,13} These complexes are active for intramolecular hydroamination of aminoolefins. It is interesting to note that the reactivity decreases with increasing atomic radius of the metal. Although the elements in this group are not well-explored for hydroamination reactions, they are potentially important for industrial use as they are inexpensive and environmentally benign.

1.3 Hydroamination with transition metals (Group 3 and 5)

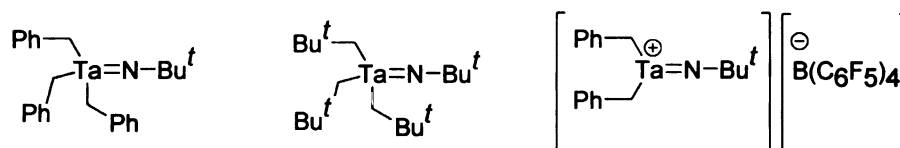
Roesky and co-workers have reported that mono- and *bis*(*N*-*iso*-propyl-2-(*iso*-propylamino)troponiminato) yttrium amides, [(Pri)₂ATI]_{*m*}Y[N(SiMe₃)₂]_{*n*} (where *m* = 1–2; *n* = 3–*m*), are effective for intramolecular hydroamination of alkynes.¹⁴ Schafer has described scandium-catalyzed hydroamination of aminoalkynes and aminoalkenes. Both neutral and cationic complexes were synthesized using aldiminato- and diketiminato-ligands (Figure 1.1). The key to this activity is the small ionic radius of scandium and the availability of an open coordination site on the cationic complex.¹⁵ Further investigation in this field has involved the synthesis of both neutral and cationic complexes of scandium and yttrium with bidentate amidinate and tetradentate triamine-amide ligands.¹⁶ The activity of the catalysts depends on the nature of the ancillary ligands.

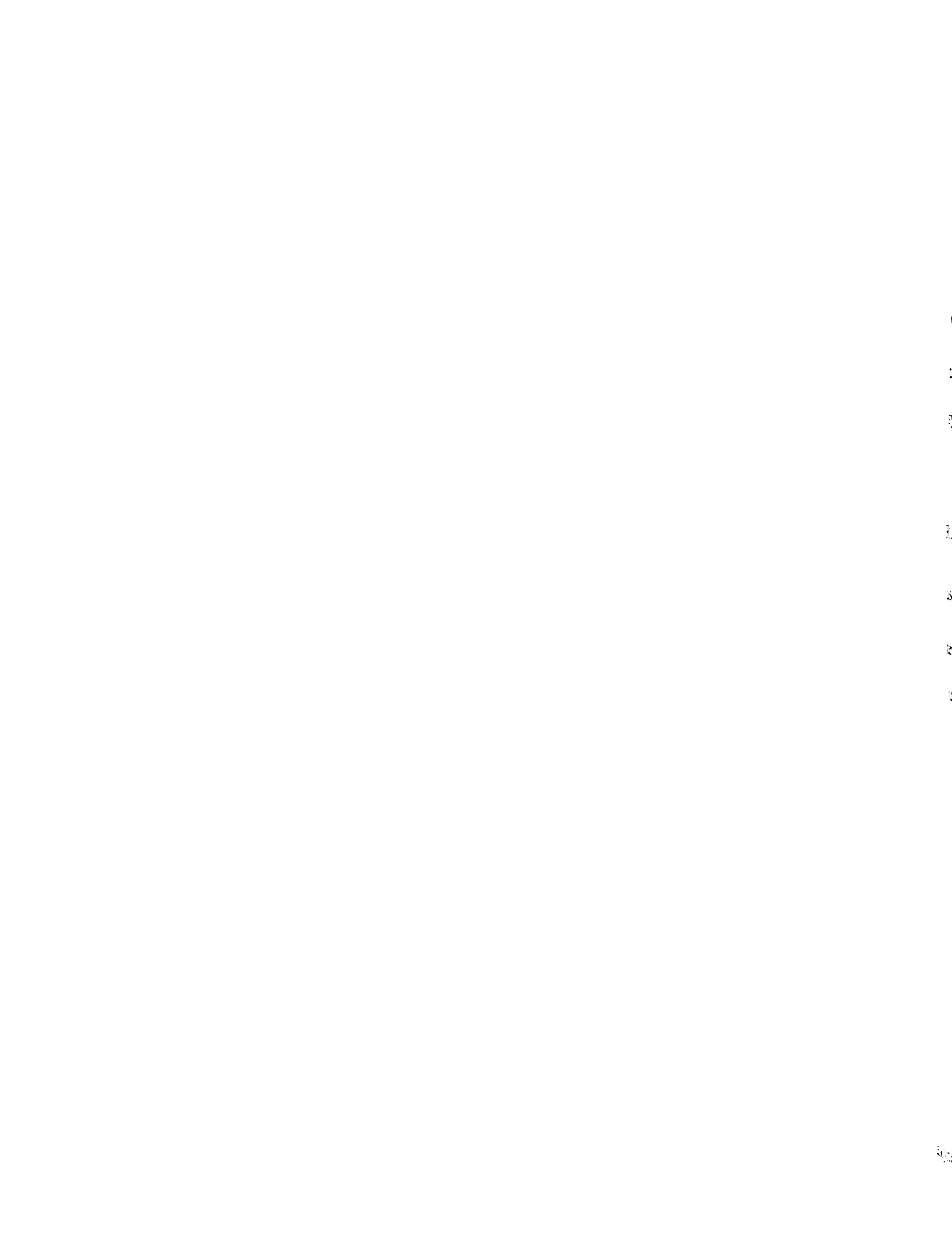
Figure 1.1 Sc-based metal complexes for intramolecular hydroamination.



Among the group 5 metals, Bergman has shown several tantalum imido complexes (both neutral and cationic) that are efficient catalysts for intermolecular hydroamination of alkynes and alkenes (Figure 1.2).¹⁷ Different amido- and imido-vanadium complexes have shown moderate reactivity towards intermolecular hydroamination of alkynes with aromatic amines.¹⁸ These catalysts generate Markovnikov imine products almost exclusively.

Figure 1.2 Tantalum catalysts (neutral and cationic) for intramolecular hydroamination.





1.4 Hydroamination with late transition metals

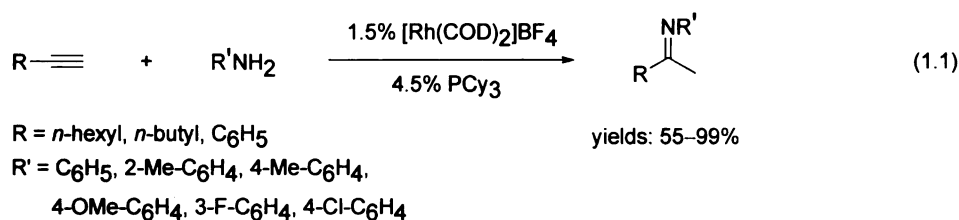
In contrast to early transition metals and f-block elements, late transition metals provide alternative catalytic systems that are less air and moisture sensitive. They are also less oxophilic and often more functional group tolerant. Until 1999, hydroamination was only known with mercury¹⁹ and thallium²⁰ among the late transition metals. However these two are toxic. Therefore, the search for more environmentally benign catalytic systems was necessary.

Wakatsuki and co-workers first reported an efficient late transition metal catalyst, $\text{Ru}_3(\text{CO})_{12}$, for intermolecular hydroamination.²¹ Only 0.1 mol% of the catalyst was used in the presence of 0.3 mol% acidic additive NH_4PF_6 for the hydroamination of terminal alkynes with aniline. Moreover, the reactions can be carried out in open air under solvent-free conditions.

More recently, Takai has expanded this methodology towards the synthesis of indene derivatives in a one-pot, two-step procedure; hydroamination was followed by C–H activation with $[\text{ReBr}(\text{CO})_3(\text{THF})]_2$ and coupling with ethyl acrylate.²² A cationic complex, $[(\text{PCy}_3)_2(\text{CO})(\text{CH}_3\text{CN})_2\text{RuH}]^+\text{BF}_4^-$, also has been used for intermolecular cyclization of amine and alkynes. The resulting quinoline products are obtained in 43–94% yield.²³

The first example of rhodium-catalyzed intermolecular hydroamination of terminal alkynes with aniline was reported by Beller in 2001.²⁴ The cationic Rh(I) catalyst,

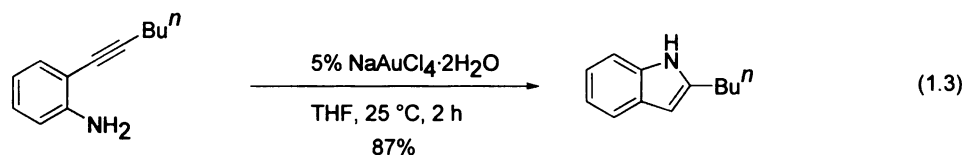
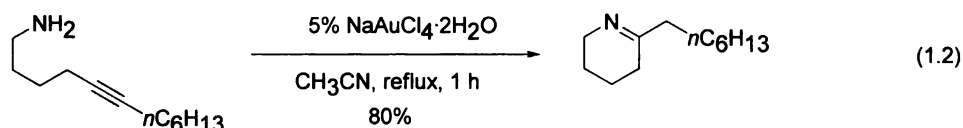
Rh(COD)₂BF₄/3 PCy₃ in THF was found to be very active for such transformations with up to 99% yield under very mild conditions (room temperature) and without any acid or base (Equation 1.1). The generated imines were further converted to secondary amines in situ by organolithium reagents. This catalyst is less oxophilic, nontoxic, and easy to handle compared to early transition metal catalysts.



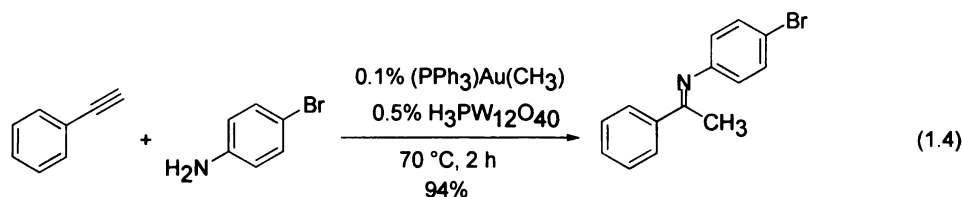
More recently, different Rh(I) and Ir(I) complexes containing bidentate phosphine-pyrazolyl ligands having the molecular formula [M(R₂PyP)(COD)]BPh₄ (R = Me, Pr^{*i*}, Ph; M = Ir, Rh) (where COD = cyclooctadiene), [Ir(R₂PyP)(COD)]BPh₄ (R = Me, Pr^{*i*}), and [M(R₂PyP)(CO)Cl] (R = Me, Pr^{*i*}, Ph, M = Ir, Rh) were reported for intramolecular hydroamination of alkynes. Cationic Ir complexes with COD ligands are more active than CO ligands. Moreover, the neutral complexes are inactive for intramolecular hydroamination. Another interesting observation is that the Rh(I) cationic complexes are less effective than their Ir(I) analogues.²⁵

Among the noble metals, a few Au(I) and Au(III) complexes are known to be active for hydroamination of alkynes. In 1987, Utimoto reported NaAuCl₄·2H₂O-catalyzed

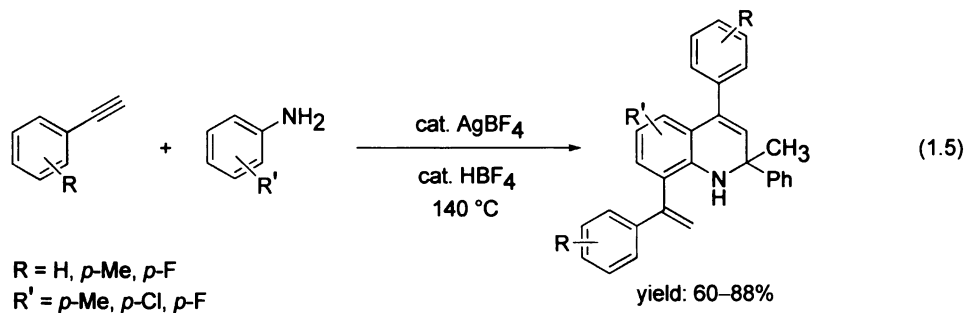
hydroamination of 5-alkynylamines to form tetrahydropyridine derivatives (Equation 1.2).^{26, 27} He also expanded this methodology towards the synthesis of indoles (Equation 1.3).²⁸ Marinelli expanded the scope of this reaction by using an ethanol/water mixed solvent system.²⁹



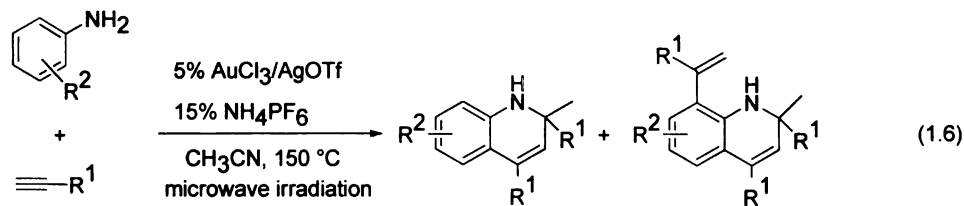
Acid-promoted intermolecular hydroamination of terminal and internal alkynes have been carried out with $(\text{PPh}_3)\text{Au}(\text{CH}_3)$ to generate imines (Equation 1.4).³⁰ Both aryl and alkyl, terminal and internal alkynes have been used. Different primary aromatic amines (electron-rich, electron-deficient, and sterically hindered) are effective in this reaction, however, alkylamines are not. More recently, a new porphyrin-based Au(III) catalyst was introduced for hydroamination of alkynes.³¹



Surprisingly, the reaction of phenylacetylene with aniline in the presence of catalytic $\text{AgBF}_4/\text{HBF}_4$ produces 1,2-dihydroquinoline derivatives instead of imine products (Equation 1.5). In this case, the products are formed by hydroamination followed by hydroarylation.³² Ag-catalyzed hydroamination are also applied to synthesize pyrroles.³³



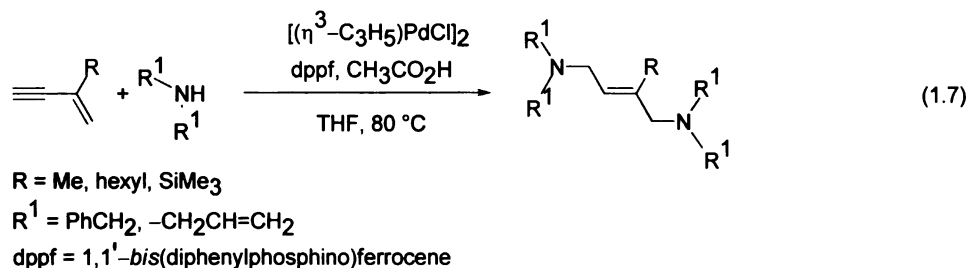
In addition, a combination of both Au/Ag-catalyzed microwave-assisted hydroamination of alkynes with amines was reported where 1,2-dihydroquinolines were obtained as the final products (Equation 1.6).³⁴



Yamamoto described the formation of pyrrolidine and piperidines by intramolecular hydroamination of amines or sulfonyl amides, bearing a terminal allene group using Pd

catalyst. This involved the addition of an M–H bond across an allenic double bond.³⁵ Pd-catalyzed hydroamination of allenes was reported for the synthesis of allylic amines.³⁶

The same group showed an efficient stereoselective hydroamination of conjugated enynes in the presence of a palladium catalyst (Equation 1.7).³⁷ The reactions only occurred in the presence of a phosphine-based ligand.

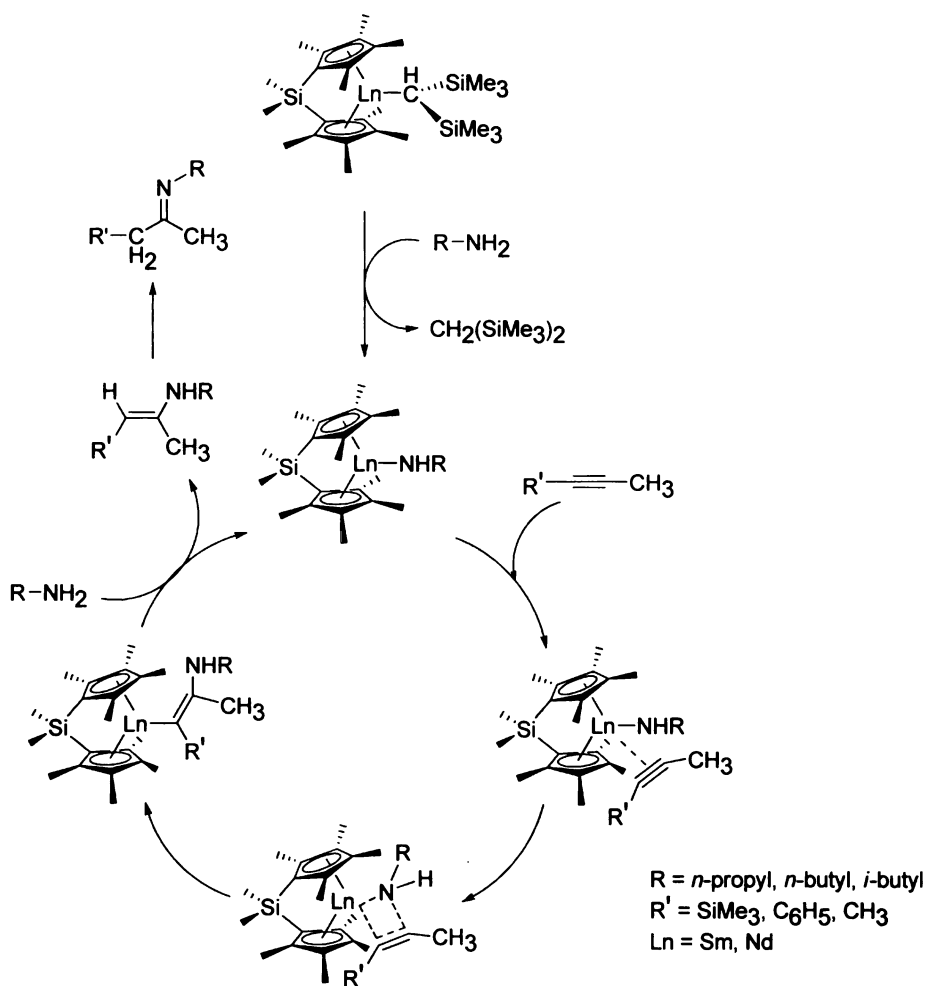


Intermolecular hydroamination of aminoalkynes using Group 7–12 metals has been reported. For example, [Cu(CH₃CN)₄]PF₆, Zn(CF₃SO₃)₂, and [Pd(triphos)](CF₃SO₃)₂ (where triphos = 1,1,1-tris(diphenylphosphinomethyl)ethane) have been used, and the products are substituted pyrrolidines and piperidines.³⁸

1.5 Hydroamination with lanthanides and actinides

Marks and co-workers discovered lanthanide-based catalysts effective for both intra- and intermolecular hydroamination of alkenes and alkynes.³⁹ The f-block elements are quite different in their activity towards activation of unsaturated organic substrates (C=C and C≡C activation in particular) and heteroatom cyclization due to their high electrophilicity, large atomic radius, and nondissociative ancillary ligation. Complexes having the structure $\text{Cp}'_2\text{LnCH}(\text{SiMe}_3)_2$ ($\text{Ln} = \text{Sm}$, $\text{Cp}' = \eta^5\text{-Me}_5\text{C}_5$) and $\text{Me}_2\text{SiCp}''_2\text{LnCH}(\text{SiMe}_3)_2$ ($\text{Ln} = \text{Nd}$, Sm , Lu ; $\text{Cp}'' = \eta^5\text{-Me}_4\text{C}_5$) are effective precatalysts for both intra- and intermolecular hydroamination of alkenes, alkynes, and dienes. However, the corresponding intramolecular processes are ~1000 times faster than the intermolecular processes. Mechanistically, the turnover limiting step is the insertion of C=C or C≡C bonds into Ln–N bond followed by rapid protonolysis of the resulting Ln–C bond (Scheme 1.4).

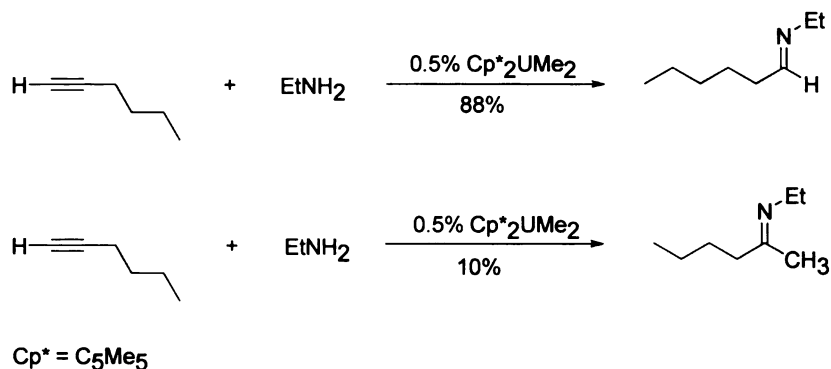
Scheme 1.4 Mechanistic pathway for hydroamination of alkynes by lanthanides



Intermolecular hydroamination of terminal alkynes (aliphatic and aromatic) with primary aliphatic amines was carried out with organoactinide complexes $\text{Cp}^*_2\text{AcR}_2$ (Ac = Th, U; R = Me, HNR) developed by Eisen and co-workers.^{40,41} Here the regioselectivity of hydroamination depends on the nature of the metal. While aldimine

products are obtained in good to excellent yield with the uranium complex, only poor to moderate yields of ketimine products were observed in the case of thorium (Scheme 1.5).

Scheme 1.5 Intermolecular hydroamination with actinides

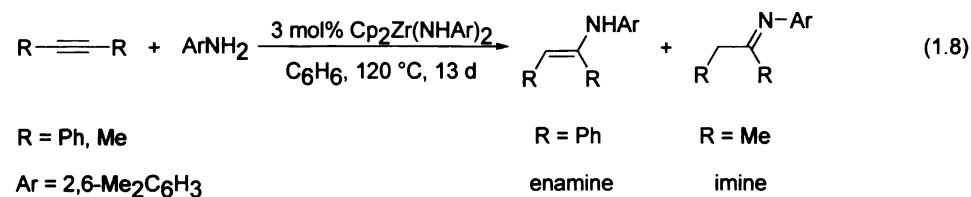


In general, there are considerable differences in the reactivity of 4f- (lanthanides) and 5f- (actinides) metal complexes in hydroamination reactions. In the case of actinides, only terminal alkynes undergo reaction with amines but not internal ones. Silyl substituent effects are minor for actinides. Hydroamination of alkenes have not been observed with actinides. Mechanistically, for actinides, the rate-determining step is the formation of the metal-imido complex after N-H σ -bond activation followed by the release of CH_4 (Scheme 1.6). The intermediate then undergoes rapid cyclization with alkyne to form a four-membered metallacycle. This is followed by protonolysis by amine. The enamine product is produced along with regeneration of the metal-imido species. The enamine product then converts into the more stable imine isomer.

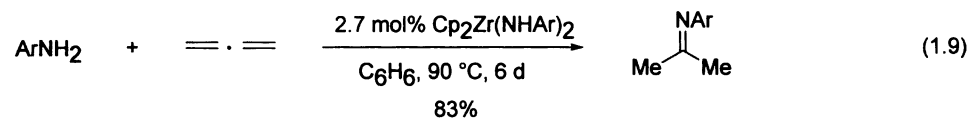
1.6 Hydroamination with Group 4 metal complexes

1.6.1 Hydroamination of alkynes with Zirconium

The earliest example of zirconium-catalyzed hydroamination appeared in the literature from the pioneering work of Bergmann in 1992.^{42,43} He discovered that the zirconocene bis(amide) $[\text{Cp}_2\text{Zr}(\text{NH}-2,6\text{-Me}_2\text{C}_6\text{H}_3)_2]$ catalyzed the intermolecular hydroamination of aromatic amines with alkynes and allenes. The reaction took place at 90-120 °C in the presence of 2–3 mol% of the catalyst. Although the catalyst seemed to be stable under these reaction conditions, the reaction was found to be relatively slow. While the enamine formed from diphenylacetylene was isolated in 60% yield, the enamine formed from 2-butyne only was observed by ^1H NMR. In the second case, the product was the more stable imine isomer (Equation 1.8).



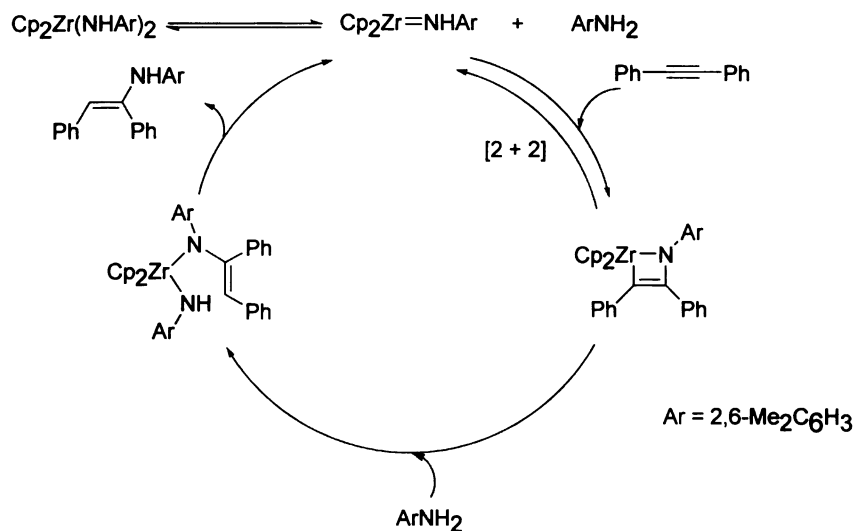
Although the above described zirconocene catalyst was inactive for alkene hydroamination, it hydroaminated allene under relatively mild conditions (Equation 1.9). The Markovnikov addition product, the imine of acetone, was isolated in 83% yield.



Ar = 2,6-Me₂C₆H₃

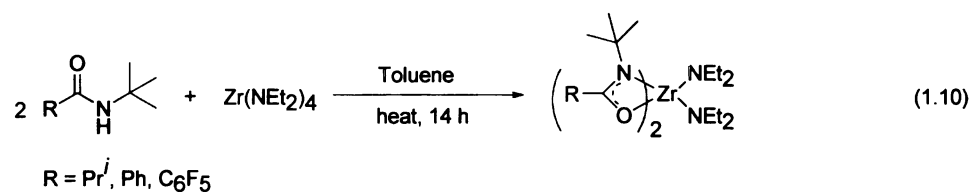
A detailed kinetic study was carried out to investigate the mechanism of the above transformation (Scheme 1.7). The catalytic cycle begins with the formation of zirconium imido complex from the zirconocene precatalyst. This is followed by the [2 + 2]-cycloaddition of the alkyne to form an azametallacyclobutene intermediate. Rapid protonation by the amine generates the enamide-amide complex, which then undergoes α -elimination of enamine to regenerate the catalytically active species.

Scheme 1.7 Mechanistic pathway for catalytic hydroamination of alkynes



Although the reaction was limited to disubstituted alkynes and bulky aromatic amines, this was a breakthrough in Group 4 alkyne hydroamination. Not surprisingly, this was followed by a series of hydroamination reactions using another Group 4 element, titanium, which are described in the next section.

More recently, Schafer has reported bis(amidate) bis(amido) zirconium complexes (Equation 1.10), which are effective precatalysts for both intra- and intermolecular hydroamination of alkynes.^{44,45}

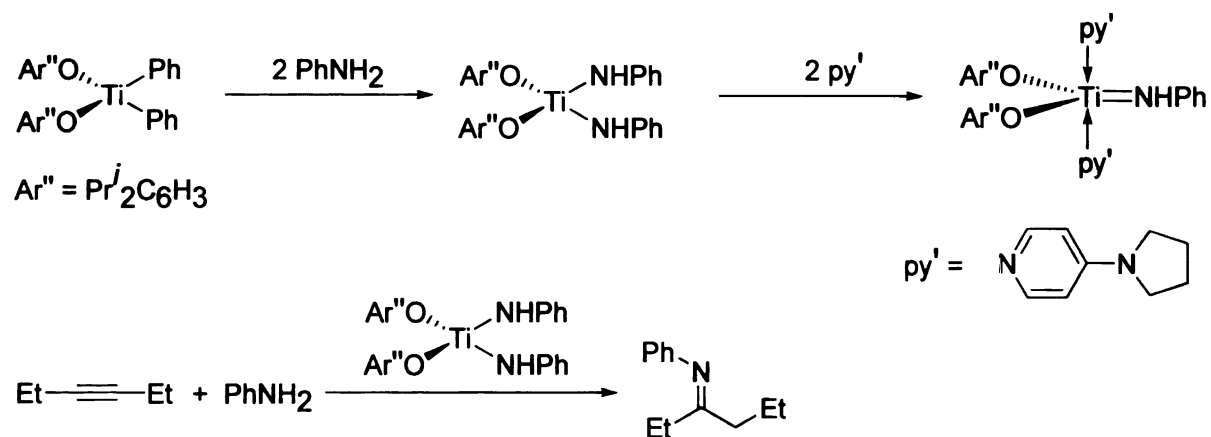


1.6.2 Hydroamination of alkynes with Titanium

The earliest example of titanium-catalyzed hydroamination was reported by Rothwell and co-workers.⁴⁶ They showed the hydroamination of 3-hexyne with aniline using bis(phenylamido) titanium(IV) complex (Scheme 1.8). They also reported for the first time a structurally characterized titanium imido complex. However, the isolated imido pyridine complex did not exhibit any reactivity towards hydroamination of 3-hexyne.

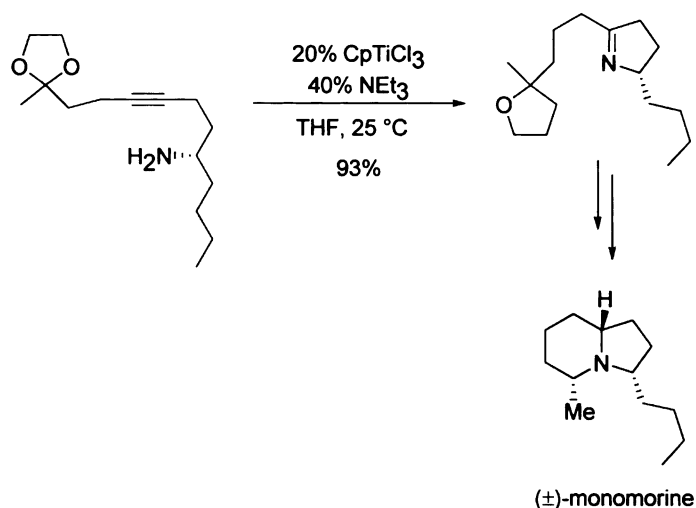
In 1992, Livinghouse reported hydroamination with a Cp-based (Cp = cyclopentadiene, $C_5H_5^-$) titanium complex. He showed intramolecular hydroamination of γ - and δ -aminoalkynes with 20 mol% $CpTiCl_3$ and 40 mol% Pr^i_2NEt .^{47,48}

Scheme 1.8 Synthesis of first titanium-based hydroamination catalyst



The mechanism is very similar to that depicted by Bergman. The cycle starts with the formation of the imido complex, followed by [2 + 2]-cycloaddition with the alkyne forming an azametallacyclobutene intermediate. The final step involves protonation to generate the product. Although this methodology was restricted to intramolecular hydroamination, it did not require a sterically bulky amine. He also extended this methodology towards the synthesis of the natural product (\pm)-monomorine.⁴⁹ The key step involves $CpTiCl_3$ -catalyzed hydroamination of aminoalkyne as shown in Scheme 1.9.

Scheme 1.9 Synthesis of (±)-monomorine



Another Cp-based titanium catalyst, Cp₂Ti(NHPh)₂, and more versatile Cp₂TiMe₂ were introduced by Doye in 1999.⁵⁰ Both aryl and alkyl amines can be used in the hydroamination with symmetrically substituted internal and terminal alkynes. The resulting imines were either converted into ketones or reduced to amines (Scheme 1.10). Although good yields were obtained with aryl amines and sterically demanding *sec*- and *tert*-alkyl amines, yields were poor for less hindered *n*-alkyl and benzyl amines. Later, a slightly modified Cp-based titanium catalyst, Cp*₂TiMe₂ (Cp* = Me₅C₅⁻), was found to be successful for hydroamination with less hindered amines.⁵¹ A recently reported catalyst for similar transformations involves an indenyl ligand, (Ind)₂TiMe₂, which is also commonly used for intermolecular hydroamination of alkynes.⁵² While *anti*-Markovnikov products were observed with arylalkynes, only Markovnikov products were

05

21

Sc

15

16

17

18

19

20

21

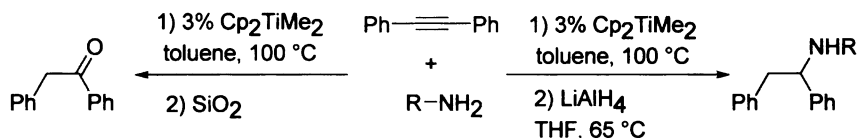
22

23

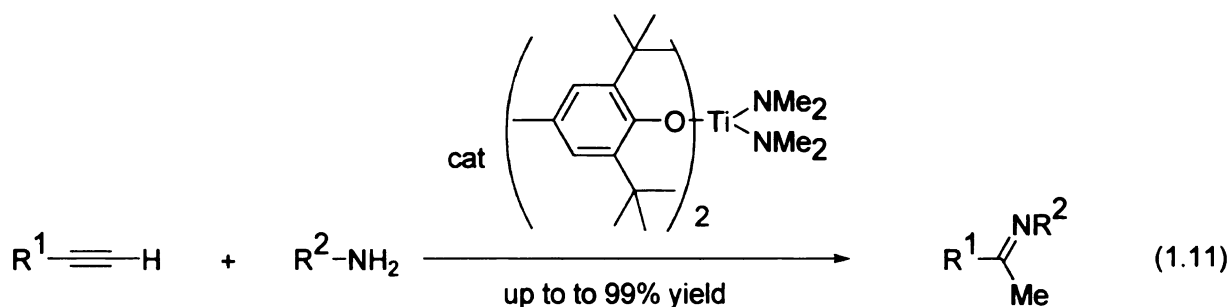
24

obtained with alkylalkynes and arylamines. Bergman has shown hydroamination of allene using Cp_2TiMe_2 as the precatalyst, and the product is the imine of acetone.⁵³

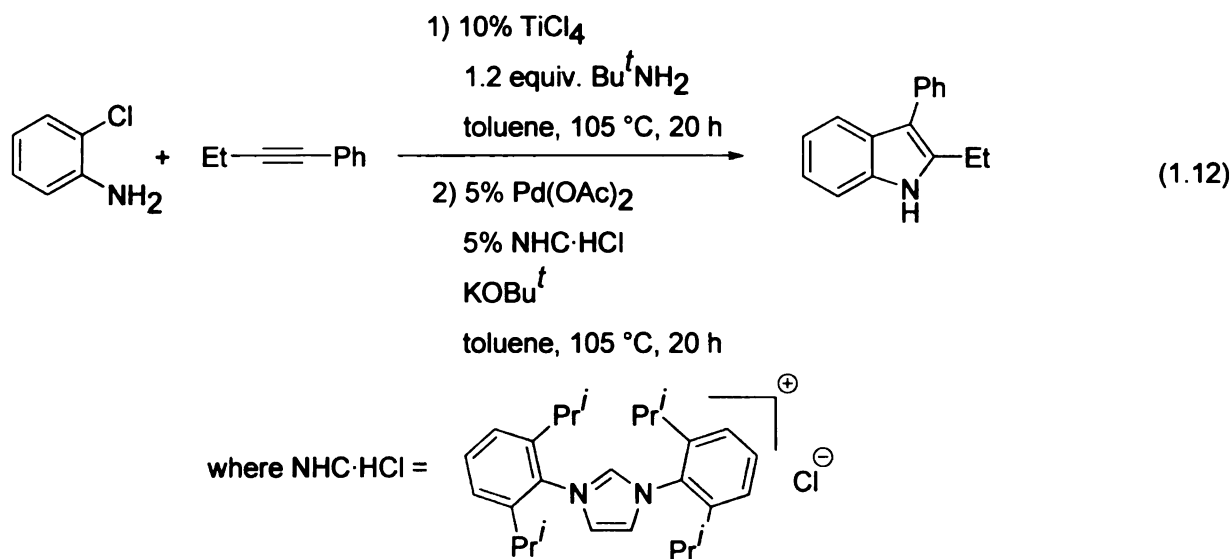
Scheme 1.10 Intermolecular hydroamination of alkyne with Cp_2TiMe_2



In 2002, Beller developed new titanocene alkyne complexes $[(\text{Cp}_2\text{Ti}(\eta^2\text{-Me}_3\text{SiC}\equiv\text{CSiMe}_3)]$ and $[(\text{Cp}_2\text{Ti}(\eta^2\text{-Me}_3\text{SiC}\equiv\text{CPh})]$ for intermolecular hydroamination of both terminal and internal alkynes.⁵⁴ Excellent *anti*-Markovnikov selectivity was observed with terminal aliphatic alkynes with *tert*-butylamine. The selectivity was observed to increase depending on the steric bulk of the amine. In the reaction of aniline with 1-hexyne, the product was obtained almost to the exclusion of the *anti*-Markovnikov product (Markovnikov:*anti*-Markovnikov = 1:99). Later, the same group introduced an aryloxo-based titanium precatalyst for chemo- and regioselective intermolecular hydroamination of terminal and internal alkynes with aliphatic and aromatic amines in good to excellent yields (Equation 1.11).⁵⁵ The regioselectivity can also be reversed by suitably changing the substituents on the aryloxo ligand.⁵⁶

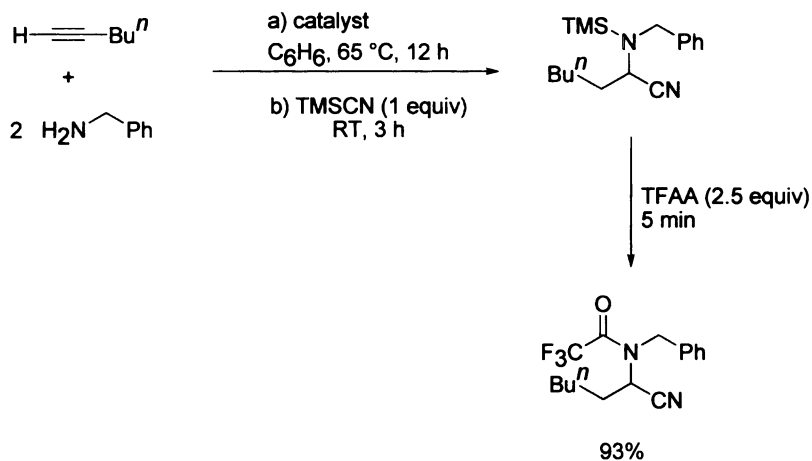


Ackermann showed another user-friendly protocol for intermolecular hydroamination of alkynes with various alkyl and arylamines using commercially available TiCl_4 . Addition of *tert*-butylamine to TiCl_4 generated the active catalyst in situ. This catalyst tolerates various halides, which enables the synthesis of various indoles via one-pot hydroamination/Heck coupling reaction sequence (Equation 1.12).^{57,58}



Another class of the intermolecular hydroaminations of internal and terminal alkynes with primary amines was developed by the Schafer group using amidate ligands (yields as high as 97%). However, the enhanced reactivity also reduced the selectivity for some terminal alkynes.^{45,59-61} This methodology was further extended to the synthesis of α -amino acids and α -amino esters (Scheme 1.11).⁶²

Scheme 1.11 Synthesis of α -amino esters via a hydroamination pathway

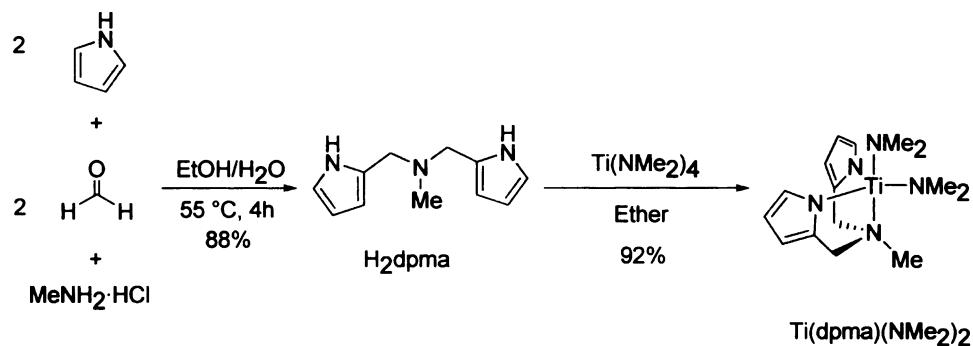


1.6.3 Research in the Odom group

The first example of non-Cp-based titanium catalyst, $\text{Ti}(\text{NMe}_2)_4$, for alkyne hydroamination was reported from our group in 2001.⁶³ Hydroaminations of terminal and internal alkynes were carried out with aniline and different aromatic amines. This precatalyst is selective for Markovnikov products, as opposed to the Cp_2TiMe_2 system which produces *anti*-Markovnikov products selectively. The reactions were carried out with 10% catalyst loading at 75°C . The reactions with terminal alkynes were faster than the internal ones. However, alkyne oligomerization and polymerization were observed with phenylacetylene, hence low yield of the imine product was obtained. Unfortunately, hydroamination reactions of alkynes with alkyl amines were not successful with this precatalyst.

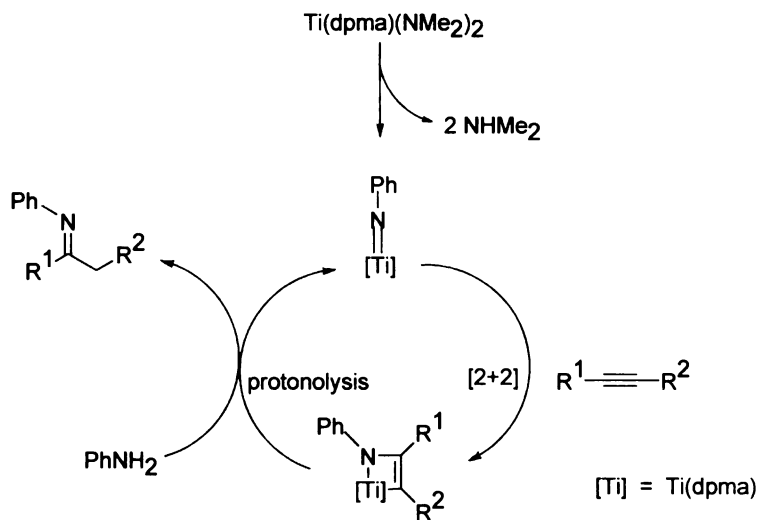
In search for a better catalytic system, a pyrrolyl-based ligand was used. Pyrrolyl ligands are less π -donating to the metal due to its competition with the aromatic stabilization of pyrrole (aromatic stabilization energy of pyrrole is $\sim 21 \text{ kcal mol}^{-1}$).⁶⁴ This makes the metal center more Lewis acidic. A pyrrolyl-based ligand, H₂dpma (dpma = di(pyrrolyl- α -methyl)methylamine), was synthesized by Mannich reaction of pyrrole, formaldehyde, and methylamine hydrochloride (88% yield). A new precatalyst, Ti(dpma)(NMe₂)₂, was synthesized (Scheme 1.12) and applied successfully to intermolecular hydroamination of alkynes.⁶⁵⁻⁶⁷ Both terminal and internal alkynes were hydroaminated by aliphatic and aromatic amines. The reaction of terminal alkynes with aniline was most effective. A large number of functional groups (*m*-, *p*-OMe, halogen) on aniline were tolerated. Although steric effects on the aniline were not dominant, a large electronic effect was observed. In addition, the reactions were successful with alkyl amines (cyclohexyl, benzyl, and benzhydrylamine). Compared to Ti(NMe₂)₄, this catalyst was more selective towards Markovnikov products for most of the alkynes (except 1-phenylpropyne) (50:1 versus 3:1 for the reaction of 1-hexyne with aniline). This was attributed to the presence of the pyrrolyl ligand in the active species during catalysis.

Scheme 1.12 Synthesis of $\text{Ti}(\text{dpma})(\text{NMe}_2)_2$



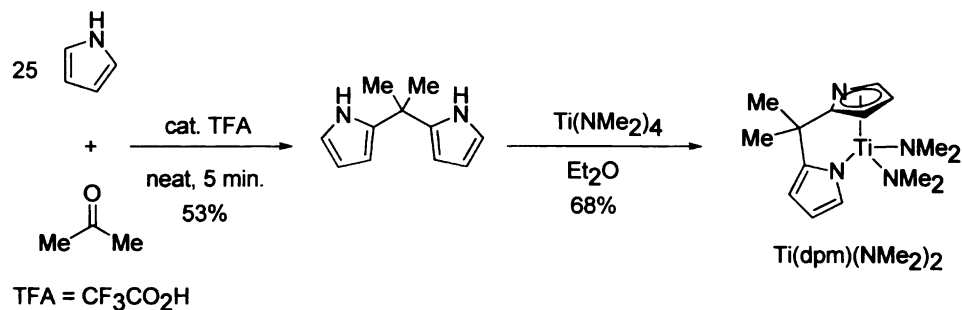
The proposed mechanistic pathway (Scheme 1.13) leading to the imine product is very similar to that for hydroamination of alkynes by zirconocene established by Bergman and co-workers. The first step is the formation of the imido complex, followed by [2 + 2]-cycloaddition of the alkyne forming an azametallacyclobutene intermediate. The metallacycle then undergoes protonolysis by amine to form the imine product and regenerates the imido species.

Scheme 1.13 Proposed mechanistic pathway for hydroamination of alkyne



However, to decrease the steric strain and increase the Lewis acidity of the metal center, a slightly different pyrrolyl ligand was used. The complex was $\text{Ti}(\text{dpm})(\text{NMe}_2)_2$, where H_2dpm is 5,5-dimethyldipyrrolylmethane (Scheme 1.14).⁶⁸ This was an improved precatalyst for intermolecular hydroamination of both terminal and internal alkynes with aliphatic and aromatic amines. In fact, this was actually an order of magnitude faster than the previous precatalyst, $\text{Ti}(\text{dpma})(\text{NMe}_2)_2$, as revealed by kinetic experiments. Several other $\text{Ti}(\text{dpm})(\text{NMe}_2)_2$ -type catalysts have been synthesized more recently. This includes the use of 2,9-diaryldipyrrolylmethane derivatives.⁶⁹ These also have been found to be active catalysts for intermolecular alkyne hydroamination.

Scheme 1.14 Synthesis of $\text{Ti}(\text{dpm})(\text{NMe}_2)_2$



1.7 Concluding Remarks

A variety of metal complexes covering most of the periodic table have been used to catalyze hydroamination of alkynes. Both inter- and intramolecular versions have been explored widely. Earlier examples of hydroamination involved harsh conditions such as high temperature and pressure, while new reactions are facile at or near room temperature. Hydroamination also has been applied towards the synthesis of amines and different heterocycles.

During the development of titanium-based precatalysts for hydroamination, a new reaction was discovered that involves hydrazines in place of amines. This process is formally known as hydrohydrazination. Details on hydrohydrazination and its synthetic applications will be discussed in the next chapter.

Reactions involving metal-ligand multiple bonds in catalysis, e.g., hydrohydrazination, are the main focus of this thesis. Expansion of this new chemistry towards multicomponent coupling reactions and synthesis of different transition metal hydrazido complexes will be discussed in the subsequent chapters.

1.8 References

1. Pohlki, F.; Doye, S. *Chem. Soc. Rev.* **2003**, 32, 104.
2. Heilen, G.; Mercker, J. H.; Frank, D.; Reck, A. R.; Jackh, R. *Ullman's Encyclopedia of Industrial Chemistry*, 1985, A2, 36.
3. Steinborn, D.; Taube, R. *Z. Chem.* **1986**, 26, 349.
4. Howk, B. W.; Little, E. L.; Scott, S. L.; Whiteman, G. M. *J. Am. Chem. Soc.* **1954**, 76.
5. Closson, R. D.; Napolitano, J. P.; Ecke, G. G.; Kolka, A. J. *J. Org. Chem.* **1957**, 22, 646.
6. Pez, G. P.; Galle, J. E. *Pure Appl. Chem.* **1985**, 57, 1917.
7. Hartung, C. G.; Breindl, C.; Tillack, A.; Beller, M. *Tetrahedron* **2000**, 56, 5157.
8. Beller, M.; Breindl, C.; Riermeier, T. H.; Eichberger, M.; Trauthwein, H. *Angew. Chem. Int. Ed.* **1998**, 37, 3389.
9. Beller, M.; Breindl, C.; Riermeier, T. H.; Tillack, A. *J. Org. Chem.* **2001**, 66, 1403.
10. Tzalis, D.; Koradin, C.; Knochel, P. *Tet. Lett.* **1999**, 40, 6193.
11. Crimmin, M. R.; Casely, I. J.; Hill, M. S. *J. Am. Chem. Soc.* **2005**, 127, 2042.
12. Datta, S.; Gamer, M. T.; Roesky, P. W. *Organometallics* **2008**, 27, 1207.
13. Datta, S.; Roesky, P. W.; Blechert, S. *Organometallics* **2007**, 26, 4392.
14. Burgstein, M. R.; Berberich, H.; Roesky, P. W. *Organometallics* **1998**, 17, 1452.
15. Lauterwasser, F.; Hayes, P. G.; Brase, S.; Piers, W. E.; Schafer, L. L. *Organometallics* **2004**, 23, 2234.
16. Bambirra, S.; Tsurugi, H.; van Leusen, D.; Hessen, B. *Dalton Trans.* **2006**, 1157.
17. Anderson, L. L.; Arnold, J.; Bergman, R. G. *Org. Lett.* **2004**, 6, 2519.
18. Lorber, C.; Choukroun, R.; Vendier, L. *Organometallics* **2004**, 23, 1845.
19. Barluenga, J.; Aznar, F.; Liz, R.; Rodes, R. *J. Chem. Soc., Perkin Trans. 1* **1980**, 2732.

20. Barluenga, J.; Aznar, F. *Synthesis* **1977**, 195.
21. Tokunaga, M.; Eckert, M.; Wakatsuki, Y. *Angew. Chem. Int. Ed.* **1999**, *38*, 3222.
22. Kuninobu, Y.; Nishina, Y.; Takai, K. *Org. Lett.* **2006**, *8*, 2891.
23. Yi, C. S.; Yun, S. Y. *J. Am. Chem. Soc.* **2005**, *127*, 17000.
24. Hartung, C. G.; Tillack, A.; Trauthwein, H.; Beller, M. *J. Org. Chem.* **2001**, *66*, 6339.
25. Field, L. D.; Messerle, B. A.; Vuong, K. Q.; Turner, P.; Failes, T. *Organometallics* **2007**, *26*, 2058.
26. Fukuda, Y.; Utimoto, K. *Synthesis* **1991**, 975.
27. Fukuda, Y.; Utimoto, K.; Nozaki, H. *Heterocycles* **1987**, *25*, 297.
28. Iritani, K.; Matsubara, S.; Utimoto, K. *Tet. Lett.* **1988**, *29*, 1799.
29. Arcadi, A.; Bianchi, G.; Marinelli, F. *Synthesis* **2004**, 610.
30. Mizushima, E.; Hayashi, T.; Tanaka, M. *Org. Lett.* **2003**, *5*, 3349.
31. Zhou, C. Y.; Chan, P. W. H.; Che, C. M. *Org. Lett.* **2006**, *8*, 325.
32. Luo, Y. M.; Li, Z. G.; Li, C. J. *Org. Lett.* **2005**, *7*, 2675.
33. Robinson, R. S.; Dovey, M. C.; Gravestock, D. *Tet. Lett.* **2004**, *45*, 6787.
34. Liu, X. Y.; Ding, P.; Huang, J. S.; Che, C. M. *Org. Lett.* **2007**, *9*, 2645.
35. Meguro, M.; Yamamoto, Y. *Tet. Lett.* **1998**, *39*, 5421.
36. Besson, L.; Goré, J.; Cazes, B. *Tet. Lett.* **1995**, *36*, 3857.
37. Radhakrishnan, U.; Al-Masum, M.; Yamamoto, Y. *Tet. Lett.* **1998**, *39*, 1037.
38. Muller, T. E.; Grosche, M.; Herdtweck, E.; Pleier, A. K.; Walter, E.; Yan, Y. K. *Organometallics* **2000**, *19*, 170.
39. Li, Y. W.; Marks, T. J. *Organometallics* **1996**, *15*, 3770.
40. Straub, T.; Haskel, A.; Neyroud, T. G.; Kapon, M.; Botoshansky, M.; Eisen, M. S. *Organometallics* **2001**, *20*, 5017.

41. Haskel, A.; Straub, T.; Eisen, M. S. *Organometallics* **1996**, *15*, 3773.
42. Baranger, A. M.; Walsh, P. J.; Bergman, R. G. *J. Am. Chem. Soc.* **1993**, *115*, 2753.
43. Walsh, P. J.; Baranger, A. M.; Bergman, R. G. *J. Am. Chem. Soc.* **1992**, *114*, 1708.
44. Thomson, R. K.; Zahariev, F. E.; Zhang, Z.; Patrick, B. O.; Wang, Y. A.; Schafer, L. L. *Inorg. Chem.* **2005**, *44*, 8680.
45. Li, C.; Thomson, R. K.; Gillon, B.; Patrick, B. O.; Schafer, L. L. *Chem. Commun.* **2003**, 2462.
46. Hill, E. J.; Profflet, D. R.; Fanwick, E. P.; Rothwell, P. I. *Angew. Chem. Int. Ed.* **1990**, *29*, 664.
47. McGrane, P. L.; Jensen, M.; Livinghouse, T. *J. Am. Chem. Soc.* **1992**, *114*, 5459.
48. McGrane, P. L.; Livinghouse, T. *J. Am. Chem. Soc.* **1993**, *115*, 11485.
49. McGrane, P. L.; Livinghouse, T. *J. Org. Chem.* **1992**, *57*, 1323.
50. Haak, E.; Bytschkov, I.; Doye, S. *Angew. Chem. Int. Ed.* **1999**, *38*, 3389.
51. Heutling, A.; Doye, S. *J. Org. Chem.* **2002**, *67*, 1961.
52. Heutling, A.; Pohlki, F.; Doye, S. *Chem. Eur. J.* **2004**, *10*, 3059.
53. Johnson, J. S.; Bergman, R. G. *J. Am. Chem. Soc.* **2001**, *123*, 2923.
54. Tillack, A.; Castro, I. G.; Hartung, C. G.; Beller, M. *Angew. Chem. Int. Ed.* **2002**, *41*, 2541.
55. Khedkar, V.; Tillack, A.; Beller, M. *Org. Lett.* **2003**, *5*, 4767.
56. Tillack, A.; Khedkar, V.; Beller, M. *Tet. Lett.* **2004**, *45*, 8875.
57. Ackermann, L.; Sandmann, R.; Villar, A.; Kaspar, L. T. *Tetrahedron* **2008**, *64*, 769.
58. Ackermann, L. *Organometallics* **2003**, *22*, 4367.
59. Bexrud, J. A.; Li, C. Y.; Schafer, L. L. *Organometallics* **2007**, *26*, 6366.
60. Lee, A. V.; Schafer, L. L. *Organometallics* **2006**, *25*, 5249.
61. Zhang, Z.; Schafer, L. L. *Org. Lett.* **2003**, *5*, 4733.

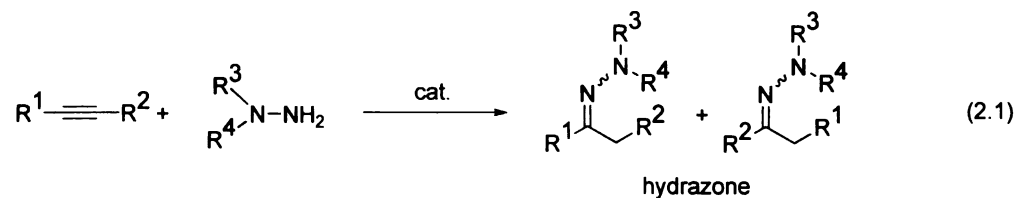
62. Lee, A. V.; Schafer, L. L. *Synlett* **2006**, 2973.
63. Shi, Y. H.; Ciszewski, J. T.; Odom, A. L. *Organometallics* **2001**, *20*, 3967.
64. March, J. *Advanced Organic Chemistry*, 4th ed.; John Wiley and Sons: New York, 1996, p 45.
65. Li, Y. H.; Turnas, A.; Ciszewski, J. T.; Odom, A. L. *Inorg. Chem.* **2002**, *41*, 6298.
66. Harris, S. A.; Ciszewski, J. T.; Odom, A. L. *Inorg. Chem.* **2001**, *40*, 1987.
67. Cao, C. S.; Ciszewski, J. T.; Odom, A. L. *Organometallics* **2001**, *20*, 5011.
68. Shi, Y.; Hall, C.; Ciszewski, J. T.; Cao, C.; Odom, A. L. *Chem. Commun.* **2003**, 586.
69. Swartz, D. L.; Odom, A. L. *Organometallics* **2006**, *25*, 6125.

CHAPTER 2

Hydrohydrazination of alkynes with monosubstituted hydrazines

2.1 Introduction

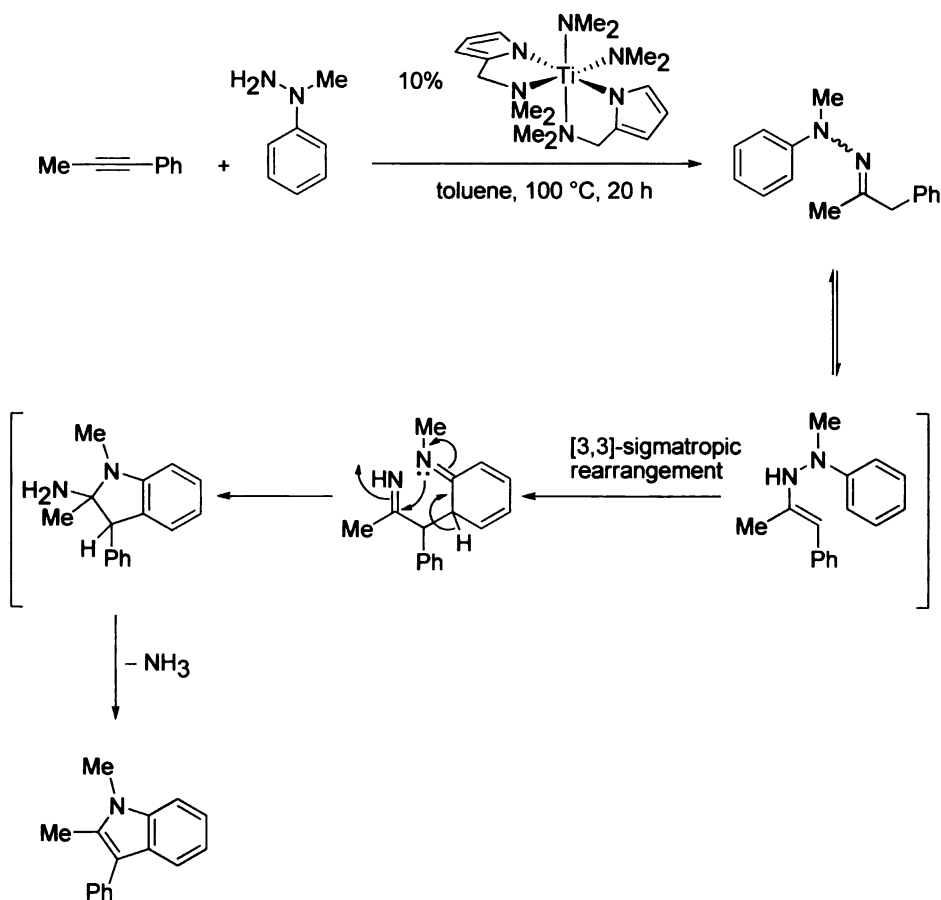
Hydrohydrazination is the formal addition of a hydrazine to an unsaturated C–C bond resulting in a hydrazone or substituted hydrazine, which is shown for alkynes in Equation 2.1. This reaction allows access to heterocyclic structures that act as the core of many natural products and pharmaceuticals.¹⁻⁴ Metal-catalyzed hydrohydrazination of alkynes is primarily known for Ti, Co, Mn, Pd, and Zn. The catalytic process for these metals will be discussed here. This is followed by the discussion of our work on hydrohydrazination of alkynes using monosubstituted hydrazines.



2.1.1 Hydrohydrazination with Titanium

The first example of titanium-catalyzed addition of 1,1-disubstituted hydrazines to alkynes was reported by our group in 2002.⁵ In these reactions, hydrazones are generated, and, if aryl-substituted hydrazines are used, Fischer indole cyclization results in isolation of the corresponding *N*-substituted indoles (Scheme 2.1).

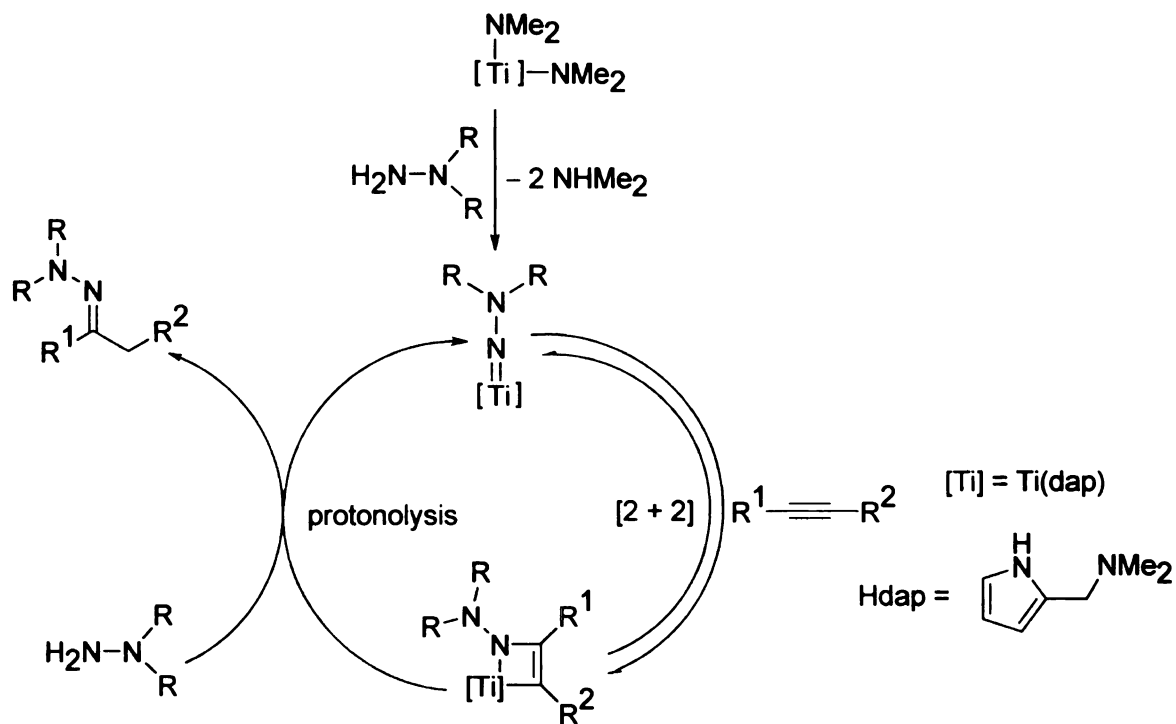
Scheme 2.1 Titanium-catalyzed hydrohydrazination of alkynes and synthesis of an *N*-substituted indole



For 1,1-disubstituted hydrazine substrates, a pyrrole-based ligand framework on titanium was found to be effective. The originally reported design was $\text{Ti}(\text{dap})_2(\text{NMe}_2)_2$ (1), where $\text{dap} = 2\text{-(dimethylaminomethyl)pyrrole}$. In addition, a thiolate-based catalyst was also found to be very active, $\text{Ti}(\text{SC}_6\text{F}_5)_2(\text{NMe}_2)_2(\text{NHMe}_2)$.

In titanium-catalyzed hydrohydrazination, the reactions are believed to follow a pathway similar to that discovered for hydroamination by Bergman and co-workers using zirconocene as catalyst (Scheme 2.2).⁶⁻⁸ In the first step, a titanium hydrazido(2-) complex is generated from the *bis*(dimethylamido) precatalyst losing two equivalents of dimethylamine.⁹ The hydrazido(2-) then undergoes [2 + 2]-cycloaddition with an alkyne forming an azatitanacyclobutene intermediate. Finally, the metallacycle undergoes protonolysis with hydrazine to form product and regenerate the metal-ligand multiple bond.

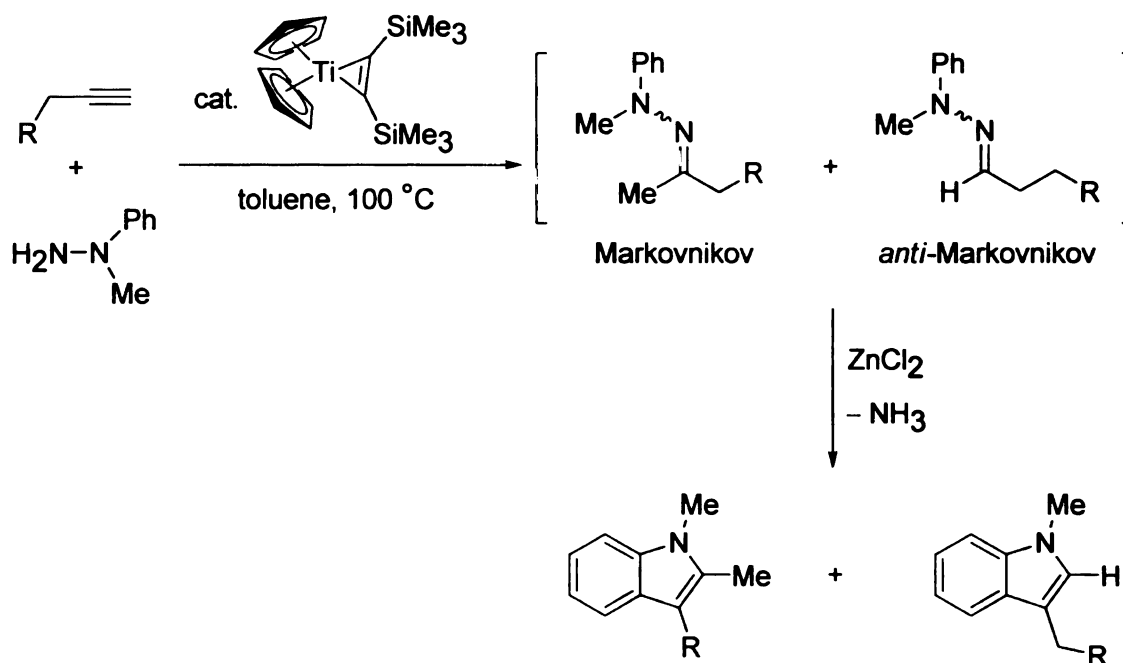
Scheme 2.2 Proposed mechanistic pathway for the hydrohydrazination reaction using 1,1-disubstituted hydrazines



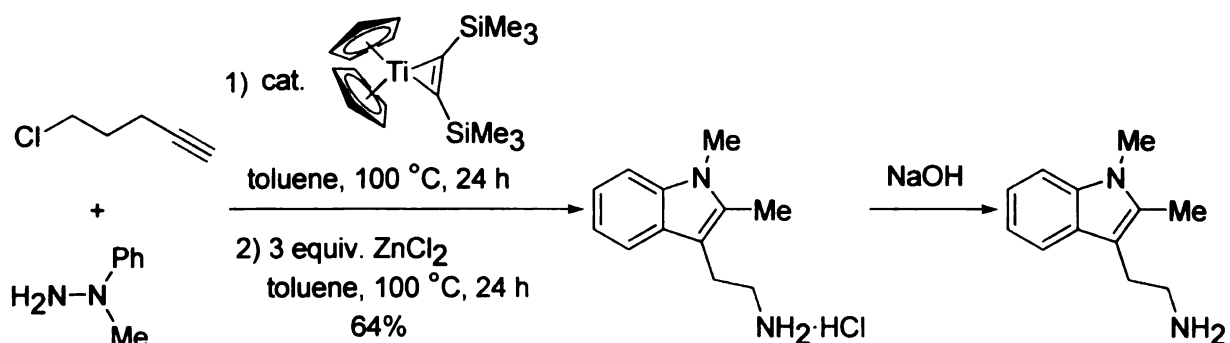
More recently, Beller and co-workers have used a Cp-based (Cp = cyclopentadiene) titanium catalyst for a similar transformation. $\eta^5\text{-Cp}_2\text{Ti}(\eta^2\text{-Me}_3\text{SiC}_2\text{SiMe}_3)$ has been used as the precatalyst for hydrohydrazination of terminal alkynes with *N*-phenyl-*N*-methyl hydrazine (Scheme 2.3).¹⁰ Typical reaction conditions involve 2.5–10 mol% catalyst at 85–100 °C, and the reactions are complete in 24 h. Addition of ZnCl_2 to the resulting hydrazones affords substituted *N*-methylindoles in 52–90% yield (Scheme 2.3). Except for phenylacetylene, high Markovnikov selectivity is observed for other terminal alkynes and 2-methyl-3-alkylsubstituted indoles are obtained as products. In the case of phenylacetylene, the ratio of the indole products is 4:1 (Markovnikov:*anti*-Markovnikov). In case of 5-chloropent-1-yne, the hydrochloride salt of *N*-methyl-3-(2-aminomethyl)-2-

methylindole is obtained, which on addition of NaOH affords *N*-methyl-3-(2-aminoethyl)-2-methyl indole in high yield (Scheme 2.4).

Scheme 2.3 Cp-based titanium-catalyzed hydrohydrazination of alkynes and synthesis of substituted *N*-methylindoles

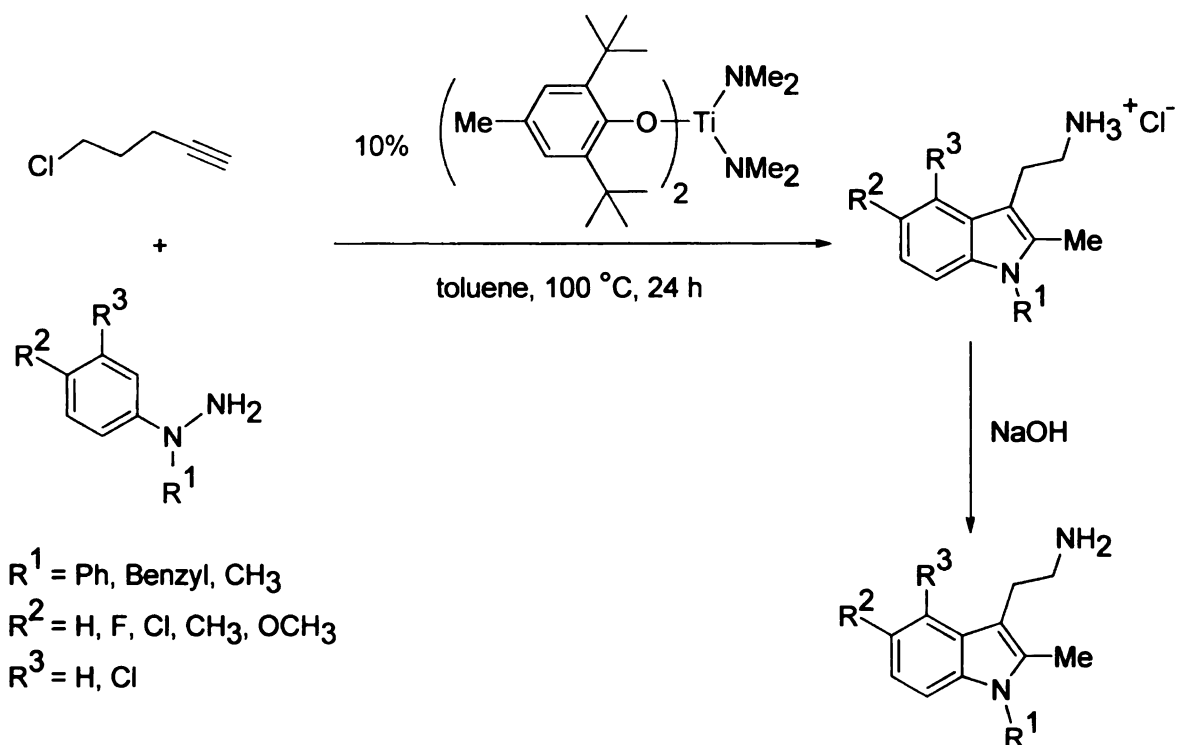


Scheme 2.4 Cp-based titanium-catalyzed hydrohydrazination of alkynes and synthesis of substituted *N*-methyltryptamines



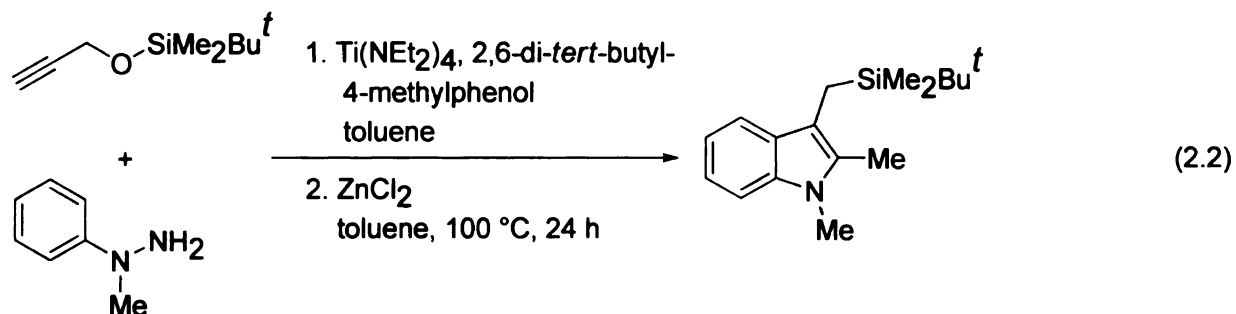
In addition, Beller has reported alkoxide-based ligands for titanium-catalyzed hydrohydrazination with 5-chloropent-1-yne to generate *N*-substituted tryptamines (Scheme 2.5).¹¹ Here, 2.5–5 mol% of *bis*(2,6-di-*tert*-butyl-4-methylphenoxy)-*bis*(dimethylamide)titanium is used as catalyst, and the reactions are carried out at 80–120 °C. The products are isolated in moderate to good yield. The steps involved in forming the tryptamine products are hydrohydrazination followed by [3,3]-sigmatropic rearrangement of the resulting hydrazone combined with the elimination of ammonia. The final step involves the nucleophilic attack of ammonia to the chloroalkane to generate the tryptamine derivatives. Both electron-donating and electron-withdrawing groups are tolerated on the hydrazine during this reaction. Note that the presence of the aryloxo ligand is necessary for the high yield of the indole product since only low yield was obtained using $\text{Ti}(\text{NMe}_2)_4$ as the precatalyst.

Scheme 2.5 Synthesis of tryptamine derivatives by aryloxo-based titanium catalyst



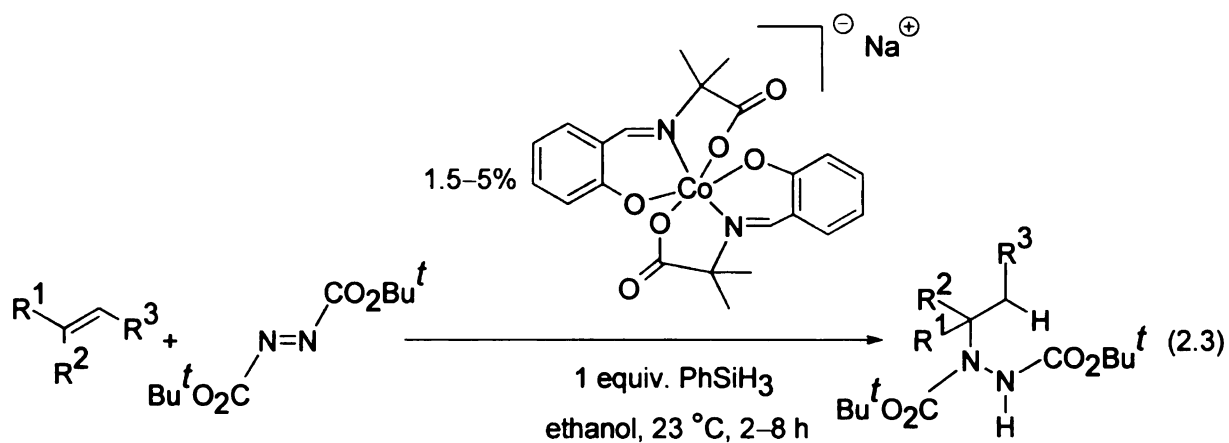
Beller and co-workers have also reported the hydrohydrazination of *tert*-butyldimethylsiloxy-2-propyne with *N*-methyl-*N*-phenylhydrazine generating 3-siloxy-2-methyl indoles (Equation 2.2).¹² The optimized conditions for this reaction involve the use of 5% $\text{Ti}(\text{NEt}_2)_4$ and 10% 2,6-di-*tert*-butyl-4-methyl-phenol at 100 °C in the presence of a slight excess of hydrazine. ZnCl_2 is used for the Fisher indole cyclization step. A range of different substituents are tolerated in the *para* position of the hydrazine. Note that the yields are higher for *N*-methyl indoles compared to *N*-benzyl indoles. Recently, they have presented a similar transformation generating different *N*-substituted tryptophol derivatives.¹³ $\text{TiCl}_4/\text{Bu}^t\text{NH}_2$ -catalyzed hydrohydrazination of alkyne with

1,1-disubstituted alkynes have also been reported and the final products are N-substituted indoles. Here, TiCl_4 is sufficiently Lewis acidic to circumvent the use of ZnCl_2 .¹⁴



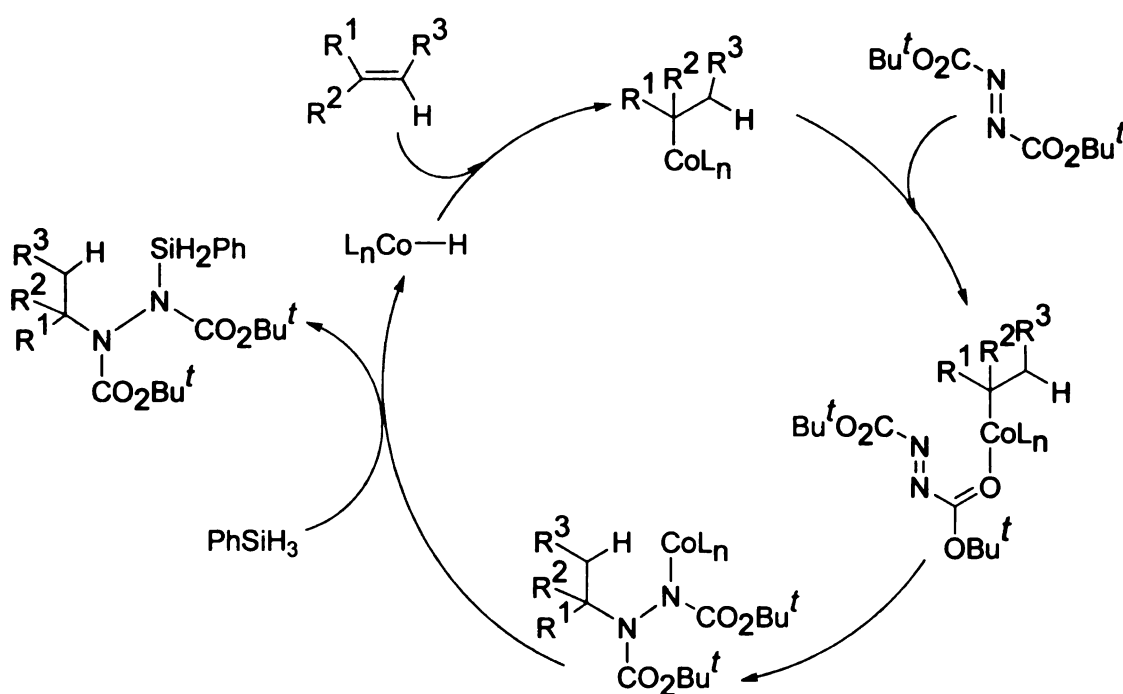
2.1.2 Hydrohydrazination with Cobalt

A cobalt(III) catalyst with a Schiff-base ligand has been reported by Carreira for olefin hydrohydrazination.¹⁵ Both cyclic and acyclic olefins including monosubstituted, 1,1- and 1,2-disubstituted, and trisubstituted olefins are used in the presence of 1–5% catalyst at 23 °C for 2–8 h (Equation 2.3). The reaction is highly selective for Markovnikov products (except for esters in the case of 1,2-disubstituted olefins). A large number of functional groups including bromides and ketones are tolerated. However, only low yields are obtained for unactivated 1,2-disubstituted olefins (crotyl alcohol and cyclohexene).

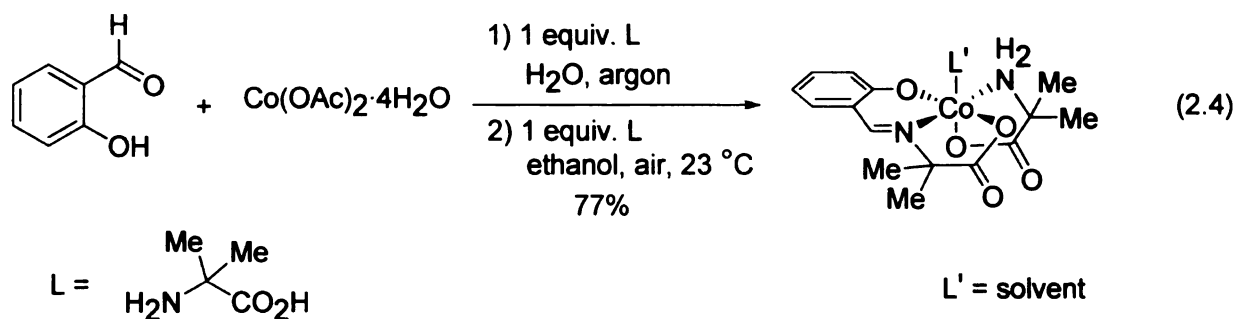


The proposed mechanistic pathway involves a hydrido cobalt intermediate, which undergoes chemoselective addition of olefin to afford an organocobalt species (Scheme 2.6). The metal alkyl then adds to the N=N bond of azodicarboxylates to generate a cobalt–nitrogen species. The final step involves σ -bond metathesis of PhSiH₃, which regenerates the cobalt-hydrido complex.

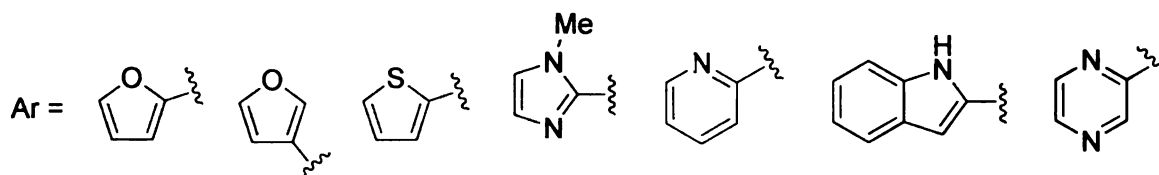
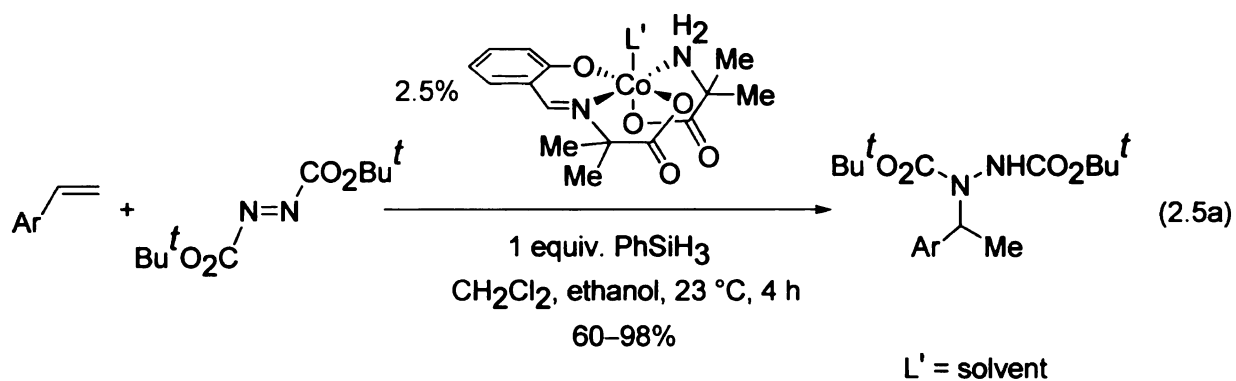
Scheme 2.6 Proposed mechanistic pathway for Co-catalyzed hydrohydrazination of olefin



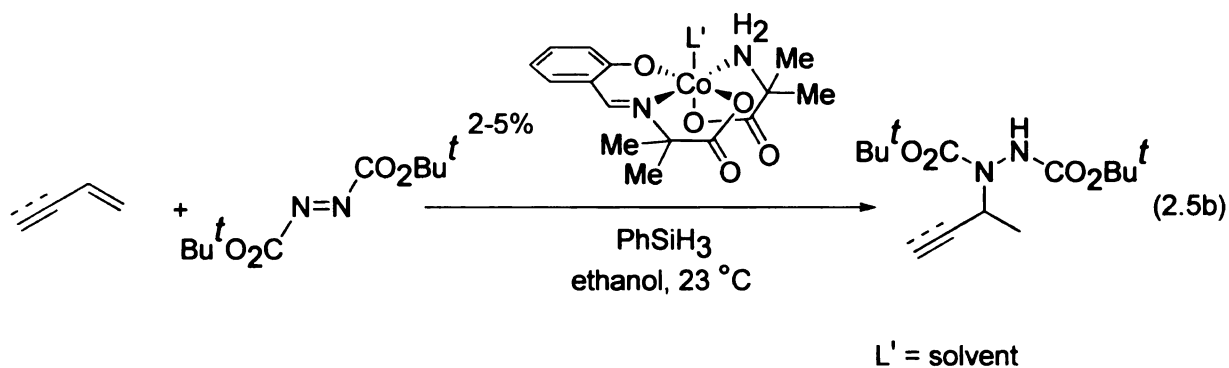
The same group later reported the synthesis and use of a neutral Co(III) catalyst active for a similar transformation. The catalyst was synthesized in a two-step procedure starting from $\text{Co}(\text{OAc})_2 \cdot 4\text{H}_2\text{O}$ and reacting with salicylaldehyde and α,α -dimethyl substituted amino acid (Equation 2.4).¹⁶



This complex is very active for hydrohydrazination of alkenes with di-*tert*-butylazodicarboxylate. At first, monosubstituted olefins containing different functional groups were used. The products, substituted hydrazines, were isolated in good yields. Next, vinyl-substituted heterocycles, as shown in Equation 2.5a, were functionalized.

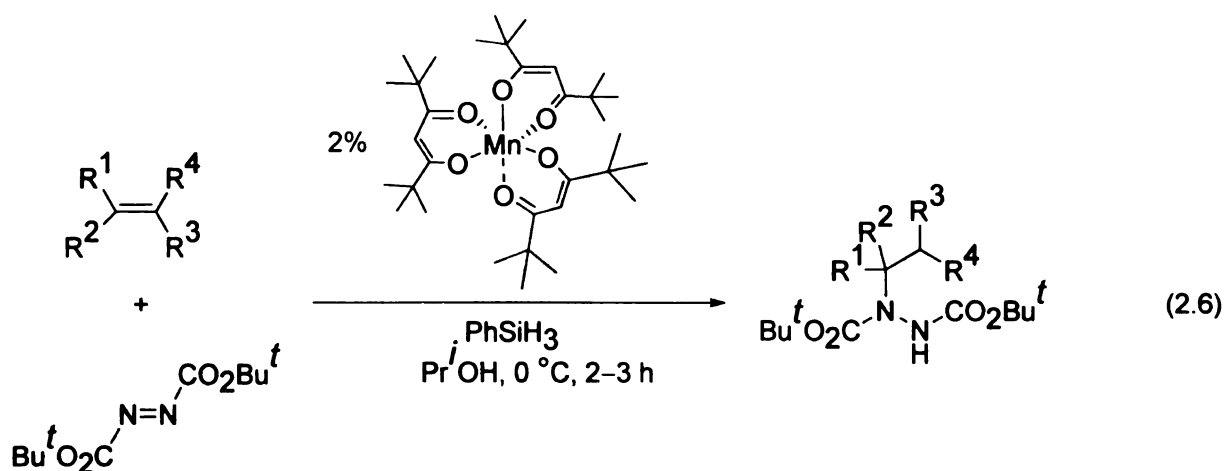


The scope of the reaction has been extended to di- and tri-substituted olefins, and a strong activating and directing effect of the phenyl group is observed. The products are di- and trisubstituted styrene derivatives with exclusive formation of the hydrazine product at the benzylic position. The use of this catalyst has also been extended to the reaction with dienes and enynes generating various substituted allylic and propargylic hydrazines as products (Equation 2.5b).¹⁷ It is interesting to note that only the C=C bond of the enyne and terminal olefinic bonds are selectively hydrohydrazinated in this reaction.



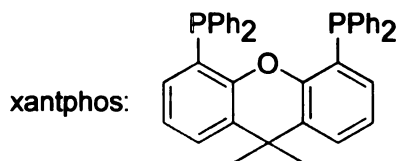
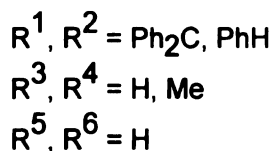
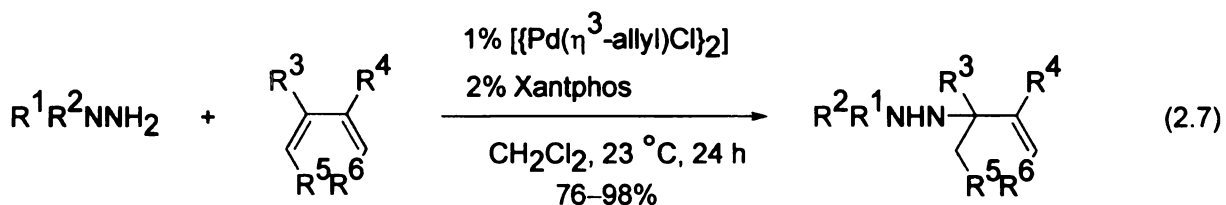
2.1.3 Hydrohydrazination with Manganese

Carreira and co-workers have reported highly efficient hydrohydrazination of alkenes with a manganese-based catalyst.¹⁸ Dipivaloylmethanato (dpm) complexes of both Mn(II) and Mn(III) are effective for this transformation. However, since Mn(dpm)₂ is very air sensitive, the Mn(dpm)₃ complex is preferentially used. The Mn(III) complex is very active, and the reaction works even at 0 °C with 2% catalyst loading (Equation 2.6). A wide range of substrates including 1,2- and 1,1-disubstituted alkenes, α,β -unsaturated esters, tetrasubstituted alkenes, homoallylic alcohols are used with this new manganese-based catalyst.



2.1.4 Hydrohydrazination with Palladium

Addition of hydrazine or hydroxylamine to a C=C bond in 1,3-dienes has been carried out in the presence of 1% [$\text{Pd}(\eta^3\text{-allyl})\text{Cl}$] $_2$ and 2% xantphos by Hartwig and co-workers. It generates branched allylation products in excellent yields (Equation 2.7).¹⁹ Various nucleophiles such as benzophenone hydrazone, fluorenone hydrazone, 1-aminobenzotriazole, and phenylhydrazine are used as substrates to add to C=C bond in 1,3-diene to yield the corresponding products. Benzophenone hydrazine has also been used to add to a C=C bond in catalytic amination of allylic esters.

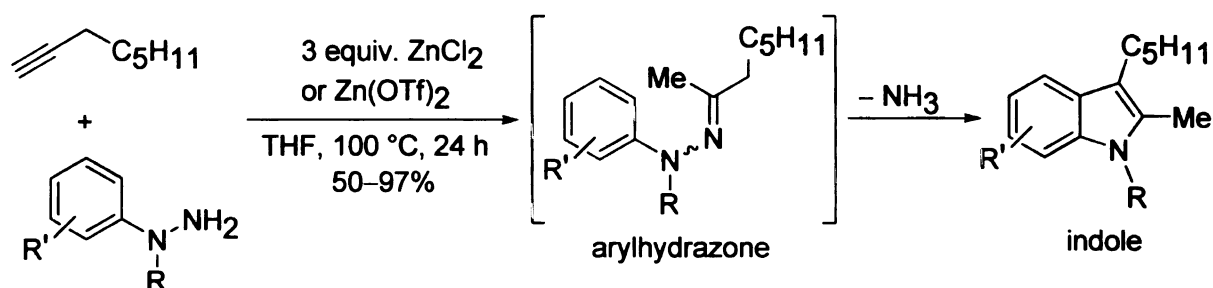


2.1.5 Hydrohydrazination with Zinc

Very recently, Beller and co-workers reported intermolecular hydrohydrazination of terminal alkynes catalyzed by zinc salts.²⁰ In particular, both ZnCl_2 and $\text{Zn}(\text{OTf})_2$ ($\text{OTf} = \text{OSO}_2\text{CF}_3$) have been used for such transformations. The reactions are carried out in THF at 100°C for 24 h, and indole products are obtained in good to excellent yields

(Scheme 2.7). Both *N*-protected and *NH*-indoles are obtained. However, only terminal alkynes are employed. Different functional groups including free and protected alcohols, esters, phthalimide-protected amines are tolerated on the alkyne. On the other hand, functional groups such as *p*-Me, *p*-pr^{*i*}, *p*-Bu^{*t*}, *p*-Br, *p*-Cl, *p*-F, *p*-OMe are tolerated on the phenylhydrazine. This appears to be an elegant approach for the synthesis of both *N*-protected and *NH*-indoles in an environmentally benign way bypassing *N*-protection of hydrazine and *N*-deprotection of indole in the final product.

Scheme 2.7 Synthesis of *NH*-indole by zinc salts

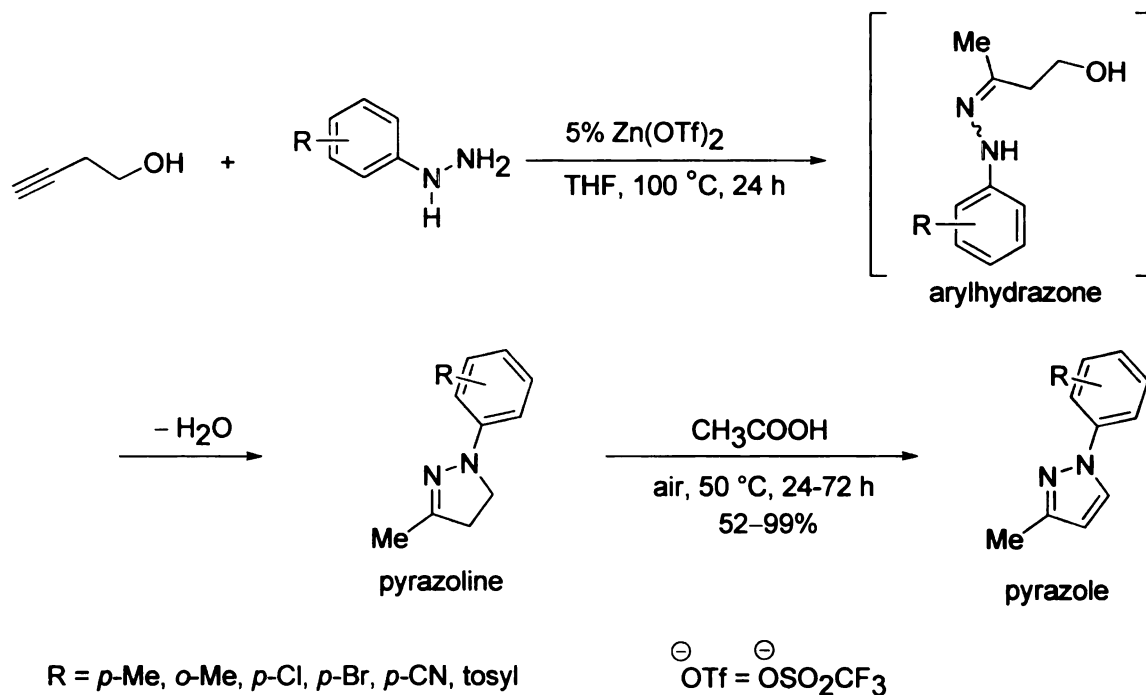


R = Me, H; R' = *p*-Me, *o*-Me, *p*-pr^{*i*}, *p*-Bu^{*t*}, *p*-F, *p*-Cl, *p*-Br, *p*-OMe; OTf = OSO₂CF₃

The Beller group has also extended the above hydrohydrazination reaction towards the synthesis of pyrazolines and pyrazoles.²¹ Reaction between 3-butynol and phenylhydrazine affords *N*-phenylpyrazoline and *N*-phenylpyrazole derivatives in the presence of Zn(OTf)₂ as catalyst (Scheme 2.8). Different substituents including *o*-Me, *p*-Me, *p*-Cl, *o*-Cl, *p*-Br, *p*-CN, *p*-tolylsulfonyl are tolerated on the phenylhydrazine. The reaction between 3-butynol and phenylhydrazine generates pyrazoline first, which on further oxidation by air in the presence of acetic acid results in the pyrazole product in

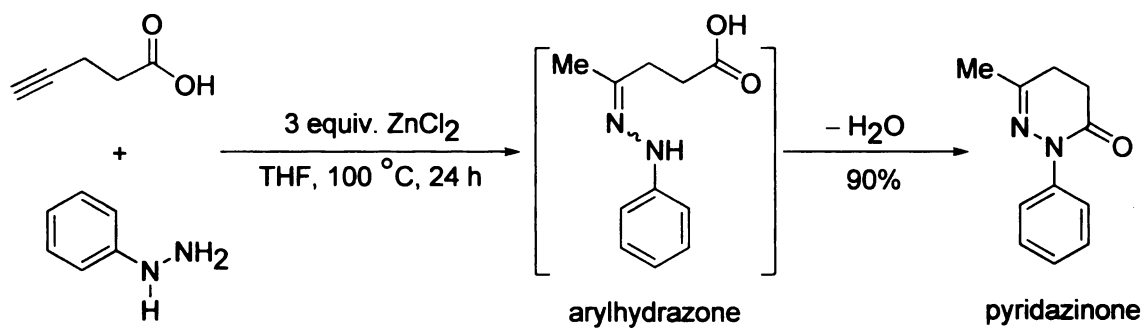
good to excellent yield. No difference is observed in the yield of the pyrazole product if the reaction is carried out with the isolated pyrazoline or all in one pot.

Scheme 2.8 Synthesis of pyrazoline and pyrazole by Zn(OTf)₂-catalyzed hydrohydrazination



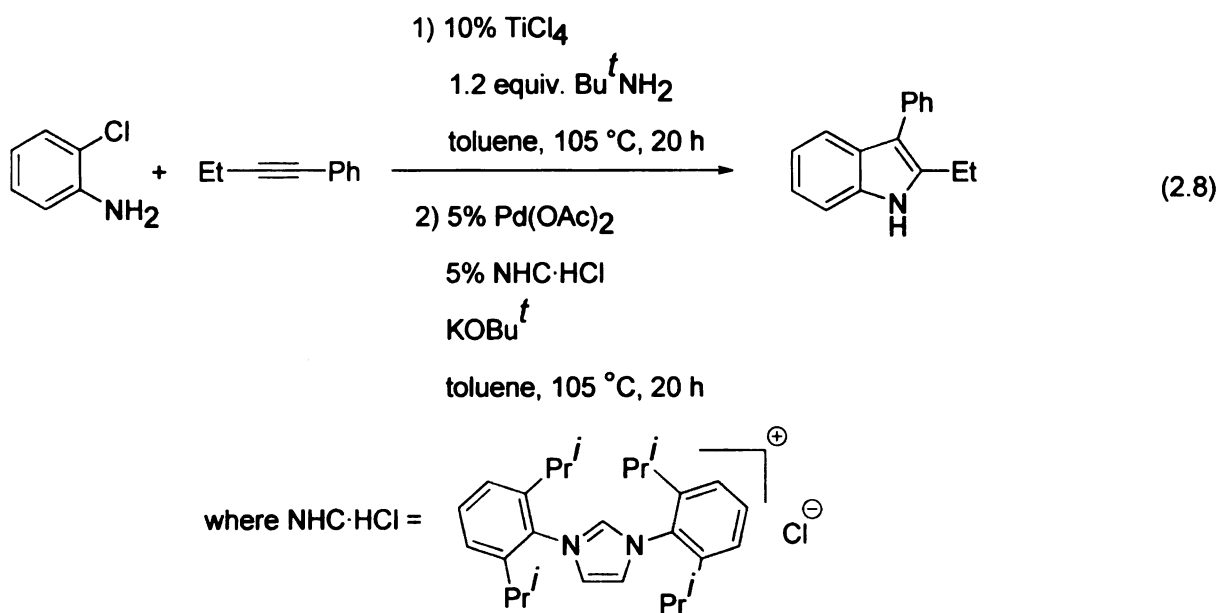
A further extension of this chemistry involves the synthesis of dihydropyridazinones.²² Hydrohydrazination of 4-pentynoic acid with different arylhydrazines generates aryl-substituted 4,5-dihydro-3(2H)-pyridazinones in the presence of ZnCl₂ (Scheme 2.9). This is a convenient method to form pyridazinones in one-pot procedure and does not require any special handling of the reagents or air- or moisture-free solvents and atmosphere.

Scheme 2.9 Synthesis of pyridazinones via hydrohydrazination using ZnCl_2



2.2 Synthesis of *NH*-indoles

Since the discovery of the Fischer indole synthesis in 1883, synthesis and functionalization of indoles continued to be an active area of research.²³ A variety of modern and well-documented methods are also available for *NH*-indole synthesis.²⁴ For example, Pd-catalyzed coupling and annulation reactions have been employed in the synthesis of indole frameworks.²⁵⁻³⁴ Recently, titanium-based hydroamination of alkynes followed by Heck couplings have been developed by Ackermann for the synthesis of *NH*-indoles (Equation 2.8).³⁵



2.3 Aim of the current project

We have seen that titanium-catalyzed hydrohydrazination of alkynes with 1,1-disubstituted hydrazines forms the corresponding hydrazones. If one of the substituents is an aryl or phenyl group, the hydrazones can be converted to *N*-substituted indoles in the presence of an external Lewis acid, ZnCl₂ (Scheme 2.1). However, indoles present in natural products and pharmaceuticals more often contain the *NH*-functionality.³⁶⁻³⁹

Our interest here is to carry out direct synthesis of *NH*-indoles using hydrohydrazination. For this we have developed a new pyrrole-based ligand for the hydrohydrazination of alkynes using monosubstituted hydrazines.⁴⁰ This is the first titanium-based catalyst active for monosubstituted hydrazines. In addition, this is the only reported catalyst that is active for both terminal and internal alkynes. *NH*-hydrazones are generated in situ by the catalytic process, and a variety of heterocycles are synthesized using this methodology. The development of this new precatalyst, its substrate scope, and applications to various heterocyclic synthesis will be described in the following sections. This project was carried out with the help of Dr. Eyal Barnea who joined our group as a post-doctoral associate during the exploration of this new methodology. Also note that during the course of our work, the Beller group developed a zinc-catalyzed hydrohydrazination to synthesize *NH*-indoles using exclusively terminal alkynes. This work was described in Section 2.1.5.

2.4 Results and Discussion

In an attempt to extend the hydrohydrazination reaction to monosubstituted hydrazines, we investigated the reaction between 1-hexyne and phenylhydrazine with our previous catalysts $\text{Ti}(\text{dap})_2(\text{NMe}_2)_2$ (**1**) and $\text{Ti}(\text{SC}_6\text{F}_5)_2(\text{NMe}_2)_2(\text{NHMe}_2)$ at 100 °C for 16 h. However, no hydrohydrazination product was observed. With $\text{Ti}(\text{NMe}_2)_4$, where all the ligands are protolytically labile, we did not observe any hydrazone product. Reaction of **1** with 10 equiv of phenylhydrazine resulted in greater than 1 equivalent of Hdap being generated per titanium. As a consequence, the dap ancillaries were assumed to be too protolytically labile to support monosubstituted hydrazine reactivity.

Therefore, we attempted to increase the protolytic stability of the ancillary ligand set by using a tetradentate ligand instead of two bidentate ligands. For the synthesis of the new tetradentate ligand (Scheme 2.10), Hdap⁴¹⁻⁴³ was converted to *N*-(Boc)-dap (**2**) with $(\text{Boc})_2\text{O}$ and DMAP (where, Boc = *tert*-butyloxycarbonyl, DMAP = *N,N*-dimethylaminopyridine). The tertiary amine of the Boc-protected dap was quarternized with methyl iodide to form the corresponding ammonium salt (**3**). Reaction of **3** with *N,N'*-dimethyl-1,2-ethylenediamine in the presence of excess K_2CO_3 formed the desired ligand H₂enp (where, H₂enp = *N,N'*-bis(α -methylpyrrol)-*N,N'*-dimethylethane-1,2-diamine) (**4**) in ~50% yield with concomitant pyrrole nitrogen deprotection.

The X-ray crystal structure of **4** is shown in Figure 2.1. There is intermolecular hydrogen bonding between the hydrogen atom of pyrrole nitrogen and the tertiary amine nitrogen.

Scheme 2.10 Synthesis of H₂enp (**4**)

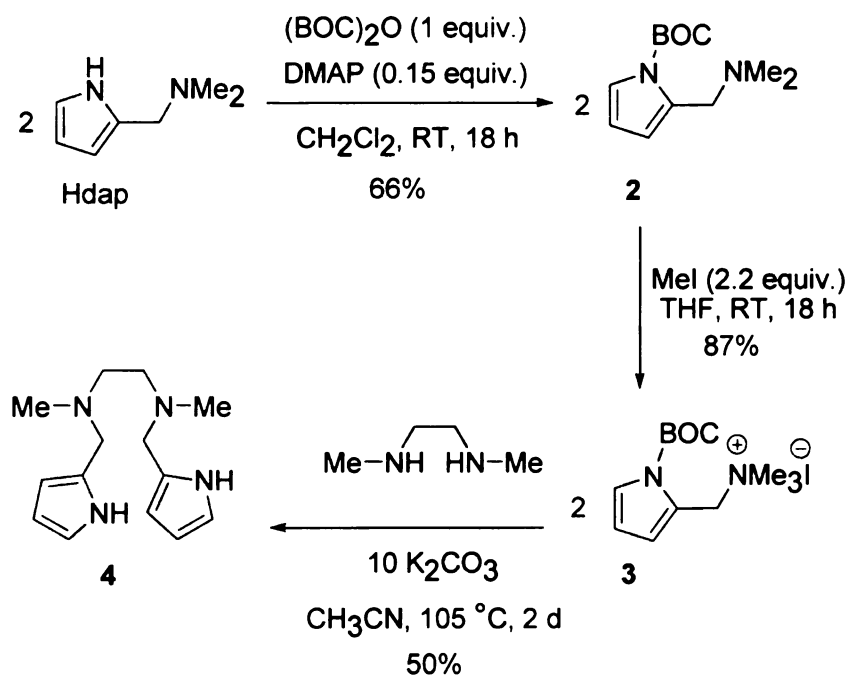
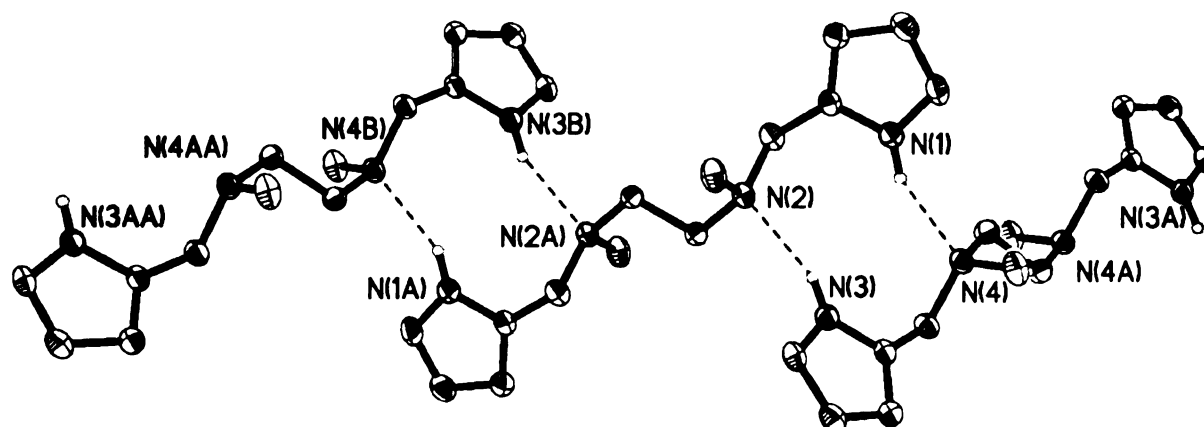
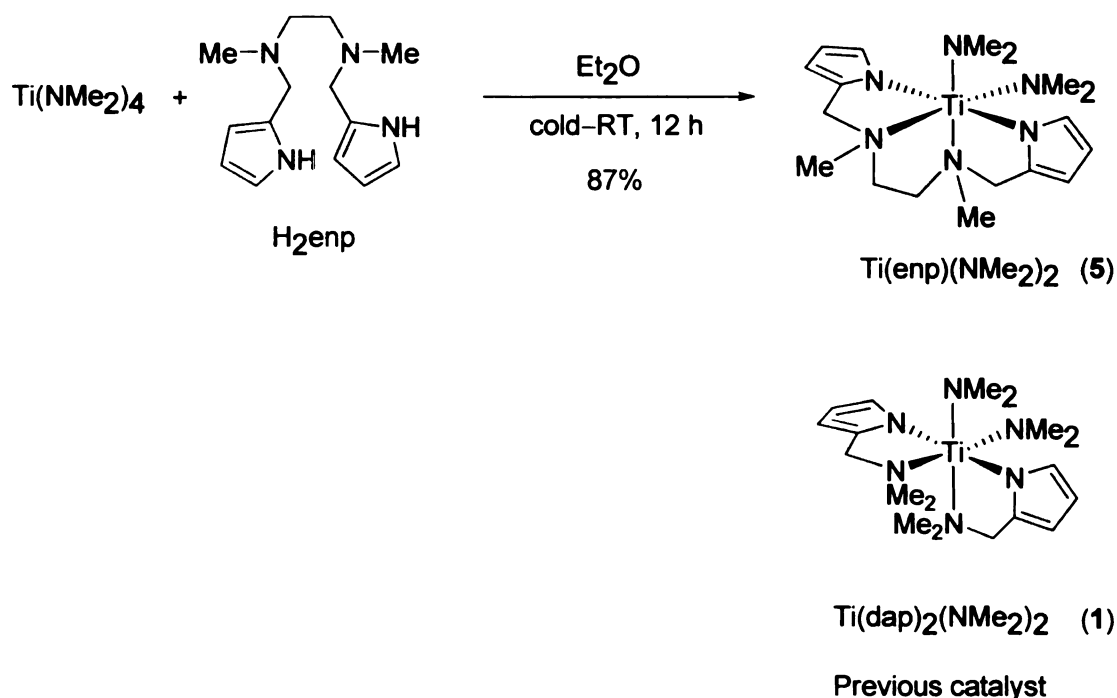


Figure 2.1 ORTEP representation (50% probability level) of H₂enp (**4**).



Next, a new titanium precatalyst $\text{Ti}(\text{enp})(\text{NMe}_2)_2$ (**5**) was prepared by reaction of one equivalent of H_2enp with $\text{Ti}(\text{NMe}_2)_4$ as shown in Figure 2.2. The expected structure has two pyrroles coordinating in an η^1 -fashion with two dimethylamido fragments mutually *cis*, which is consistent with the spectroscopic properties of the molecule.⁴⁴

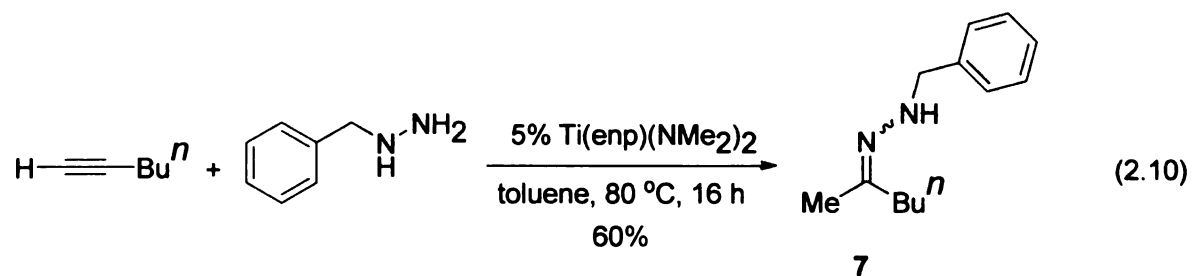
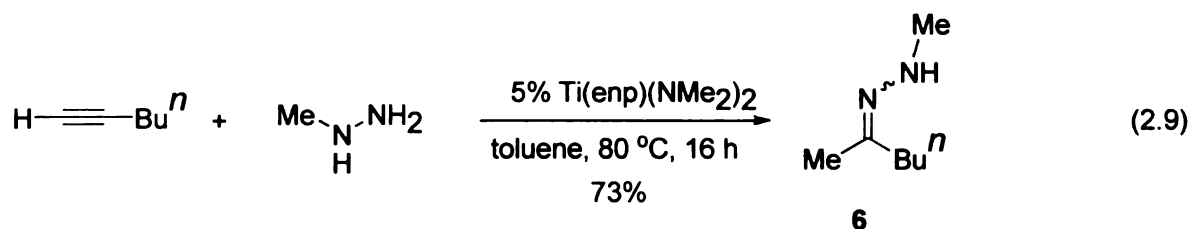
Figure 2.2 Synthesis of $\text{Ti}(\text{enp})(\text{NMe}_2)_2$ (**5**) and comparison with $\text{Ti}(\text{dap})_2(\text{NMe}_2)_2$ (**1**).



In order to probe the substrate scope of $\text{Ti}(\text{enp})(\text{NMe}_2)_2$ (**5**), both terminal and internal alkynes were treated with different monosubstituted hydrazines in the presence of catalytic **5**. Test reactions using 1-hexyne and phenylhydrazine with 10 mol% catalyst loading at room temperature proceeded to near full conversion, but the reaction rates

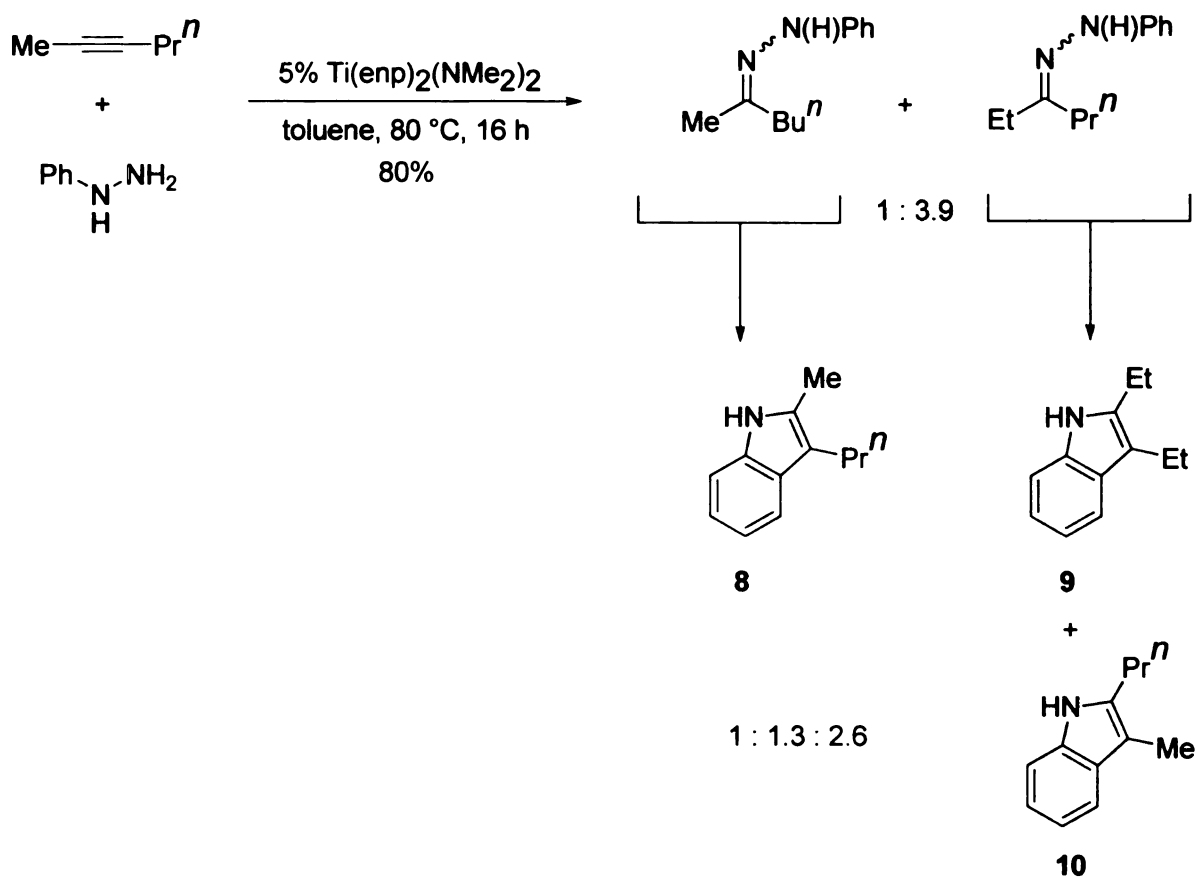
were impractically slow requiring ~ 5 days to reach completion. The reaction of 1-hexyne with phenylhydrazine was optimized to run at 80 °C with 5 mol% **5** and was complete in 2 h. Under the optimized conditions, reactions were carried out with 5 mol% **5** in toluene at 80 °C for 4.5–41 h (Table 2.1). Hydrazones of 1-hexyne were also obtained with methyl- and benzylhydrazine. Only the Markovnikov product was observed in these cases (Equations 2.9 and 2.10).

In order to apply this methodology towards indole synthesis, arylhydrazines were reacted with different alkynes. In large part for expediency of product isolation and characterization, arylhydrazones (observed by GC/FID and GCMS) were converted to indoles in a one-pot procedure with excess ZnCl₂. In all cases, the hydrazones were cleanly generated and observed prior to ZnCl₂ addition. Therefore, this methodology is in general applicable to hydrazone synthesis.



The regioselectivity of the products was dependent on the electronic and steric properties of the alkyne. Only the Markovnikov product was obtained for reaction of 1-hexyne with phenylhydrazine (Entry 1, Table 2.1). For 2-hexyne (Entry 2, Table 2.1), the apparent hydrohydrazination regioselectivity, based on the ratios of isolated indoles, is 1:4 with a preference for hydrazine addition to the 3-carbon (Scheme 2.11). If the two alkyl groups (methyl and *n*-propyl) in this alkyne are considered electronically equivalent, this reaction demonstrates the preference of the catalyst to create the new C–N bond at the more hindered carbon in the triple bond.

Scheme 2.11 Reaction of 2-hexyne with phenylhydrazine catalyzed by **5**

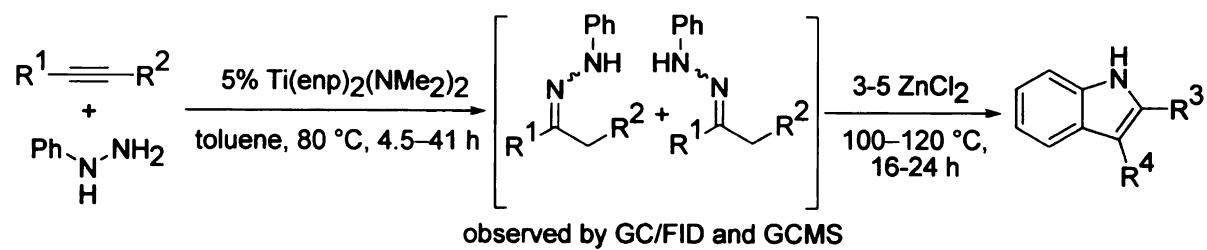


For symmetrical 3-hexyne, a 1:2.5 mixture of indole products are obtained due to a lack of selectivity in the Fischer indole cyclization (Entry 3, Table 2.1).

For aryl-substituted alkynes, there is an electronic preference for generating the new C–N bond β to the phenyl group. Consequently, for phenylacetylene there is a steric preference for addition α to the phenyl group and an electronic preference β to the phenyl group. This leads to a mixture of products for this substrate (Entry 6, Table 2.1), and the hydrohydrazination reaction with phenylhydrazine resulted in a 1:2.6 mixture favoring the electronically preferred indole from *anti*-Markovnikov addition. Adding even a small amount of sterics to the terminal carbon lessens the steric preference, and for the 1-phenylpropyne reaction, only the indole product from electronically preferred β -addition of hydrazine with respect to the phenyl group was observed (Entry 4, Table 2.1).

Protected alcohols and amines on the alkyne were employed to provide TBS-protected (where TBS = *tert*-butyldimethylsilyl) 2-methyltryptophol and 2-methyl-*N,N*-diethyltryptamine, respectively, after the Fischer indole cyclization (Entries 7 and 8, Table 2.1).

Table 2.1 Hydrohydrazination of alkynes with phenylhydrazine



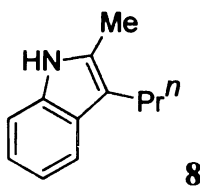
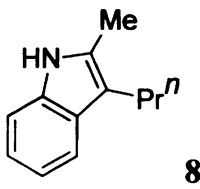
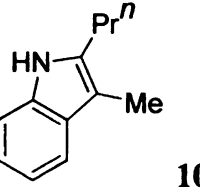
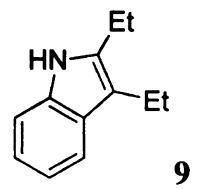
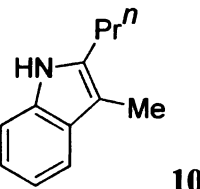
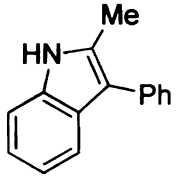
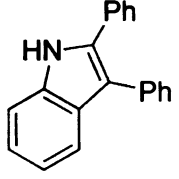
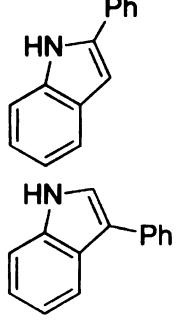
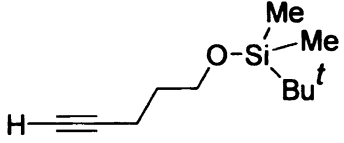
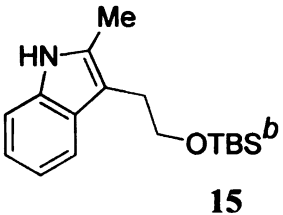
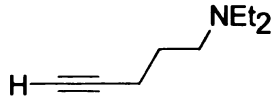
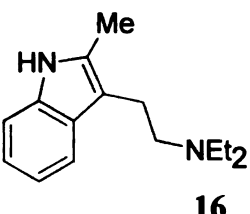
Entry	Substrate	Product(s)	Ratio (a:b or a:b:c)	Yield (%) ^a
1	H—≡—Bu ⁿ	 <p style="text-align: center;">8</p>	—	87
2	Me—≡—Pr ⁿ	 <p style="text-align: center;">8</p>  <p style="text-align: center;">9</p>  <p style="text-align: center;">10</p>	1:1.3:2.6	80
3	Et—≡—Et	 <p style="text-align: center;">9</p>  <p style="text-align: center;">10</p>	1:2.5	76

Table 2.1 (Cont'd.)

4	$\text{Me} \equiv \text{Ph}$	 11	—	70
5	$\text{Ph} \equiv \text{Ph}$	 12	—	55
6	$\text{H} \equiv \text{Ph}$	 13 14	1:2.6	70
7		 15	—	62
8		 16	—	48

^a Reaction time for the first step: 16 h for entries 2-4 and 7; 4.5 h for entries 1 and 6; 41 h for entry 5, 24 h for entry 8. ^b TBS = *tert*-butyldimethylsilyl

The effect of using coordinating solvents instead of toluene was also studied. It was found that using THF or acetonitrile as the solvent had no obvious effect on the hydrohydrazination reactions. In addition, these solvent changes had no obvious effect on the indole cyclization for hydrazone derived from 1-hexyne and phenylhydrazine.

To determine the sensitivity of the titanium catalysis to a variety of potential amine bases, we ran the reaction between 1-hexyne and phenylhydrazine in the presence of several amines. It was observed that there was no significant effect for addition of quinclidine, triethylamine, 2,6-lutidine, or pyridine. The conversions after 18 h at 80 °C with 10 mol% **5** and 20 mol% base were approximately the same (66–71%) as in the absence of these bases (75%).

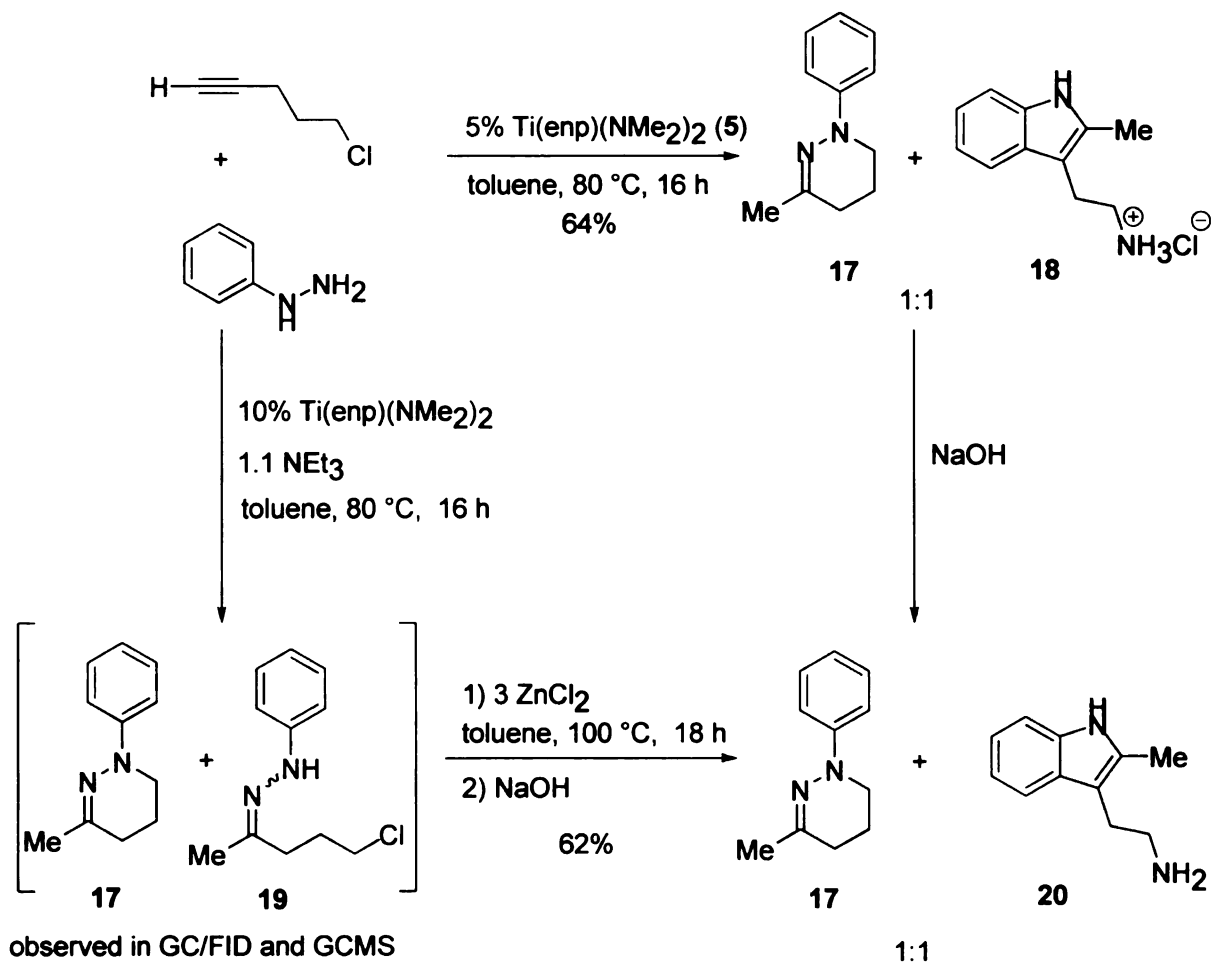
From the reaction of 5-chloropent-1-yne with phenylhydrazine two products were obtained (Scheme 2.12). One product, 3-methyl-1-phenyl-1,4,5,6-tetrahydropyridazine (**17**), was obtained by hydrohydrazination followed by intramolecular elimination of hydrochloric acid and cyclization in situ. The remaining hydrazone **19** undergoes Fisher cyclization, perhaps catalyzed by HCl in the reaction mixture, generating the salt of 2-methyltryptamine (**18**). Free 2-methyltryptamine (**20**) was obtained on basification. Compound **17** was found to be very stable in the presence of HCl generated in the reaction mixture, and also external Lewis acid as observed previously in the literature.⁴⁵

⁴⁶ The products were obtained in a 1:1 ratio, in an overall yield of 64%.

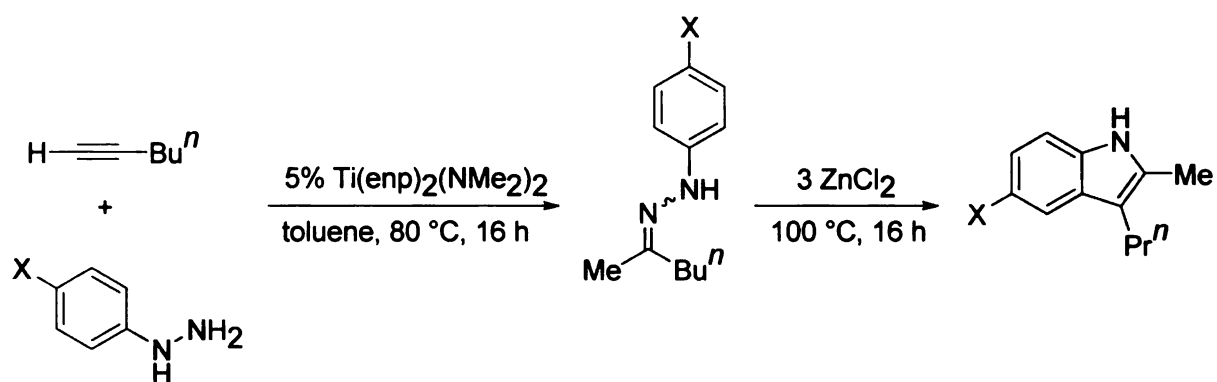
Addition of 1.1 equivalents of triethylamine to a similar reaction between 5-chloropent-1-yne and phenylhydrazine resulted in the formation of two compounds, **17**

and **19**, which were observable by GCMS. Sequential addition of ZnCl_2 and NaOH provided 2-methyltryptamine **20** (Scheme 2.12).

Scheme 2.12 Hydrohydrazination of 5-chloropent-1-yne with phenylhydrazine



Substituted phenylhydrazines were also used in reactions with 1-hexyne, and the products were isolated in good yield. Corresponding indoles were obtained when *p*-Me, *p*-F, and *p*-OMe substituted phenylhydrazines were used. Only the products derived from Markovnikov addition to the alkyne were obtained in all of these cases (Table 2.2).

Table 2.2 Hydrohydrazination with substituted phenylhydrazines

Entry	X	Product	Yield (%)
1	Me	 21	64
2	F	 22	70
3	OMe	 23	76

The scope of the reaction was also extended to diynes. When nona-1,4-diyne was reacted with phenylhydrazine at 80 °C for 16 h, it led to the formation of substituted dihydropyridazine (**24**) in one step along with a substituted pyrazole product (**25**) (Entry 1, Table 2.3). In this particular case, the dihydropyridazine (**24**) was obtained as the minor product (**24**:**25** = 1:2.6). The hydrazone generated was due to exclusive addition of the phenylhydrazine in a Markovnikov fashion to the terminal triple bond. The formation of the observed products can be explained as shown in Scheme 2.13. We speculate that cyclizations may occur through an allene intermediate under the reaction conditions, which can then undergo either 6-*endo* or 5-*exo trig* cyclization, giving rise to **24** or **25** respectively.^{47,48} An alternative 1,2-insertion pathway involving the alkyne and a titanium hydrazido(1-) of the initial hydrohydrazination product cannot be ruled out under these reaction conditions.^{49-53,54}

When octa-1,7-diyne was reacted with 2.2 equivalents of phenylhydrazine at 100 °C for 24 h, hydrohydrazination at both the triple bonds results. Fischer indole cyclization in one pot furnished 1,2-bis(2-methyl-1*H*-indol-3-yl)ethane⁵⁵ (**26**) in 70% yield (Entry 2, Table 2.3).

Scheme 2.13 Possible pathways to **24** and **25**

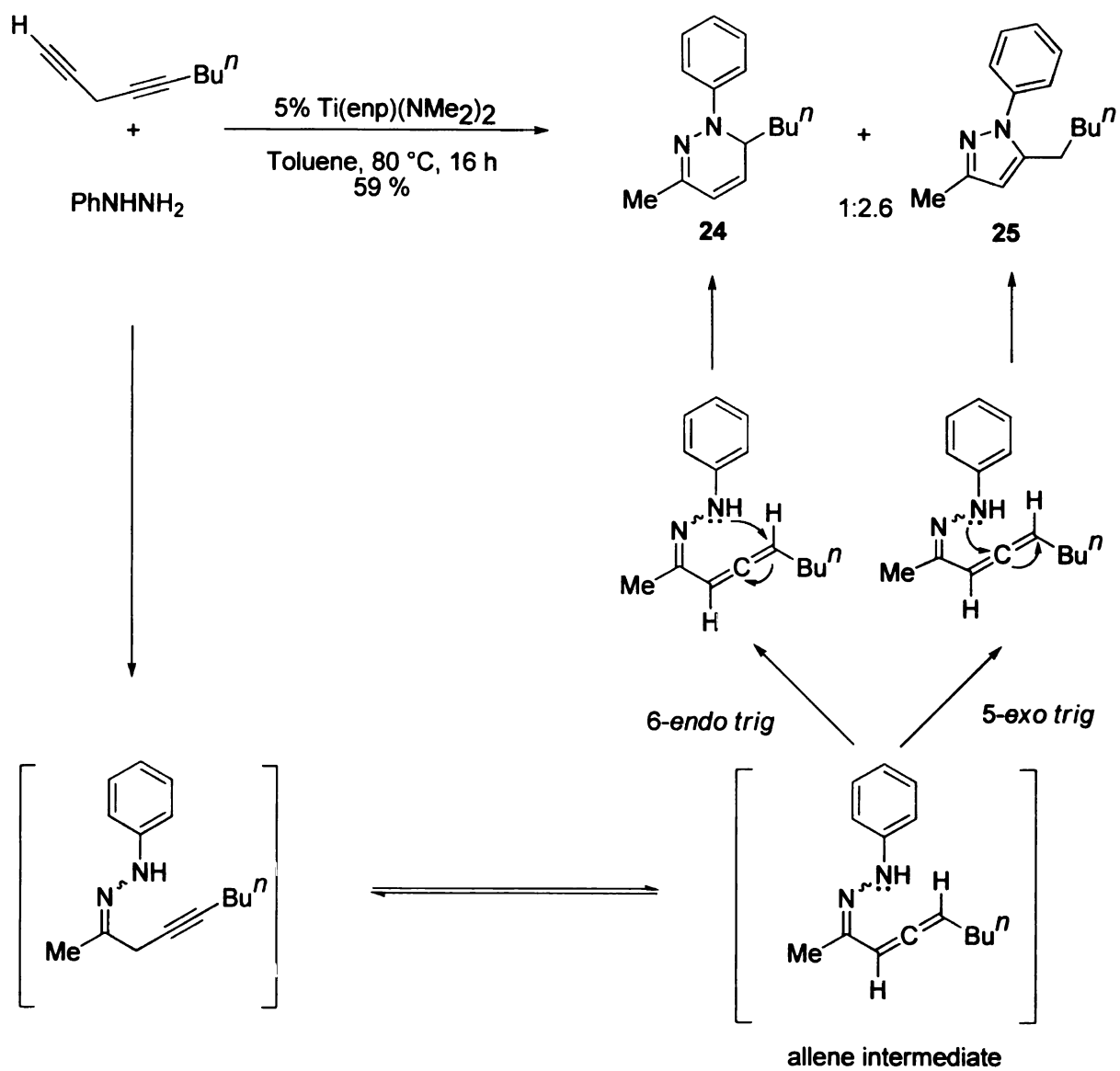
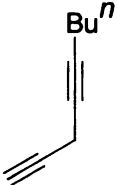
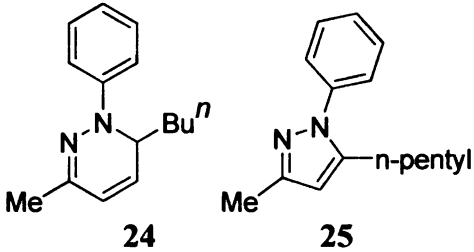
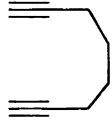
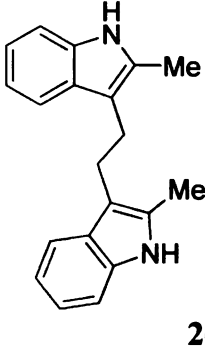
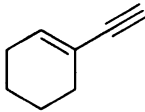
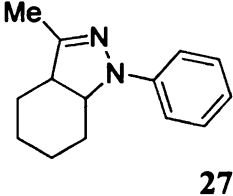


Table 2.3 Hydrohydrazination with diynes and enyne

Entry	Substrate	Conditions ^a	Product	Isolated Yield (%)
1		A	 24 → 25	59 ^b
2		B	 26	70
3		C	 27	52

^a A is 5 mol% **5** at 80 °C for 16 h, B is 5 mol% **5** at 100 °C for 24 h followed by 4 equiv ZnCl₂ at 100 °C for 24 h, C is 5 mol% **5** at 80 °C for 24 h followed by 3 equiv ZnCl₂ at 100 °C for 36 h. ^b **24:25** = 1:2.6.

One enyne substrate was examined with phenylhydrazine, 1-ethynylcyclohex-1-ene (Entry 3, Table 2.3). After the formation of the hydrazone, which was not isolated, addition of ZnCl₂ resulted in Michael addition of the β-nitrogen of the hydrazone across the C=C bond of the cyclohexenyl moiety to yield the substituted indazole^{56,57} **27** in 52% yield.

2.5 Concluding Remarks

A new catalytic hydrohydrazination reaction of monosubstituted hydrazines with alkynes has been developed. This was accomplished by suitably designing the ligand framework on the titanium center. Both terminal and internal alkynes have been used with aliphatic as well as aromatic hydrazines. The regioselectivity of the addition is highly dependent on the electronic and steric nature of the alkyne, and the catalyst is applicable to generating both *N*-alkyl- and *N*-arylhydrazones. This methodology has also been applied to the synthesis of different *NH*-indoles including 2-methyltryptamine and tryptophol derivatives, which are important building blocks of different natural products. As discussed here, many different 5- and 6-membered heterocycles are available using titanium-catalyzed hydrohydrazination.

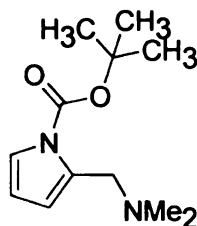
2.6 Experimental

General Considerations

All manipulations of air sensitive compounds were carried out in an MBraun drybox under a purified nitrogen atmosphere. Pentane (Spectrum Chemical Mfg. Corp.), toluene (Spectrum Chemical Mfg. Corp.), ether (Columbus Chemical Industries Inc.), dichloromethane (EM Science), acetonitrile (Spectrum Chemical), and tetrahydrofuran (JADE Scientific) were sparged with nitrogen to remove oxygen then dried by passing through activated alumina. Hydrazines were purchased from Aldrich Chemical Company and dried by distillation from KOH under dry nitrogen. Alkynes were distilled from CaO under dry nitrogen. Octa-1,7-diyne was purchased from GFS chemicals, and distilled over CaO under dry nitrogen. Nona-1,4-diyne,⁵⁸ and 1-ethynylcyclohex-1-ene⁵⁹ were prepared according to the literature procedures. (BOC)₂O (BOC = *t*-butyloxycarbonyl) and DMAP (4-dimethylaminopyridine) were purchased from Aldrich and used as received. Ti(NMe₂)₄⁶⁰ was prepared using the literature procedure. The Hdap (where dap = 2-(dimethylaminomethyl)pyrrole) ligand was prepared as described in the literature.²² Deuterated solvents were dried over purple sodium benzophenone ketyl (C₆D₆) or phosphoric anhydride (CDCl₃) and distilled under nitrogen. ¹H and ¹³C spectra were recorded on Inova-300 or VXR-500 spectrometers. ¹H and ¹³C assignments were confirmed when necessary with the use of two-dimensional ¹H-¹H and ¹³C-¹H correlation NMR experiments. Routine coupling constants in ¹³C NMR are not reported.

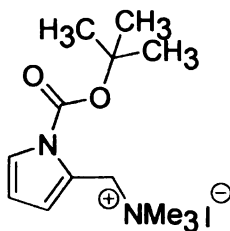
All spectra were referenced internally to residual protiosolvent (^1H) or solvent (^{13}C) resonances. Chemical shifts are quoted in ppm, and coupling constants in Hz.

Synthesis of butyl-2-((dimethylamino)methyl)-1H-pyrrole-1-carboxylate (2)



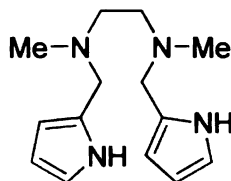
A 500 mL round bottom flask was charged with Hdap (2.617 g, 21.10 mmol), (BOC)₂O (4.600 g, 21.10 mmol), and DMAP (0.386 g, 3.1 mmol) in dichloromethane (250 mL) and was allowed to stir at room temperature overnight. The solution was quenched with water (20 mL) and extracted with ether (3 × 20 mL). Combined organic layers were washed with water. The organic layer was then dried over MgSO₄, filtered, and volatiles were removed under vacuum. The product was isolated by distillation under vacuum (~65 °C, 0.1 Torr) as a colorless oil in 66% yield (3.120 g, 13.90 mmol). ¹H NMR (499.7 MHz, CDCl₃): 7.18 (dd, 1 H, *J*_{HH} = 1.8, 3.4 Hz, 5*H*-pyrrole), 6.11 (m, 1 H, 4*H*-pyrrole), 6.08 (t, *J*_{HH} = 3.3 Hz, 1 H, 3*H*-pyrrole), 3.65 (s, 2 H, CH₂), 2.26 (s, 6 H, NCH₃), 1.57 (s, 9 H, CCH₃). ¹³C{¹H} NMR (125.7 MHz, CDCl₃): 149.9, 132.7, 121.5, 113.3, 109.7, 83.3, 56.6, 45.5, 28.0. Elemental Analysis; Experimental (Calc.), C: 63.88 (64.26). H: 8.98 (8.99). N: 13.11 (12.49). MS (EI) *m/z* = 224 (M⁺).

Synthesis of [N-(t-butoxycarbonyl)-2-(trimethylaminomethyl)pyrrole]I (3)



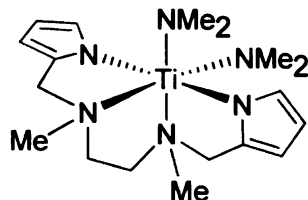
To a 500 mL round bottom flask was added **2** (9.870 g, 44.00 mmol), methyl iodide (6.870 g, 48.40 mmol), and THF (250 mL). The reaction was allowed to stir at room temperature overnight. A white precipitate appeared during the reaction. The precipitate was filtered, washed with THF, and dried under vacuum to yield the product as a white powder in 87% yield (14.00 g, 38.00 mmol). ^1H NMR (499.7 MHz, CDCl_3): 7.35 (d, $J_{\text{HH}} = 3.4$ Hz, 1 H, 5H-pyrrole), 6.85 (dd, $J_{\text{HH}} = 1.7, 3.6$ Hz, 1 H, 4H-pyrrole), 6.27 (t, $J_{\text{HH}} = 3.4$ Hz, 1 H, 3H-pyrrole), 5.22 (s, 2 H, CH_2), 3.37 (s, 9 H, NCH_3), 1.58 (s, 9 H, CCH_3). $^{13}\text{C}\{^1\text{H}\}$ NMR (125.7 MHz, CDCl_3): 149.4, 125.5, 123.3, 120.9, 111.4, 86.0, 61.4, 52.8, 27.9. Elemental Analysis; Experimental (Calc.), C: 42.81 (42.63). H: 6.52 (6.33). N: 7.75 (7.65). m.p. 180 °C (dec).

Synthesis of H₂enp (4)



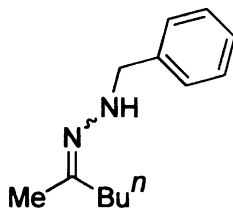
A round bottom flask (500 mL) was charged with K₂CO₃ (7.561 g, 54.80 mmol) in dry acetonitrile (250 mL) and *N,N'*-dimethylethylenediamine (0.483 g, 5.50 mmol). To the flask was added **3** (4.091 g, 10.90 mmol). Initially, the reaction was a light brown colored suspension and was refluxed at 105 °C for 2 d. After that, the suspension was allowed to cool to room temperature and sit, producing a brown solution with white precipitate. The mixture was filtered, and the filtrate was dried by rotary evaporation. Ethylacetate was added to the brown oily product, which led to additional white precipitate. The brown solution was filtered, and the filtrate was dried under vacuum. The dark brown resulting oil was subjected to column chromatography on alumina using 60% ethylacetate:pentane followed by 10% MeOH:ethylacetate. The product was isolated as a pale yellow solid in 50% yield (0.670 g, 2.70 mmol). X-ray quality crystals were grown at room temperature from dichloromethane solution of **4** with one drop of toluene by slow evaporation. ¹H NMR (499.7 MHz, CDCl₃): 9.38 (b, 2 H, NH), 6.69 (q, *J*_{HH} = 2.4 Hz, 2 H, 5*H*-pyrrole), 6.12 (q, *J*_{HH} = 2.7 Hz, 2 H, 4*H*-pyrrole), 5.99 (m, 2 H, 3*H*-pyrrole), 3.58 (s, 4 H, CH₂-pyrrole), 2.48 (s, 4 H, CH₂CH₂), 2.22 (s, 6 H, CH₃). ¹³C{¹H} NMR (125.7 MHz, CDCl₃): 128.9, 117.4, 108.0, 107.0, 54.8, 54.1, 42.8. m.p.: 95-97 °C.

Synthesis of $\text{Ti}(\text{enp})(\text{NMe}_2)_2$ (**5**)



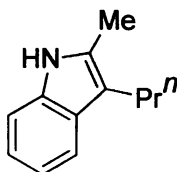
All the manipulations were carried out inside an inert atmosphere glove box. A filter flask (125 mL) was loaded with $\text{Ti}(\text{NMe}_2)_4$ (0.388 g, 1.70 mmol) in ether (2 mL) and cooled inside the cold well. To the solution was added cold **4** (0.427 g, 1.70 mmol) in ether (25 mL) dropwise over a period of 15 min. The reaction was allowed to warm to room temperature and stir overnight producing a dark red solution. Volatiles were removed in vacuo. The product was recrystallized from 1:1 ether:pentane as an orange solid in 87% yield (0.560 g, 1.50 mmol). ^1H NMR (499.7 MHz, CDCl_3): 6.98-7.02 (m, 2 H, 5*H*-pyrrole), 6.10 (app t, $J_{\text{HH}} = 2.3$ Hz, 2 H, 4*H*-pyrrole), 5.80-5.84 (m, 2 H, 3*H*-pyrrole), 4.50 (d, $J_{\text{HH}} = 15.4$ Hz, 2 H, CH*H*-pyrrole), 3.67 (d, $J_{\text{HH}} = 15.3$ Hz, 2 H, CH*H*-pyrrole), 3.38 (s, 12 H, $\text{N}(\text{CH}_3)_2$), 2.55 (d, $J_{\text{HH}} = 9.2$ Hz, 2 H, CH*H*-CH*H*), 2.14 (d, $J_{\text{HH}} = 8.8$ Hz, 2 H, CH*H*-CH*H*), 1.96 (s, 6 H, CH_2NCH_3). $^{13}\text{C}\{^1\text{H}\}$ NMR (75.4 MHz, CDCl_3): 138.4, 126.0, 107.0, 99.8, 62.3, 62.1, 49.1, 47.6. m.p. 126-128 °C. Complex **5** after many attempts did not pass elemental analysis. Spectra for the complex are included in the supporting information.

Synthesis of the *E*-benzylhydrazone of 2-hexanone (7)



Under an atmosphere of dry nitrogen, a threaded pressure tube was loaded with **5** (0.057 g, 0.15 mmol) in toluene (750 μ L), benzylhydrazine (300 μ L, 3.00 mmol), and 1-hexyne (350 μ L, 3.00 mmol). The reaction vessel was sealed and removed from the dry box to be heated at 80 $^{\circ}$ C for 16 h. The solution was then cooled to room temperature, diluted with ether, and passed through a pad of alumina in a fritted funnel. Volatiles were removed from the filtrate under vacuum. The resulting dark brown oil was subjected to column chromatography on alumina using 4:1 hexanes:ethylacetate as eluent. The product was isolated as brown oil in 60% (0.360 g, 1.80 mmol). ^1H NMR (499.7 MHz, CDCl_3): 7.34 (m, 2 H, *o*-H Ph), 7.31 (d, 2 H, *m*-H Ph), 7.26 (t, 1 H, $J_{\text{HH}} = 7.1$ Hz, *p*-H Ph), 1.36-1.23 (br s, 1 H, NH), 4.34 (s, 2 H, NH- CH_2 Ph), 2.21 (t, 2 H, $J_{\text{HH}} = 8.2$ Hz, C(=N) CH_2), 1.69 (s, 3 H, C(=N) CH_3), 1.52-1.40 (m, 2 H, $J_{\text{HH}} = 7.9$ Hz, C(=N) CH_2CH_2), 1.36-1.22 (m, 2 H, $J_{\text{HH}} = 8.0$ Hz, CH_3CH_2), 0.98 (t, 3 H, $J_{\text{HH}} = 7.5$ Hz, CH_2CH_3). $^{13}\text{C}\{^1\text{H}\}$ NMR (125.7 MHz, CDCl_3): 149.7, 139.6, 128.4, 128.3, 127.1, 55.4, 38.8, 29.1, 22.4, 14.3, 13.9. MS (EI) $m/z = 204$ (M^+).

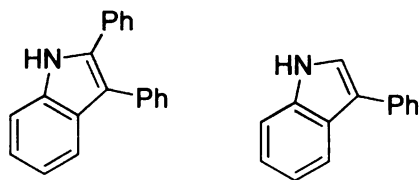
Synthesis of 2-methyl-3-propyl-1*H*-indole (8)



Under an atmosphere of dry nitrogen, a threaded pressure tube was loaded with **5** (0.114 g, 0.30 mmol) in toluene (1.5 mL), phenylhydrazine (295 μ L, 3.00 mmol), and 1-hexyne (350 μ L, 3.00 mmol). The tube was sealed and removed from the dry box for heating at 80 $^{\circ}$ C for 4.5 h. The reaction was then allowed to cool to room temperature, taken inside the box, and excess ZnCl_2 (1.227 g, 9.00 mmol) was added. It was heated at 100 $^{\circ}$ C for 24 h. After that, the reaction was allowed to cool to room temperature, diluted with ether, and passed through a pad of silica in a fritted funnel. Volatiles were removed from the filtrate in vacuo. The resulting dark brown oil was subjected to column chromatography on silica gel with 7:3 dichloromethane:pentane as eluent. The product⁶¹ was isolated as pale yellow oil in 87% yield (0.450 g, 2.60 mmol). ^1H NMR (299.8 MHz, CDCl_3): 7.65 (br s, 1 H, *NH*), 7.48 (d, 1 H, $J_{\text{HH}} = 7.5$ Hz, 4*H*-indole), 7.24 (dd, 1 H, $J_{\text{HH}} = 3.5, 6.2$ Hz, 7*H*-indole), 7.12 – 7.02 (m, 2 H, 5*H*- and 6*H*-indole), 2.66 (t, 2 H, $J_{\text{HH}} = 7.5$ Hz, $\text{CH}_3\text{CH}_2\text{CH}_2$), 2.53 (s, 3 H, 2-*CH}_3*), 1.63 (m, 2 H, $\text{CH}_3\text{CH}_2\text{CH}_2$), 0.93 (t, 3 H, $J_{\text{HH}} = 7.3$ Hz, CH_3CH_2). $^{13}\text{C}\{^1\text{H}\}$ NMR (75.4 MHz, CDCl_3): 135.3, 130.7, 128.9, 120.7, 118.9, 118.2, 112.3, 110.0, 26.2, 23.8, 14.1, 11.7. Elemental analysis;

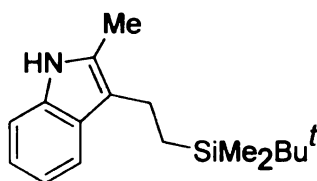
Experimental (Calc.), C: 83.17 (83.19). H: 8.88 (8.73). N: 8.05 (8.08). MS (EI) $m/z = 173$
(M^+).

Synthesis of 2-phenylindole (13) and 3-phenylindole (14)



Under an atmosphere of dry nitrogen, a threaded pressure tube was loaded with **5** (0.093 g, 0.25 mmol) in toluene (1.2 mL), phenylhydrazine (518 μ L, 4.90 mmol), and phenylacetylene (538 μ L, 4.90 mmol). The tube was sealed and removed from the dry box for heating at 80 $^{\circ}$ C for 4.5 h. The reaction was then allowed to cool to room temperature, taken inside the box, and excess ZnCl_2 (3.279 g, 24.50 mmol) was added. The tube then was heated at 120 $^{\circ}$ C for 24 h. After that, the mixture was allowed to cool to room temperature, diluted with ether, and passed through a pad of silica in a fritted funnel. Volatiles were removed from the filtrate in vacuo. The resulting dark brown oil was subjected to column chromatography on silica gel with 1:1 petroleum ether:ether as eluent. The products⁶² were isolated as a pale yellow oil in 70% yield (0.660 g, 2.60 mmol). ^1H NMR (299.8 MHz, CDCl_3): 8.40 (br s, 1 H, *NH*), 8.38 (br s, 1 H, *NH*), 7.95 (s, 1 H, 2-*CH*), 7.78-7.15 (m, 9 H, Ph), 7.38-7.18 (m, 9 H, Ph) 6.81 (s, 1 H, 3-*CH*). $^{13}\text{C}\{^1\text{H}\}$ NMR (75.4 MHz, CDCl_3): 137.9, 136.8, 136.6, 135.5, 132.4, 129.3, 129.0-125.1, 122.4-119.8, 118.4, 113.2, 111.4, 110.9, 100.0 (b). MS (EI) m/z = 193 (M^+).

Synthesis of 2-methyl-3-(2-(dimethyl(*t*-butyl)siloxy)ethyl)indole (15)

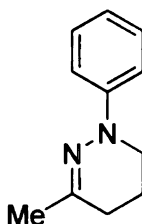


Under an atmosphere of dry nitrogen, a threaded pressure tube was loaded with **5** (0.024 g, 0.07 mmol) in toluene (315 μ L), phenylhydrazine (124 μ L, 1.30 mmol), and (pent-4-ynyloxy)*t*-butyldimethylsilane (0.250 g, 1.30 mmol). The tube was sealed and removed from the dry box for heating at 80 $^{\circ}$ C for 16 h. The solution was then allowed to cool to room temperature, taken inside the box, and excess ZnCl_2 (0.506 g, 3.90 mmol) was added. The reaction was heated at 100 $^{\circ}$ C for 16 h. The mixture was allowed to cool to room temperature, diluted with ether, and passed through a pad of silica in a fritted funnel. Volatiles were removed from the filtrate in vacuo. The resulting dark red oil was subjected to column chromatography on silica gel with 7:3 hexanes:ethylacetate as eluent. The product was isolated as pale yellow oil in 62% yield (0.220 g, 0.80 mmol).

^1H NMR (499.7 MHz, CDCl_3): 7.74 (br s, 1 H, NH), 7.52 (d, 1 H, $J_{\text{HH}} = 7.4$ Hz, 7H-indole), 7.28 (d, 1 H, $J_{\text{HH}} = 6.9$ Hz, 4H-indole), 7.17 (m, 2 H, 5H- and 6H-indole), 3.65 (t, 2 H, $J_{\text{HH}} = 8.9$ Hz, OCH_2), 2.98 (t, 2 H, $J_{\text{HH}} = 7.4$ Hz, OCH_2CH_2), 2.41 (s, 3 H, 2- CH_3), 0.86 (s, 9 H, CCH_3), 0.11 (s, 6 H, SiCH_3). $^{13}\text{C}\{^1\text{H}\}$ NMR (125.7 MHz, CDCl_3): 135.2, 131.7, 128.9, 120.9, 119.1, 117.9, 110.1, 108.4, 63.6, 28.2, 26.0, 18.4, 11.7, -5.3.

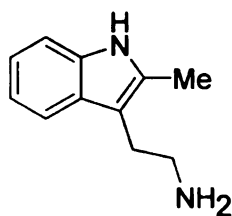
MS (EI) $m/z = 289$ (M^+).

Synthesis of 1-phenyl-3-methyl-tetrahydropyridazine (17)



Under an atmosphere of dry nitrogen, a threaded pressure tube was loaded with **5** (0.139 g, 0.37 mmol) in toluene (1.8 mL), phenylhydrazine (717 μ L, 7.30 mmol), and 5-chloropent-1-yne (775 μ L, 7.30 mmol). The tube was sealed and removed from the dry box for heating at 80 $^{\circ}$ C for 24 h. The reaction was then allowed to cool to room temperature, diluted with dichloromethane (20 mL), and saturated NaHCO_3 solution was added. The organic layer was separated. The aqueous layer was extracted with dichloromethane (3×15 mL). The combined organics were washed with water, and the final combined organics were dried over MgSO_4 , filtered, and dried in vacuo. This yielded a dark brown oil, which was subjected to column chromatography on silica gel using 4:1 petroleum ether:ether as eluent. The product⁴⁵ was isolated in 32% yield (0.400 g, 2.30 mmol) as yellow oil, which turned to red on standing. ^1H NMR (499.7 MHz, CDCl_3): 7.29 (t, 2 H, $J_{\text{HH}} = 4.1$ Hz, 8.7 Hz, *o*-Ph), 7.22 (d, 2 H, $J_{\text{HH}} = 7.8$ Hz, *m*-Ph), 6.87 (t, 1 H, $J_{\text{HH}} = 7.4$ Hz, *p*-Ph), 3.51 (t, 2 H, $J_{\text{HH}} = 6.1$ Hz, NCH_2), 2.21 (t, 3 H, $J_{\text{HH}} = 6.1$ Hz, C(=N)CH_2), 2.08 (m, 2 H, $(=\text{N})\text{CH}_2\text{CH}_2$), 2.02 (s, 3 H, CH_3). $^{13}\text{C}\{^1\text{H}\}$ NMR (125.7 MHz, CDCl_3): 148.3, 143.6, 128.8, 119.1, 113.5, 42.2, 25.6, 24.3, 19.0. MS (EI) $m/z = 174$ (M^+).

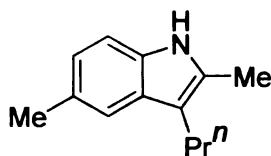
Synthesis of 2-methyltryptamine (20)



Under an atmosphere of dry nitrogen, a threaded pressure tube was loaded with **5** (0.185 g, 0.49 mmol) in toluene (2.4 mL), phenylhydrazine (964 μ L, 9.80 mmol), and 5-chloropent-1-yne (1034 μ L, 9.80 mmol). The tube was sealed and removed from the dry box for heating at 80 °C for 24 h. The reaction then was allowed to cool to room temperature. The hydrochloride salt (**18**) of the product precipitated during reaction. The precipitate was washed with ethylacetate (50 mL), which contained crude **17**. To the crude **18** was added NaOH (20%, 25 mL), and the product was extracted with ethylacetate (3 \times 20 mL). The combined organic layers were dried over Na₂SO₄, filtered, and volatiles were removed under vacuum. To the resulting brown oil was added hexanes (20 mL), and then HCl in ether until it reached pH \sim 2. A brown solid precipitated from the solution. The solid was filtered and volatiles were again removed under vacuum. Next, the solids were dissolved in dichloromethane (20 mL), and saturated NaHCO₃ solution was added to the solution (pH \sim 7). The mixture was shaken, and the organic layer was separated. The aqueous layer was extracted with dichloromethane (3 \times 15 mL). The combined organic layers were washed with water. The final organic layer was dried over MgSO₄, filtered, and volatiles removed in vacuo. This yielded **20** as a brown oil⁶³ in 32% yield (0.400 g, 2.30 mmol). ¹H NMR (499.7 MHz, CDCl₃): 7.76 (br s, 1 H, NH),

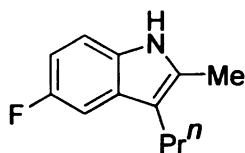
7.85 (d, 1 H, $J_{\text{HH}} = 8.1$ Hz, 7*H*-indole), 7.26 (d, 1 H, $J_{\text{HH}} = 5.6$ Hz, 4*H*-indole), 7.18-7.04 (m, 2 H, k, 5*H*-indole), 2.96 (t, 2 H, $J_{\text{HH}} = 6.6$ Hz, 3- CH_2), 2.84 (t, 2 H, $J_{\text{HH}} = 6.6$ Hz, NH_2CH_2), 2.38 (s, 3 H, 2- CH_3), 1.74 (br s, 2 H, NH_2). $^{13}\text{C}\{^1\text{H}\}$ NMR (125.7 MHz, CDCl_3): 135.3, 131.8, 128.8, 121.0, 119.2, 118.0, 110.2, 109.0, 42.5, 28.0, 11.8. MS (EI) $m/z = 174$ (M^+).

Synthesis of 2,5-dimethyl-3-propyl-NH-indole (21)



Under an atmosphere of dry nitrogen, a threaded pressure tube was loaded with **5** (0.029 g, 0.08 mmol) in toluene (375 μ L), *p*-methylphenylhydrazine (0.183 g, 1.50 mmol), and 1-hexyne (175 μ L, 1.50 mmol). The tube was sealed and removed from the dry box for heating at 80 $^{\circ}$ C for 16 h. The solution was then allowed to cool to room temperature, taken inside the box, and excess ZnCl_2 (0.602 g, 4.50 mmol) was added. The reaction was heated at 100 $^{\circ}$ C for 16 h. After that, the solution was allowed to cool to room temperature, diluted with ether, and passed through a pad of silica in a fritted funnel. Volatiles were removed from the filtrate in vacuo. The resulting dark red oil was subjected to column chromatography on silica gel with 1:1 hexanes:ethylacetate as eluent. The product was isolated as a red oil in 64% yield (0.180 g, 0.90 mmol). ^1H NMR (299.8 MHz, CDCl_3): 7.61 (br s, 1 H, NH), 7.26 (s, 1 H, 4H-indole), 7.13 (d, 1 H, $J_{\text{HH}} = 8.1$ Hz, 6H-indole), 6.91 (dd, 1 H, $J_{\text{HH}} = 1.4, 8.1$ Hz, 7H-indole), 2.61 (t, 2 H, $J_{\text{HH}} = 7.3$ Hz, 3- CH_2), 2.43 (s, 3 H, 5- CH_3), 2.33 (s, 3 H, 2- CH_3), 1.63 (m, 2 H, CH_3CH_2), 0.94 (t, 3 H, $J_{\text{HH}} = 7.4$ Hz, CH_2CH_3). $^{13}\text{C}\{^1\text{H}\}$ NMR (75.4 MHz, CDCl_3): 133.5, 130.9, 129.1, 128.0, 122.2, 118.0, 111.9, 109.7, 26.2, 23.8, 21.5, 14.1, 11.7. MS (EI) $m/z = 187$ (M^+).

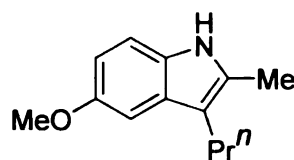
Synthesis of 2-methyl-5-fluoro-3-propyl-NH-indole (22)



Under an atmosphere of dry nitrogen, a threaded pressure tube was loaded with **5** (0.029 g, 0.08 mmol) in toluene (375 μ L), *p*-fluorophenylhydrazine (0.192 g, 1.50 mmol), and 1-hexyne (175 μ L, 1.50 mmol). The tube was sealed and removed from the dry box for heating at 80 $^{\circ}$ C for 16 h. The reaction then was allowed to cool to room temperature, taken inside the box, and excess ZnCl₂ (0.602 g, 4.50 mmol) was added. The mixture was heated at 100 $^{\circ}$ C for 16 h. After that, the reaction was allowed to cool to the room temperature, diluted with ether, and passed through a pad of silica in a fritted funnel. Volatiles were removed from the filtrate in vacuo. The resulting dark red oil was subjected to column chromatography on silica gel with 2:1 ether:pentane as eluent. The product was isolated as a red oil in 70% yield (0.200 g, 1.05 mmol). ¹H NMR (499.7 MHz, CDCl₃): 7.61 (br s, 1 H, NH), 7.17-7.15 (dd, 1 H, $J_{HH} = 2.5, 9.9$ Hz, 4*H*-indole), 7.14-7.11 (dd, 1 H, $J_{HH} = 4.4, 8.6$ Hz, 7*H*-indole), 6.87 – 6.83 (dt, 1 H, $J_{HH} = 2.5, 9.0$ Hz, 6*H*-indole), 2.63 (t, 2 H, $J_{HH} = 7.7$ Hz, 3-CH₂), 2.35 (s, 3 H, 2-CH₃), 1.63 (m, 2 H, CH₃CH₂), 0.95 (t, 3 H, $J_{HH} = 6.5$ Hz, CH₂CH₃). ¹³C{¹H} NMR (125.7 MHz, CDCl₃): 158.6, 156.7, 132.9, 129.3 (d, $J_{CF} = 9.7$ Hz), 112.5 (d, $J_{CF} = 4.5$ Hz), 110.5 (d, $J_{CF} = 9.7$ Hz), 108.7 (d, $J_{CF} = 26.2$ Hz), 103.3, (d, $J_{CF} = 23.6$ Hz), 26.1, 23.7, 14.0, 11.7.

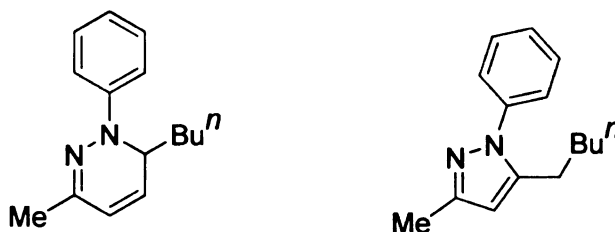
Elemental Analysis; Experimental (Calc.), C: 75.04 (75.36). H: 7.65 (7.38). N: 7.18
(7.32). MS (EI) $m/z = 191$ (M^+).

Synthesis of 2-methyl-5-methoxy-3-propyl-NH-indole (23)



Under an atmosphere of dry nitrogen, a threaded pressure tube was loaded with **5** (0.057 g, 0.15 mmol) in toluene (750 μ L), *p*-methoxyphenylhydrazine (0.421 g, 3.0 mmol), and 1-hexyne (350 μ L, 3.0 mmol). The tube was sealed and removed from the dry box for heating at 80 $^{\circ}$ C for 16 h. The reaction then was allowed to cool to room temperature, taken inside the box, and excess ZnCl_2 (0.602 g, 9.00 mmol) was added. The mixture was heated at 100 $^{\circ}$ C for 16 h. After that, the reaction was allowed to cool to the room temperature, diluted with ether, and passed through a pad of silica in a fritted funnel. Volatiles were removed from the filtrate in vacuo. The resulting dark brown-red oil was subjected to column chromatography on silica gel with 1:1 hexanes:ethylacetate as eluent. The product was isolated as red oil in 76% yield (0.460 g, 2.30 mmol). ^1H NMR (499.7 MHz, CDCl_3): 7.58 (br s, 1 H, NH), 7.25 (d, 1 H, $J_{\text{HH}} = 8.8$ Hz, 7H-indole), 6.94 (d, 1 H, $J_{\text{HH}} = 2.5$ Hz, 4H-indole), 6.76-6.72 (dd, 1 H, $J_{\text{HH}} = 2.5, 8.5$ Hz, 6H-indole), 3.85 (s, 3H, OCH_3), 2.62 (t, 2 H, $J_{\text{HH}} = 7.4$ Hz, 3- CH_2), 2.32 (s, 3 H, 2- CH_3), 1.68-1.59 (m, 2 H, CH_3CH_2), 0.96 (t, 3 H, $J_{\text{HH}} = 7.4$ Hz, CH_2CH_3). $^{13}\text{C}\{^1\text{H}\}$ NMR (125.7 MHz, CDCl_3): 153.7, 131.8, 130.4, 129.3, 112.1, 110.6, 110.2, 100.9, 56.0, 26.2, 23.7, 14.1, 11.8. Elemental Analysis; Experimental (Calc.), C: 76.62 (76.81). H: 8.85 (8.43). N: 6.34 (6.89). MS (EI) $m/z = 203$ (M^+).

Reaction of 1,4-nonadiyne with phenylhydrazine to synthesize **24** and **25**



Under an atmosphere of dry nitrogen, a threaded pressure tube was loaded with **5** (0.040 g, 0.11 mmol) in toluene (525 μ L), phenylhydrazine (204 μ L, 2.10 mmol), and nona-1,4-diyne (0.250 g, 2.10 mmol). The tube was sealed and removed from the dry box for heating at 80 $^{\circ}$ C for 16 h. The reaction was then allowed to cool to room temperature, diluted with ether, and passed through a pad of alumina in a fritted funnel. Volatiles were removed from the filtrate in vacuo. The resulting dark red oil was subjected to column chromatography on alumina. Isomer **24** eluted with 5:1 hexanes:ether as the first fraction. After removing volatiles in vacuo, **24** was isolated in 17% yield (0.080 g, 0.35 mmol). Isomer **25** eluted using 1:1 hexanes:ether in the second fraction. After removing volatiles in vacuo, **25** was isolated in 42% yield (0.203 g, 0.89 mmol). Isomer **24**: ^1H NMR (499.7 MHz, CDCl_3): 7.26-7.19 (m, 4 H, *o,m*-Ph), 6.83 (t, 1 H, $J_{\text{HH}} = 7.0$ Hz, *p*-Ph), 6.04 (dd, 1 H, $J_{\text{HH}} = 6.6, 9.3$ Hz, 5*H*-pyridazine), 5.87 (d, 1 H, $J_{\text{HH}} = 9.9$ Hz, 3*H*-pyridazine), 4.62 (m, 1 H, 6*H*-pyridazine), 2.06 (s, 3 H, 3- CH_3), 1.61-1.47 (m, 2 H, 6- CH_2), 1.28 (m, 4 H, CH_3CH_2 and $\text{CH}_3\text{CH}_2\text{CH}_2$), 0.84 (t, $J_{\text{HH}} = 6.9$ Hz, 3H, CH_3CH_2). $^{13}\text{C}\{^1\text{H}\}$ NMR (125.7 MHz, CDCl_3): 146.0, 142.8, 129.0, 127.4, 120.0, 119.6, 113.7, 51.0, 30.6, 26.2, 22.7, 21.2, 14.0. MS (EI) $m/z = 228$ (M^+). Isomer **25**: ^1H NMR (499.7 MHz, CDCl_3): 7.46-7.32 (m, 5 H, Ph), 6.00 (s, 1 H, 4*H*-pyrazole), 2.58 (t, 2 H, $J_{\text{HH}} = 8.0$ Hz, 5- CH_2),

2.29 (s, 3 H, 3-CH₃), 1.55 (m, 2 H, CH₂CH₂), 1.25 (m, 4 H, CH₃CH₂CH₂ and CH₃CH₂CH₂), 0.84 (t, 3 H, $J_{HH} = 7.1$ Hz, CH₂CH₃). ¹³C{¹H} NMR (125.7 MHz, CDCl₃): 148.9, 144.6, 140.0, 129.0, 127.4, 125.3, 105.2, 31.4, 28.5, 26.2, 22.3, 13.9, 13.6. MS (EI) m/z = 228 (M⁺).

X-ray Crystallography

Crystals grown from concentrated solutions at room temperature were moved quickly from a scintillation vial to a microscope slide containing Paratone N. Samples were selected and mounted on a glass fiber in wax and Paratone. Data were collected using a Bruker CCD diffractometer equipped with an Oxford Cryostream low-temperature apparatus operating at 173 K. The data were processed and reduced utilizing the program SAINTPLUS supplied by Bruker AXS. Data reduction was performed using the SAINT software. Scaling and absorption corrections were applied using SADABS multi-scan technique supplied by George Sheldrick. The structure was solved by the direct method using the SHELXS-97 program and refined by the least squares method on F^2 , SHELXL-97, incorporated in SHELXTL-PC V 6.10.

2.7 References

1. Kitajima, M. *J. Nat. Med.* **2007**, *61*, 14.
2. Sanchez, C.; Mendez, C.; Salas, J. A. *Nat. Prod. Rep.* **2006**, *23*, 1007.
3. Kitajima, M.; Misawa, K.; Kogure, N.; Said, I. M.; Horie, S.; Hatori, Y.; Murayama, T.; Takayama, H. *J. Nat. Med.* **2006**, *60*, 28.
4. Chen, F. E.; Huang, J. *Chem. Rev.* **2005**, *105*, 4671.
5. Cao, C. S.; Shi, Y. H.; Odom, A. L. *Org. Lett.* **2002**, *4*, 2853.
6. Straub, B. F.; Bergman, R. G. *Angew. Chem. Int. Ed.* **2001**, *40*, 4632.
7. Baranger, A. M.; Walsh, P. J.; Bergman, R. G. *J. Am. Chem. Soc.* **1993**, *115*, 2753.
8. Walsh, P. J.; Baranger, A. M.; Bergman, R. G. *J. Am. Chem. Soc.* **1992**, *114*, 1708.
9. Patel, S.; Li, Y.; Odom, A. L. *Inorg. Chem.* **2007**, *46*, 6373.
10. Tillack, A.; Jiao, H. J.; Castro, I. G.; Hartung, C. G.; Beller, M. *Chem. Eur. J.* **2004**, *10*, 2409.
11. Khedkar, V.; Tillack, A.; Michalik, M.; Beller, M. *Tet. Lett.* **2004**, *45*, 3123.
12. Schwarz, N.; Alex, K.; Sayyed, I. A.; Khedkar, V.; Tillack, A.; Beller, M. *Synlett* **2007**, 1091.
13. Khedkar, V.; Tillack, A.; Michalik, M.; Beller, M. *Tetrahedron* **2005**, *61*, 7622.
14. Ackermann, L.; Born, R. *Tet. Lett.* **2004**, *45*, 9541.
15. Waser, J.; Carreira, E. M. *J. Am. Chem. Soc.* **2004**, *126*, 5676.
16. Waser, J.; Gaspar, B.; Nambu, H.; Carreira, E. M. *J. Am. Chem. Soc.* **2006**, *128*, 11693.
17. Waser, J.; Gonzalez-Gomez, J. C.; Nambu, H.; Huber, P.; Carreira, E. M. *Org. Lett.* **2005**, *7*, 4249.
18. Waser, J.; Carreira, E. M. *Angew. Chem. Int. Ed.* **2004**, *43*, 4099.
19. Johns, A. M.; Liu, Z. J.; Hartwig, J. F. *Angew. Chem. Int. Ed.* **2007**, *46*, 7259.

20. Alex, K.; Tillack, A.; Schwarz, N.; Beller, M. *Angew. Chem. Int. Ed.* **2008**, *47*, 2304.
21. Alex, K.; Tillack, A.; Schwarz, N.; Beller, M. *Org. Lett.* **2008**, *10*, 2377.
22. Alex, K.; Tillack, A.; Schwarz, N.; Beller, M. *Tet. Lett.* **2008**, *49*, 4607.
23. Robinson, B. *The Fischer Indole Synthesis*, Wiley & Sons: Chichester, UK, 1982.
24. Humphrey, G. R.; Kuethe, J. T. *Chem. Rev.* **2006**, *106*, 2875.
25. Hulcoop, D. G.; Lautens, M. *Org. Lett.* **2007**, *9*, 1761.
26. Barluenga, J.; Jimenez-Aquino, A.; Valdes, C.; Aznar, F. *Angew. Chem. Int. Ed.* **2007**, *46*, 1529.
27. Patil, S.; Buolamwini, J. K. *Curr. Org. Synth.* **2006**, *3*, 477.
28. Lu, B. Z.; Zhao, W. Y.; Wei, H. X.; Dufour, M.; Farina, V.; Senanayake, C. H. *Org. Lett.* **2006**, *8*, 3271.
29. Hostyn, S.; Maes, B. U. W.; Van Baelen, G.; Gulevskaya, A.; Meyers, C.; Smits, K. *Tetrahedron* **2006**, *62*, 4676.
30. Fayol, A.; Fang, Y. Q.; Lautens, M. *Org. Lett.* **2006**, *8*, 4203.
31. Djakovitch, L.; Dufaud, V.; Zaidi, R. *Adv. Synth. Catal.* **2006**, *348*, 715.
32. Ambrogio, I.; Cacchi, S.; Fabrizi, G. *Org. Lett.* **2006**, *8*, 2083.
33. Abbiati, G.; Arcadi, A.; Beccalli, E.; Bianchi, G.; Marinelli, F.; Rossi, E. *Tetrahedron* **2006**, *62*, 3033.
34. Cacchi, S.; Fabrizi, G. *Chem. Rev.* **2005**, *105*, 2873.
35. Ackermann, L.; Kaspar, L. T.; Gschrei, C. J. *Chem. Commun.* **2004**, 2824.
36. Lipinska, T. M. *Tetrahedron* **2006**, *62*, 5736.
37. Garg, N. K.; Stoltz, B. M. *Chem. Commun.* **2006**, 3769.
38. Schmidt, A. M.; Eilbracht, P. *J. Org. Chem.* **2005**, *70*, 5528.
39. Tietze, L. F.; Modi, A. *Med. Res. Rev.* **2000**, *20*, 304.
40. Banerjee, S.; Barnea, E.; Odom, A. L. *Organometallics* **2008**, *27*, 1005.

41. Kim, I. T.; Elsenbaumer, R. L. *Tetrahedron Lett.* **1998**, *39*, 1087.
42. Raines, S.; Kovacs, C. A. *J. Heterocycl. Chem.* **1970**, *7*, 223.
43. Herz, W.; Dittmer, K. *J. Am. Chem. Soc.* **1947**, *69*, 1698.
44. The zirconium derivative has the geometry described in a structure determined by X-ray diffraction and is spectroscopically similar. Barnea, E.; Odom, A. L. *Dalton Trans.* **2008** 4050.
45. Benincori, T.; Brenna, E.; Sannicolo, F. *J. Chem. Soc. Perkin Trans. 1.* **1991**, 2139.
46. Grandberg, I. I.; Kost, A. N.; Terentev, A. P. *Russ. J. Gen. Chem.* **1957**, *27*, 3378.
47. Similar dihydropyridazine compounds are known. For references see: Kaneko, C.; Tsuchiya, T.; Igeta, H. *Chem. Pharm. Bull.* **1974**, *22*, 2894.
48. Crosslan, I.; Kelstrup, E. *Acta. Chem. Scand.* **1968**, *22*, 1669.
49. For some examples of similar insertion of alkynes into transition metal-nitrogen bonds see: Katayev, E.; Li, Y. H.; Odom, A. L. *Chem. Commun.* **2002**, 838.
50. Boncella, J. M.; Eve, T. M.; Rickman, B.; Abboud, K. A. *Polyhedron* **1998**, *17*, 725.
51. Vanderlende, D. D.; Abboud, K. A.; Boncella, J. M. *Inorg. Chem.* **1995**, *34*, 5319.
52. Villanueva, L. A.; Abboud, K. A.; Boncella, J. M. *Organometallics* **1992**, *11*, 2963.
53. Kemmitt, R. D. W.; Mason, S.; Moore, M. R.; Fawcett, J.; Russell, D. R. *J. Chem. Soc. Chem. Commun.* **1990**, 1535.
54. Hydroamination of alkynes using lanthanides also involved similar insertion. For a review see: Hong, S.; Marks, T. J. *Acc. Chem. Res.* **2004**, *37*, 673.
55. Bergman, J.; Carlsson, R. *J. Heterocyclic Chem.* **1972**, *9*, 833.
56. Similar Michael type reaction is known with acetic acid. For references see: Ferres, H.; Hamdam, M. S.; Jackson, W. R. *J. Chem. Soc., Perkin Trans.* **1973**, 936.
57. Alexandre, C. W.; Jackson, W. R.; Hamdam, M. S. *J. Chem. Soc., Chem. Commun.* **1972**, 94.
58. Verkruijsse, H. D.; Hasselaar, M. *Synthesis* **1979**, 292.

59. Brandsma, L. *Preparative Acetylenic Chemistry*, Elsevier Publishers: Amsterdam-London-New York, 1971, 137.
60. Bradley, D. C.; Thomas, I. M. *J. Chem. Soc.* **1960**, 3859.
61. Jackson, A. H.; Smith, A. E. *Tetrahedron* **1965**, *21*, 989.
62. Minakata, S.; Kasano, Y.; Ota, H.; Oderaotoshi, Y.; Komatsu, M. *Org. Lett.* **2006**, *8*, 3693.
63. Jackson, A. H.; Smith, A. E. *J. Chem. Soc.* **1964**, 5510.

CHAPTER 3

Iminohydrazination of alkynes: scope, mechanistic investigation, and applications towards pyrazole synthesis

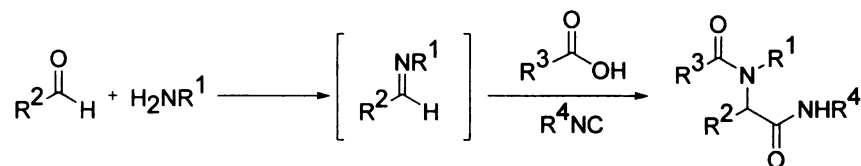
3.1 Introduction

Iminohydrazination is the conversion of an alkyne to an α,β -unsaturated β -aminohydrazone, making both C–C and C–N bonds in a single step. This is a new multicomponent reaction (MCR) between an alkyne, 1,1-disubstituted hydrazine, and isonitrile in the presence of a catalyst.

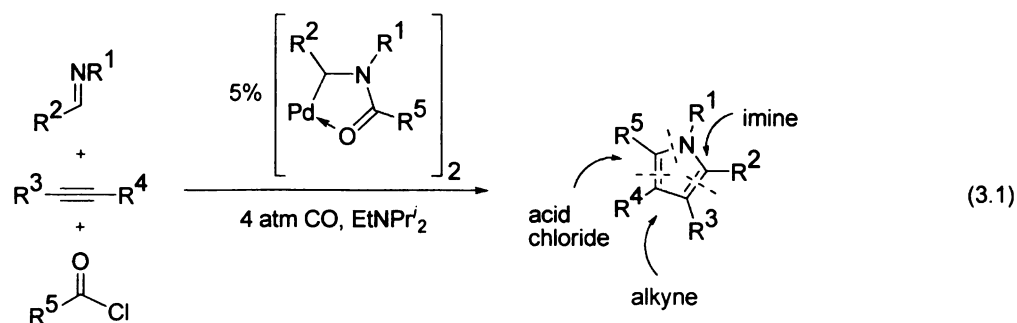
Multicomponent reactions are valuable tools for the preparation of complex structures from simple starting materials. Multicomponent reactions are well suited for the rapid and highly atom-economical assembly of large compound libraries. As a consequence, the application of MCR to the drug discovery process has drawn considerable attention in recent years. A few of the earlier examples are Mannich,^{1,2} Strecker,³⁻⁶ Hantzsch,⁷ and Biginelli⁸ reactions. In 1959, Ugi and co-workers reported the one-pot condensation of a carbonyl (aldehyde or ketone), amine, carboxylic acid, and isonitrile (Scheme 3.1).⁹ This reaction, now referred to as the Ugi 4-component reaction

(Ugi-4CR), provides an efficient method to construct functionalized acylamidoacetamides. Later, this protocol was adopted by Guanti et al. for the synthesis of α -amino acid derivatives in a very stereoselective manner.¹⁰

Scheme 3.1 Ugi 4-component reaction

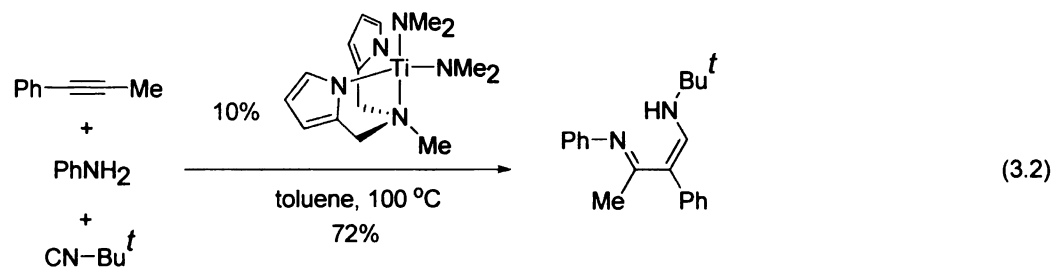


Further development in this area involves transition metal catalyzed MCR. Transition metals such as Pd,^{11,12} Cu,¹³ Ag,¹⁴ Zn,¹⁵ Ni,¹⁶ Ti,¹⁷⁻²¹ Zr,²² and Rh²³ have been effectively used for different multicomponent transformations. One example of Pd catalyzed MCR is shown in Equation 3.1.



In the previous chapters, we have shown that Group 4 metal complexes can be widely used in catalytic transformations of organic molecules, e.g., hydroamination and

hydrohydrazination reactions. They can be used in MCR as well.¹⁷⁻²² For example, Odom and co-workers have explored the titanium-catalyzed 3-component coupling reaction between alkyne, amine, and isonitrile to generate α,β -unsaturated β -iminoamines (Equation 3.2).²¹

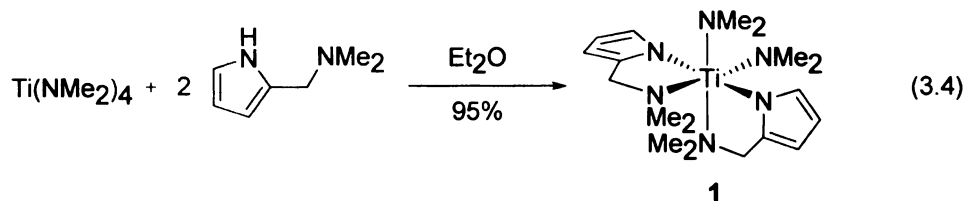
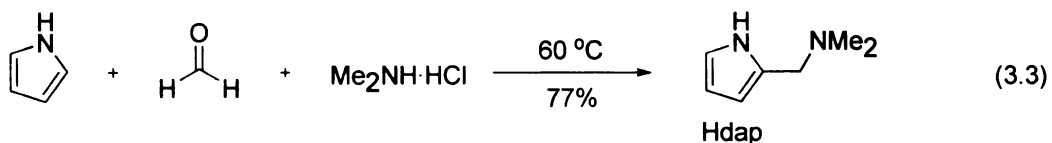


As an extension of this work, a new multicomponent reaction has been carried out between alkyne, 1,1-disubstituted hydrazine, and isonitrile to generate α,β -unsaturated β -aminohydrazone in the presence of pyrrolyl-based titanium catalysts.²⁴ This reaction is formally the iminohydrazination of the alkyne. The results of this reaction, mechanistic studies, and applications are discussed in detail in the following sections of this chapter.

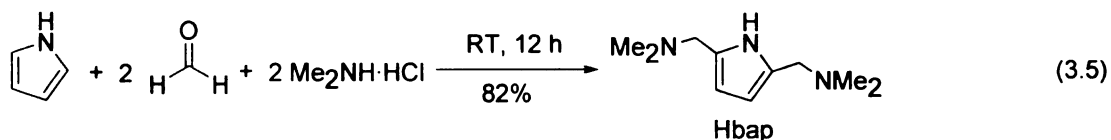
3.2 Results and Discussion

3.2.1 Iminohydrazination Results

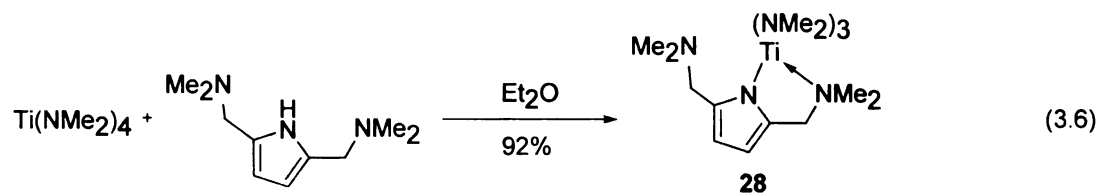
Iminohydrazination is a modification of alkyne hydrohydrazination. In hydrohydrazination reaction, an alkyne is allowed to react with a 1,1-disubstituted hydrazine in the presence of a catalyst to generate a hydrazone. In iminohydrazination, an alkyne is reacted with 1,1-disubstituted hydrazine and isonitrile in the presence of a catalyst to generate α,β -unsaturated β -aminohydrazone. For this reaction, three different titanium-based catalysts were used: $\text{Ti}(\text{NMe}_2)_2(\text{dap})_2$ (**1**), where dap is 2-(*N,N*-dimethylaminomethyl)pyrrolyl, $\text{Ti}(\text{NMe}_2)_3(\text{bap})$ (**28**), where bap is *bis*-2,5-(*N,N*-dimethylaminomethyl)pyrrolyl, and $\text{Ti}(\text{NMe}_2)_2(\text{SC}_6\text{F}_5)_2(\text{NHMe}_2)$ (**29**). The Hdap ligand was synthesized by the reaction of one equivalent each of pyrrole, formaldehyde, and dimethylamine hydrochloride. The ligand was isolated in 77% yield (Equation 3.3).²⁵ Catalyst **1** was then synthesized by adding two equivalents of Hdap to $\text{Ti}(\text{NMe}_2)_4$ and isolated in 95% yield (Equation 3.4).²⁶



The Hdap ligand was synthesized by adding two equivalents each of formaldehyde and dimethylamine hydrochloride to one equivalent of pyrrole and isolated in 82% yield (Equation 3.5).²⁷



Catalyst **28** was synthesized in 92% yield by adding one equivalent of Hbap to $\text{Ti}(\text{NMe}_2)_4$ (Equation 3.6). The solution NMR spectrum reveals that the two arms of the bap ligand are equivalent to each other. However, as shown in Figure 3.1, the solid state structure shows that only one arm is coordinated. The uncoordinated amine nitrogen is 4.1 Å away from titanium. This suggests that the equivalency of the two dimethylamine donors in solution is likely due to fast exchange processes.



Catalyst **29** was synthesized by adding two equivalents of $\text{C}_6\text{F}_5\text{SH}$ to $\text{Ti}(\text{NMe}_2)_4$ and isolated in 65% yield (Equation 3.7).²⁶

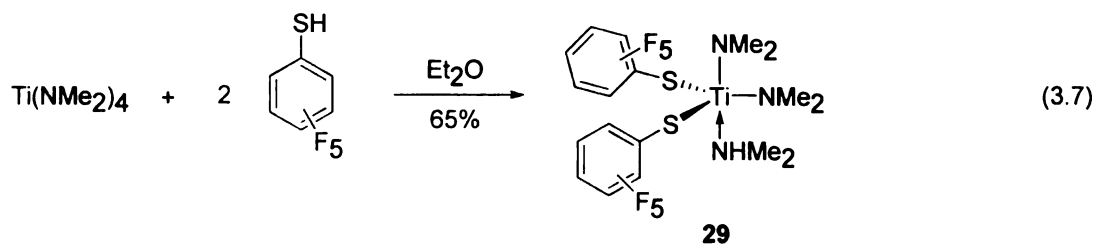
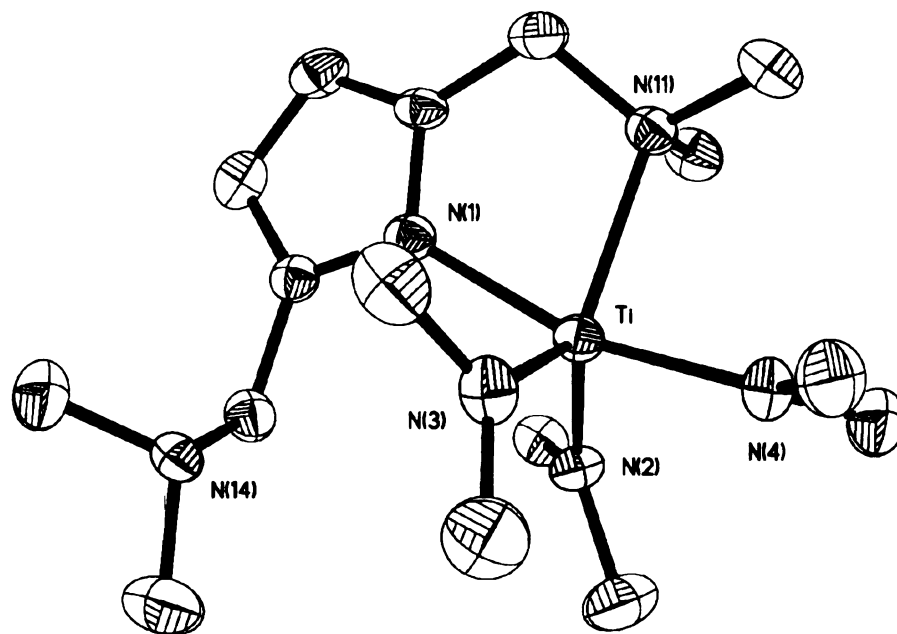


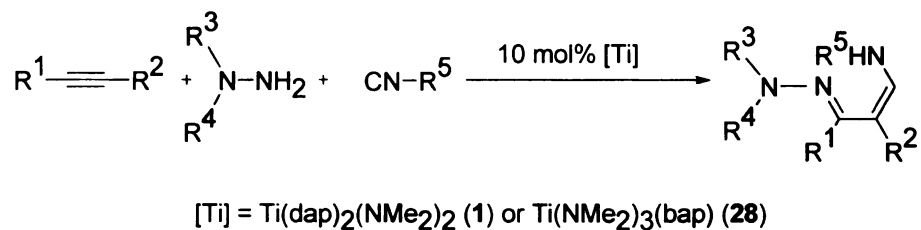
Figure 3.1 Solid-state structure of $\text{Ti}(\text{NMe}_2)_3(\text{bap})$ (**28**) from X-ray diffraction.



This new iminohydrazination reaction tolerates a wide range of substrates, including terminal and internal alkynes with aliphatic and aromatic isonitriles (Table 3.1). In all these reactions, 10 mol% catalysts **1** and **28** were used. The reactions are more facile with terminal alkynes and alkyl isonitriles. Interestingly, if diphenylhydrazine is used, only a small amount of the product and a significant amount of diphenylamine are obtained. Note that in the iminoamination reaction, which is a 3-component coupling of alkyne, amine, and isonitrile, we did not observe the expected 3-component coupling product when cyclohexylisonitrile was used.²¹ Iminoamination required a quaternary carbon adjacent to the nitrogen atom in the isonitrile. However, in the present study of

iminohydrazination, the expected product is formed even with cyclohexylisonitrile. The need for an isonitrile having a quaternary carbon adjacent to the nitrogen atom is eliminated by using hydrazine as a substrate. Therefore, this process can be generalized for a wide range of substrates. The product yields varied from 12–73%.

Table 3.1 Examples of alkyne iminohydrazination



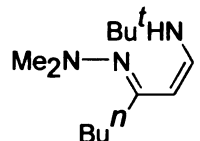
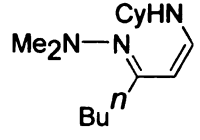
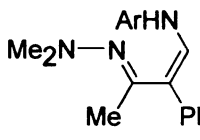
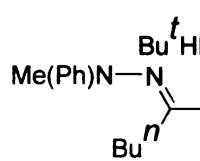
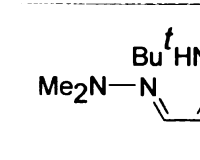
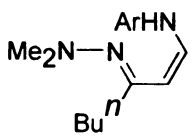
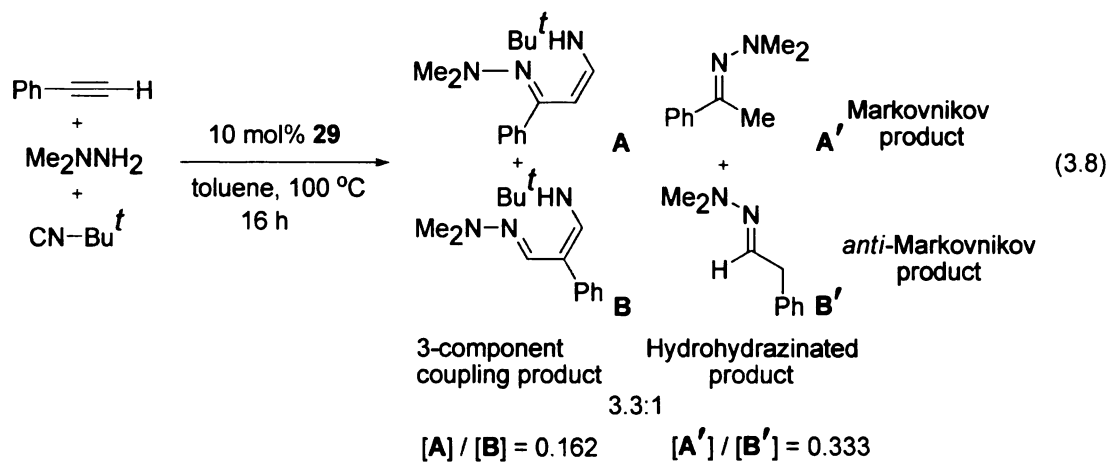
Entry	R ¹ , R ²	R ³ , R ⁴	R ⁵	Conditions ^a	Product	Yield (%)
1	Bu ⁿ , H	Me, Me	Bu ^t	A, 16 h	 30	63
2	Bu ⁿ , H	Me, Me	Cy ^b	A, 16 h	 31	73
3	Me, Ph	Me, Me	Ar ^c	B, 43 h	 32	15
4	Bu ⁿ , H	Ph, Me	Bu ^t	A, 16 h	 33	27
5	H, Ph	Me, Me	Bu ^t	C, 16 h	 34	43

Table 3.1 (Cont'd.)

6	Bu ⁿ , H	Me, Me	Ar ^c	A, 16 h		12
35						

^a **A** = 10 mol% **1** in toluene at 100 °C, **B** = 10 mol% **1** in toluene at 130 °C, **C** = 10 mol% **28** in toluene at 100 °C. ^b Cy = cyclohexyl. ^c Ar = 2,6-dimethylphenyl

The catalytic activity of **29** in iminohydrazination reaction was also explored. Unfortunately, **29** did not generate the desired 3-component coupling product except for the substrates in Entry 5 of Table 3.1, where the quite reactive alkyne phenylacetylene was used. The reaction with phenylecetylene produced a significant amount of hydrohydrazinated product, making **29** less effective than **28**. In this case, as shown in Equation 3.8, the major product was dimethylhydrazone of phenyl acetaldehyde (*anti*-Markovnikov product) and the minor product was dimethylhydrazone of acetophenone (Markovnikov product). In addition, **29** also showed some activity for the substrates in Entry 1, but produced a 4-component coupling product that corresponds to the mass of two isonitriles, one alkyne, and one hydrazine (Equation 3.9).

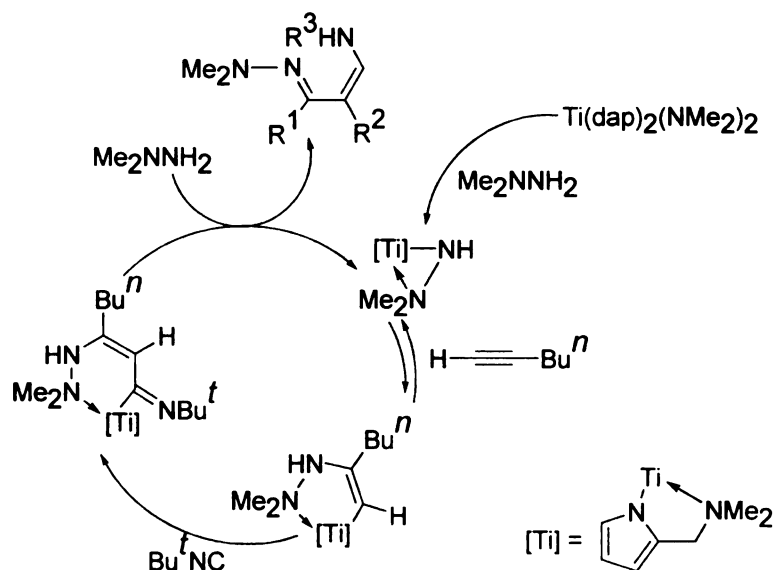


3.3 Mechanistic Investigation

3.3.1 Pathway via 1,2-insertion

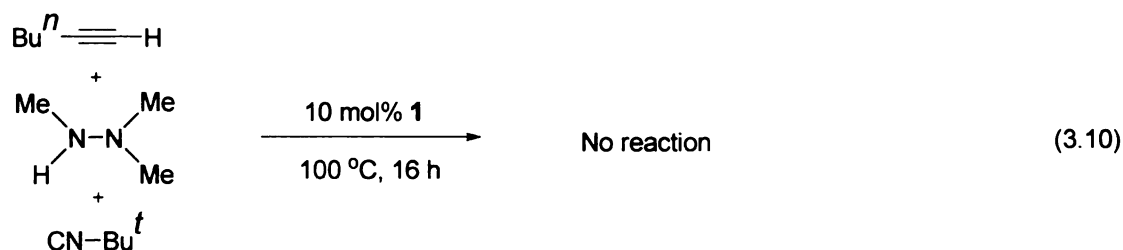
We proposed two possible mechanisms for iminohydrazination. The first one was a 1,2-insertion pathway. This involved 1,2-insertion of an alkyne into a titanium hydrazido(1-) intermediate, a pathway extensively studied by Marks and co-workers for amide.²⁸ If the isonitrile traps the resulting vinyl intermediate via 1,1-insertion, a 3-component coupling product would result according to Scheme 3.2.

Scheme 3.2 Possible 1,2-insertion pathway for the iminohydrazination reaction



For the above mechanism, the formation of a hydrazido(1-) intermediate is necessary. If the alkyne inserts into this intermediate, then reactions with trimethylhydrazine should generate an iminohydrazination product similar to Entry 1 in Table 3.1. To verify this

point, a 3-component coupling reaction with 1-hexyne, *N,N,N'*-trimethylhydrazine, and *tert*-butylisocyanide was attempted (Equation 3.10). However, no reaction was observed when monitored by GC/FID. Therefore, it is unlikely that the iminohydrazination reaction involves a 1,2-insertion pathway. Alternatively, the reaction may involve a hydrazido(2-) intermediate and follow a mechanism similar to the zirconocene-based hydroamination of alkynes established by Bergman which is discussed in the next section.

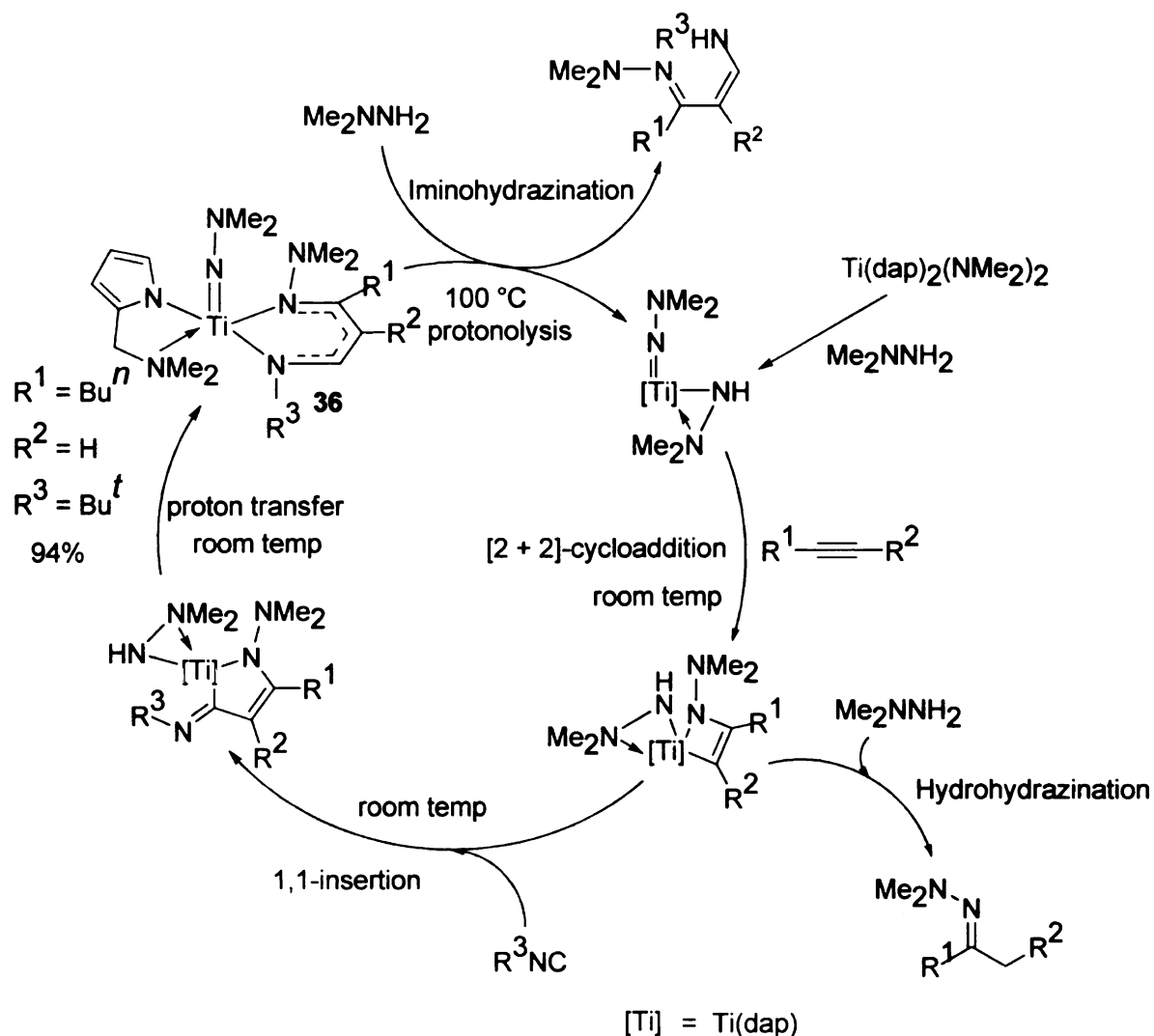


3.3.2 [2 + 2]-cycloaddition mechanism

An alternative mechanistic pathway for the iminohydrazination reaction can be anticipated following the Bergman mechanism^{29,30} for zirconocene-catalyzed hydroamination as shown in Scheme 3.3. Catalyst **1** forms a titanium hydrazido(2-) intermediate, which undergoes [2 + 2]-cycloaddition with alkyne to form an azatitanacyclobutene. This cycloaddition step is followed by 1,1-insertion of isocyanide forming a new Ti-C bond. The five-membered metallacycle then rearranges to form an

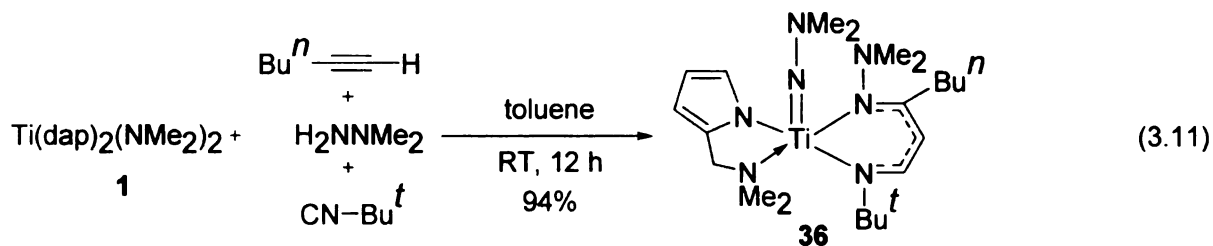
isolable intermediate **36**. Compound **36** finally undergoes intermolecular protonolysis generating the 3-component coupling product.

Scheme 3.3 Possible mechanistic pathway of iminohydrazination by **1** for Entry 1 in Table 3.1



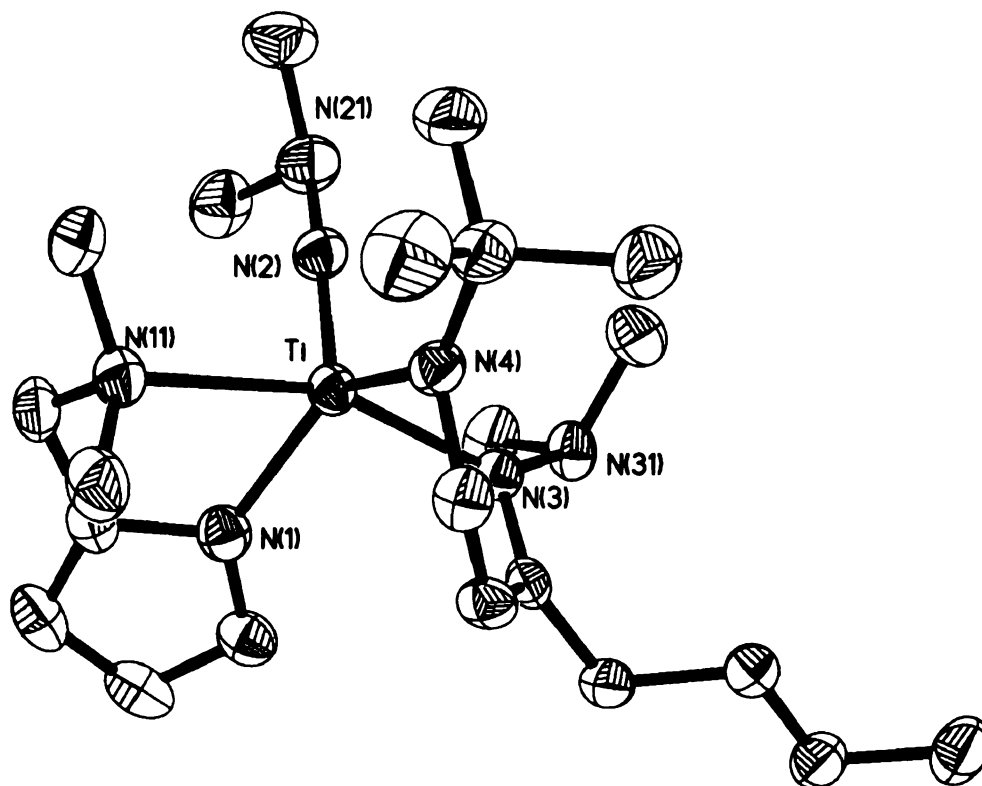
In an attempt to isolate an intermediate, a reaction was carried out involving **1** with 1 equivalent each of 1-hexyne, 1,1-dimethylhydrazine, and *tert*-butylisocyanide. The reaction was very facile and generated $\text{Ti}(\text{NNMe}_2)(\text{dap})[\text{N}(\text{Bu}^t)\text{CHCHC}(\text{Bu}^n)\text{N}(\text{NMe}_2)-k^2\text{N}]$

(36), at room temperature (Equation 3.11). The compound was isolated in 94% yield with respect to limiting hydrazine.



The structure of **36** was solved by X-ray diffraction and is shown in Figure 3.2. It has many features in common with another structurally characterized titanium dimethylhydrazido(2-) complex, $\text{Ti}(\text{NNMe}_2)(\text{bpy})(\text{dpma})$, where dpma is *N,N*-di(pyrrolyl- α -methyl)-*N*-methylamine.³¹ Both have approximately linear terminal hydrazido(2-) Ti–N–N angles, which measured $169.6(2)^\circ$ in **36**.

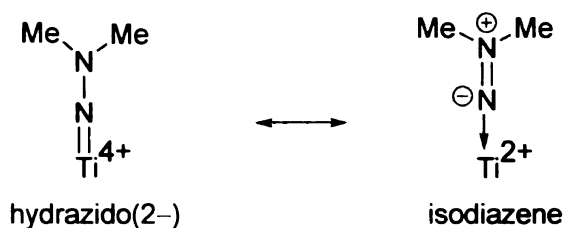
Figure 3.2 Structure of hydrazido(2-) complex **36** from X-ray diffraction. Selected bond distances (Å) and angles (°): Ti–N(2), 1.709(3); Ti–N(3), 2.077(2); Ti–N(4), 2.055(3); Ti–N(1), 2.119(3); Ti–N(11), 2.323(3); N(2)–N(21), 1.403(4); N(3)–N(31), 1.457(3); Ti–N(2)–N(21), 169.6(2).



The Ti=N(hydrazido) bond distance in **36** is 1.709(3) Å and is in the usual range for a titanium-nitrogen double to triple bond. The hydrazido(2-) N–N distance of 1.402(4) Å is slightly shorter than an N–N single bond, which is 1.451 ± 0.005 Å in hydrazine.³² The shortening of the hydrazido(2-) N–N distance is perhaps due to contribution from the isodiazene resonance form (Figure 3.3). While the hydrazido(2-) form is favored for the electropositive titanium center, which is very reducing as titanium(II), for more weakly π -donating metal centers the isodiazene form strongly prevails. The isodiazene resonance form is known to be favored in many other compounds. For example, in an

isodiazene iron porphyrin complex, the N–N bond distance is 1.232(5) Å,³³ indicating a bond order of ~2.0 (discussed in more details in Section 4.2, Chapter 4).³⁴

Figure 3.3 Possible resonance forms of **36**. (For simplicity, the other ligands are not shown).



Most often, N is planar in hydrazido(2-) complexes and only a few examples with pyramidalized nitrogens have been structurally characterized.³⁵ The angles around N_β in **36** sum up to 335.5(3)°, only slightly higher than that expected for an *sp*³ hybridized nitrogen in NR₃ compound (328.0°). Therefore, the dimethylhydrazido(2-) complex of titanium (**36**) has a pyramidalized N_β, consistent with the preferred hydrazido(2-) resonance form in these early metal derivatives.^{36,37}

The overall geometry of the five-coordinate complex, **36**, is intermediate between a square pyramidal and a trigonal bipyramidal, the former is slightly more favored. The complex **36** has a continuous symmetry parameter value of $\tau = 0.36$, where $\tau = 0$ represents a square pyramid and $\tau = 1$ represents a trigonal bipyramid.^{38,39} The nacnac ligand^{20,40} of **36**, although quite unsymmetrically substituted, is symmetrically bound to

titanium, where the Ti–N(NMe₂) and Ti–N(Bu^t) distances are 2.080(3) and 2.055(3) Å, respectively. The other C–C and C–N distances within the 6-membered ring are also consistent with a highly delocalized system.

Examination of the ¹H NMR spectrum of this hydrazido(2–) complex reveals a slight broadening of the methyl groups associated with the multiple bonded ligand due to relatively slow exchange. The barrier associated with the exchange of the two methyl groups has been measured as 12 kcal mol^{–1} using variable temperature NMR spectroscopy. Apparently, the barrier is associated with steric interactions between the hydrazido(2–) methyl groups and groups on the nacnac ligand, an observation also supported by the corresponding Density Functional Theory (DFT) calculations.

Attempts to increase the yield of **36** by adding more than one equivalent (two equivalents) of Me₂NNH₂ to **1** yielded a new dinuclear compound Ti₂(dap)₃(μ₂:^{1,2}-NNMe₂)(μ₁:¹-NHNMe₂) (**37**), which has two bridging hydrazido(2–) ligands and one dap protolytically replaced with a hydrazido(1–) ligand (Equation 3.12). The compound has been isolated in 61% yield as yellow crystals from a 1:1 solution of dichloromethane and pentane. From the structure of the isolated dinuclear compound, it is obvious that at least one of the dap ligands is cleaved during the reaction (Figure 3.4). Hence one dap is protolytically labile in the presence of 1,1-dimethylhydrazine.

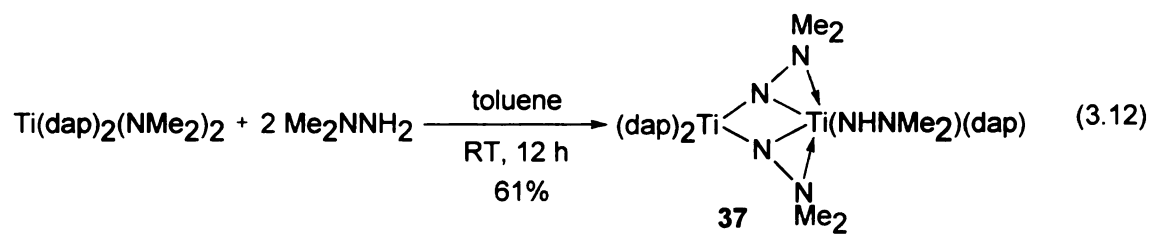
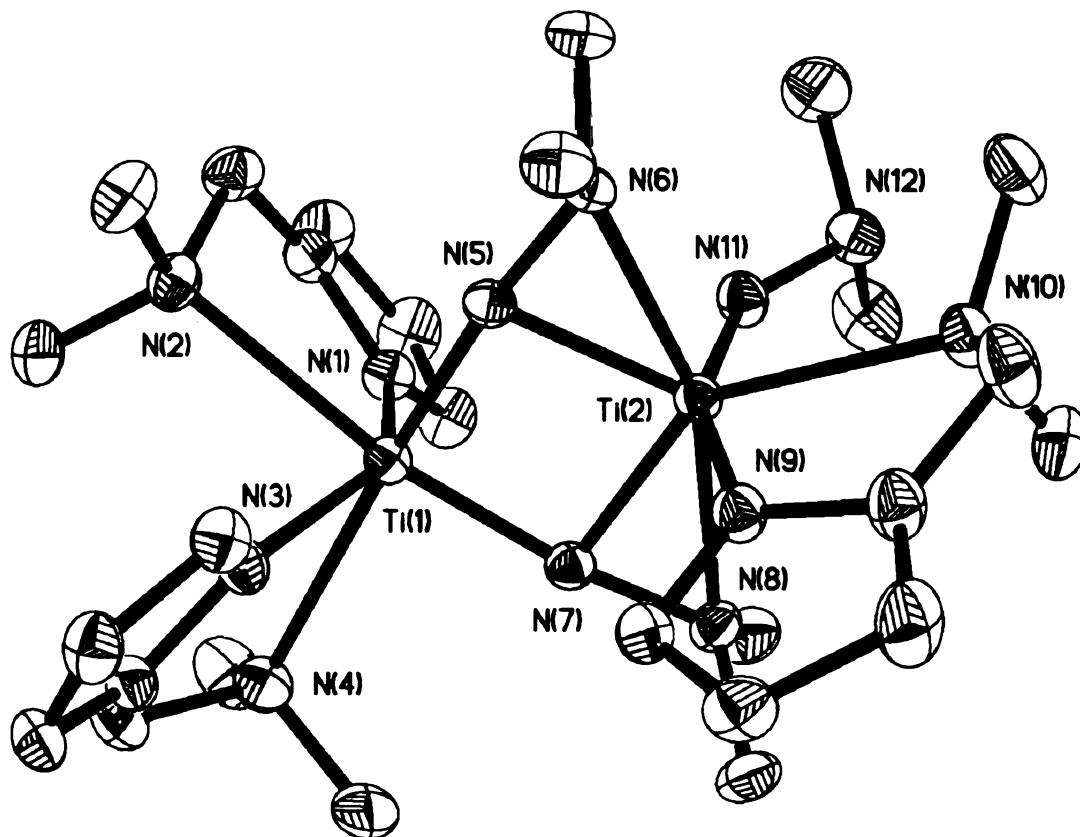


Figure 3.4 ORTEP representation of $\text{Ti}_2(\text{dap})_3(\mu_2:\eta^1, \eta^2\text{-NNMe}_2)_2(\mu_1:\eta^1\text{-NHNMe}_2)$ (37) at 50% probability level.



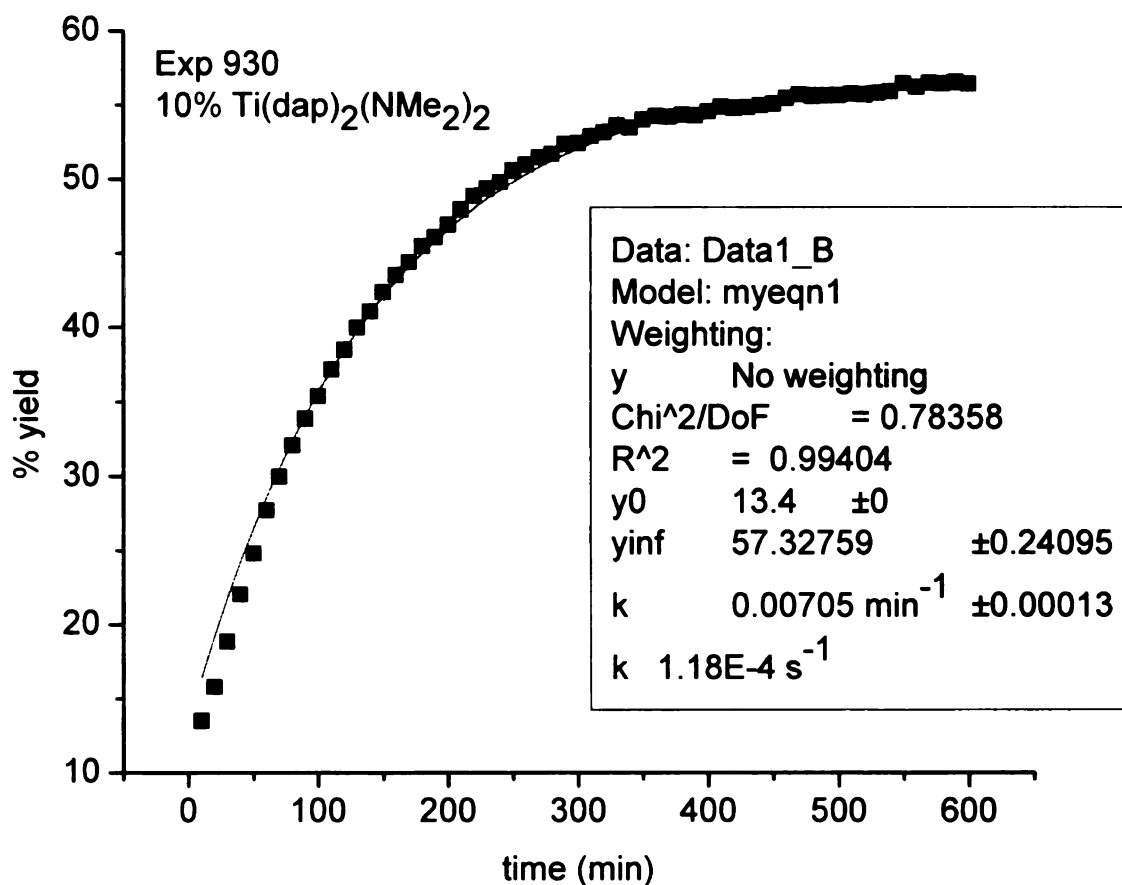
3.3.3 Kinetic studies

To further elucidate the role of **36** in the iminohydrazination reaction, the rate of the catalysis with **36** was studied and compared to the rate observed with **1**. The reactions were monitored using ^1H NMR setting the probe temperature at 100 °C for 10 h. The overall yield of the reaction varied from 55–100% depending on the type of the reactions studied (Table 3.2). The progress of the reaction was monitored vs time with respect to an internal standard. The percent yield of the product is plotted vs time, and the data are fit to a first order equation using the scientific graphing program OriginPro 7.5. The equation used for the plots was $Y_t = Y_{inf} + (Y_0 - Y_{inf}) \times \exp(-k_{obs}t)$ where Y_{inf} = product yield at time infinity, Y_0 = product yield at initialization, and k_{obs} = the rate constant, t = time in minute, and Y_t = amount of the product formed at time t .⁴¹ The rates are based on the average of four kinetic runs, and the error is calculated to the 99% confidence limit. The results of the kinetic experiments are shown in Table 3.2.

The rate of the reaction was studied using 10 mol% of $\text{Ti}(\text{dap})_2(\text{NMe}_2)_2$ (**1**), as shown in Case A in Table 3.2. A graph of percent yield versus time (min) has been plotted, and a representative plot is shown in Figure 3.5. The k_{obs} value was found to be $(1.07 \pm 0.42) \times 10^{-4} \text{ s}^{-1}$. The remaining plots are shown in Appendix B (Figures B1.1 to B1.3). It is noteworthy that the yield of the reaction was only 55–60%. The relatively low yield for this reaction is due to the formation of the titanium dinuclear complex **37**, which is not

kinetically competent (*vide infra*). The in situ generation of this complex deactivates the precatalyst **1**, which may be the reason for the low product formation.

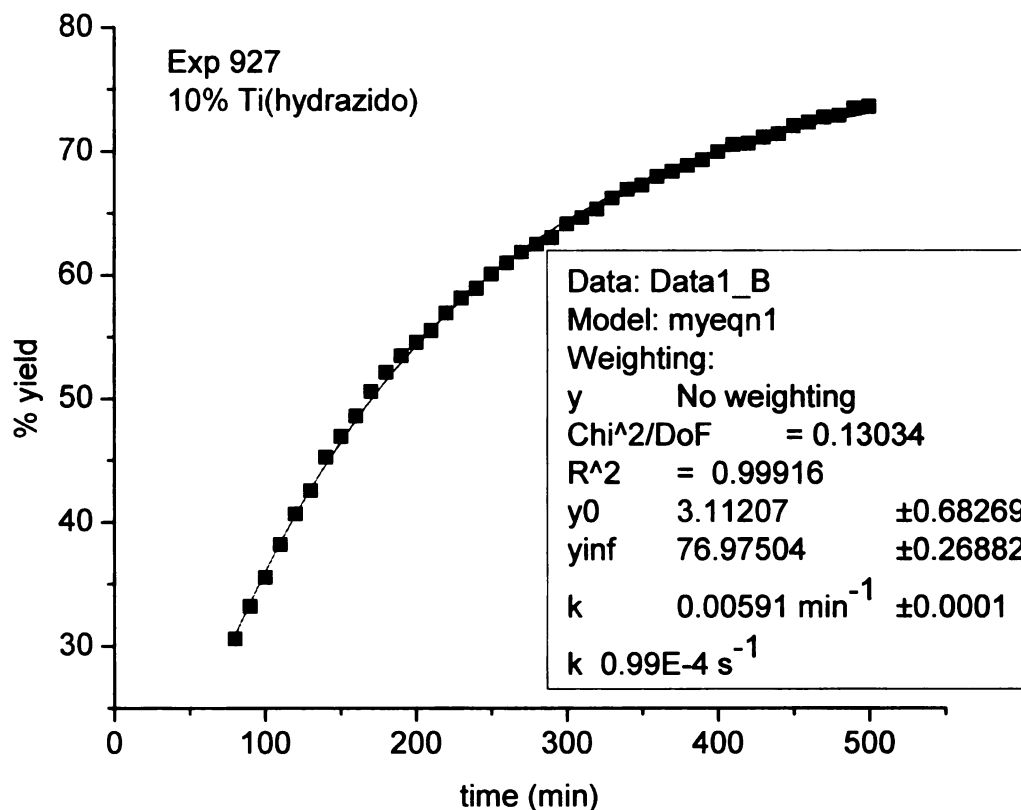
Figure 3.5 Representative plot for the catalysis with $\text{Ti}(\text{dap})_2(\text{NMe}_2)_2$ (**1**).



The intermediacy of the titanium hydrazido(2-) complex **36** in the catalytic cycle was probed by studying the reaction as shown in Case B in Table 3.2. A graph of percent yield versus time (minute) is shown in Figure 3.6. The individual plots for the other reactions are given in Figures B2.1 to B2.3. The k_{obs} value for **36** was determined to be

$(0.98 \pm 0.11) \times 10^{-4} \text{ s}^{-1}$. The rate constants for catalysis involving **36** are similar to those of **1** within the error range. This suggests that **36** is an intermediate of the reaction. Based on all these observations, we propose that the mechanistic pathway for iminohydrazination reaction involves the following steps prior to the formation of **36**: i) formation of η^1 -hydrazido(2-) intermediate, ii) [2 + 2]-cycloaddition of alkyne, iii) 1,1-insertion of isonitrile and proton transfer to generate **36**. Compound **36** was generated at *room temperature*, and it contains one molecule of the product as a ligand. The required temperature for the iminohydrazination reactions was 100 °C. This suggests that all the steps prior to the formation of **36** are fast, and the protonolysis step to liberate the final product is the slowest step in the formation of the iminohydrazination product.

Figure 3.6 Representative plot for the catalysis with **36**.



To further verify this mechanism, the reaction of **36** with 10 equivalents of 1,1-dimethylhydrazine was studied kinetically (Case C, Table 3.2). A graph of percent yield versus time (min) is shown in Figure 3.7. The value of k_{obs} was found to be $(1.11 \pm 0.30) \times 10^{-4} \text{ s}^{-1}$. This suggests that the protonolysis step is the rate determining for the reaction. Once again, the plots for the other reactions are in the appendix (Figures B3.1 to B3.3).

Figure 3.7 Representative plot for the reaction of **36** with 1,1-dimethylhydrazine.

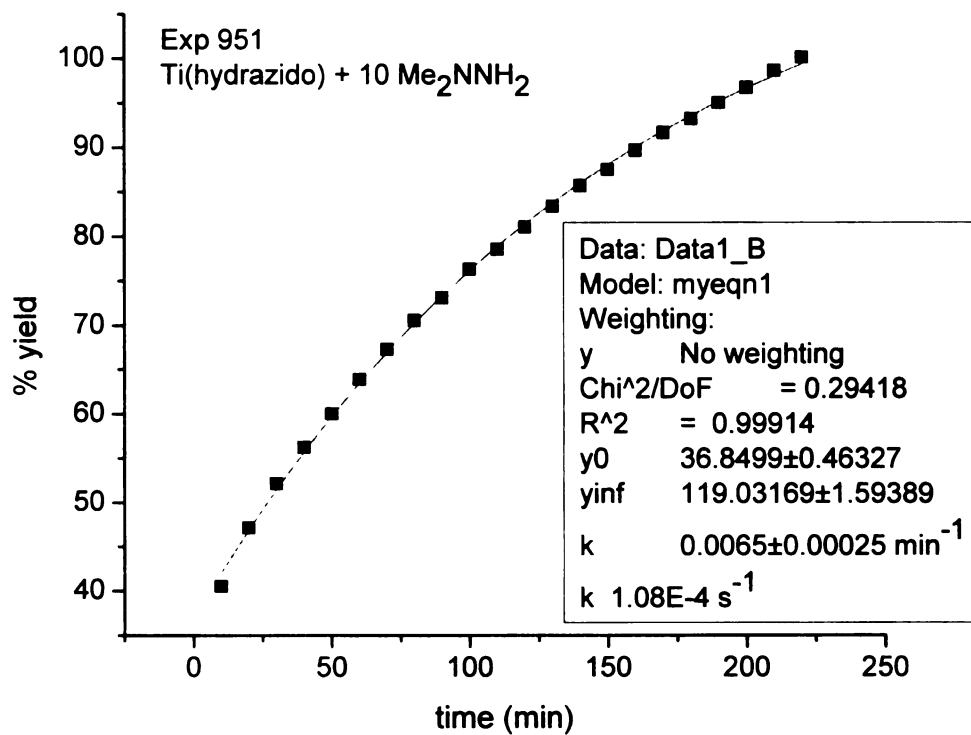
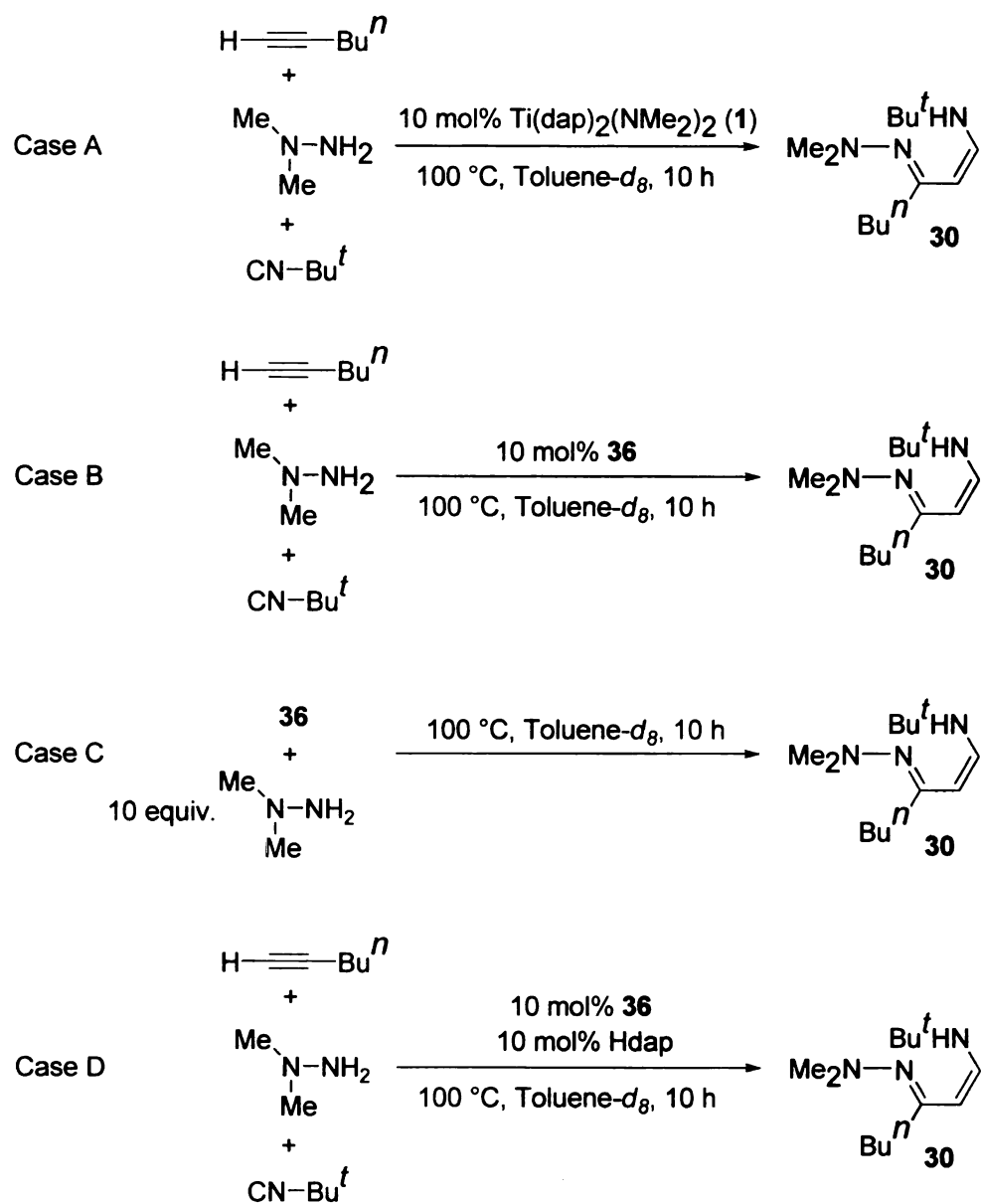


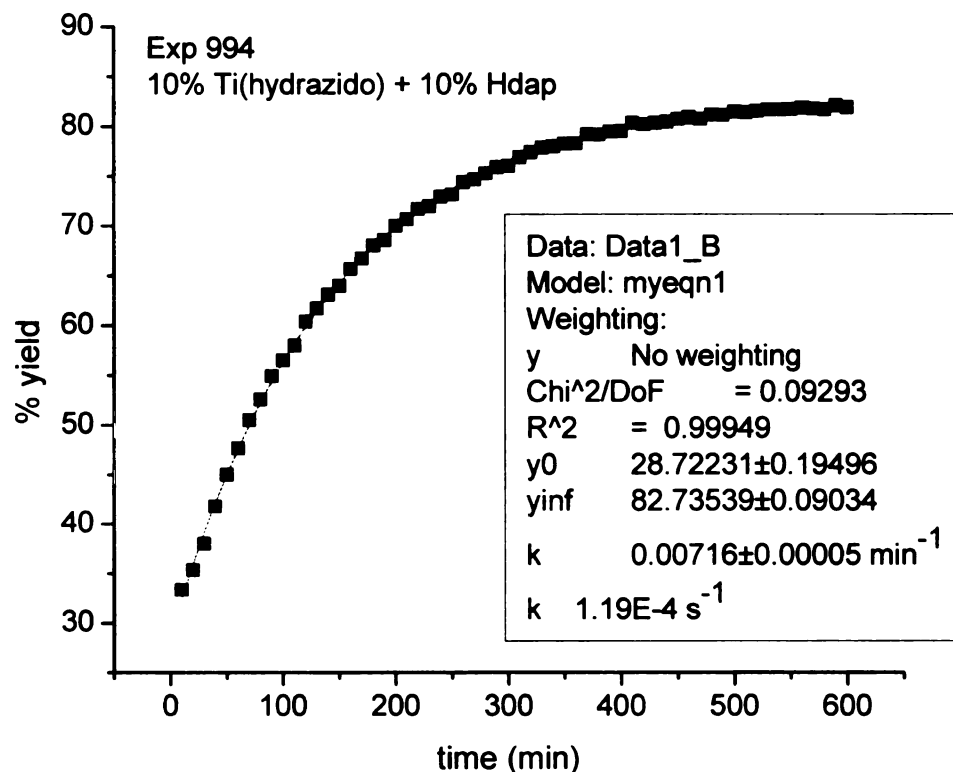
Table 3.2 Rate Constants and conditions for kinetic experiments



Reaction	concentration (M)			k_{obs} ($\times 10^{-4} \text{ s}^{-1}$)
	Catalyst	Hdap	Me_2NNH_2	
Case A	0.06	—	0.6	1.07 ± 0.42
Case B	0.06	—	0.6	0.98 ± 0.11
Case C	0.06	—	0.6	1.11 ± 0.30
Case D	0.06	0.06	0.6	1.19 ± 0.23

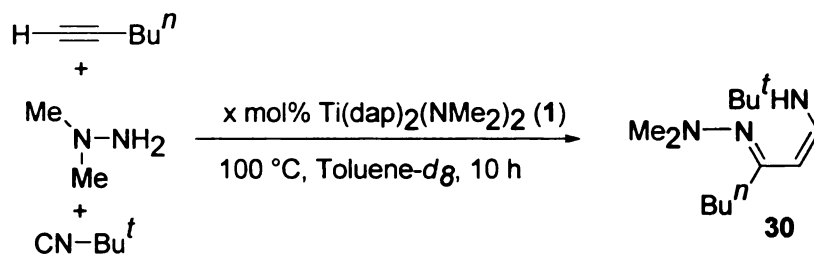
The precatalyst **1** contains two dap ligands. Interestingly, in the intermediate **36**, only one dap ligand is present. This suggests that one dap is lost prior to the formation of **36** and was present in the reaction medium. Hence we investigated the effect of excess Hdap on the rate of the catalysis. Kinetic reactions were carried out as shown in Case D, Table 3.2. The plots are shown in Figure 3.8 and Figures B4.1 to B4.3. The value of k_{obs} was found to be $(1.19 \pm 0.23) \times 10^{-4} \text{ s}^{-1}$. This is similar to the k_{obs} value of Case A in Table 3.2 within error, where the catalysis involves precatalyst **1**. This indicates that there is essentially no effect of additional Hdap ligand on the reaction rate.

Figure 3.8 Representative plot for the catalysis with 10 mol% of **36** and Hdap.

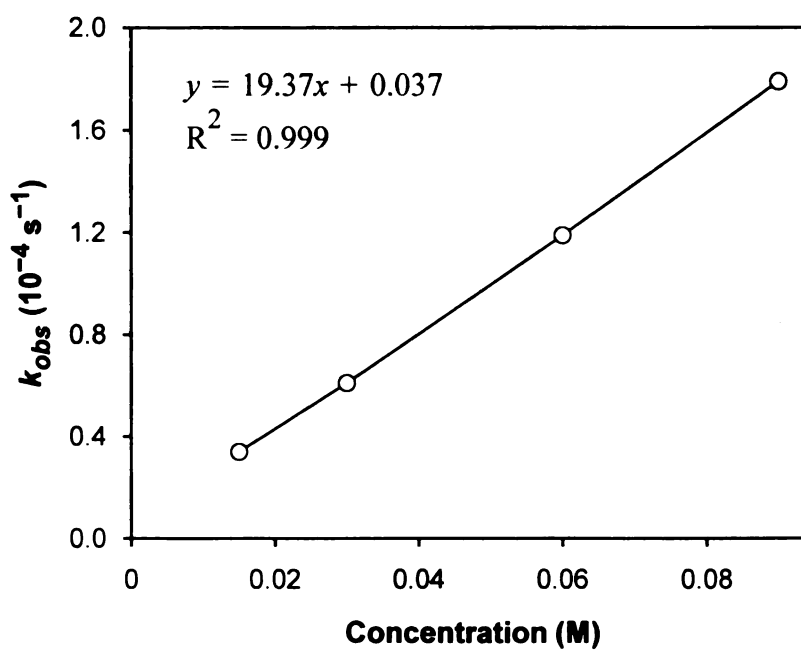


The intermediacy of dinuclear compound **37** in the catalytic cycle was also investigated. The reactions were carried out in a similar way to Case A, Table 3.2. However, compound **37** yielded only 22% of the desired product, and the k_{obs} value for this reaction was $4.8 \times 10^{-6} \text{ s}^{-1}$ (Figure B5.1). This shows that compound **37** is not kinetically competent to be involved in catalysis involving **1**. Instead, **37** is perhaps a mode of catalyst deactivation.

The dependence of the reaction rate on catalyst concentration was also studied. The reactions were carried out using the conditions in Table 3.3. The progress of the reactions was plotted vs time, and the resulting k_{obs} values are shown in Table 3.3 (Figures B6.1, B6.2, B6.3). Next, the individual k_{obs} values were plotted vs catalyst concentration (M). A straight line is obtained with $R^2 = 0.999$ (Figure 3.9), suggesting a first order dependence of k_{obs} on catalyst concentration.

Table 3.3 Observed rate constant vs catalyst concentration

Entry	X mol%	Catalyst conc. (M)	$k_{obs} (\times 10^{-4} \text{ s}^{-1})$
1	15	0.09	1.79
2	10	0.06	1.19
3	5	0.03	0.61
4	2.5	0.015	0.34

Figure 3.9 Dependence of k_{obs} on catalyst concentration

3.3.4 Overall mechanism for Iminohydrazination reaction

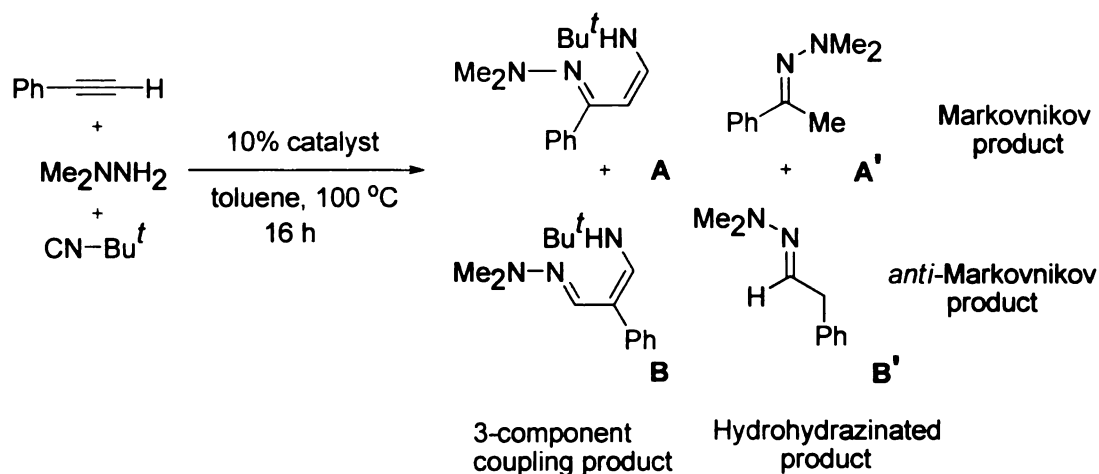
For iminohydrazination, the proposed catalytic cycle begins with the generation of a titanium hydrazido(2-) complex, followed by [2 + 2]-cycloaddition to generate an azametallacyclobutene intermediate, which after protonolysis yields the hydrohydrazination product (Scheme 3.3). Isonitrile insertion forms a 5-membered metallacycle, which, following a proton rearrangement, yields the isolable titanium hydrazido(2-) complex **36**. Compound **36** undergoes protonolysis at 100 °C with Me₂NNH₂ to yield the product regenerating the active species.

3.3.5 Experimental observations on regioselectivities

The multicomponent reaction between phenylacetylene, 1,1-dimethylhydrazine, and *tert*-butylisonitrile generated both hydrohydrazination and iminohydrazination products. Moreover, the products were obtained as mixture of regioisomers. The ratios of the isomers were obtained from the GC/FID of the crude reaction mixture (Table 3.4). In all these reactions, the *anti*-Markovnikov product was the major product with the phenyl group in the 2-position of the 1,3-hydrazonylimine (same as Entry 5, Table 3.1). The reaction was repeated six times using **1** as catalyst. The ratio of iminohydrazination products was found to be 0.453 ± 0.117 (99% confidence level, $n=5$), with the range from 0.351 to 0.510. In the same experiment, the ratio of hydrohydrazination products was found to be 0.442 ± 0.339 (99% confidence level, $n=5$), with the range from 0.236 to 0.750. The ranges were fairly large; however, the product ratios are sensitive to the

structure of the ligand present on the catalyst. For example, *anti*-Markovnikov product has been obtained exclusively when **28** is used instead of **1** for the above reaction.

Although the errors are relatively large, the mean values are very close. This suggests that the ratio of different isomers is nearly the same for both iminothiazination and hydrothiazination reactions. The similar ratios are associated with the regiochemistry prior to the protonolysis or 1,1-insertion, i.e., associated with the [2 + 2]-cycloaddition and/or alkyne coordination step. This is consistent with the recent assertion by the Beller group that titanium hydroamination regioselectivities correlate with the alkyne coordination regioselectivities.⁴² The equilibrium between the two azatitanacyclobutenes forms the regioisomers for both iminothiazination and hydrothiazination products. Therefore, the mean values are remarkably close. The relative rates of trapping for the azatitanacyclobutene by proton (protonolysis) or *tert*-butylisocyanide (1,1-insertion of isocyanide) are different leading to the slight difference in the ratios of the products (hydrothiazination vs iminothiazination). Changing the ancillary ligand set on titanium greatly affects the product ratios. In particular, the *anti*-Markovnikov product is obtained exclusively when **28** is used instead of **1**. But the iminothiazination and hydrothiazination products are obtained in the same ratio as obtained for **1** (the observed ratios between 3-component coupling product and hydrothiazinated product are 4:1 for **1**, and 3.2:1 for **28**). This suggests that the [2 + 2]-cycloaddition step is dramatically affected by changing the ancillary ligand set but relative rates of protonolysis or 1,1-insertion of isocyanide are not affected much.

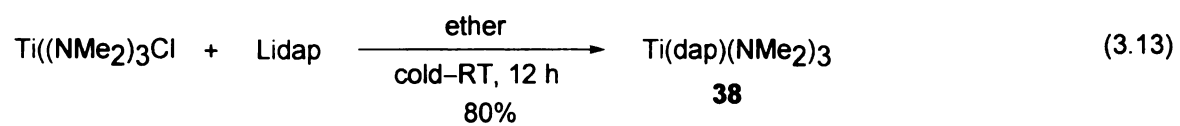
Table 3.4 Iminohydrazination of phenylacetylene by different catalysts

Catalyst	[A] / [B]	[A'] / [B']
1	0.453 ± 0.117	0.442 ± 0.339
36	0.558	0.364
38	0.478	0.238

We also note that the observed ratios of the regioisomers for iminohydrazination and hydrohydrazination products using **36** as catalyst are 0.558 and 0.364 respectively (Table 3.4). This is comparable to the ratios obtained using **1** (Table 3.4). This suggests that **36** is also an effective catalyst for this iminohydrazination reaction.

The structure of **36** reveals that it has one dap ligand attached to the titanium center. So the actual catalytically active species might involve only one dap ligand on titanium. To verify this, a new molecule $\text{Ti}(\text{dap})(\text{NMe}_2)_3$ (**38**) was synthesized by adding Lidap to $\text{Ti}(\text{NMe}_2)_3\text{Cl}$ (Equation 3.13). The catalytic activity of **38** was compared with **1** by comparing the ratios of the regioisomers for the reactions shown in Table 3.4. The ratios for the iminohydrazination and hydrohydrazination products are found to be 0.478 and

0.238. These are again comparable to the product ratios obtained for **1** as the precatalyst. Therefore, the active species might involve a titanium center carrying only one dap ligand.

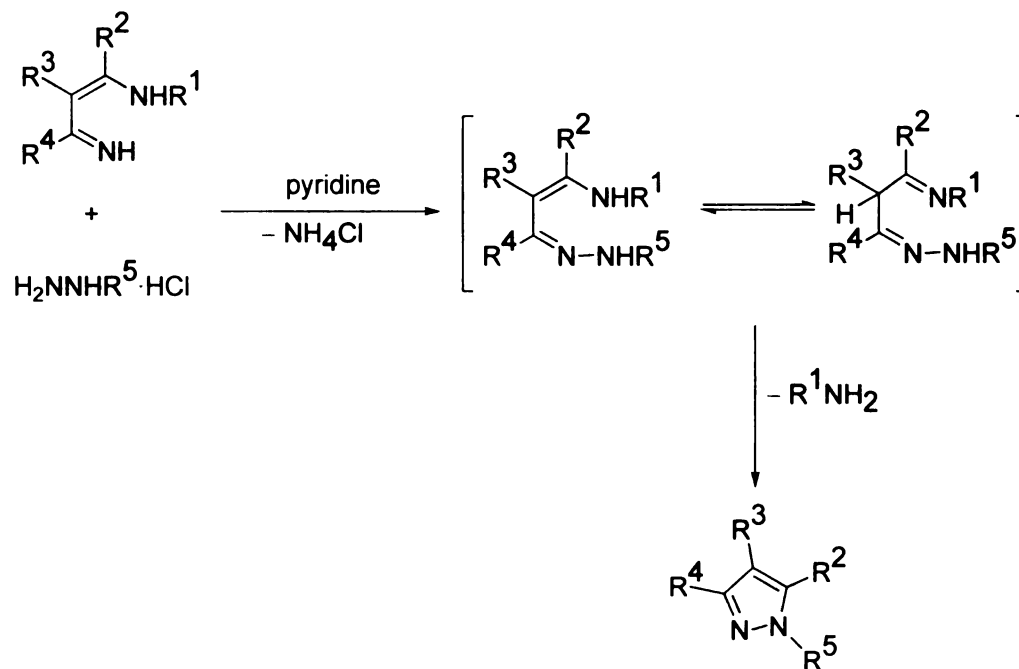


3.4 Applications of the Iminohydrazination reaction towards the synthesis of pyrazoles

3.4.1 Background information

The products of iminohydrazination reactions are basically α,β -unsaturated β -aminohydrazones. Barluenga and co-workers have shown the formation of different heterocycles starting from 4-amino-1-azabutadienes (in other words, α,β -unsaturated β -aminoimines) as shown in Scheme 3.4.⁴³⁻⁴⁵

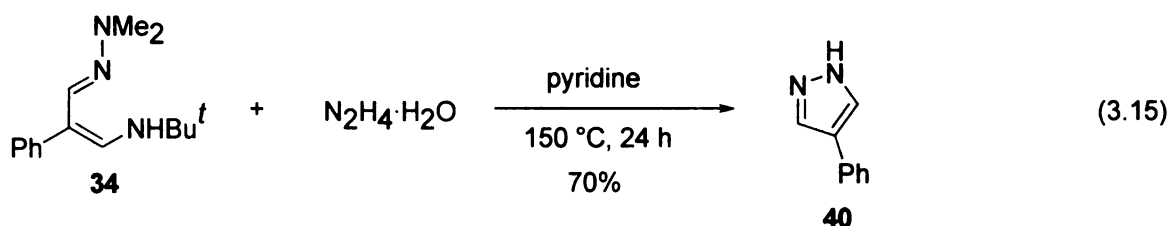
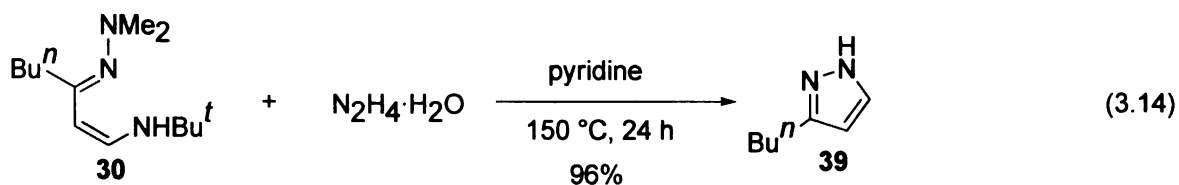
Scheme 3.4 Synthesis of pyrazole from 4-amino-1-azabutadienes



We have been exploring similar reactions with our iminohydrazination products.

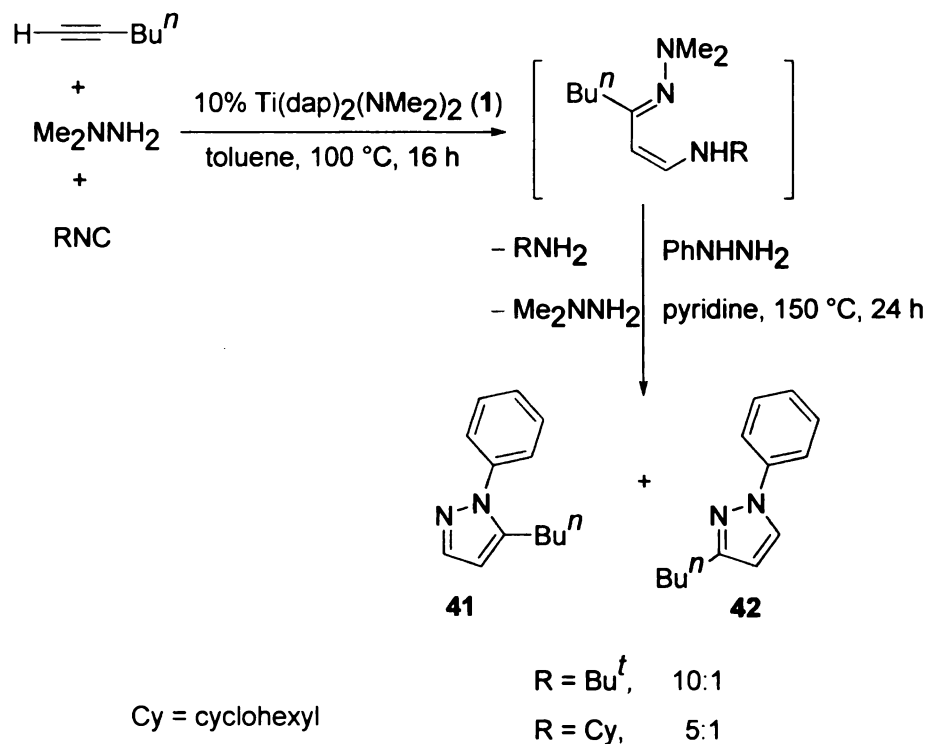
3.4.2 Results and Discussion

The isolated 3-component coupling product from iminohydrazination was allowed to react with $\text{N}_2\text{H}_4 \cdot \text{H}_2\text{O}$ at 150 °C for 24 h in pyridine (Equations 3.14 and 3.15). In these cases only one pyrazole product was obtained in good to excellent yield.



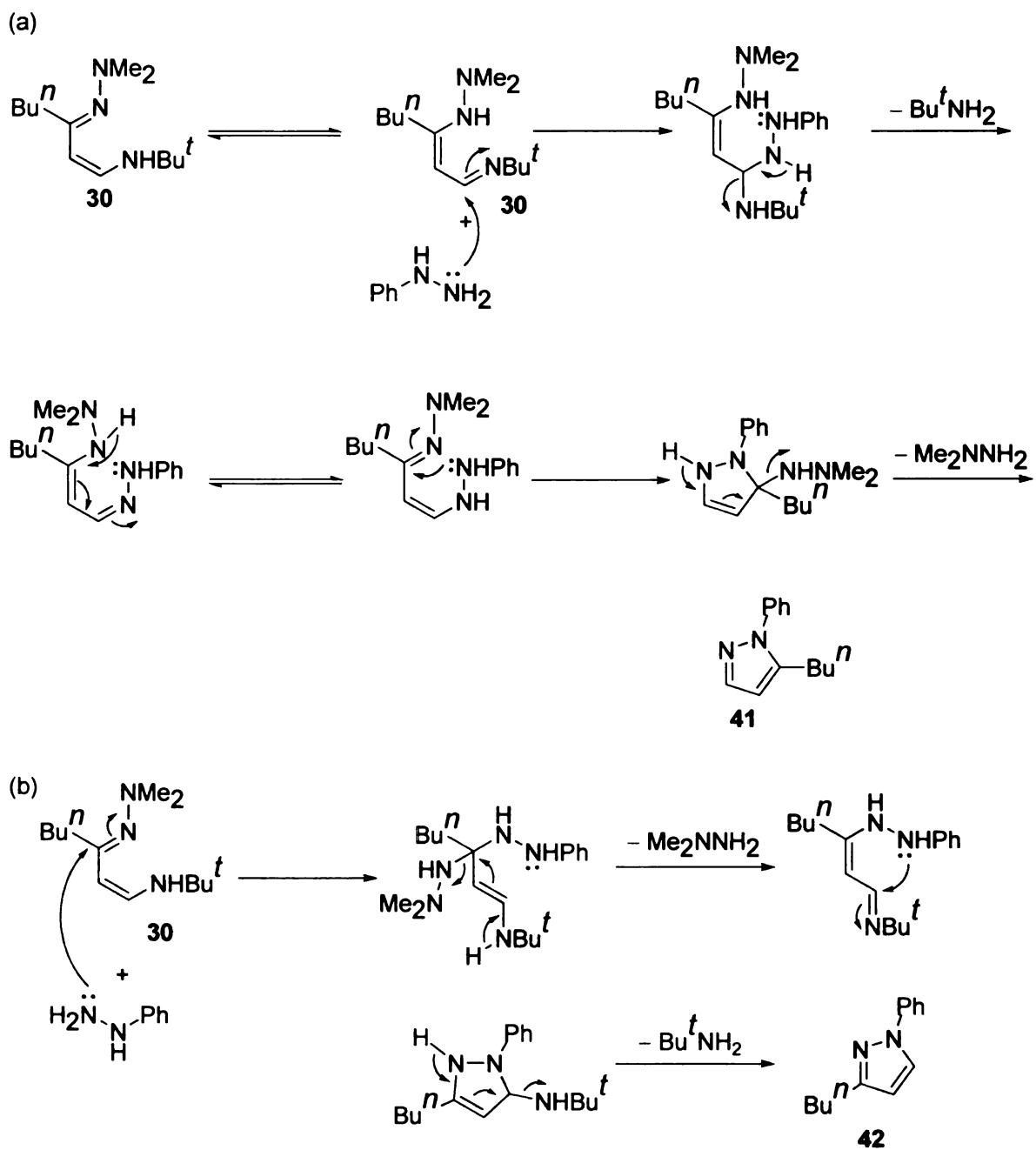
To investigate the mechanism of this reaction, we performed the reaction of compound **30** with phenylhydrazine where there is the possibility of forming two different pyrazoles. Both the titanium-catalyzed reaction and the cyclization with phenylhydrazine were carried out in a one-pot procedure (Scheme 3.5). Two different isomers were obtained in 10:1 ratio (using Bu^tNC) under the specified reaction conditions.

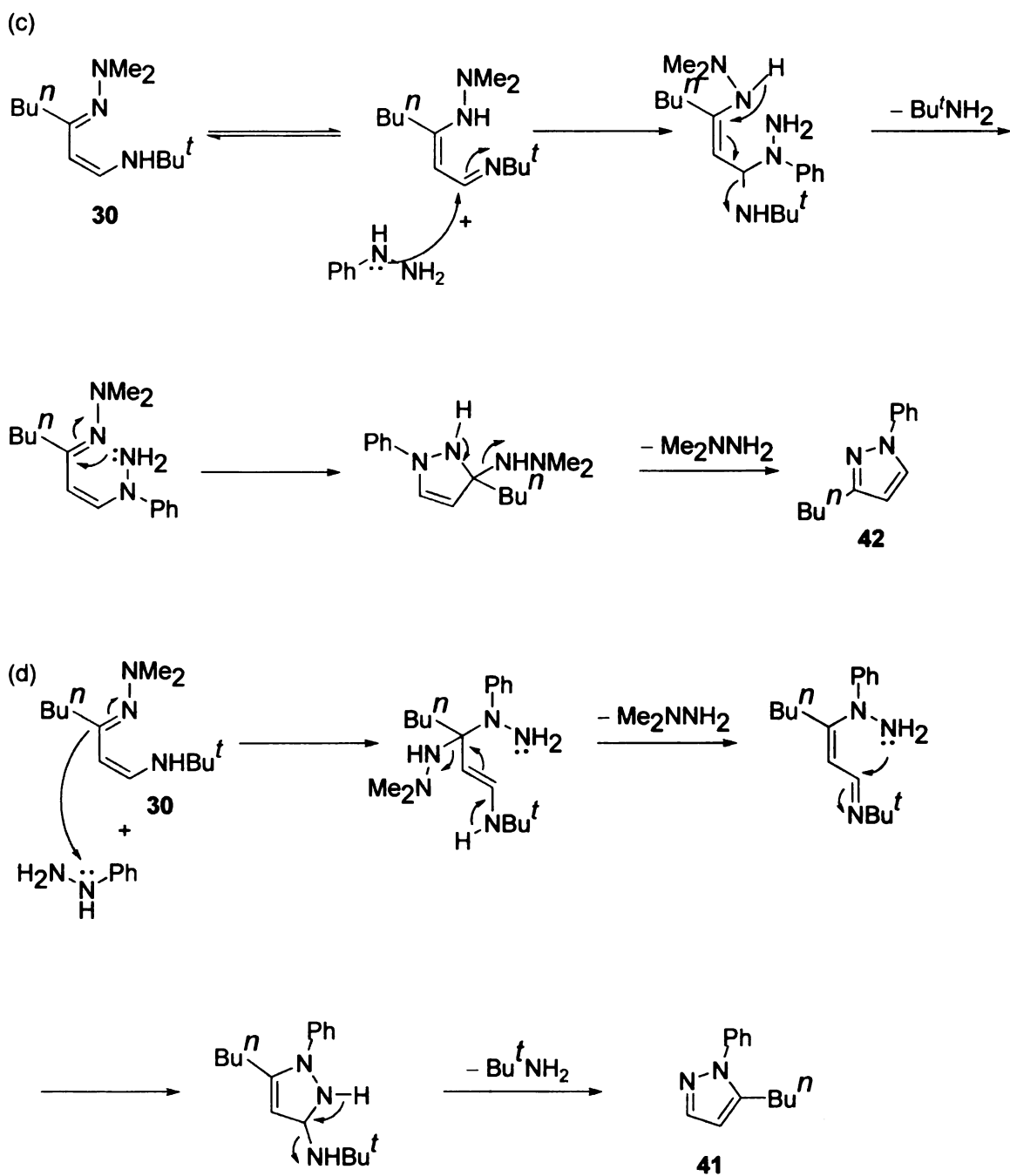
Scheme 3.5 Synthesis of *N*-phenyl-5-*n*-butylpyrazole and *N*-phenyl-3-*n*-butylpyrazole



Mechanistically, the formation of the products can be understood by considering four different modes of attack of the two nitrogen atoms on phenylhydrazine (Scheme 3.6) However, among these four possibilities, pathways (a), and (c) are more likely from the steric point as well as the nucleophilic attack by phenylhydrazine can be considered as 1,4-addition to α,β -unsaturated imine.

Scheme 3.6 Possible mechanistic pathways for the pyrazole formation





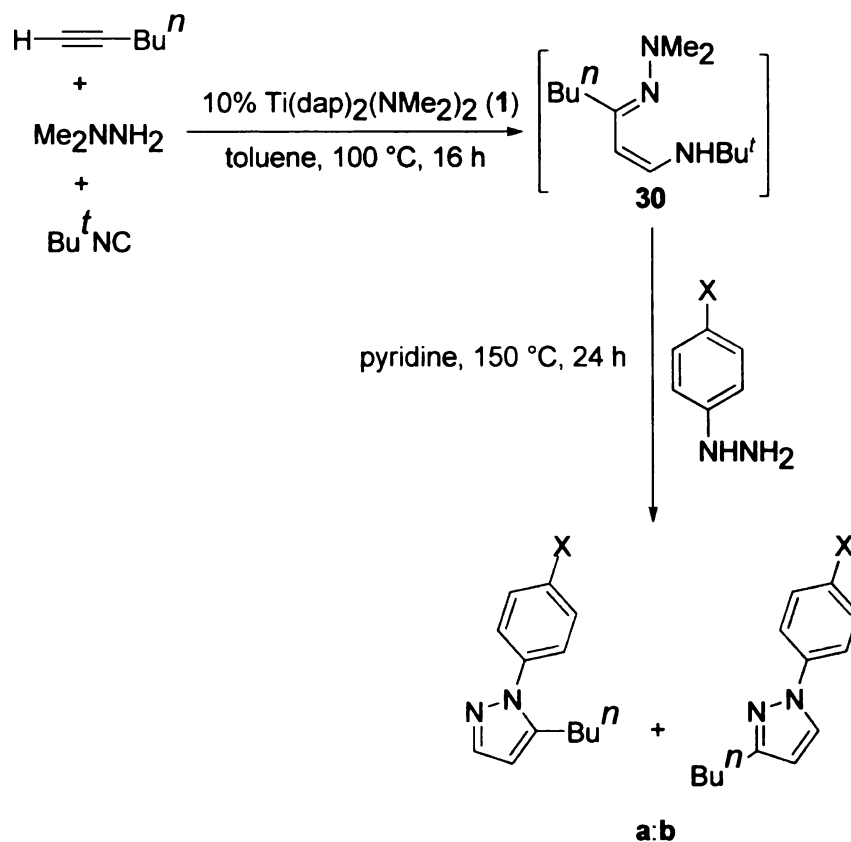
From the observed ratio of the products in Scheme 3.5, it is clear that the major product has been obtained following pathway (a) under the conditions of the reaction. In (a), phenylhydrazine attacks on the carbon atom coming from the isonitrile group as

opposed to the other carbon atom adjacent to dimethylhydrazine in the 3-component coupling product (pathway (b)).

We further wanted to explore the effect of isonitrile sterics on the mode of attack shown in (a). For this, we carried out reactions with two different isonitriles as shown in Scheme 3.5. Since a cyclohexyl group is smaller in size than a *tert*-butyl group, the ratio of the pyrazole products should change if steric factor is important. From the experimental data, we observed similar product ratios for both of them. This indicates that there is no obvious effect of isonitrile sterics in the cyclization step.

We also carried out experiments to discover how the electronics of the substituents on the phenyl ring affects the regioselectivity. For this, three different *para*-substituted phenylhydrazines were used, and the ratio of the corresponding pyrazole products was observed by ^1H NMR spectroscopy (Table 3.5).

Table 3.5 Effect of *p*-substituents on arylhydrazine on pyrazole formation



Entry	X	Ratio (a : b)
1	H	10:1
2	OMe	2:1
3	F	4.5:1
4	CN	1:6

From the data shown in Table 3.5, it is observed that isomer **a** is preferred when $\text{X} = \text{H}$. This can be explained following pathway (a) in Scheme 3.6. However, when $\text{X} = \text{OMe}$, substantial amount of isomer **b** (minor) is produced along with **a** (major). This can be explained following pathway (c) in Scheme 3.6, which includes the attack by α -

nitrogen atom of arylhydrazine. This can happen due to the π -donor ability of OMe group. So the observed ratio of the products **a**:**b** is 2:1. When X = F, it has both electron withdrawing effect and π -donor ability. This makes α -nitrogen atom sufficiently nucleophilic so that isomer **b** can be formed following pathway (c). But the selectivity is more than the case when X = OMe since F also has electron withdrawing effect, which produces isomer **a** according to pathway (a). When X = CN, which has both electron withdrawing effect and π -accepting ability, formation of isomer **b** is favored. This can be due to the attack by α -nitrogen atom of arylhydrazine following pathway (c). In this case, α -nitrogen is preferred over β -nitrogen in arylhydrazine because the hydrogen on α -nitrogen is more acidic due to the presence of *p*-CN group.

3.5 Multicomponent Coupling Reactions of alkynes, monosubstituted hydrazines, and isonitriles

After the success of using a tetradentate ligand (H₂enp, **4**) on titanium(IV) for hydrohydrazination of alkynes with monosubstituted hydrazines (discussed in Chapter 2), we have attempted application of this ligand framework towards 3-component couplings with isonitriles. Unfortunately, multicomponent coupling reactions of alkynes, monosubstituted hydrazines, and isonitriles did not produce the expected 3-component coupling product using Ti(enp)(NMe₂)₂ (**5**) as precatalyst. Instead, only hydrohydrazination products were obtained. Therefore, we have screened other catalysts for this transformation.

We have observed (Scheme 3.3) that the active species in the iminohydrazination reaction contains only one dap attached to the metal center. Hence, one dap is protolytically labile under the reaction conditions. The presence of the tetradentate enp is possibly inhibiting the formation of species that would be active for 3-component coupling. The enp ligand on the metal center forms a stable five-membered metallacycle with titanium, and it may be difficult to remove one of the pyrrolyl groups. So, we decided to investigate the effect of the Hdap^{3-mes} ligand on titanium(IV), and its catalytic efficiency for the 3-component coupling reaction with monosubstituted hydrazines.

Hdap^{3-mes} (**43**) was synthesized as shown in Scheme 3.7. At first, Boc-pyrrole was borylated at the 3- position using Smith borylation,⁴⁶ followed by Suzuki coupling⁴⁷ in the presence of catalytic Pd(PPh₃)₄ (Boc is *tert*-butyloxycarbonyl). The next step was

removal of BOC-group by heating the reaction mixture at 100 °C for 24 h in BuⁿOH and excess K₃PO₄·nH₂O (Scheme 3.7). All of these steps were carried out in a single pot. The final product, 3-mesitylpyrrole (**43**), was isolated in 85% overall yield. An ORTEP representation of the X-ray crystal structure of **43** is shown in Figure 3.10. The next step involved Mannich reaction with formaldehyde and dimethylamine hydrochloride in ethanol at 45 °C. The final product, Hdap^{3-mes} (**44**) was isolated in 89% yield.

Scheme 3.7 Synthesis of 3-mesitylpyrrole (**43**)

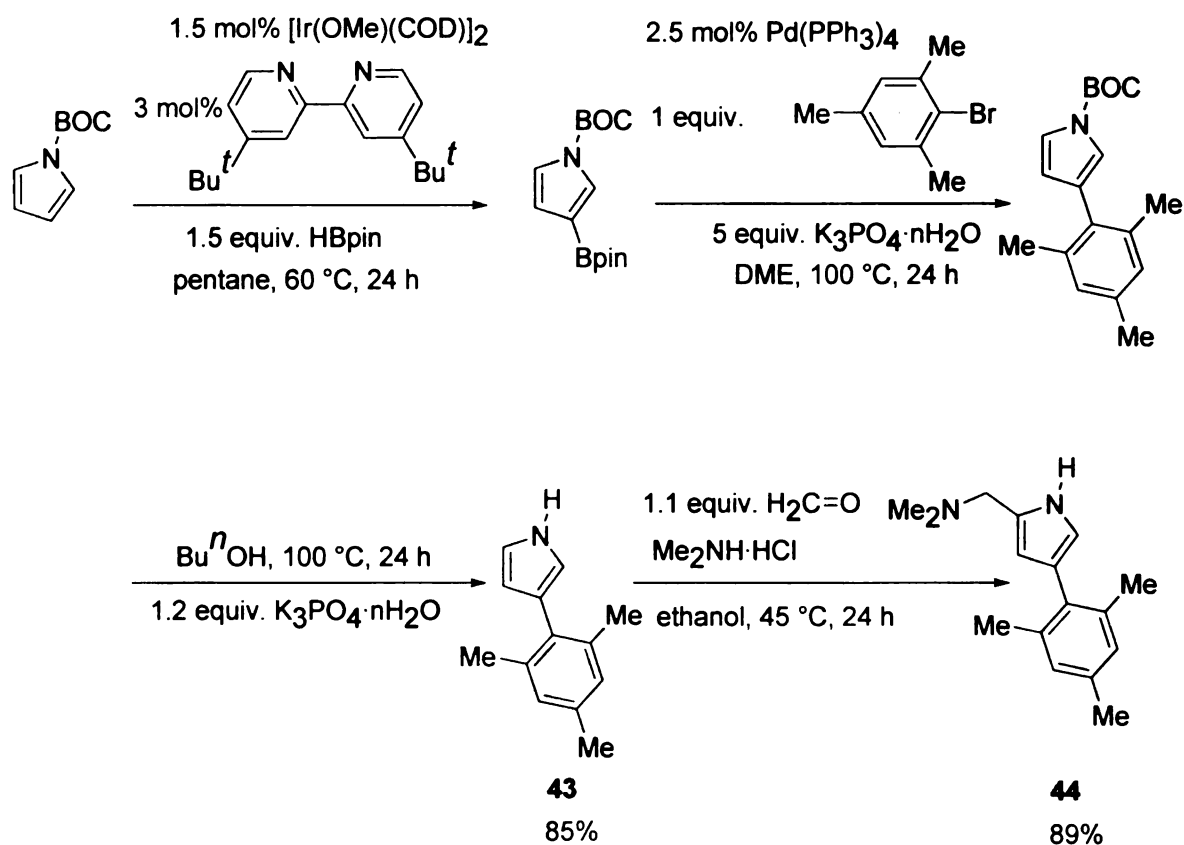
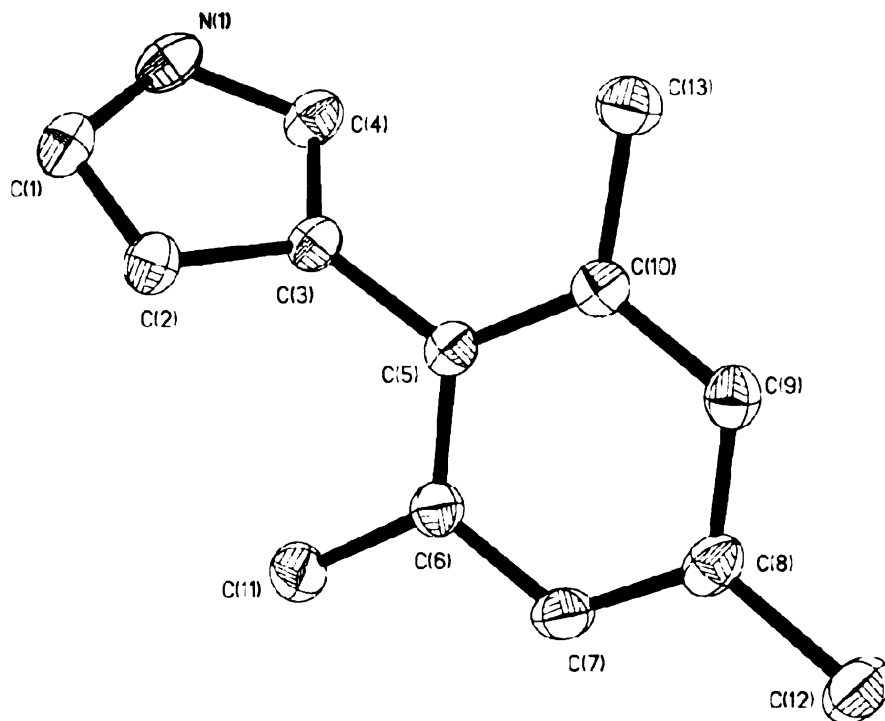
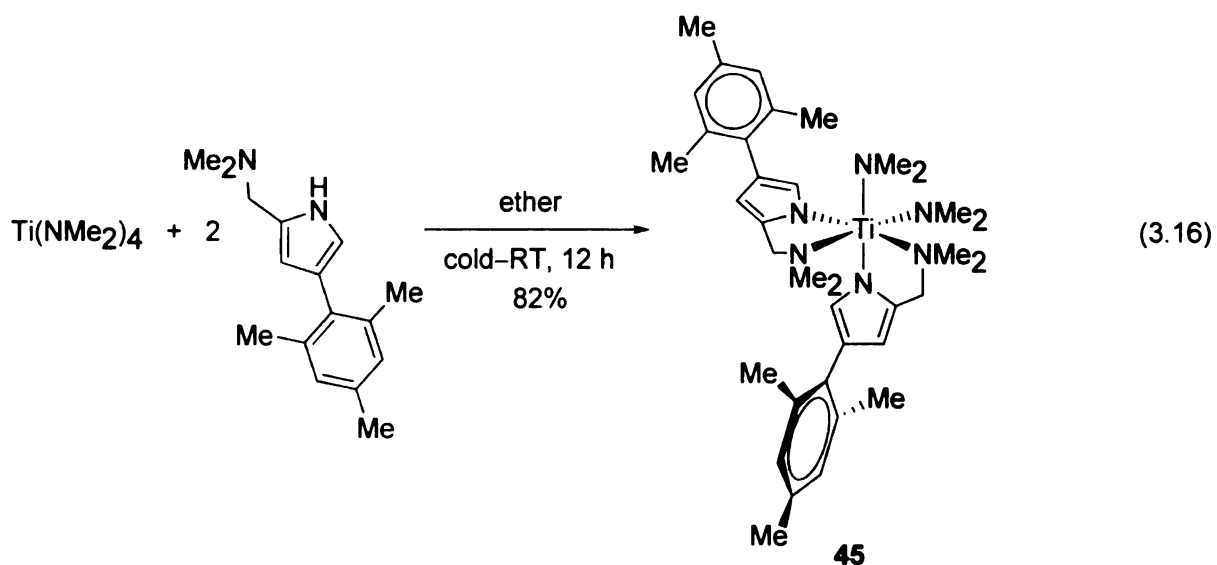


Figure 3.10 ORTEP representation of 3-mesitylpyrrole (**43**).

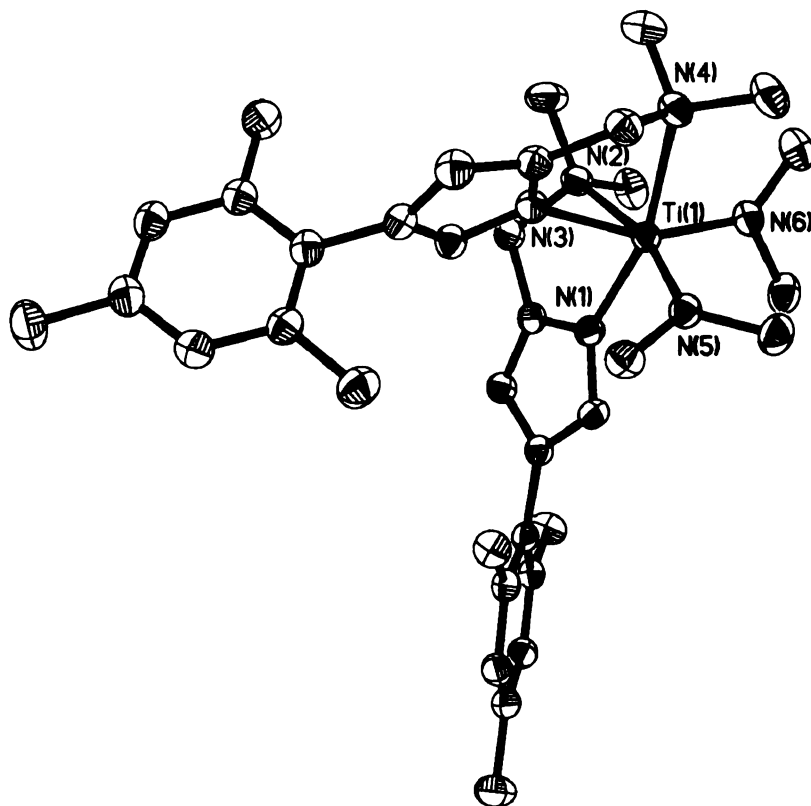


In the next step, the precatalyst $\text{Ti}(\text{dap}^{3\text{-mes}})_2(\text{NMe}_2)_2$ (**45**) was synthesized by adding two equiv of $\text{Hdap}^{3\text{-mes}}$ to $\text{Ti}(\text{NMe}_2)_4$, and the catalyst was isolated in 82% yield (Equation 3.16).



Complex **45** was also crystallographically characterized as shown in Figure 3.11. One of the amido groups has a pyrrolyl group in the *trans*-position instead of an amine donor nitrogen as might be expected (donor ability of the ligands are amido > pyrrolyl > amine). This might be due to the sterically bulky substituents present on the pyrrolyl group.

Figure 3.11 ORTEP representation of $\text{Ti}(\text{dap}^{3\text{-mes}})_2(\text{NMe}_2)_2$ (**45**). Selected bond lengths(Å) and bond angles(°) are: $\text{Ti}(1)\text{--N}(5) = 1.9076(15)$, $\text{Ti}(1)\text{--N}(6) = 1.9156(16)$, $\text{Ti}(1)\text{--N}(1) = 2.0548(15)$, $\text{Ti}(1)\text{--N}(3) = 2.1035(15)$, $\text{Ti}(1)\text{--N}(4) = 2.4276(15)$, $\text{Ti}(1)\text{--N}(2) = 2.5510(16)$, $\text{N}(5)\text{--Ti}(1)\text{--N}(6) = 100.08(7)$, $\text{N}(5)\text{--Ti}(1)\text{--N}(1) = 93.33(6)$, $\text{N}(6)\text{--Ti}(1)\text{--N}(1) = 105.75(6)$, $\text{N}(5)\text{--Ti}(1)\text{--N}(3) = 93.26(6)$, $\text{N}(6)\text{--Ti}(1)\text{--N}(3) = 157.45(7)$, $\text{N}(1)\text{--Ti}(1)\text{--N}(3) = 91.41(6)$, $\text{N}(5)\text{--Ti}(1)\text{--N}(4) = 90.41(6)$, $\text{N}(6)\text{--Ti}(1)\text{--N}(4) = 89.15(6)$, $\text{N}(1)\text{--Ti}(1)\text{--N}(4) = 163.71(6)$.



Unfortunately, three-component coupling of alkyne with monosubstituted hydrazine and isonitrile was not generally successful using **45** as the catalyst except for where phenylacetylene was used as the alkyne. Using phenylacetylene, two different products were formed; the uncyclized 3-component coupling product and the pyrazole (Equation 3.17). They were obtained in ~ 40% yield as observed by GC/FID. No reaction was

3.6 Concluding Remarks

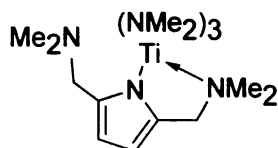
Alkynes have been successfully transformed into α,β -unsaturated β -aminohydrazones through multicomponent coupling of alkyne, 1,1-disubstituted hydrazine, and isonitrile. This reaction has been effectively catalyzed by titanium pyrrolyl-based catalysts. The reaction is quite general in the sense that it tolerates both terminal and internal alkynes with aliphatic and aromatic isonitriles. Mechanistically, the reaction involves a titanium hydrazido(2-) complex **36** as the intermediate (Scheme 3.3). The reaction also involves the formation of a titanium dinuclear species **37**, which is not kinetically competent for the iminohydrazination reaction. Consequently, the catalyst concentration may be constantly changing during these catalyses. However, with the available data from the kinetic experiments, the mechanism can be envisioned as follows: the formation of the product involves a hydrazido(2-) intermediate, followed by [2 + 2]-cycloaddition of alkyne to form an azatitanacyclobutene. This cycloaddition is followed by 1,1-insertion of isonitrile forming a new Ti-C bond. The five-membered metallacycle then undergoes intramolecular proton transfer to form the isolable intermediate **36**. Compound **36** finally undergoes protonolysis by hydrazine forming the 3-component coupling product (Scheme 3.3). The reaction has also been efficiently applied to the synthesis of different pyrazoles by adding hydrazine to the 3-component coupling product.

3.7 Experimental

General Considerations

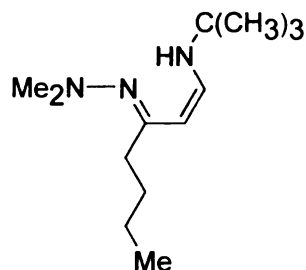
All manipulations of air sensitive compounds were carried out in an MBraun drybox under a purified nitrogen atmosphere. All the solvents were purified according to the standard procedure. Hydrazines were purchased from Aldrich Chemical Company and dried by distillation from KOH under dry nitrogen. Alkynes were distilled under dry nitrogen over CaO. $\text{Ti}(\text{NMe}_2)_4$,⁴⁸ $\text{TiCl}(\text{NMe}_2)_3$,⁴⁹ Hdap,²⁵ Hbap,²⁷ *tert*-butyl isonitrile,⁵⁰ and 2,6-xylyl isonitrile⁵¹ were prepared using the literature procedures. Lidap was prepared by addition of 1.1 equivalents of LiBu^n to a toluene solution of Hdap; the Lidap was collected by filtration and washed with pentane to afford the colorless product. Cyclohexyl isonitrile was purchased from Aldrich Chemical Company and distilled under dry nitrogen prior to use. Deuterated solvents were dried over purple sodium benzophenone ketyl (C_6D_6) or phosphoric anhydride (CDCl_3) and distilled under nitrogen. ^1H and ^{13}C spectra were recorded on Inova-300 or VXR-500 spectrometers. ^1H and ^{13}C assignments were confirmed when necessary with the use of two-dimensional ^1H - ^1H and ^{13}C - ^1H correlation NMR experiments. All spectra were referenced internally to residual protiosolvent (^1H) or solvent (^{13}C) resonances. Many common coupling constants are not listed. Chemical shifts are quoted in ppm and coupling constants in Hz.

Synthesis and characterization of Ti(bap)(NMe₂)₃ (28)



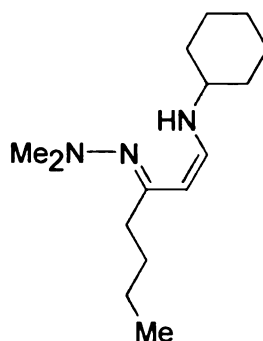
Under an atmosphere of dry nitrogen, a solution of Ti(NMe₂)₄ (2.000 g, 8.9 mmol) in ether (20 mL) was frozen in a liquid nitrogen cooled cold well. The solution was allowed to warm enough to be stirred. Then, a cold solution of Hbap (1.610 g, 8.900 mmol) in 10 mL ether was added to the above solution dropwise over a period of 20 min. It was allowed to warm up to room temperature and stir overnight. The volatiles were removed under vacuum. The solid was purified by crystallization as orange-red crystals from pentane (2.950 g, 8.200 mmol) in 92% yield. ¹H NMR (299.8 MHz, CDCl₃): 6.34 (s, 2 H, 3*H*-pyrrole), 3.48 (s, 4 H, CH₂), 3.13 (s, 12 H, CH₂N(CH₃)₂), 2.07 (s, 18 H, N(CH₃)₂). ¹³C{¹H} NMR (75.4 MHz, CDCl₃): 137.9, 106.9, 60.0, 47.1, 45.8. Elemental analysis; Experimental (Calc.), C: 53.19 (53.33). H: 10.09 (10.07). N: 22.82 (23.32). M.p. 118-120 °C.

Synthesis of compound 30



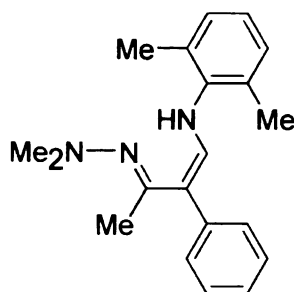
Under an atmosphere of dry nitrogen, a threaded pressure tube was loaded with toluene (6000 μ L), Ti(dap)₂(NMe₂)₂ (0.458 g, 1.200 mmol), 1,1-dimethylhydrazine (910 μ L, 12 mmol), 1-hexyne (1399 μ L, 12 mmol), and *tert*-butyl isocyanide (1355 μ L, 12 mmol). The tube was sealed with a Teflon cap and heated at 100 $^{\circ}$ C for 16 h. The solvent was removed under vacuum. The product was isolated by distillation under vacuum (\sim 65 $^{\circ}$ C, 0.65 torr) in 63% yield (1.702 g, 7.564 mmol) as red oil. ¹H NMR (299.8 MHz, CDCl₃): 9.82 (br s, 1 H, NH^c), 6.88 (d, 1 H, J_{HH} = 8.1 Hz, HNCH), 4.68 (d, 1 H, J_{HH} = 8.1 Hz, HNCHCH), 2.71 (m, 8 H, N(CH₃)₂ and N=CCH₂), 1.77 (m, 2 H, N=CCH₂CH₂), 1.64 (m, 2 H, N=CCH₂CH₂CH₂), 1.52 (s, 9 H, CCH₃), 1.17 (t, 3 H, J_{HH} = 8.0 Hz, C(CH₃)₃). ¹³C{¹H} NMR (75.4 MHz, CDCl₃): 171.5, 139.6, 89.5, 51.5, 48.9, 47.5, 31.2, 30.4, 23.1, 13.9. Elemental analysis; Experimental (Calc.), C: 69.41 (69.33). H: 12.35 (12.00). N: 18.85 (18.67). MS (EI) m/z = 225(M⁺).

Synthesis of compound 31



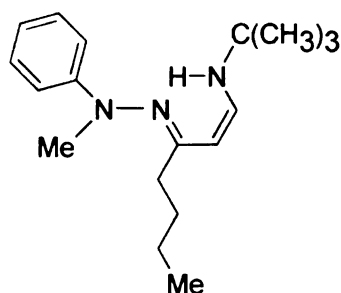
Under an atmosphere of dry nitrogen, a threaded pressure tube was loaded with toluene (6000 μ L), $\text{Ti}(\text{dap})_2(\text{NMe}_2)_2$ (0.457 g, 1.200 mmol), 1,1-dimethylhydrazine (910 μ L, 12 mmol), 1-hexyne (1399 μ L, 12 mmol), and cyclohexyl isocyanide (1790 μ L, 14.400 mmol). The tube was sealed with a Teflon cap and heated at 100 $^\circ\text{C}$ for 16 h. The solvent was removed under vacuum. The product was isolated by distillation under vacuum (\sim 110 $^\circ\text{C}$, 0.65 torr) in 73% yield (2.205 g, 8.785 mmol) as brown oil. ^1H NMR (299.8 MHz, CDCl_3): 9.61 (br s, 1 H, NH), 6.74 (d, 1 H, $J_{\text{HH}} = 8.1$ Hz, HNCH), 4.61 (d, 1 H, $J_{\text{HH}} = 8.1$ Hz, HNCHCH), 2.68 (m, 8 H, $\text{N}(\text{CH}_3)_2$ and $\text{N}=\text{CCH}_2$), 2.09-1.93 (m, 11 H, cyclohexyl), 1.73 (m, 2 H, $\text{N}=\text{CCH}_2\text{CH}_2$), 1.57 (m, 2 H, $\text{N}=\text{CCH}_2\text{CH}_2\text{CH}_2$), 1.14 (t, 3 H, $J_{\text{HH}} = 7.1$ Hz, CH_3). $^{13}\text{C}\{^1\text{H}\}$ NMR (75.4 MHz, CDCl_3): 171.9, 142.5, 89.9, 56.0, 49.8, 47.9, 34.8, 31.5, 26.2, 24.9, 23.0, 13.9. Elemental analysis; Experimental (Calc.), C: 71.71 (71.71). H: 11.96 (11.55). N: 16.80 (16.73). MS (EI) $m/z = 251(\text{M}^+)$.

Synthesis of compound 32



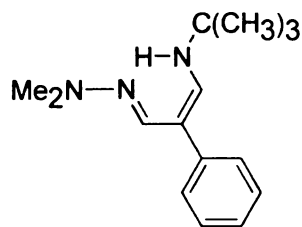
Under an atmosphere of dry nitrogen, a threaded pressure tube was loaded with toluene (4500 μ L), $\text{Ti}(\text{dap})_2(\text{NMe}_2)_2$ (0.344 g, 0.900 mmol), 1,1-dimethylhydrazine (1024 μ L, 13.500 mmol), 1-phenylpropyne (1078 μ L, 9 mmol), and xylyl isocyanide (1.769 g, 13.500 mmol). The tube was sealed with a Teflon cap and heated at 130 $^\circ\text{C}$ for 43 h. The volatiles were removed under vacuum. The product was then isolated by column chromatography on Florisil. The impurities were removed as the first fraction using 1:1 pentane:ethyl acetate mixture. The product was then isolated with pure ethyl acetate in 14% yield (0.401 g, 1.306 mmol) as a dark brown viscous oil. ^1H NMR (299.8 MHz, CDCl_3): 11.31 (br s, 1 H, *NH*), 7.35 – 6.69 (m, 8 H, Ph), 6.82 (d, 1 H, $J_{\text{HH}} = 7.3$ Hz, *HNCH*), 2.66 (s, 6 H, $\text{N}(\text{CH}_3)_2$), 2.43 (s, 6 H, 2,6- $(\text{CH}_3)_2\text{C}_6\text{H}_3$), 2.23 (s, 3 H, $\text{N}=\text{CCH}_3$). $^{13}\text{C}\{^1\text{H}\}$ NMR (75.4 MHz, CDCl_3): 166.3, 142.7, 143.0, 142.0, 141.8, 131.0, 129.0, 128.1, 126.8, 125.9, 123.9, 108.3, 48.2, 19.5, 17.9. Elemental analysis; Experimental (Calc.), C: 77.88 (78.17). H: 8.33 (8.14). N: 13.49 (13.68). MS (EI) $m/z = 307(\text{M}^+)$.

Synthesis of compound 33



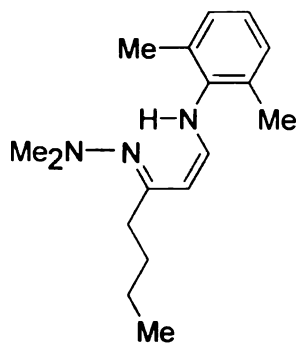
Under an atmosphere of dry nitrogen, a threaded pressure tube was loaded with toluene (4500 μ L), $\text{Ti}(\text{dap})_2(\text{NMe}_2)_2$ (0.344 g, 0.900 mmol), 1-methyl-1-phenylhydrazine (1059 μ L, 9 mmol), 1-hexyne (1119 μ L, 9 mmol), and *tert*-butyl isocyanide (1018 μ L, 9 mmol). The tube was sealed with a Teflon cap and heated at 100 $^\circ\text{C}$ for 13 h. The solvent was removed under vacuum. The product was isolated by distillation under vacuum (\sim 110 $^\circ\text{C}$, 0.65 torr) in 27% yield (0.693 g, 2.414 mmol) as dark brown oil. ^1H NMR (299.8 MHz, CDCl_3): 9.69 (br s, 1 H, NH), 7.27-6.83 (m, 5 H, Ph), 6.93 (m, 1 H, HNCH), 4.57 (d, 1 H, $J_{\text{HH}} = 8.1$ Hz, HNCHCH), 3.11 (s, 3 H, $\text{N}(\text{CH}_3)_2$), 2.36 (t, 2 H, $J_{\text{HH}} = 7.7$ Hz, $\text{N}=\text{CCH}_2$), 1.50 (m, 2 H, $\text{N}=\text{CCH}_2\text{CH}_2$), 1.39 (m, 2 H, $\text{N}=\text{CCH}_2\text{CH}_2\text{CH}_2$), 1.29 (s, 9 H, CH_3), 0.89 (t, 3 H, $J_{\text{HH}} = 7.2$ Hz, $\text{C}(\text{CH}_3)_3$). $^{13}\text{C}\{^1\text{H}\}$ NMR (75.4 MHz, CDCl_3): 176.3, 152.2, 140.9, 128.5, 118.0, 113.9, 89.1, 51.0, 42.8, 32.0, 30.3, 30.1, 22.8, 13.8. Elemental analysis; Experimental (Calc.), C: 75.29 (75.26). H: 10.49 (10.10). N: 14.72 (14.63). MS (EI) $m/z = 287(\text{M}^+)$.

Synthesis of compound 34



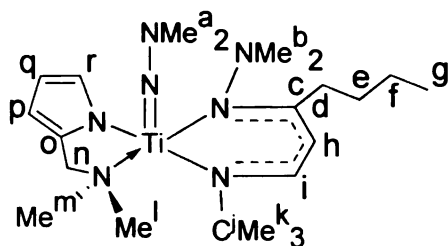
Under an atmosphere of dry nitrogen, a threaded pressure tube was loaded with toluene (4900 μ L), Ti(bap)(NMe₂)₃ (0.353 g, 0.980 mmol), 1,1-dimethylhydrazine (743 μ L, 9.800 mmol), phenylacetylene (1075 μ L, 9.800 mmol), and *tert*-butyl isocyanide (1107 μ L, 9.800 mmol). The tube was sealed with a Teflon cap and heated at 100 °C for 16 h. The solvent was removed under vacuum. The product was isolated by distillation under vacuum (~125 °C, 0.65 torr) in 43% yield (1.030 g, 4.204 mmol) as a red oil. ¹H NMR (299.8 MHz, CDCl₃): 9.03 (br d, 1 H, $J_{\text{HH}} = 13.0$ Hz, NH), 7.65 (s, 1 H, N=CCH), 7.40-7.15 (m, 5 H, Ph), 6.89 (d, 1 H, $J_{\text{HH}} = 2.3$ Hz, HNCH), 2.83 (s, 6 H, N(CH₃)₂), 1.36 (s, 9 H, C(CH₃)₃). ¹³C{¹H} NMR (75.4 MHz, CDCl₃): 143.0, 142.0, 136.0, 128.5, 125.0, 124.0, 102.9, 50.9, 42.0, 30.0. Elemental analysis; Experimental (Calc.), C: 73.58 (73.47). H: 9.26 (9.39). N: 17.05 (17.14). MS (EI) $m/z = 245(\text{M}^+)$.

Synthesis of compound 35



Under an atmosphere of dry nitrogen, a threaded pressure tube was loaded with toluene (6000 μ L), Ti(dap)₂(NMe₂)₂ (0.4319 g, 1.200 mmol), 1,1-dimethylhydrazine (910 μ L, 12 mmol), 1-hexyne (1399 μ L, 12 mmol), and xylyl isocyanide (1.573 g, 12 mmol). The tube was sealed with a Teflon cap and heated at 100 °C for 16 h. The volatiles were removed under vacuum. The product was then isolated by column chromatography on Florisil. The impurities were removed as the first fraction using 1:1 dichloromethane:ethyl acetate mixture. The product was then isolated with ethyl acetate as the eluent in 12% yield (0.401 g, 1.469 mmol) as a viscous oil. ¹H NMR (299.8 MHz, CDCl₃): 10.89 (br s, 1 H, NH), 7.15 – 6.85 (m, 3 H, *o*, *m*-CH), 6.78 (d, 2 H, *J*_{HH} = 7.8 Hz, HNCH), 4.62 (d, 1 H, *J*_{HH} = 8.0 Hz, N=CCH), 2.58 (m, 8 H, N(CH₃)₂ and N=CCH₂), 2.38 (s, 6 H, 2,6-(CH₃)₂C₆H₃), 1.59 (m, 2 H, N=CCH₂CH₂), 1.41 (m, 2 H, N=CCH₂CH₂CH₂), 0.99 (t, 3 H, *J*_{HH} = 7.3 Hz, CH₂CH₃). ¹³C{¹H} NMR (75.4 MHz, CDCl₃): 170.4, 143.1, 141.8, 131.7, 128.7, 128.6, 124.1, 122.1, 117.9, 92.0, 48.8, 46.6, 31.4, 23.0, 19.3, 14.0. High Resolution MS (EI) *m/z* = 273.2200, calc. = 273.2205.

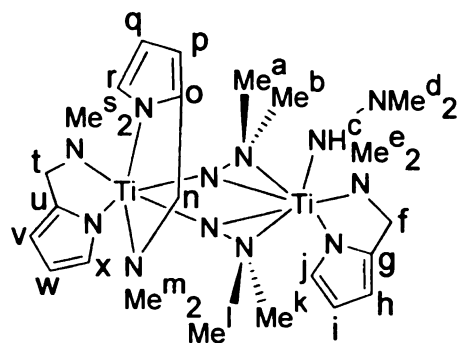
Synthesis of $\text{Ti}(\text{NNMe}_2)(\text{dap})[\text{N}(\text{Bu}^t)\text{CHCHC}(\text{Bu}^n)\text{N}(\text{NMe}_2)-k^2\text{N}]$ (36)



All the manipulations were done inside the glove-box filled with nitrogen. 1,1-Me₂NNH₂ (91 μL, 1.2 mmol) was added to Ti(dap)₂(NMe₂)₂ (0.4538 g, 1.2 mmol) dissolved in 600 μL of toluene in a vial. It was then cooled in the cold well filled with liquid nitrogen. To this were added cold solutions of 1-hexyne (0.1 g, 1.2 mmol) and Bu^tNC (136 μL, 1.2 mmol). It was then allowed to warm up to the room temperature and stir for 12 h. It was then kept at –35 °C for overnight. The solvent was then pumped down and the reddish-brown residue was crystallized from pentane as orange-red colored plate-shaped crystals in 94% yield (0.256 g, 0.565 mmol) with respect to limiting hydrazine. ¹H NMR (499.7 MHz, C₆D₆): 7.09 (d, 1 H, i), 6.73 (t, 1 H, *J*_{HH} = 2.1 Hz, r), 6.59 (t, 1 H, *J*_{HH} = 2.3 Hz, q), 6.47 (m, 1 H, p), 4.67 (d, 1 H, *J*_{HH} = 12.4 Hz, n), 4.56 (d, 1 H, *J*_{HH} = 7.4 Hz, i), 3.34 (d, 2 H, *J*_{HH} = 12.4 Hz, n), 3.09 (m, 1 H, d), 2.87 (br s, 6 H, a), 2.60 (br s, 3 H, l or m), 2.56 (s, 6 H, b), 2.29 (m, 1 H, d), 1.74 (br s, 3 H, l or m), 1.51 (m, 2 H, e), 1.31 (s, 9 H, k), 1.29 (m, 2 H, f), 0.89 (t, 3 H, *J*_{HH} = 7.3 Hz, g). ¹³C{¹H} NMR (125.7 MHz, C₆D₆): 166.7, 146.9, 136.2, 126.8, 107.1, 104.1, 93.2, 63.3, 56.9,

50.1, 49.7, 49.1, 33.7, 32.0, 31.7, 31.5, 23.3, 14.2. Elemental analysis; Experimental (Calc.), C: 57.83 (58.27). H: 9.25 (9.56). N: 21.36 (21.62). M.p. decomp. 230 °C. Structural details: (Monoclinic, P2(1)/c, Formula: C₂₂H₄₃N₇Ti, a = 9.180(1), b = 19.161(3), c = 15.043(2), β = 102.598(3)°, Z = 4, D_{calc} = 1.167 g/mL, μ = 0.353 mm⁻¹, F(000) = 984, θ range = 1.75 to 23.33°, total ref = 22066, unique ref = 3737, parameters = 272, GOF = 1.012, ε = 0.020(2), largest peak and hole = 0.414 and -0.398 eÅ⁻³, R (I > 2σ(I)) = 0.0436, wR² (I > 2σ(I)) = 0.1040.)

Synthesis and characterization of $\text{Ti}_2(\text{dap})_3(\text{NHNMe}_2)(\text{NNMe}_2)_2$ (**37**)



All the manipulations were done inside a nitrogen filled glove-box. In a vial, $\text{Ti}(\text{dap})_2(\text{NMe}_2)_2$ (0.200 g, 0.500 mmol) was dissolved in toluene (250 μL). It was then cooled in a liquid nitrogen-cooled cold well. To this solution was added 1,1- Me_2NNH_2 (76 μL , 1.000 mmol). Then, the solution was allowed to warm up to room temperature and stir for 1 h. The solution was kept in the refrigerator at $-35\text{ }^\circ\text{C}$ overnight. The volatiles were removed in vacuo, and the yellow-brown residue was crystallized from a 1:1 dichloromethane:pentane to obtain **37** as yellow plates in 61% yield (0.195 g, 0.305 mmol). ^1H NMR (499.7 MHz, C_6D_6): 7.68 (br, 1 H, c), 6.89 (br, 1 H, r or x), 6.56 (t, 1 H, $J_{\text{HH}} = 2.7$ Hz, q or w), 6.40 (t, 2 H, $J_{\text{HH}} = 2.5$ Hz, q or w and r or x), 6.34 (br, 1 H, p or v), 6.22 (br, 1 H, j), 6.17 (t, 1 H, $J_{\text{HH}} = 2.6$ Hz, i), 6.08 (br, 1 H, p or v), 5.77 (br, 1 H, h), 3.99 (d, 1 H, $J_{\text{HH}} = 13.8$ Hz, f), 3.87 (d, 1 H, $J_{\text{HH}} = 13.8$ Hz, n or t), 3.78 (d, 1 H, $J_{\text{HH}} = 13.4$ Hz, n or t), 3.57 (d, 1 H, $J_{\text{HH}} = 13.4$ Hz, n or t), 3.52 (d, 1 H, n or t, $J_{\text{HH}} = 13.8$), 3.12 (d, 1 H, f, $J_{\text{HH}} = 13.8$), 2.95 (br, 3 H, a or b or k or l), 2.85 (br, 6 H, m or s), 2.68 (br, 3 H, a or b or k or l), 2.42 (br, 6 H, d), 2.32 (br, 3 H, a or b or k or l), 2.29 (br, 3

H, a or b or k or l), 2.26 (br, 6 H, m or s), 1.86 (br, 6 H, e). $^{13}\text{C}\{^1\text{H}\}$ NMR (125.7 MHz, C_6D_6): 137.2, 136.1, 133.5, 130.6, 129.5, 108.0, 107.3, 106.7, 102.1, 101.8, 101.4, 65.5, 63.0, 62.9, 54.4, 54.3, 51.0, 50.6, 50.3, 49.8, 49.4. Elemental analysis; Experimental (Calc.), C: 50.93 (50.64). H: 8.48 (8.12). N: 26.07 (26.25). M.p. decomp. 230 °C.

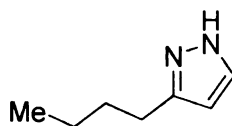
Synthesis and characterization of Ti(dap)(NMe₂)₃ (38)

Under an atmosphere of dry nitrogen, Ti(NMe₂)₃(Cl) (0.200 g, 0.9 mmol) was dissolved in 15 mL ether in a filter flask. Lidap (0.121 g, 0.9 mmol) was dissolved in 5 mL ether in a vial. Both of them were cooled in the cold well. Then Lidap solution was added to the solution of Ti(NMe₂)₃Cl and allowed to warm up to the room temperature and stir overnight. Then it was filtered, and the solvent was pumped down. The product was isolated by crystallization from 1:1 ether: pentane as reddish-brown crystals in 80% yield (0.218 g, 0.7 mmol). ¹H NMR (299.8 MHz, CDCl₃): 6.80 (q, 1 H, 5-pyrrolyl), 6.02 (t, 1 H, *J*_{HH} = 2.6 Hz, 4H-pyrrolyl), 5.82 (m, 1 H, 3H-pyrrolyl), 3.51 (s, 2 H, CH₂), 3.22 (s, 18 H, amido CH₃), 2.36 (s, 6 H, amine CH₃). ¹³C{¹H} NMR (75.4 MHz, CDCl₃): 142.9, 133.3, 122.0, 107.5, 65.2, 53.3, 51.6. M.p. 148-150 °C.

Attempted reaction of 1-hexyne, N,N,N'-trimethylhydrazine, and tert-butylisocyanide in presence of Ti(dap)₂(NMe₂)₂ (1)

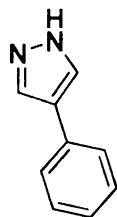
Under an atmosphere of dry nitrogen, a threaded pressure tube was loaded with toluene (300 μL), Ti(dap)₂(NMe₂)₂ (1) (0.023 g, 0.06 mmol), N,N,N'-trimethylhydrazine (0.044 g, 0.6 mmol), 1-hexyne (0.050 g, 0.6 mmol), and *tert*-butyl isocyanide (68 μL, 0.6 mmol). The tube was sealed with a Teflon cap and heated at 100 °C for 16 h. The residue was analyzed with GC-FID. Only starting materials were observed, and no product was detected under these reaction conditions.

Synthesis of 3-n-butylpyrazole (39)



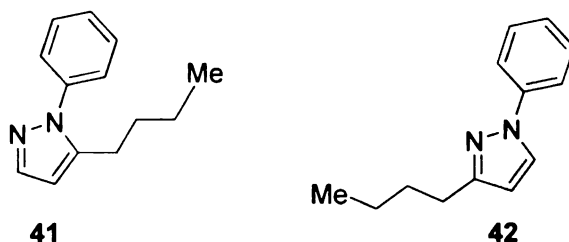
A pressure tube was loaded with **30** (0.100 g, 0.4 mmol), hydrazine (0.0156 g, 0.4 mmol), and pyridine (1 mL). The solution was heated at 150 °C for 24 h. The tube was allowed to cool to room temperature. CH₂Cl₂ (25 mL) was added, and the solution was extracted with water. The organic layer was dried over Na₂SO₄, filtered, and dried under vacuum. This yielded the pure product⁵² in 96% (0.0476 g, 0.380 mmol) yield. ¹H NMR (499.7 MHz, CDCl₃): 8.60 (br s, 1 H, NH), 7.46 (d, 1 H, *J*_{HH} = 2.0 Hz, NCHC), 6.06 (d, 1 H, *J*_{HH} = 1.9 Hz, NC(Buⁿ)CH), 2.66 (t, 2 H, *J*_{HH} = 7.6 Hz, NCCH₂), 1.62 (m, 2 H, NCCH₂CH₂), 1.35 (m, 2 H, CH₂CH₃), 0.91 (t, 3 H, *J*_{HH} = 7.4 Hz, CH₃). ¹³C {¹H} NMR (125.7 MHz, CDCl₃): 147.9, 135.1, 103.4, 31.5, 26.3, 22.3, 13.8. MS (EI) *m/z* = 124 (M⁺).

Synthesis of 4-phenylpyrazole (40)



A pressure tube was loaded with **34** (0.05 g, 0.200 mmol), hydrazine (0.0064 g, 0.200 mmol), and pyridine (1 mL). The mixture was heated at 150 °C for 24 h. The solution was allowed to cool to room temperature. CH₂Cl₂ (25 mL) was added, and the solution was extracted with water. The organic layer was dried over Na₂SO₄, filtered, and dried under vacuum. This resulted in a white solid. The product was isolated by crystallization from 3:1 methanol:ethylacetate at 5 °C. The product⁵³ was isolated as colorless crystals in 70% (0.02 g, 0.14 mmol) yield. ¹H NMR (499.7 MHz, DMSO): 12.9 (br s, 1 H, NH), 7.65 (m, 2 H, *ortho*-CH), 7.39 (tt, 2 H, *J*_{HH} = 1.21, 7.55 Hz, *meta*-CH), 7.22 (tt, 1 H, *J*_{HH} = 1.20, 7.35 Hz, *para*-CH). ¹³C {¹H} NMR (125.7 MHz, CDCl₃): 133.9, 129.7, 126.7, 126.0, 122.1. MS (EI) *m/z* = 144 (M⁺). M.p. 230-232 °C.

Synthesis of 5-n-butyl-1-phenylpyrazole (41) and 3-n-butyl-1-phenylpyrazole (42)

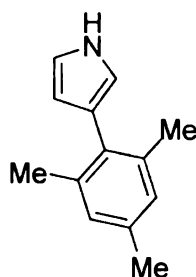


Inside a glove box, a pressure tube was loaded with $\text{Ti}(\text{dap})_2(\text{NMe}_2)_2$ (0.2326 g, 0.609 mmol), Me_2NNH_2 (462 μL , 6.09 mmol), 1-hexyne (699 μL , 6.09 mmol), *tert*-butylisocyanide (688 μL , 6.09 mmol), and toluene (610 μL). The tube was taken outside the box and heated at 100 °C for 16 h. The volatiles were removed under vacuum. This resulted in a dark brown semisolid. To this solid was added PhNHNH_2 (60 μL , 6.09 mmol) in pyridine (2 mL). The solution was heated at 150 °C for 24 h. The solution was then allowed to cool to room temperature, and the volatiles were removed under vacuum. This resulted in a dark brown semisolid which was dissolved in CH_2Cl_2 (30 mL) and extracted with water (2 \times 25 mL). The organic layer was collected, dried over Na_2SO_4 , and filtered. The volatiles were removed from the filtrate under vacuum. This resulted in a brown mass, which was characterized by ^1H NMR spectroscopy. This showed that the products were formed in 10:1 ratio (**41**:**42**). The products were then subjected to column chromatography on alumina using 20% ethyl acetate:hexanes. Compound **41** was isolated in the first fraction as a red-yellow oil. Compound **42** was isolated in the second fraction as a dark red oil. The mixture of products was obtained in 64% (0.78 g, 3.9 mmol) overall isolated yield. Compound **41**: ^1H NMR (299.8 MHz, CDCl_3): 7.57 (d, 1 H, $J_{\text{HH}} = 1.7$

Hz, 3*H*-pyrazole), 7.56-7.36 (m, 5 H, Ph), 6.19 (td, 1 H, $J_{HH} = 0.7, 1.7$ Hz, 4*H*-pyrazole), 2.63 (t, 2 H, $J_{HH} = 7.6$ Hz, NCCH₂), 1.53 (m, 2 H, NCCH₂CH₂), 1.29 (m, 2 H, CH₂CH₃), 0.85 (t, 3 H, $J_{HH} = 7.3$ Hz). ¹³C {¹H} NMR (75.4 MHz, CDCl₃): 143.8, 140.1, 139.8, 129.0, 127.8, 125.4, 105.3, 30.9, 25.9, 22.3, 13.7. MS (EI) *m/z* = 200 (M⁺).

Compound **42**: ¹H NMR (299.8 MHz, CDCl₃): 7.80 (d, 1 H, $J_{HH} = 2.5$ Hz, 5*H*-pyrazole), 7.64 (d, 2 H, $J_{HH} = 8.2$ Hz, *o*-CH-phenyl), 7.47 (t, 2 H, $J_{HH} = 7.6$ Hz, *m*-CH-phenyl), 7.23 (t, 1 H, $J_{HH} = 7.0$ Hz, *p*-CH-phenyl). ¹³C {¹H} NMR (75.4 MHz, CDCl₃): 155.4, 129.3, 127.2, 125.9, 125.6, 118.9, 106.4, 31.8, 28.1, 22.5, 13.9. MS (EI) *m/z* = 200 (M⁺).

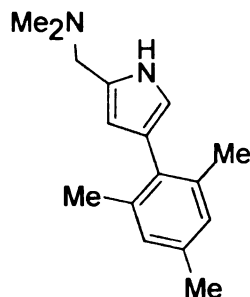
Synthesis of 3-mesitylpyrrole (43)



Inside a glove box, a Schlenk tube (100 mL) was loaded with $[\text{Ir}(\text{OMe})(\text{COD})]_2$, (0.1786 g, 0.264 mmol), HBPIn (3.4486 g, 26.946 mmol), 4,4'-di-*tert*-butyl-4,4'-bipyridine (0.1446 g, 0.538 mmol), BOC-pyrrole (3.0 g, 17.960 mmol), and pentane (3 mL). The tube was taken outside the box, and heated at 60 °C for 18 h. The tube was then taken inside the box, and the volatiles were removed under vacuum. This resulted in a brown solid. The crude reaction mixture was characterized by ^1H NMR spectroscopy to ensure that the reaction was complete. To this mixture was added $\text{Pd}(\text{PPh}_3)_4$ (0.5189 g, 0.449 mmol), mesityl bromide (3.5757 g, 17.960 mmol), $\text{K}_3\text{PO}_4 \cdot n\text{H}_2\text{O}$ (23.8688 g, 89.980 mmol), and DME (6 mL). The solution was refluxed at 100 °C for 24 h. After the reaction was over, the solution was allowed to cool to room temperature. The volatiles were removed under vacuum. This resulted in a brown solid. To this solid was added $\text{K}_3\text{PO}_4 \cdot n\text{H}_2\text{O}$ (5.7285 g, 21.552 mmol) and Bu^nOH (6 mL). The solution was then refluxed at 100 °C for 24 h. The solution was allowed to cool to room temperature, and 1:1 ether: H_2O (50 mL) was added. The solution was stirred for 15 min. The organic layer was separated, dried over Na_2SO_4 , and filtered. The volatiles were removed under

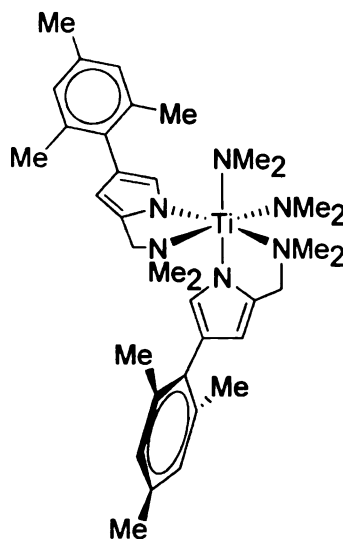
vacuum. This resulted in a dark brown solid, which was subjected to column chromatography on silica gel with 4:1 ether:pentane solution. The product was isolated from the first fraction as a pale brown solid in 85% (2.824 g, 15.3 mmol) yield. ^1H NMR (499.7 MHz, CDCl_3): 8.22 (br s, 1 H, *NH*), 6.92 (s, 2 H, *CH-Ph*), 6.85 (q, 1 H, $J_{\text{HH}} = 2.7$ Hz, *4H-pyrrole*), 6.61 (q, 1 H, $J_{\text{HH}} = 2.3$ Hz, *1H-pyrrole*), 6.11 (m, 1 H, *4H-pyrrole*), 2.30 (s, 3 H, *4-CH₃-phenyl*), 2.14 (s, 6 H, *2,6-CH₃-phenyl*). ^{13}C $\{^1\text{H}\}$ NMR (125.7 MHz, CDCl_3): $\delta = 137.9, 136.1, 133.7, 128.1, 122.3, 117.6, 116.5, 110.3, 21.4, 21.2$. MS (EI) $m/z = 185$ (M^+). Elemental analysis; Experimental (Calc.), C: 84.42 (84.28). H: 8.02 (8.16). N: 7.23 (7.56). M. p. 96-98 °C.

Synthesis of 3-Hdap^{3-mes} (44)



A round bottom flask (250 mL) was charged with 3-mesityl pyrrole (2.2231 g, 12 mmol), formaldehyde (0.9739 g, 13.2 mmol, 37% solution), *N,N*-dimethylamine hydrochloride. The solution was allowed to cool to room temperature. 10% NaOH solution (100 mL) was added, and the reaction stirred for 30 min. The reaction was then extracted with ether (3×100 mL). The combined organic layers were washed with water (100 mL). The final organic layer was dried over Na₂SO₄, filtered, and the volatiles were removed under vacuum. This resulted in a dark brown oil, which was subjected to column chromatography on alumina using 10% methanol:ethyl acetate. The product was isolated as brown oil in 89% yield (2.600 g, 10.7 mmol). ¹H NMR (499.7 MHz, CDCl₃): 9.78 (br s, 1 H, NH), 6.98 (s, 2 H, CH-Ph), 6.57 (s, 1 H, 2H-pyrrole), 5.98 (s, 1 H, 4H-pyrrole), 3.62 (s, 2 H, CH₂), 2.41 (s, 6 H, N(CH₃)₂), 2.39 (s, 3 H, 4-CH₃-phenyl), 2.19 (s, 6 H, 2,6-CH₃-phenyl). ¹³C {¹H} NMR (125.7 MHz, CDCl₃): δ = 137.4, 135.5, 133.6, 127.7, 126.9, 121.3, 116.8, 110.1, 56.3, 44.3, 21.2, 20.9. MS (EI) m/z = 242 (M⁺). M.p. 62-64 °C.

Synthesis of $\text{Ti}(\text{dap}^{3\text{-mes}})_2(\text{NMe}_2)_2$ (45)



All manipulations were carried out inside the glove box. A filter flask (100 mL) was loaded with $\text{Ti}(\text{NMe}_2)_4$ in ether (1.5 mL) (0.4668 g, 2.08 mmol) and cooled inside the cold-well. To this solution was added cold ether solution of ligand (1.0092 g, 4.2 mmol). The solution was allowed to warm up to room temperature and stir overnight. The solution changed to red with an orange-red precipitate. The mixture was filtered, and the precipitate was dried under vacuum. Suitable X-ray quality crystals were grown from 1:1 dichloromethane:pentane at $-35\text{ }^\circ\text{C}$ as red plates (1.0552 g, 1.71 mmol). ^1H NMR (499.7 MHz, CDCl_3): 6.88 (s, 4 H, *CH*-Ph), 6.56 (d, 2 H, $J_{\text{HH}} = 1.5$ Hz, 2*H*-pyrrole), 5.67 (d, 2 H, $J_{\text{HH}} = 1.5$ Hz, 4*H*-pyrrole), 3.58-3.42 (br, 4 H, CH_2), 3.32 (s, 12 H, $\text{N}(\text{CH}_3)_2$), 2.46 (s, 12 H, $\text{N}(\text{CH}_3)_2$), 2.28 (s, 6 H, phenyl-4- CH_3), 2.18 (s, 12 H, phenyl-3,5- $(\text{CH}_3)_2$). ^{13}C $\{^1\text{H}\}$ NMR (125.7 MHz, CDCl_3): 137.6, 135.7, 135.3, 134.6, 127.6, 127.1, 120.6, 104.2, 63.0, 51.9, 49.1, 48.7, 21.4, 20.9. M. p. 158-160 $^\circ\text{C}$.

Experimental for Table 3.5

Entry 2, Table 3.5:

Inside a glove box, a pressure tube was loaded with $\text{Ti}(\text{dap})_2(\text{NMe}_2)_2$ (0.0458 g, 0.119 mmol), Me_2NNH_2 (92 μL , 1.190 mmol), 1-hexyne (140 μL , 1.190 mmol), *tert*-butylisocyanide (136 μL , 1.190 mmol), and toluene (600 μL). The tube was taken outside the box and heated at 100 °C for 16 h. The volatiles were removed under vacuum. This resulted in a dark brown semisolid. To this solid was added *p*-OMeC₆H₄NHNH₂·HCl (0.2021 g, 1.190 mmol) in pyridine (2 mL). The solution was heated at 150 °C for 24 h until the conversion was complete. The solution was then allowed to cool to room temperature, and the volatiles were removed under vacuum. This resulted in a dark brown semisolid which was dissolved in CH₂Cl₂ (30 mL) and extracted with water (2×25 mL). The organic layer was collected, dried over Na₂SO₄, and filtered. The volatiles were removed from the filtrate under vacuum. This resulted in a brown mass, which was characterized by ¹H NMR spectroscopy. It produced the two isomers in 2:1 ratio. ¹H NMR (299.8 MHz, CDCl₃): 7.57 (d, 1 H, $J_{\text{HH}} = 1.7$ Hz, 3*H*-pyrazole), 7.56-7.36 (m, 5 H, Ph), 6.19 (td, 1 H, $J_{\text{HH}} = 0.7, 1.7$ Hz, 4*H*-pyrazole), 2.63 (t, 2 H, $J_{\text{HH}} = 7.6$ Hz, NCCH₂), 1.53 (m, 2 H, NCCH₂CH₂), 1.29 (m, 2 H, CH₂CH₃), 0.85 (t, 3 H, $J_{\text{HH}} = 7.3$ Hz).

Entry 3, Table 3.5:

Inside a glove box, a pressure tube was loaded with $\text{Ti}(\text{dap})_2(\text{NMe}_2)_2$ (0.0458 g, 0.119 mmol), Me_2NNH_2 (92 μL , 1.190 mmol), 1-hexyne (140 μL , 1.190 mmol), *tert*-butylisocyanide (136 μL , 1.190 mmol), and toluene (600 μL). The tube was taken outside the box and heated at 100 °C for 16 h. The volatiles were removed under vacuum. This resulted in a dark brown semisolid. To this solid was added *p*- $\text{FC}_6\text{H}_4\text{NHNH}_2$ (0.1537 g, 1.22 mmol) in pyridine (2 mL). The solution was heated at 150 °C for 24 h until the conversion was complete. The solution was then allowed to cool to room temperature, and the volatiles were removed under vacuum. This resulted in a dark brown semisolid which was dissolved in CH_2Cl_2 (30 mL) and extracted with water (2×25 mL). The organic layer was collected, dried over Na_2SO_4 , and filtered. The volatiles were removed from the filtrate under vacuum. This resulted in a brown mass, which was characterized by ^1H NMR spectroscopy as a mixture of isomers. It produced the two isomers in 4.5:1 ratio. ^1H NMR (299.8 MHz, CDCl_3): 8.02-6.62 (m, 14 H, pyrazole, Ph), 6.24 (d, 0.46 H, $J_{\text{HH}} = 1.7$ Hz, 4*H*-pyrazole. minor), 6.19 (td, 1 H, $J_{\text{HH}} = 0.7, 1.7$ Hz, 4*H*-pyrazole, major), 3.86-3.76 (m, 7 H, OCH_3), 2.79-2.56 (m, 4 H, NCCH_2), 1.83-1.55 (m, 4 H, NCCH_2CH_2), 1.53-1.21 (m, 4 H, CH_2CH_3), 0.99-0.89 (m, 5 H, CH_3).

Entry 4, Table 3.5:

Inside a glove box, a pressure tube was loaded with $\text{Ti}(\text{dap})_2(\text{NMe}_2)_2$ (0.0458 g, 0.119 mmol), Me_2NNH_2 (92 μL , 1.190 mmol), 1-hexyne (140 μL , 1.190 mmol), *tert*-butylisocyanide (136 μL , 1.190 mmol), and toluene (600 μL). The tube was taken outside the box and heated at 100 °C for 16 h. The volatiles were removed under vacuum. This resulted in a dark brown semisolid. To this solid was added *p*-CNC₆H₄-NHNH₂·HCl (0.2068 g, 1.220 mmol) in pyridine (2 mL). The solution was heated at 150 °C for 24 h until the conversion was complete. The solution was then allowed to cool to room temperature, and the volatiles were removed under vacuum. This resulted in a dark brown semisolid which was dissolved in CH_2Cl_2 (30 mL) and extracted with water (2×25 mL). The organic layer was collected, dried over Na_2SO_4 , and filtered. The volatiles were removed from the filtrate under vacuum. This resulted in a brown mass, which was characterized by ¹H NMR spectroscopy as a mixture of two different isomers. It produced the two isomers in 1:6 ratio. ¹H NMR (299.8 MHz, CDCl_3): 7.62 (d, 1 H, $J_{\text{HH}} = 1.7$ Hz, 3*H*-pyrazole), 7.78-7.36 (m, 10 H, Ph, pyrazole), 6.41-6.01 (m, 3 H, Ph), 6.31 (d, 1 H, $J_{\text{HH}} = 1.7$ Hz, 4*H*-pyrazole, major), 6.25 (td, 0.1 H, $J_{\text{HH}} = 0.7, 1.7$ Hz, 4*H*-pyrazole, minor) 2.72 (m, 3 H, NCCH_2), 1.73-1.62 (m, 4 H, NCCH_2CH_2), 1.42-1.34 (m, 4 H, CH_2CH_3), 0.85 (t, 5 H, $J_{\text{HH}} = 7.3$ Hz, CH_3).

Experimental for kinetic reactions

Representative procedure for the catalysis with 10% Ti(dap)₂(NMe₂)₂ (Case A, Table 3.2)

Under an atmosphere of dry nitrogen, a vial was loaded with Ti(dap)₂(NMe₂)₂ (**1**) (0.0229 g, 0.060 mmol), toluene-*d*₈ (500 μL), 1,1-Me₂NNH₂ (46 μL, 0.600 mmol), 1-hexyne (70 μL, 0.6 mmol), *tert*-butylisocyanide (68 μL, 0.600 mmol), and hexamethyldisiloxane (0.0486 g, 0.300 mmol). The volume was adjusted to 1 mL with toluene-*d*₈ in a volumetric flask, and the solution was transferred to a J-Young tube. The progress of the reaction was monitored over time at 100 °C by ¹H NMR spectroscopy. The yields were calculated with respect to internal standard (hexamethyldisiloxane). A graph of percent yield was then plotted vs time (in min). The value of the rate constant was calculated using OriginPro 7.5.

*k*_{obs} values:

$$k_{obs} = 0.84 \times 10^{-4} \text{ s}^{-1}, R^2 = 0.997$$

$$k_{obs} = 0.92 \times 10^{-4} \text{ s}^{-1}, R^2 = 0.992$$

$$k_{obs} = 1.32 \times 10^{-4} \text{ s}^{-1}, R^2 = 0.991$$

$$k_{obs} = 1.18 \times 10^{-4} \text{ s}^{-1}, R^2 = 0.994$$

$$\text{Average } k_{obs} = (1.07 \pm 0.42) \times 10^{-4} \text{ s}^{-1}$$

Representative procedure for the catalysis with 10% 36 (Case B, Table 3.2)

Under an atmosphere of dry nitrogen, a vial was loaded with **36** (0.0276 g, 0.060 mmol), toluene-*d*₈ (500 μL), 1,1-Me₂NNH₂ (46 μL, 0.600 mmol), 1-hexyne (70 μL, 0.6 mmol), *tert*-butylisocyanide (68 μL, 0.600 mmol), and hexamethyldisiloxane (0.0486 g, 0.300 mmol). The volume was adjusted to 1 mL with toluene-*d*₈ in a volumetric flask, and the solution was transferred to a J-Young tube. The progress of the reaction was monitored over time at 100 °C by ¹H NMR spectroscopy. The yields were calculated with respect to the internal standard (hexamethyldisiloxane). A graph of percent yield was then plotted vs time (in min). The value of the rate constant was calculated using OriginPro 7.5.

*k*_{obs} values:

$$k_{obs} = 0.99 \times 10^{-4} \text{ s}^{-1}, R^2 = 0.999$$

$$k_{obs} = 1.01 \times 10^{-4} \text{ s}^{-1}, R^2 = 0.999$$

$$k_{obs} = 0.89 \times 10^{-4} \text{ s}^{-1}, R^2 = 0.999$$

$$k_{obs} = 1.01 \times 10^{-4} \text{ s}^{-1}, R^2 = 0.999$$

$$\text{Average } k_{obs} = (0.98 \pm 0.11) \times 10^{-4} \text{ s}^{-1}$$

Representative procedure for the reaction of 36 with 10 equivalent Me₂NNH₂ (Case C, Table 3.2)

Under an atmosphere of dry nitrogen, a vial was loaded with **36** (0.0276 g, 0.060 mmol), toluene-*d*₈ (500 μL), 1,1-Me₂NNH₂ (46 μL, 0.600 mmol), and hexamethyldisiloxane (0.0098 g, 0.600 mmol). The volume was adjusted to 1 mL with toluene-*d*₈ in a volumetric flask, and the solution was transferred to a J-Young tube. The progress of the reaction was monitored over time at 100 °C by ¹H NMR spectroscopy. The yields were calculated with respect to the internal standard (hexamethyldisiloxane). A graph of percentage yield was then plotted vs time (in min). The value of the rate constant was calculated using OriginPro 7.5.

*k*_{obs} Values:

$$k_{obs} = 1.08 \times 10^{-4} \text{ s}^{-1}, R^2 = 0.999$$

$$k_{obs} = 0.94 \times 10^{-4} \text{ s}^{-1}, R^2 = 0.999$$

$$k_{obs} = 1.09 \times 10^{-4} \text{ s}^{-1}, R^2 = 0.998$$

$$k_{obs} = 1.32 \times 10^{-4} \text{ s}^{-1}, R^2 = 0.994$$

$$\text{Average } k_{obs} = (1.11 \pm 0.30) \times 10^{-4} \text{ s}^{-1}$$

Representative procedure for reaction with 10% 36 and 10% Hdap (Case D, Table 3.2)

Under an atmosphere of dry nitrogen, a vial was loaded with **36** (0.0276 g, 0.060 mmol), toluene-*d*₈ (500 μL), 1,1-Me₂NNH₂ (46 μL, 0.600 mmol), 1-hexyne (70 μL, 0.6 mmol), *tert*-butylisocyanide (68 μL, 0.600 mmol), Hdap (0.0076 g, 0.060 mmol), and hexamethyldisiloxane (0.0486 g, 0.300 mmol). The volume was adjusted to 1 mL with toluene-*d*₈ in a volumetric flask, and the solution was transferred to a J-Young tube. The progress of the reaction was monitored over time at 100 °C by ¹H NMR spectroscopy. The yields were calculated with respect to the internal standard (hexamethyldisiloxane). A graph of percent yield was then plotted vs time (in min). The value of the rate constant was calculated using OriginPro 7.5.

*k*_{obs} Values:

$$k_{obs} = 1.19 \times 10^{-4} \text{ s}^{-1}, R^2 = 0.999$$

$$k_{obs} = 1.04 \times 10^{-4} \text{ s}^{-1}, R^2 = 0.999$$

$$k_{obs} = 1.19 \times 10^{-4} \text{ s}^{-1}, R^2 = 0.999$$

$$k_{obs} = 1.34 \times 10^{-4} \text{ s}^{-1}, R^2 = 0.999$$

$$\text{Average } k_{obs} = (1.19 \pm 0.23) \times 10^{-4} \text{ s}^{-1}$$

Represtativ e procedure for the reactions shown in Table 3.3

The reactions were carried out following the procedure shown in Case A (Table 3.2) for the kinetics experiment with **1**. Only the amount of the catalyst was varied.

For Entry 1, Table 3.3. Catalyst (**1**) loading: (0.0349 g, 0.900 mmol)

For Entry 2, Table 3.3. Catalyst (**1**) loading: (0.0229 g, 0.600 mmol)

For Entry 3, Table 3.3. Catalyst (**1**) loading: (0.0115 g, 0.300 mmol)

For Entry 4, Table 3.3. Catalyst (**1**) loading: (0.0058 g, 0.150 mmol)

X-ray Crystallography

Crystals grown from concentrated solutions at $-35\text{ }^{\circ}\text{C}$ were moved quickly from a scintillation vial to a microscope slide containing Paratone N. Samples were selected and mounted on a glass fiber in wax and Paratone. The data collections were carried out at a sample temperature of 173 K on a Bruker AXS platform three-circle goniometer with a CCD detector. The data were processed and reduced utilizing the program SAINTPLUS supplied by Bruker AXS. The structures were solved by direct methods (SHELXTL v5.1, Bruker AXS) in conjunction with standard difference Fourier techniques.

3.8 References

1. Arend, M.; Westermann, B.; Risch, N. *Angew. Chem. Int. Ed.* **1998**, *37*, 1044.
2. Cortes, E.; Martinez, R.; Avila, J. G.; Toscano, R. A. *J. Heterocycl. Chem.* **1988**, *25*, 895.
3. Li, J.; Jiang, W. Y.; Han, K. L.; He, G. Z.; Li, C. *J. Org. Chem.* **2003**, *68*, 8786.
4. Yet, L. *Angew. Chem. Int. Ed.* **2001**, *40*, 875.
5. Sigman, M. S.; Vachal, P.; Jacobsen, E. N. *Angew. Chem. Int. Ed.* **2000**, *39*, 1279.
6. Strecker, A. *Ann. Chem. Pharm.* **1850**, *75*, 27.
7. Dondoni, A.; Massi, A.; Minghini, E.; Bertolasi, V. *Tetrahedron* **2004**, *60*, 2311.
8. Shimokawa, J.; Shirai, K.; Tanatani, A.; Hashimoto, Y.; Nagasawa, K. *Angew. Chem. Int. Ed.* **2004**, *43*, 1559.
9. Domling, A.; Ugi, I. *Angew. Chem. Int. Ed.* **2000**, *39*, 3169.
10. Basso, A.; Banfi, L.; Riva, R.; Guanti, G. *J. Org. Chem.* **2005**, *70*, 575.
11. Xi, C. J.; Chen, C.; Lin, J.; Hong, X. Y. *Org. Lett.* **2005**, *7*, 347.
12. Dhawan, R.; Arndtsen, B. A. *J. Am. Chem. Soc.* **2004**, *126*, 468.
13. Bae, I.; Han, H.; Chang, S. *J. Am. Chem. Soc.* **2005**, *127*, 2038.
14. Bon, R. S.; van Vliet, B.; Sprenkels, N. E.; Schmitz, R. F.; de Kanter, F. J. J.; Stevens, C. V.; Swart, M.; Bickelhaupt, F. M.; Groen, M. B.; Orru, R. V. A. *J. Org. Chem.* **2005**, *70*, 3542.
15. Bazin, S.; Feray, L.; Vanthuyne, N.; Bertrand, M. P. *Tetrahedron* **2005**, *61*, 4261.
16. Hratchian, H. P.; Chowdhury, S. K.; Gutierrez-Garcia, V. M.; Amarasinghe, K. K. D.; Heeg, M. J.; Schlegel, H. B.; Montgomery, J. *Organometallics* **2004**, *23*, 4636.
17. Vujkovic, N. F., J. L.; Ward, B. D.; Wadepohl, H.; Mountford, P.; Gade, L. H. *Organometallics* **2008**, 2518.
18. Aneetha, H.; Basuli, F.; Bollinger, J.; Huffman, J. C.; Mindiola, D. J. *Organometallics* **2006**, *25*, 2402.
19. Ghosh, A. K.; Xu, C. X.; Kulkarni, S. S.; Wink, D. *Org. Lett.* **2005**, *7*, 7.

20. Basuli, F.; Bailey, B. C.; Huffman, J. C.; Mindiola, D. J. *Organometallics* **2005**, *24*, 3321.
21. Cao, C. S.; Shi, Y. H.; Odom, A. L. *J. Am. Chem. Soc.* **2003**, *125*, 2880.
22. Ruck, R. T.; Zuckerman, R. L.; Krska, S. W.; Bergman, R. G. *Angew. chem. int. ed.* **2004**, *43*, 5372.
23. Nair, V.; Mathai, S.; Nair, S. M.; Rath, N. P. *Tet. Lett.* **2003**, *44*, 8407.
24. Banerjee, S.; Shi, Y. H.; Cao, C. S.; Odom, A. L. *J. Organomet. Chem.* **2005**, *690*, 5066.
25. Herz, W.; Dittmer, K.; Cristol, S. J. *J. Am. Chem. Soc.* **1947**, *69*, 1698.
26. Cao, C. S.; Shi, Y. H.; Odom, A. L. *Org. Lett.* **2002**, *4*, 2853.
27. Kim, I. T.; Elsenbaumer, R. L. *Tet. Lett.* **1998**, *39*, 1087.
28. Li, Y. W.; Marks, T. J. *Organometallics* **1996**, *15*, 3770.
29. Baranger, A. M.; Walsh, P. J.; Bergman, R. G. *J. Am. Chem. Soc.* **1993**, *115*, 2753.
30. Walsh, P. J.; Baranger, A. M.; Bergman, R. G. *J. Am. Chem. Soc.* **1992**, *114*, 1708.
31. Li, Y.; Shi, Y.; Odom, A. L. *J. Am. Chem. Soc.* **2004**, *126*, 1794.
32. Gordon, A. J., Ford, R. A. *The Chemist's Companion* 1972, John Wiley & Sons: New York. Here the parentheses denote estimated standard deviations from model used in the X-ray diffraction experiment, and the \pm denotes standard deviation from the average found from multiple experiments.
33. Mahy, J. P.; Battioni, P.; Mansuy, D.; Fisher, J.; Weiss, R.; Mispelter, J.; Morgensternbadarau, I.; Gans, P. *J. Am. Chem. Soc.* **1984**, *106*, 1699.
34. Allman, R., Structural Chemistry. In *The Chemistry of the Hydrazo, Azo, and Azoxy Groups*, Saul, P., Ed. John Wiley and Sons: London, 1975; Vol. 1, p 23.
35. Kahlal, S.; Saillard, J. Y.; Hamon, J. R.; Manzur, C.; Carrillo, D. *J. Chem. Soc., Dalton Trans.* **1998**, 1229.
36. Parsons, T. B.; Hazari, N.; Cowley, A. R.; Green, J. C.; Mountford, P. *Inorg. Chem.* **2005**, *44*, 8442.
37. Walsh, P. J.; Carney, M. J.; Bergman, R. G. *J. Am. Chem. Soc.* **1991**, *113*, 6343.

38. Alvarez, S.; Llunell, M. *J. Chem. Soc., Dalton Trans.* **2000**, 3288.
39. Zabrodsky, H.; Peleg, S.; Avnir, D. *J. Am. Chem. Soc.* **1992**, *114*, 7843.
40. Basuli, F.; Aneetha, H.; Huffman, J. C.; Mindiola, D. J. *J. Am. Chem. Soc.* **2005**, *127*, 17992.
41. Espenson, J. H. *Chemical Kinetics and Reaction Mechanisms*, McGraw-Hill: New York, 1995.
42. Tillack, A.; Jiao, H. J.; Castro, I. G.; Hartung, C. G.; Beller, M. *Chem. Eur. J.* **2004**, *10*, 2409.
43. Barluenga, J.; Rubio, E.; Rubio, V.; Muniz, L.; Iglesias, J.; Gotor, V. *J. Chem. Res. (S)* **1985**, 124.
44. Barluenga, J.; Jardon, J.; Rubio, V.; Gotor, V. *J. Org. Chem.* **1983**, *48*, 1379.
45. Barluenga, J.; Rubio, V.; Gotor, V. *J. Org. Chem.* **1982**, *47*, 1696.
46. Cho, J. Y.; Tse, M. K.; Holmes, D.; Maleczka, R. E.; Smith, M. R. *Science* **2002**, *295*, 305.
47. Suzuki, A. *J. Organomet. Chem.* **1999**, *576*, 147.
48. Bradley, D. C.; Thomas, I. M. *J. Chem. Soc.* **1960**, 3857.
49. Benzing, E.; Kornicker, W. *Chem. Ber.* **1961**, *94*, 2263.
50. Gokel, G. W.; Widera, R. P.; Weber, W. P. *Org. Synth.* **1979**, *55*, 96.
51. Walborski, H.; Niznik, G. E. *J. Org. Chem.* **1972**, *37*, 187.
52. Heuisgen, R.; Koszinowski, J.; Ohta, A.; Schiffer, R. *Angew. Chem. Int. Ed.* **1980**, *19*, 202.
53. Reger, D. L.; Gardinier, J. R.; Grattan, T. C.; Smith, M. R.; Smith, M. D. *New J. Chem.* **2003**, *27*, 1670.

CHAPTER 4

Synthesis of Vanadium(V) hydrazido(2–) thiolate imine alkoxide complexes

4.1 Introduction

Metal hydrazido(2–) complexes are well known intermediates in dinitrogen activation to produce NH_3 .¹⁻³ Hydrazido(2–) complexes have been synthesized for a large variety of metal centers including Mo and W,⁴⁻⁹ Ti,¹⁰⁻¹⁷ Zr,¹⁸⁻²⁰ Re,²¹⁻²⁴ V,²⁵⁻³² Nb,³³ Ta,³⁴ Os,³⁵⁻³⁷ Pt,³⁸ Au,³⁹ Li,⁴⁰ U,⁴¹ and Tc.⁴² Among these, molybdenum-based hydrazido complexes have been studied extensively due to their presence in nitrogenase enzymes.⁴³ Similarly, there has been considerable interest in vanadium hydrazido(2–) complexes since the discovery of vanadium in the active sites of similar enzymes.⁴⁴⁻⁴⁶ The reduction of dinitrogen by these nitrogenase enzymes is believed to involve metal-bound (Fe, Mo, V) hydrazine and hydrazido intermediates.^{47,48} The FeMoco enzyme has been studied extensively and was shown by X-ray crystallography to contain a cluster with the molybdenum atom ligated by one nitrogen, three sulfurs, and two oxygen atoms.⁴³ It is generally believed that vanadium in nitrogenase enzymes occupies a similar site.⁴⁹ Since vanadium, like

molybdenum, may be the coordinating site for N₂, it is important to understand the hydrazido(2-) chemistry of vanadium with ligands containing S, N, and O atoms. In particular, reduction of N₂ to NH₃ by these enzymes might involve the intermediate species N₂H_{*m*} and NH_{*n*} (*m* = 0–4, *n* = 0–3) bound to vanadium.^{47,48}

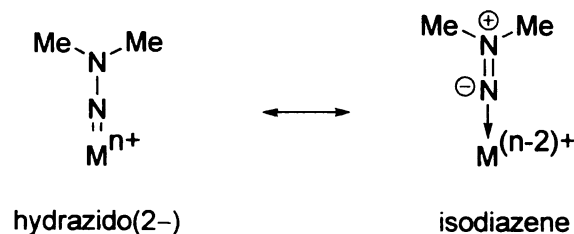
In terms of mode of action for vanadium-containing nitrogenase, it has been demonstrated that S₃-ligated vanadium in cluster anions such as [Fe₃S₄X₃V(DMF)₃]⁻ (X = Cl, Br, or I) binds hydrazines⁵⁰ and imides,⁵¹ and catalyzes their reduction.

Examples and syntheses of a few vanadium hydrazido(2-) complexes will be discussed in the following sections. For comparison, hydrazido(2-) chemistry of adjacent titanium will be briefly reviewed.

4.2 Hydrazido versus isodiazene bonding in $MNNR_2$ complexes

The degree of donation of the β -N lone pair into the $M=N$ π^* orbital in terminal $M-N-N$ ligands determines participation of the two different resonance forms. Cases where N_β is strongly donating with weak π -donation from the metal center results in an N-N bond order ~ 2.0 . This is represented as the isodiazene form (Figure 4.1, right).^{52,53} This is favored in metal complexes with a low formal oxidation state. This is analogous to a singlet Fischer-type carbene complex, where the metal center is present in a relatively low formal oxidation state. Conversely, in the cases where the lower oxidation state of the metal is very reducing, e.g. titanium(II), the hydrazido(2-) resonance form predominates (Figure 4.1, left).⁵⁴⁻⁵⁶ Here the metal center is present in a higher formal oxidation state, and the M-N bond order is between 2 and 3. This situation is reminiscent of the triplet Schrock-type carbene complex where the metal center is present in a relatively high formal oxidation state. Different reactivities have been observed depending on the nature of the bonding in $M-N-N$ moiety.

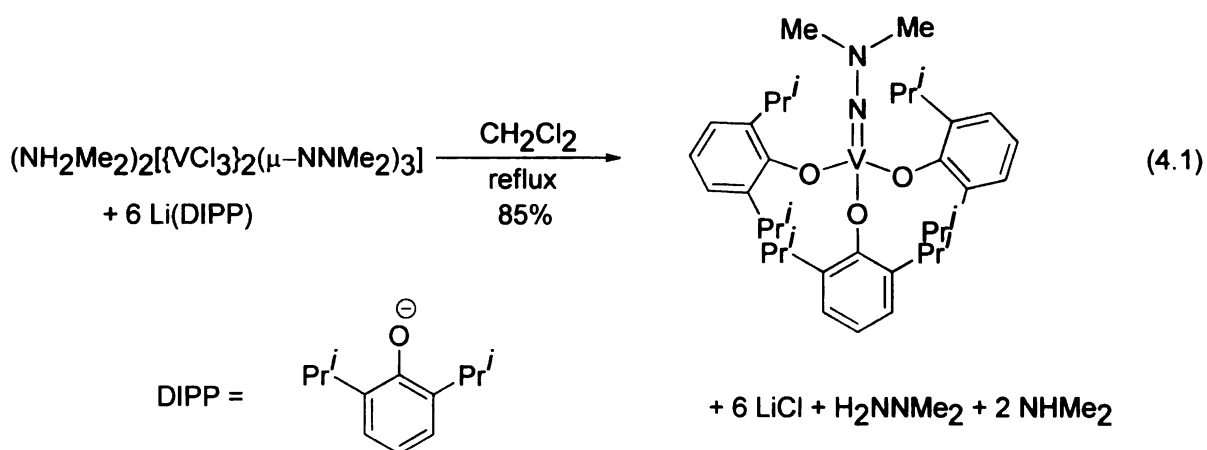
Figure 4.1 Hydrazido(2-) vs isodiazene resonance forms.



Most often, N_{β} is planar in hydrazido(2-) complexes. This is observed in the complexes where phenyl groups are present on the N_{β} atom in M–N–N moiety.^{13,20,56} This occurs due to the conjugation of the β -nitrogen with the phenyl ring. However, in the complexes where N_{β} has only alkyl groups as substituents, the geometry around the β -nitrogen atom is very different. In this case, N_{β} is sp^3 -hybridized, and the sum of the angles around it can be $\sim 328.0^{\circ}$. Only a few examples of hydrazido(2-) ligands with pyramidalized β -nitrogens have been structurally characterized.^{12,14} In the isodiazene complexes, considerable contribution from N_{β} into M=N π^* orbital results in significant delocalization of electrons in M–N–N moiety. This results in a planar N_{β} , and the sum of the angles around that atom is $\sim 360^{\circ}$.^{57,58}

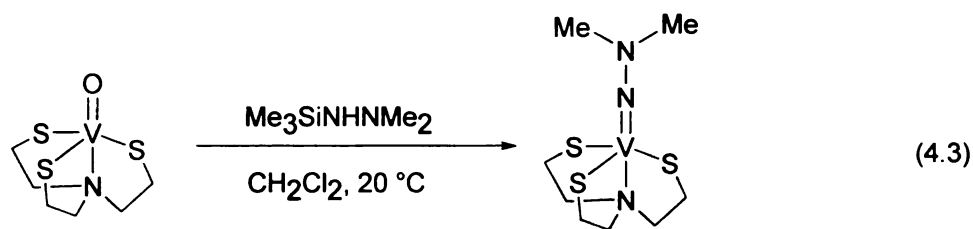
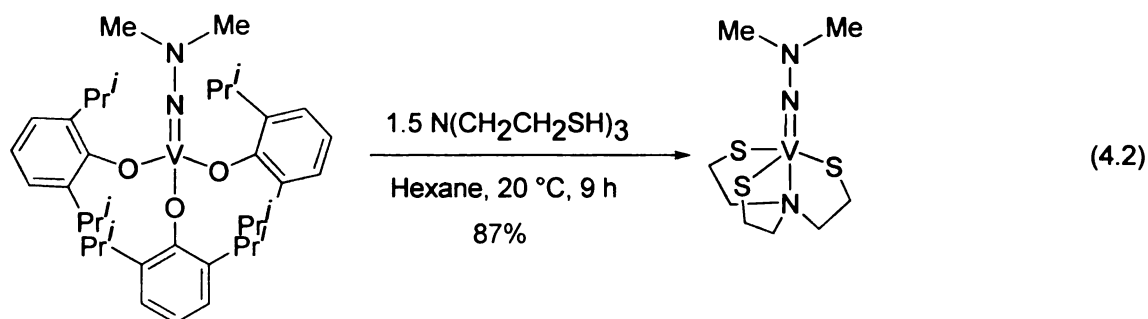
4.3 Vanadium(V) hydrazido(2-) complexes

Vanadium(V) hydrazido(2-) complexes with different ligands are known in the literature.²⁹⁻³¹ A vanadium(V) hydrazido(2-) complex with aryloxy ligands, $\text{Me}_2\text{NNV}(\text{OAr})_3$, where $\text{Ar} = 2,6\text{-Pr}^i_2\text{C}_6\text{H}_3$ has been reported (Equation 4.1).²⁸ This compound was very stable to reduction by zinc or Na/Hg. The hydrazido(2-) group can not be protonated by anhydrous HCl. However, it undergoes metathesis with $\text{N}(\text{CH}_2\text{CH}_2\text{SH})_3$ to give $[\text{V}(\text{NNMe}_2)\{\text{N}(\text{CH}_2\text{CH}_2\text{S})_3\}]$, (Equation 4.2).³⁰ This is the first example of Vanadium(V) hydrazido(2-) complex with sulfur-donor atoms as the ancillary ligand.

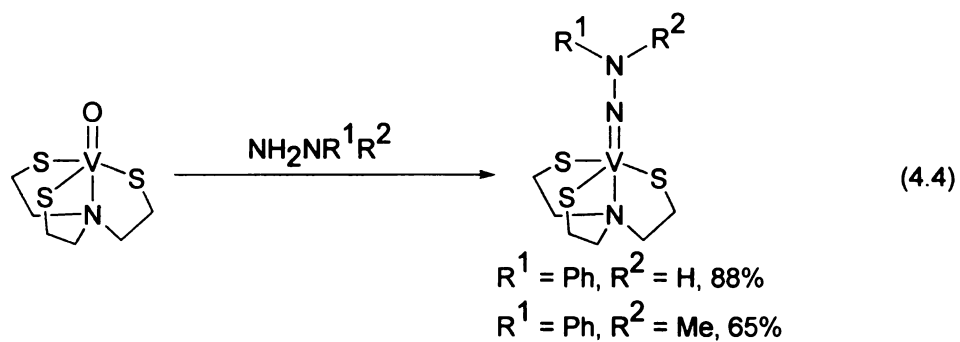


Alternatively, $\text{Me}_2\text{NNV}(\text{OAr})_3$ can be prepared from the corresponding vanadium(V) oxo compound by treating with $\text{Me}_3\text{SiNHNMe}_2$ as shown in Equation 4.3.³⁰ From the X-ray crystal structure of this compound, the V-N distance was found to be 1.681(3) Å. The N-N distance was 1.305(5) Å, and the V-N-N angle was

173.9(4)°. The N–N bond distance of 1.295(17) Å is similar to that observed in $[\text{VCl}_2(\text{NH}_2\text{NMePh})_2(\text{NNMePh})]^-$.³¹

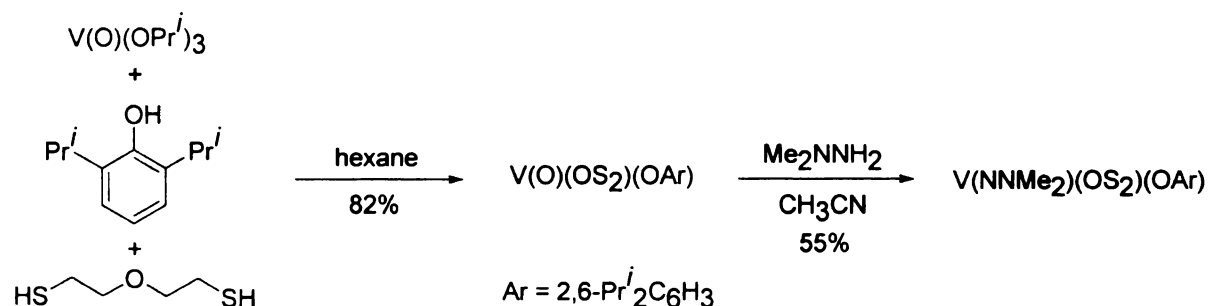


Vanadium(V) hydrazido(2-) complexes with different β -nitrogen substituents have been reported (Equation 4.4).²⁷ Here, the N–N bond distances in the corresponding NNPhMe and NNHPh complexes are 1.305(5) Å and 1.310(3) Å, respectively.

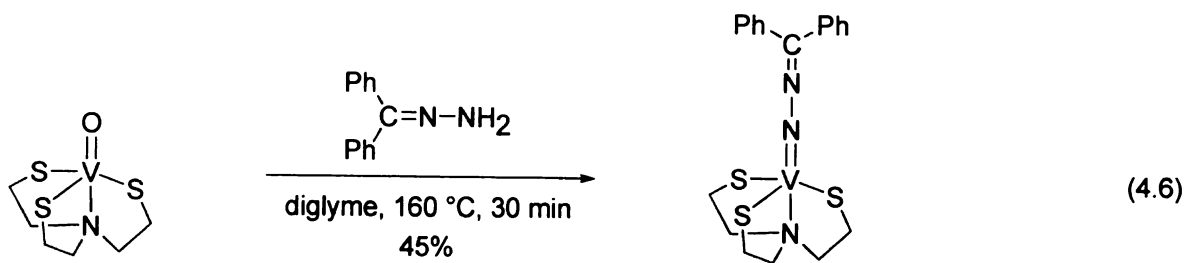
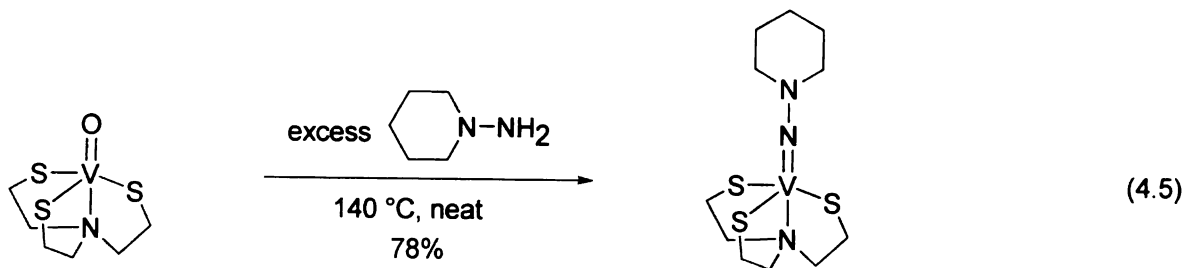


Hydrazido(2-) complexes were also synthesized using $[\text{O}(\text{SCH}_2\text{CH}_2)_2]^{2-}$ (OS_2) as the ancillary ligand on vanadium(V).²⁷ For example, the reaction of $\text{V}(\text{O})(\text{OPr}^i)_3$ with 2,6-di-*iso*-propylphenol and $\text{O}(\text{CH}_2\text{CH}_2\text{SH})_2$ generated $\text{V}(\text{OS}_2)\text{O}(\text{OAr})$, which was then treated with Me_2NNH_2 to form $\text{V}(\text{OS}_2)(\text{NNMe}_2)(\text{OAr})$ as the final product (Scheme 4.1).¹⁶

Scheme 4.1 Synthesis of a vanadium hydrazido(2-) complex with $[\text{O}(\text{SCH}_2\text{CH}_2)_2]^{2-}$ as co-ligand

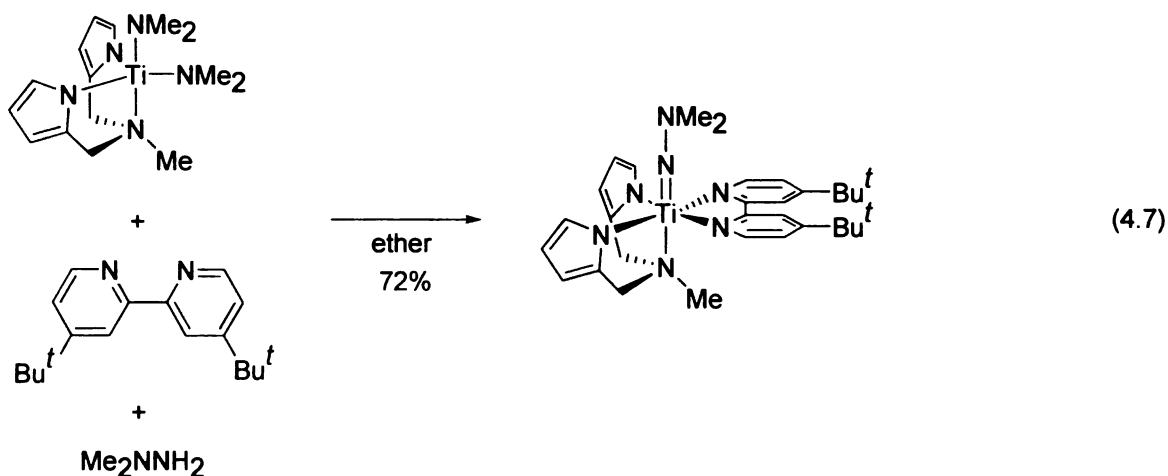


In a more recent example, $\text{V}(\text{NS}_3)(\text{NNC}_5\text{H}_{10})$ was synthesized using 1-aminopiperidine to introduce the hydrazido(2-) moiety (Equation 4.5).²⁶ It was synthesized by reaction of $[\text{V}(\text{NS}_3)\text{O}]$ with 1-aminopiperidine at 140 °C. The V–N distance was 1.677(2) Å; the N–N distance was 1.324(3) Å. The V–N–N(hydrazido) angle is almost linear at 177.0(2)°. A derivative from benzophenone hydrazone ($\text{Ph}_2\text{C}=\text{NNH}_2$) to give $\text{V}(\text{NS}_3)(\text{NNCPh}_2)$ was also prepared (Equation 4.6).²⁶

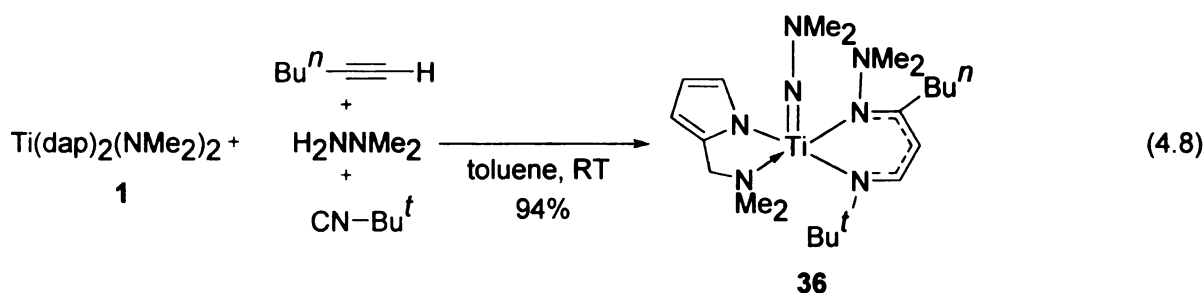


4.4 Titanium hydrazido(2-) complexes

A handful of examples of terminal Group-4 hydrazido(2-) complexes are known in the literature. The first example of a terminal titanium hydrazido(2-) complex, e.g. $\text{Cp}_2\text{Ti}\{\text{NN}(\text{SiMe}_3)_2\}$, was reported in 1978 by Wiberg and co-workers.¹⁷ In 1999, Mountford's group reported tetraazamacrocyclic-supported titanium and zirconium hydrazido(2-) complexes and their reactions with carbon dioxide, isocyanide, and isocyanates.¹⁶ Woo and Thorman developed porphyrin-based hydrazido(2-) complexes of titanium.¹⁵ The first crystallographically characterized terminal titanium hydrazido(2-) complex, $\text{Ti}(\text{NNMe}_2)(\text{dpma})(\text{Bu}^t\text{-bpy})$, where dpma = *N,N*-di(pyrrolyl- α -methyl)-*N*-methylamine, and $\text{Bu}^t\text{-bpy}$ = 4,4'-di-*tert*-butyl-2,2'-bipyridine, was reported by our group in 2004 (Equation 4.7).¹⁴



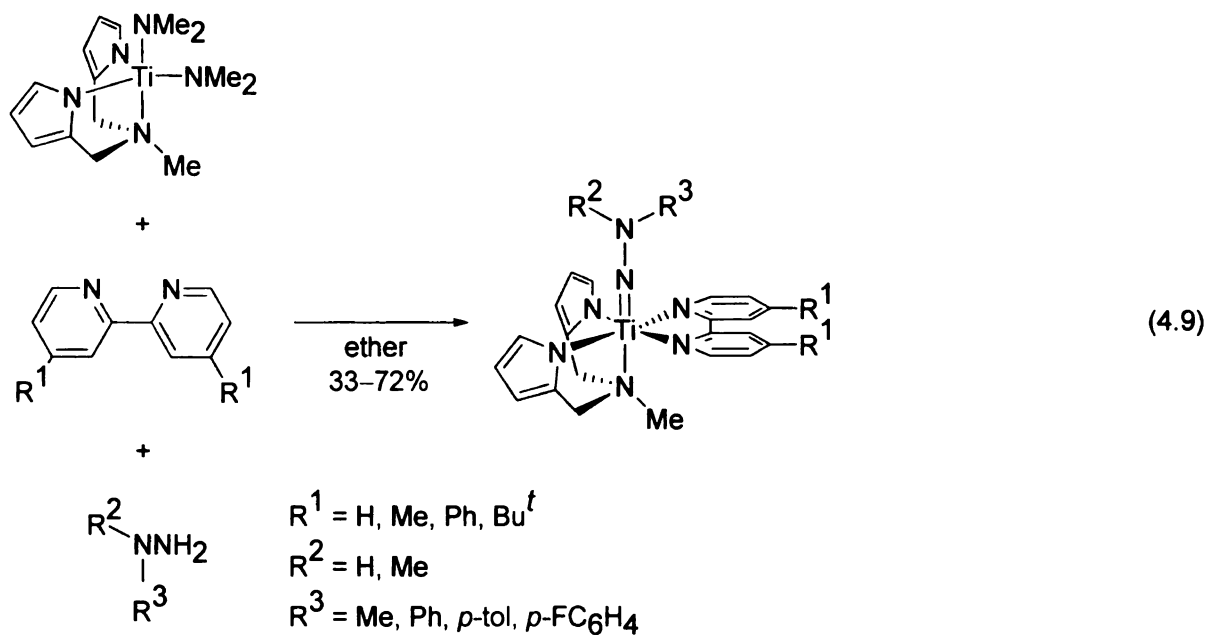
Another example of a structurally characterized titanium hydrazido(2-) complex from our group was $\text{Ti}(\text{NNMe}_2)(\text{dap})(\text{nacnac})$, where $\text{dap} = 2\text{-(dimethylaminomethyl)pyrrolyl}$ and $\text{nacnac} = [\text{N}(\text{Bu}^t)\text{CHCHC}(\text{Bu}^n)\text{N}(\text{NMe}_2)\text{-}k^2\text{N}]$ (Equation 4.8). Complex **(36)** was prepared as a possible intermediate in iminohydrazination of alkynes (*Vide supra*).¹²



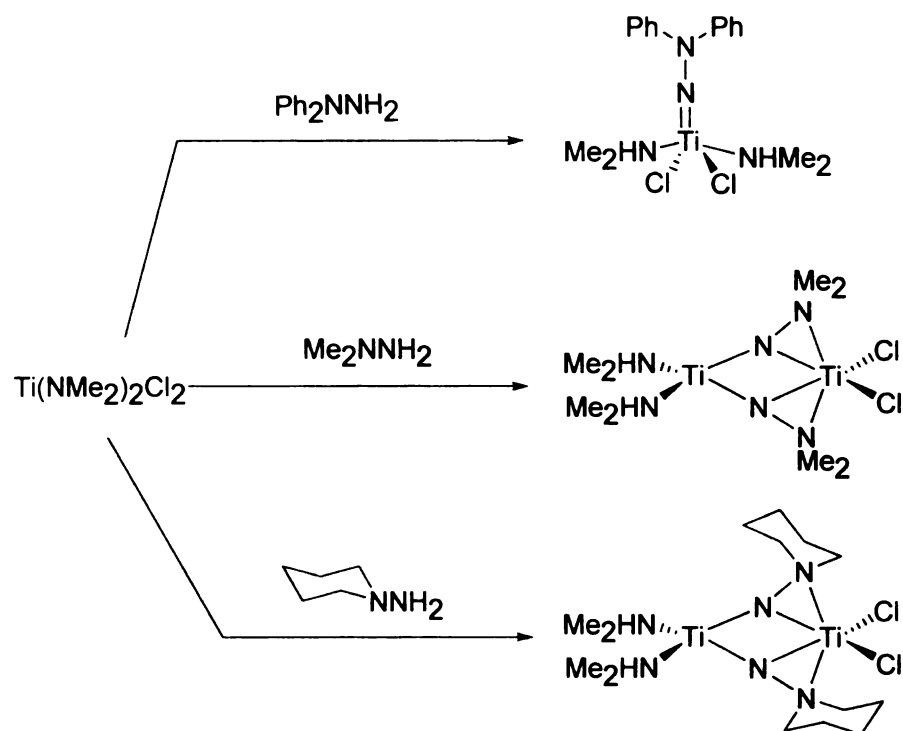
More recently, a series of terminal titanium(IV) hydrazido(2-) complexes were reported.¹¹ The complexes were synthesized by the addition of bpy, where, $\text{bpy} = 2,2'$ -bipyridine, to a solution of $\text{Ti}(\text{dpma})(\text{NMe}_2)_2$ followed by substituted hydrazines (Equation 4.9). In contrast to the normal yellow to red color of titanium(IV) complexes, these complexes are blue to green. This is due to an unusual low-energy ligand to ligand charge transfer (LLCT) transition from the hydrazido(2-) ligand to an empty π^* orbital of bipyridine.

In 2005, Mountford described the synthesis and bonding analysis of both terminal and bridging hydrazido(2-) complexes of titanium. The terminal complex was

synthesized by reacting $\text{Ti}(\text{NMe}_2)_2\text{Cl}_2$ with Ph_2NNH_2 (Scheme 4.2).¹³ In contrast, sterically smaller substituents on the hydrazines, such as Me_2NNH_2 or *N*-aminopiperidine, yielded bridging hydrazido(2-) complexes as shown in Scheme 4.2.

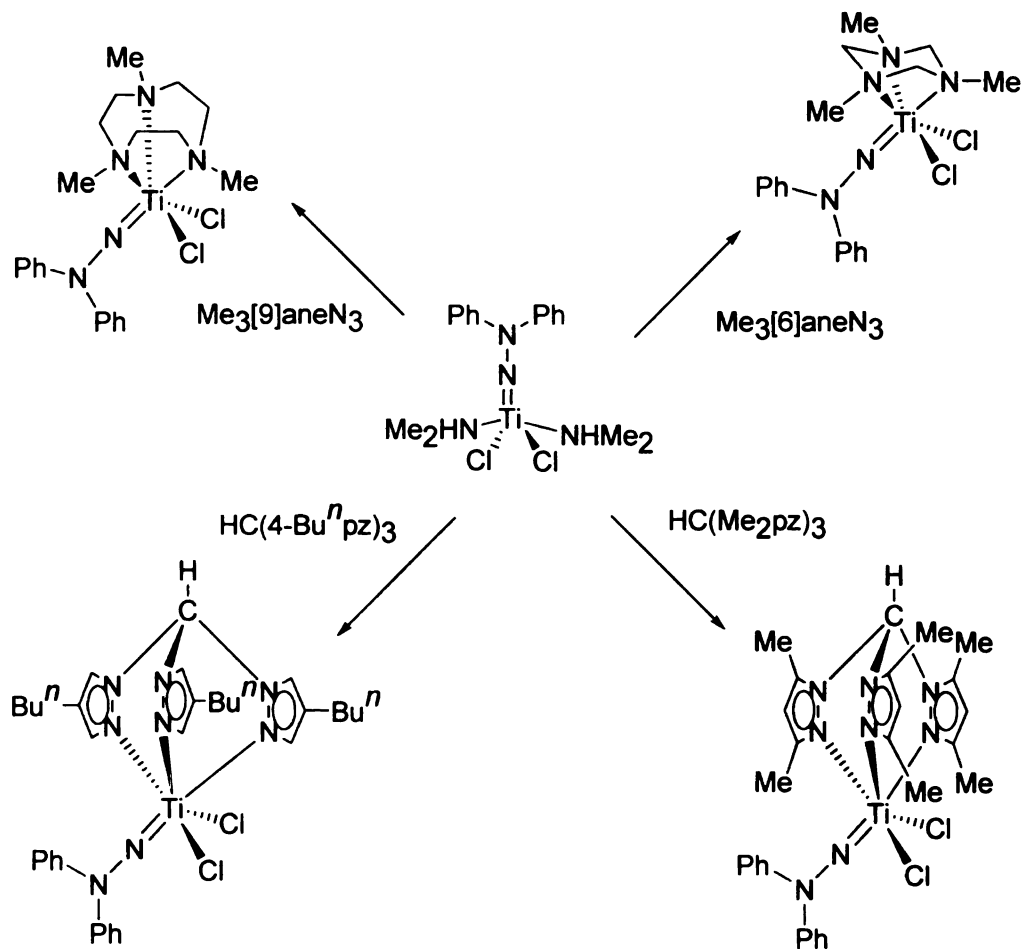


Scheme 4.2 Synthesis of titanium hydrazido(2-) complexes



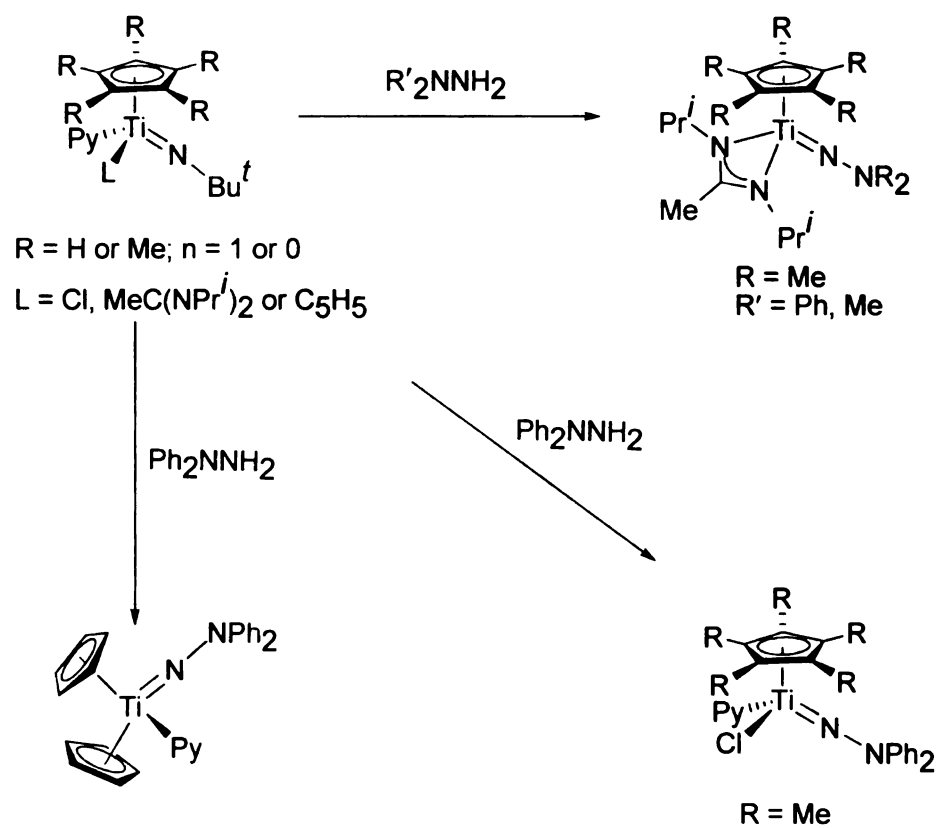
$\text{Ti}(\text{NNPh}_2)\text{Cl}_2(\text{NHMe}_2)_2$, synthesized according to Scheme 4.2, has been used to synthesize a variety of hydrazido(2-) complexes by metathesis with a *fac*- N_3 donor ligands as shown in Scheme 4.3.¹³

Scheme 4.3 Synthesis of titanium hydrazido(2-) complexes with different *fac*-N₃ donor ligands



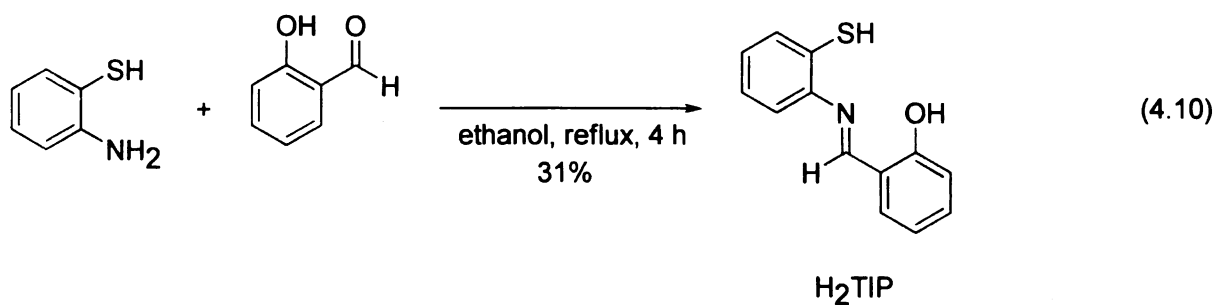
In addition, both sandwich and half-sandwich complexes of titanium carrying hydrazido(2-) ligands have been reported. They were synthesized from the corresponding imido complexes by reacting with hydrazine as shown in Scheme 4.4.¹⁰

Scheme 4.4 Synthesis of titanium hydrazido(2-) complexes from imido complexes



4.5 Aim of the current project

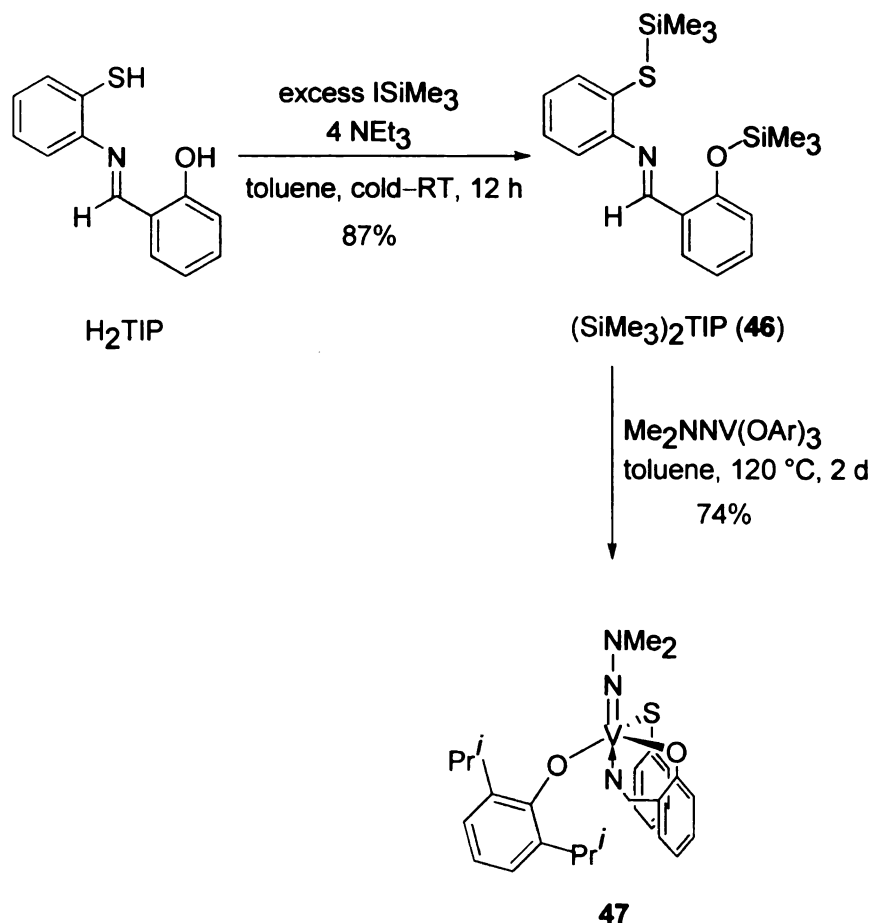
Although different types of vanadium(V) hydrazido(2-) complexes are known in the literature, no examples of vanadium hydrazido(2-) complexes are known where all of the elemental connections found in the enzyme, e.g., S, N, and O, are in the same coordination sphere. As part of our ongoing interest in the study of transition metal hydrazido(2-) complexes,^{11,12,14} we pursued the syntheses of vanadium(V) hydrazido(2-) complexes with a chelating ligand containing a thiolate, alkoxide, and donor imine, 2-((2-thiol-phenylimino)methylene)phenol H₂TIP, Equation 4.10.²⁵ The synthesis of different vanadium(V) hydrazido complexes with this ancillary ligand will be discussed in the following sections.⁵⁹



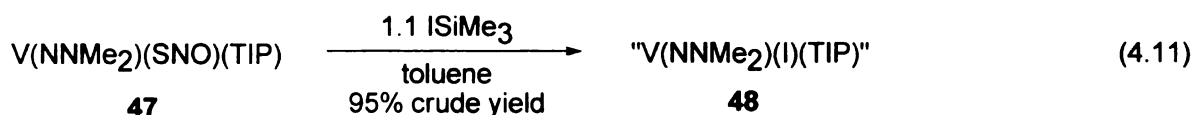
4.6 Results and Discussion

In order to synthesize vanadium(V) hydrazido(2-) complexes with the TIP ancillary, we initially attempted direct reaction of H₂TIP with V(NNMe₂)(OAr)₃,²⁸ where Ar = 2,6-Pr^{*i*}₂C₆H₃. Unfortunately, these reagents did not result in the elimination of 2 ArOH and the synthesis of V(NNMe₂)(OAr)(TIP) (**47**). However, we were able to readily synthesize (Me₃Si)₂TIP (**46**) which on reaction with V(NNMe₂)(OAr)₃ produced **47** in good yield (Scheme 4.5).

Scheme 4.5 Synthesis of V(NNMe₂)(OAr)(TIP) (**46**) (where Ar = 2,6-Pr^{*i*}₂C₆H₃)

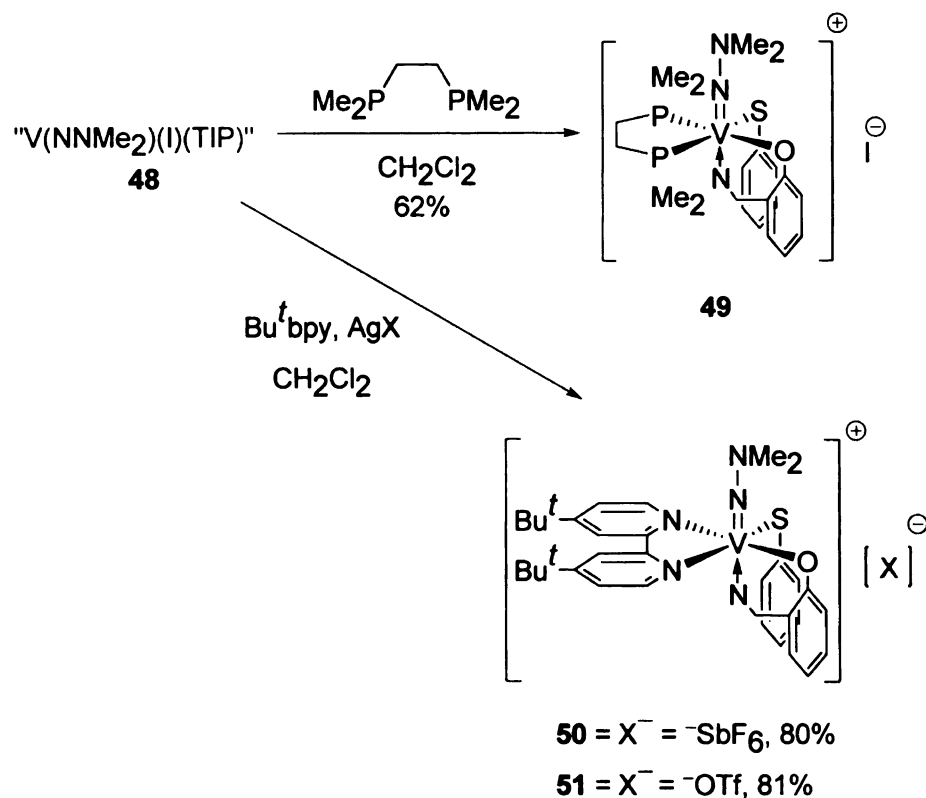


In order to explore the chemistry of the V(NNMe₂)(TIP) framework further, we exchanged the aryloxy ligand in **47** with iodide. Treatment of **47** with ISiMe₃ in toluene eliminated Me₃SiOAr and produced V(NNMe₂)(TIP)(I) (**48**) in 95% crude yield (Equation 4.11). The iodide complex was quite insoluble in most solvents but was effective as a starting material without further purification.



A brown suspension of **48** in CH₂Cl₂ reacted with dmpe, 1,2-(dimethylphosphino)ethane, to generate a dark red solution (Scheme 4.6). The new complex, [V(NNMe₂)(TIP)(dmpe)]I (**49**), was isolated in 62% yield. Similarly, treatment of **48** with 4,4'-*tert*-butyl-2,2'-bipyridine (Bu^tbpy) and triflate or hexafluoroantimonate silver(I) salts formed cationic, hexacoordinate complexes in good yields (Scheme 4.6).

Scheme 4.6 Synthesis of cationic hydrazido(2-) complexes



The dmpme complex **49** was characterized by single crystal X-ray diffraction, and an ORTEP representation is shown in Figure 4.2. Unlike the titanium dimethylhydrazido(2-) complexes reported,^{11,12,14} this hexacoordinate complex has a planar Me–N–Me moiety, which is common for hydrazido(2-) complexes of most metals.⁵⁶ This cationic complex has a short N–N bond of 1.293(3) Å. The shortest hydrazido N–N distance was found in an iron porphyrin complex, and was measured as ~1.232(5) Å.⁵³ The metric parameters in the hydrazido ligand are similar to a related cationic vanadium complex reported by Dilworth and co-workers.³¹ The short N–N bond is indicative of a double bond, and the NNMe₂ ligand in this case may be

better described as an isodiazeno (Figure 4.3, (a)). However, the metric parameters of V–N–N moiety in **49** are different from the known vanadium *bis*(isodiazeno) complex, $[(C_9H_{18}N_2)_2(OSiMe_3)_2(OSiMe_3)_2V(\mu-O)V(O)(OSiMe_3)_2]$ (**52**) (Figure 4.3, (b)). The selected bond lengths and bond angles in **52** are as follows: V–N = 1.725(2) – 1.781(3) Å, N–N = 1.285(3) – 1.245(4) Å, V–N–N = 176.4(2)°, 174.3(2)°.³⁴ Thus compound **49** can not be unambiguously described as an isodiazeno complex. While quite different from hydrazido(2–) ligands of titanium in many respects, the short V=N bond in **49** of 1.698(2) Å suggests a significant contribution from the hydrazido(2–) resonance form as well.

Figure 4.2 ORTEP representation of the cationic part in **49**. Hydrogens and iodide ion are not shown. Ellipsoids are drawn at the 50% probability level. Selected bond lengths (Å) and angles (°): V(1)–N(1) 1.698(2), N(1)–N(2) 1.293(3), V(1)–O(1) 1.908(2), V(1)–N(3) 2.162(2), V(1)–S(1) 2.3383(8), V(1)–P(1) 2.5078(8), V(1)–P(2) 2.5079(8), N(2)–N(1)–V(1) 168.5(2), O(1)–V(1)–S(1) 119.53(6).

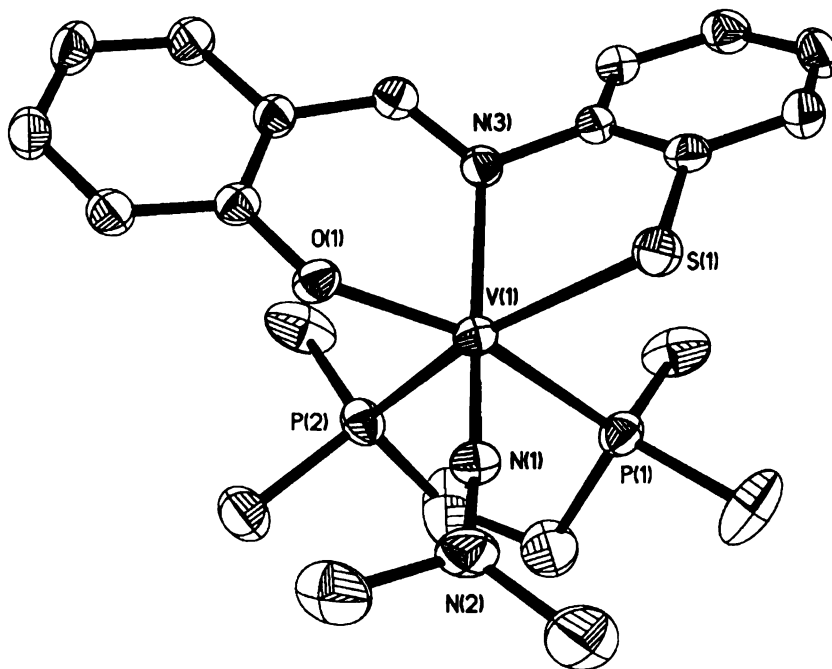
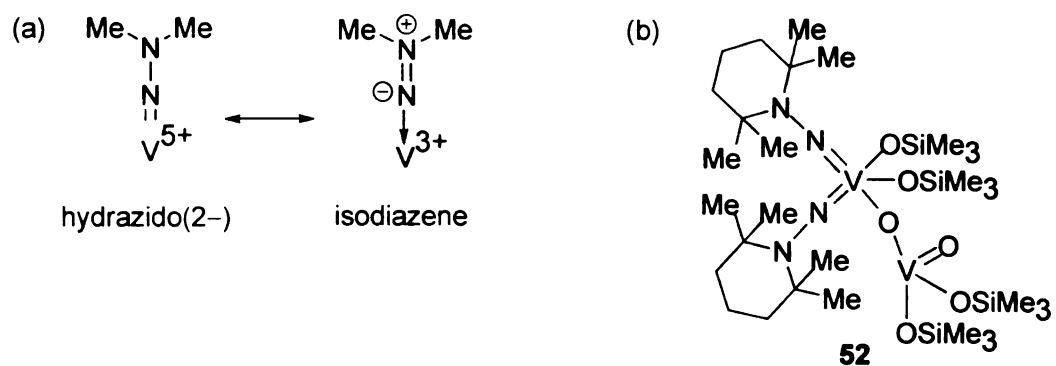


Figure 4.3 (a) Hydrazido(2-) vs isodiazeno resonance forms in vanadium complex. (b) Structure of **52**.



4.7 Concluding Remarks

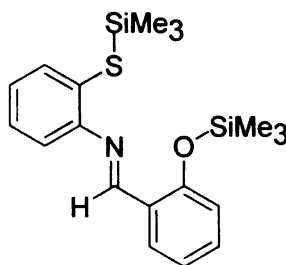
Using readily prepared $V(NNMe_2)(OAr)_3$ as a starting material, an example of a hydrazido(2-) TIP complex, $V(NNMe_2)(OAr)(TIP)$ (**46**) where $Ar = 2,6-Pr^i_2C_6H_3$, can be prepared. Replacement of the OAr ligand with iodide proceeds smoothly with $ISiMe_3$. While iodide **48** was not fully characterizable due to very low solubility in common solvents, it served as starting material for cationic hydrazido complexes. An X-ray diffraction study on one of the cationic vanadium complexes, $[V(NNMe_2)(TIP)(dmpe)]I$ (**49**), revealed a quite short N–N bond. This short N–N bond is indicative of the V(III) cation having poor backbonding into the $N=N \pi^*$ orbital of the isodiazene.

4.8 Experimental

General Considerations

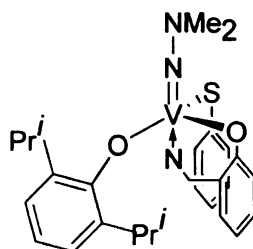
All manipulations of air sensitive compounds were carried out in an MBraun drybox under a purified nitrogen atmosphere. Pentane (Spectrum Chemical Mfg. Corp.), toluene (Spectrum Chemical Mfg. Corp.), ether (Columbus Chemical Industries Inc.), dichloromethane (EM Science), acetonitrile (Spectrum Chemical), and tetrahydrofuran (JADE Scientific) were sparged with nitrogen to remove oxygen then dried by passing through activated alumina. $\text{VCl}_3(\text{THF})_3$ was purchased from Strem Chemical Co. and used as received. 1,1-dimethylhydrazine was purchased from Aldrich Chemical Co. and distilled from KOH prior to use. 4,4'-di-*tert*-butyl-2,2'-bipyridine (Bu^tbpy) was purchased from Aldrich Chemical Co. and used as received. $\text{H}_2\text{TIP}^{25}$ and $\text{V}(\text{NNMe}_2)(\text{OAr})_3^{28}$ were synthesized according to the literature procedures. Deuterated solvents were dried over purple sodium benzophenone ketyl (C_6D_6) or phosphoric anhydride (CDCl_3) and distilled under nitrogen. ^1H and ^{13}C NMR spectra were recorded on Inova 300 or VXR-500 spectrometers. ^1H and ^{13}C NMR spectral assignments were confirmed, when necessary, with the use of 2-D ^1H - ^1H and ^{13}C - ^1H correlation NMR experiments. Routine coupling constants in ^{13}C NMR spectra are not reported. All spectra were referenced internally to residual protiosolvent (^1H) or solvent (^{13}C) resonances. Chemical shifts are quoted in ppm and coupling constants in Hz.

Synthesis of (Me₃Si)₂TIP (46)



All the manipulations were carried out inside an inert atmosphere glove box. An Erlenmeyer flask (100 mL) was loaded with H₂TIP (1.00 g, 4.36 mmol) and toluene (1.5 mL). The solution was cooled in a liquid nitrogen cooled cold well inside the box. Triethylamine (1.78 g, 17.6 mmol) in toluene (0.5 mL) was added to the solution. Trimethylsilyl iodide (3.52 g, 17.6 mmol) in toluene (0.5 mL) then was added. After the additions, the reaction was then allowed to warm to room temperature and stir overnight. The reaction mixture became pale yellow with a white precipitate. The precipitate was filtered with a fritted funnel, and the volatiles were removed in vacuo. The product was collected as a viscous, pale yellow oil in 87% yield (1.43 g, 3.9 mmol). ¹H NMR (299.8 MHz, C₆D₆): 7.56 (d, *J* = 7.48 Hz, 1 H, imine-*CH*), 7.01-6.61 (m, 8 H, aryl), 0.23 (s, 9 H, SiCH₃), 0.15 (s, 9 H, SiCH₃). ¹³C{¹H} NMR (125.7 MHz, C₆D₆): 150.7, 147.9, 136.1, 128.3, 128.0, 126.2, 124.8, 122.5, 121.4, 120.0, 118.0, 110.7, 64.9, 0.69, 0.23.

Synthesis of V(NNMe₂)(TIP)(OAr) (47)

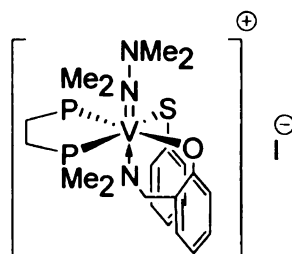


Under an atmosphere of dry nitrogen, a threaded pressure tube was loaded with V(NNMe₂)(OAr)₃ (1.50 g, 2.30 mmol) and (SiMe₃)₂TIP (0.87 g, 2.30 mmol) in toluene (9 mL). The pressure tube was taken outside the box and heated at 120 °C for 2 d. After cooling the tube to room temperature, the reaction mixture was filtered using a fritted funnel. Volatiles were removed from the brown filtrate in vacuo. This resulted in a dark brown solid. The brown solid was washed with cold pentane, and the residue was dried in vacuo. Finally, the product was crystallized as a dark brown solid from 1:1 ether:pentane in 74% yield (0.87 g, 1.70 mmol). ¹H NMR (499.7 MHz, C₆D₆): 9.21 (s, 1 H, imine-CH), 7.82 – 6.76 (m, 11 H, aryl-CH), 3.08 (s, 6 H, NCH₃), 2.80 (m, 2 H, CHMe₂), 0.84 (d, 6 H, *J*_{HH} = 6.9 Hz, CHCH₃), 0.81 (d, 6 H, *J*_{HH} = 6.8 Hz, CHCH₃). ¹³C{¹H} NMR (75.4 MHz, CDCl₃): 167.2, 159.5, 147.8, 145.4, 134.8, 134.3, 134.0, 128.0, 127.2, 124.3, 122.3, 121.6, 120.7, 119.5, 119.4, 116.7, 43.8, 26.2, 22.9, 22.5. ⁵¹V NMR (131.6 MHz, CDCl₃): 215.2 (*ν*_{1/2} = 1813 Hz). Elemental analysis: Exp. (Calc.), C: 63.47 (63.17); H: 6.44 (6.24); N: 8.00 (8.19). M.p.: 152-154 °C.

Synthesis of V(NNMe₂)(TIP)(I) (48)

Under an atmosphere of dry nitrogen, a threaded pressure tube (20 mL) was loaded with V(NNMe₂)(TIP)(OAr) (0.76 g, 1.50 mmol) and ISiMe₃ (0.33 g, 1.70 mmol) in toluene (6 mL). The solution was then heated at 45 °C overnight. A brown precipitate appeared from the reaction mixture. The precipitate was filtered using a fritted funnel. The solid was dried in vacuo. The product was isolated as brown powder in 95% crude yield (0.66 g, 1.40 mmol). Several attempts to purify this compound were unsuccessful as it was highly insoluble, and the compound was used without further purification. M.p. 216-218 °C.

Synthesis of [V(NNMe₂)(TIP)(dmpe)]I (49)



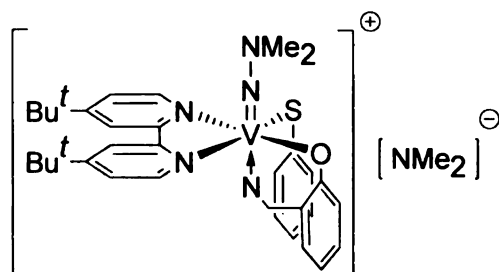
Under an atmosphere of dry nitrogen, a vial (20 mL) was loaded with V(NNMe₂)(TIP)(I) (0.18 g, 0.39 mmol), and the powder was suspended in CH₂Cl₂ (1.9 mL). To the stirred suspension was added dmpe (0.058 g, 0.39 mmol). The mixture was stirred overnight. The brown suspension gradually turned into a bright red solution. The volatiles were removed in vacuo. The product was crystallized from 1:1 CH₂Cl₂:THF in 62% yield (0.15 g, 0.24 mmol). ¹H NMR (499.7 MHz, CDCl₃): 9.47 (s, 1 H, imine-CH), 8.19 (s, 1 H, aryl-CH), 7.93 (d, 1 H, *J*_{HH} = 7.6 Hz, aryl-CH), 7.70 (t, 1 H, *J*_{HH} = 4.5 Hz, aryl-CH), 7.65 (t, 1 H, *J*_{HH} = 7.6 Hz, aryl-CH), 7.34 (q, 2 H, *J*_{HH} = 2.4 and 3.0 Hz, aryl-CH), 7.28 (d, 1 H, *J*_{HH} = 8.34 Hz, aryl-CH), 7.18 (t, 1 H, *J*_{HH} = 6.8 Hz, aryl-CH), 3.69 (s, 6 H, NCH₃), 2.11-2.03 (br s, 2 H, CH₂), 1.78-1.75 (dd, 6 H, *J* = 1.7 and 10.3 Hz, PCH₃), 1.78-1.66 (br s, 2 H, CH₂), 0.54-0.37 (dd, 6 H, *J* = 9.9 and 10.3 Hz, PCH₃). ¹³C{¹H} NMR (125.7 MHz, CDCl₃): 165.6, 164.7, 149.8, 144.1, 144.1, 134.9, 134.7, 129.2, 127.3, 126.1, 121.7, 121.2, 119.2, 44.2, 29.3 (dd, *J*_{CP} = 12.5 and 27.5 Hz, CH₂), 25.2 (dd, *J*_{CP} = 9.6 and 26.8, CH₂), 18.9 (dd, *J*_{CP} = 3.0 and 27.8, PCH₃), 14.6 (dd, *J*_{CP} = 17.2 and 22.2, PCH₃). ³¹P{¹H} NMR (200

MHz): 39.2 (br s). ^{51}V NMR (131.6 MHz, CDCl_3): -21.7 ($\nu_{1/2} = 1382$ Hz).

Elemental analysis: Exp. (Calc.), C: 41.11 (41.12); H: 5.15 (5.09); N: 6.77 (6.85).

M.p.: 179-181 °C.

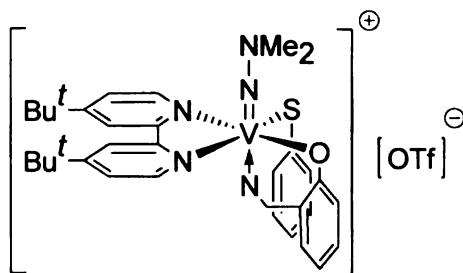
Synthesis of $[V(NNMe_2)(TIP)(Bu^t\text{bpy})][SbF_6]$ (**50**)



Under an atmosphere of dry nitrogen, a filter flask (125 mL) was loaded with **2** (0.30 g, 0.65 mmol) and CH_2Cl_2 (30 mL). The filter flask was cooled inside a liquid nitrogen cooled cold well. Two separate vials (20 mL) were loaded with $Bu^t\text{bpy}$ (0.17 g, 0.65 mmol) and $AgSbF_6$ (0.21 g, 0.61 mmol). To each reagent vial was added CH_2Cl_2 (0.5 mL). Both the vials were cooled inside the cold well. The cold solution of $Bu^t\text{bpy}$ was added to the filter flask. The mixture was allowed to stir for 10 min followed by addition of the $AgSbF_6$ suspension. The reaction mixture then was allowed to warm up to room temperature, sealed, and stirred overnight. The dark brown suspension gradually turned into a reddish-purple solution. The volatiles were removed in vacuo. Then solid products were stirred with THF (25 mL), and AgI separated as a grey solid. The solid was filtered using a fritted funnel. The volatiles were removed in vacuo from the filtrate resulting in a reddish-purple solid containing the crude product. The product was crystallized from 1:1 CH_2Cl_2 :pentane in 80% yield (0.34 g, 0.48 mmol). 1H NMR (299.8 MHz, $CDCl_3$): 8.82 (d, 1 H, $J_{HH} = 6$ Hz, $bpy-CH$), 8.77 (d, 1 H, $J_{HH} = 6$ Hz, $bpy-CH$), 8.73 (s, 1 H, imine CH), 7.84-6.83 (m,

12 H, aryl-CH and bpy-CH), 3.76 (s, 6 H, NCH₃), 1.22 (s, 9 H, CCH₃), 1.20 (s, 9 H, CCH₃). ¹³C{¹H} NMR (75.4 MHz, CDCl₃): 166.2, 165.9, 164.7, 163.0, 155.8, 153.2, 152.3, 150.4, 149.1, 147.6, 134.7, 134.1, 127.08, 127.06, 125.7, 122.7, 122.3, 121.7, 121.5, 119.5, 119.1, 118.2, 117.7, 43.6, 35.5, 29.99, 29.92. ⁵¹V NMR (131.6 MHz, CDCl₃): 423.8 (ν_{1/2} = 2832 Hz). Elemental analysis: Exp. (Calc.), C: 47.74 (47.16); H: 4.82 (4.68); N: 8.01 (8.33). M.p.: 186-188 °C.

Synthesis of [V(NNMe₂)(TIP)(Bu^tbpy)][OSO₂CF₃] (51)



Under an atmosphere of dry nitrogen, a filter flask (125 mL) was loaded with **3** (0.30 g, 0.65 mmol) and CH₂Cl₂ (30 mL). The filter flask was cooled inside a liquid nitrogen cooled cold well. To the suspension was added a cold solution of Bu^tbpy (0.17 g, 0.66 mmol) in CH₂Cl₂ (10 mL) followed by a cold suspension of AgOTf (0.17 g, 0.65 mmol) in CH₂Cl₂ (5 mL). The reaction mixture was allowed to warm up to room temperature and stir overnight. The brown suspension gradually turned into a dark purple solution. The volatiles were removed in vacuo resulting in a dark purple solid. The solid was stirred in THF (25 mL) for 5 h. AgI separated as a grey solid, which was filtered away using a fritted funnel. The volatiles were removed in vacuo from the filtrate. The product was crystallized from 1:1 THF:pentane in 81% yield (0.31 g, 0.49 mmol). ¹H NMR (299.8 MHz, CDCl₃): 8.87 (d, 1 H, *J*_{HH} = 8 Hz, bpy-CH), 8.80 (d, 1 H, *J*_{HH} = 8 Hz, bpy-CH), 8.79 (s, 1 H, imine-CH), 7.96–6.84 (m, 12 H, bpy-CH and Ph-CH), 3.75 (s, 6 H, H₃CN), 1.27 (s, 9 H, CCH₃), 1.23 (s, 9 H, CCH₃). ¹³C{¹H} NMR (75.4 MHz, CDCl₃): 166.3, 166.0, 164.8, 163.2, 155.9, 153.1, 152.3, 150.6, 149.1, 147.6, 134.6, 134.3, 127.2, 125.6, 122.7, 122.3, 121.5, 119.9,

119.4, 118.4, 117.7, 43.6, 35.6, 30.1, 30.0. ^{19}F NMR (282.4 MHz, CDCl_3): $\delta = -79.4$.
 ^{51}V NMR (131.6 MHz, CDCl_3): 423.6 ($\nu_{1/2} = 2046$ Hz). Elemental analysis: Exp. (Calc.), C: 54.43 (54.18); H: 5.07 (5.22); N: 9.18 (9.29). M.p.: 178-180 °C.

Crystal Structure Determination of $[\text{V}(\text{NNMe}_2)(\text{TIP})(\text{dmpe})]\text{I}$ (49): A red needle crystal with dimensions $0.28 \times 0.12 \times 0.10$ mm was mounted on a Nylon loop using paratone oil. Data were collected using a Bruker CCD diffractometer equipped with an Oxford Cryostream low-temperature apparatus operating at 173 K. Data were measured using ω and ϕ scans of $0.5^\circ/\text{frame}$ for 10 s. The total number of images was based on results from the program COSMO⁶⁰ where redundancy was expected to be 4.0 and completeness of 100% out to 0.83 \AA . Cell parameters were retrieved using APEX II software and refined using SAINT on all observed reflections. Data reduction was performed using the SAINT software. Scaling and absorption corrections were applied using SADABS multi-scan technique supplied by George Sheldrick. The structure was solved by the direct method using the SHELXS-97 program and refined by the least squares method on F^2 , SHELXL-97, incorporated in SHELXTL-PC V 6.10. The structure was solved in the space group Pbca . All non-hydrogen atoms are refined anisotropically. Hydrogens were calculated by geometrical methods and refined as a riding model. **Crystal Data:** $\text{C}_{21}\text{H}_{31}\text{IN}_3\text{OP}_2\text{SV}$, $M = 613.33$, orthorhombic, $a = 10.8685(2) \text{ \AA}$, $b = 18.3385(3) \text{ \AA}$, $c = 26.2108(5) \text{ \AA}$, $U = 5224.13(16) \text{ \AA}^3$, space group Pbca , $Z = 8$, 67170 reflections were collected, 6199 were unique ($R_{\text{int}} = 0.0556$) which were all used in calculations. The

final $R_1 = 0.0566$ and $wR(F_2) = 0.0701$ for all data. The final $R_1 = 0.0325$ and $wR(F_2)$
 $= 0.0627$ for all data $I > 2\sigma(I)$.

4.9 References

1. Yandulov, D. V.; Schrock, R. R. *Inorg. Chem.* **2005**, *44*, 1103.
2. Yandulov, D. V.; Schrock, R. R.; Rheingold, A. L.; Ceccarelli, C.; Davis, W. M. *Inorg. Chem.* **2003**, *42*, 796.
3. Yandulov, D. V.; Schrock, R. R. *Science* **2003**, *301*, 76.
4. Greco, G. E.; Schrock, R. R. *Inorg. Chem.* **2001**, *40*, 3861.
5. Carrillo, D. *Org. Organometallic Synth.* **2000**, *3*, 175.
6. Gouzerh, P.; Proust, A. *Chem. Rev.* **1998**, *98*, 77.
7. Niemoth-Anderson, J. D.; Debord, J. R. D.; George, T. A.; Ross, C. R.; Stezowski, J. J. *Polyhedron* **1996**, *15*, 4031.
8. Sutton, D. *Chem. Rev.* **1993**, *93*, 995.
9. Einstein, F. W. B.; T., J.; Hanlan, A. J. L.; Sutton, D. *Inorg. Chem.* **1982**, *21*, 2585.
10. Selby, J. D.; Manley, C. D.; Feliz, M.; Schwarz, A. D.; Clot, E.; Mountford, P. *Chem. Commun.* **2007**, 4937.
11. Patel, S.; Li, Y.; Odom, A. L. *Inorg. Chem.* **2007**, *46*, 6373.
12. Banerjee, S.; Odom, A. L. *Organometallics* **2006**, *25*, 3099.
13. Parsons, T. B.; Hazari, N.; Cowley, A. R.; Green, J. C.; Mountford, P. *Inorg. Chem.* **2005**, *44*, 8442.
14. Li, Y. H.; Shi, Y. H.; Odom, A. L. *J. Am. Chem. Soc.* **2004**, *126*, 1794.
15. Thorman, J. L.; Woo, L. K. *Inorg. Chem.* **2000**, *39*, 1301.
16. Blake, A. J.; McInnes, J. M.; Mountford, P.; Nikonov, G. I.; Swallow, D.; Watkin, D. J. *J. Chem. Soc., Dalton Trans.* **1999**, 379.
17. Wiberg, N.; Haring, H. W.; Huttner, G.; Friedrich, P. *Chem. Ber.* **1978**, *111*, 2708.
18. Herrmann, H.; Wadepohl, H.; Gade, L. H. *Dalton Trans.* **2008**, 2111.
19. Herrmann, H.; Fillol, J. L.; Wadepohl, H.; Gade, L. H. *Angew. Chem. Int. Ed.* **2007**, *46*, 8426.

20. Walsh, P. J.; Carney, M. J.; Bergman, R. G. *J. Am. Chem. Soc.* **1991**, *113*, 6343.
21. Kettler, P. B.; Chang, Y.; Zubieta, J. *Inorg. Chem.* **1994**, *33*, 5864.
22. Dilworth, J. R.; Jobanputra, P.; Parrott, S. J.; Thompson, R. M.; Povey, D. C.; Zubieta, J. A. *Polyhedron* **1992**, *11*, 147.
23. Nicholson, T.; Lombardi, P.; Zubieta, J. *Polyhedron* **1987**, *6*, 1577.
24. Dilworth, J. R.; Harrison, S. A.; Walton, D. R. M.; Schweda, E. *Inorg. Chem.* **1985**, *24*, 2594.
25. El-Ansary, A. L.; Soliman, A. A.; Sherif, O. E.; Ezzat, J. A. *Synthesis and Reactivity in Inorganic and Metal-Organic Chemistry* **2002**, *32*, 1301.
26. Davies, S. C.; Hughes, D. L.; Konkol, M.; Richards, R. L.; Sanders, J. R.; Sobota, P. *Dalton Trans.* **2002**, 2811.
27. Davies, S. C.; Hughes, D. L.; Janas, Z.; Jerzykiewicz, L. B.; Richards, R. L.; Sanders, J. R.; Silverston, J. E.; Sobota, P. *Inorg. Chem.* **2000**, *39*, 3485.
28. Henderson, R. A.; Janas, Z.; Jerzykiewicz, L. B.; Richards, R. L.; Sobota, P. *Inorg. Chim. Acta* **1999**, *285*, 178.
29. Kahlal, S.; Saillard, J. Y.; Hamon, J. R.; Manzur, C.; Carrillo, D. *J. Chem. Soc., Dalton Trans.* **1998**, 1229.
30. Davies, S. C.; Hughes, D. L.; Janas, Z.; Jerzykiewicz, L.; Richards, R. L.; Sanders, J. R.; Sobota, P. *Chem. Commun.* **1997**, 1261.
31. Bultitude, J.; Larkworthy, L. F.; Povey, D. C.; Smith, G. W.; Dilworth, J. R.; Leight, G. J. *J. Chem. Soc., Chem. Commun.* **1986**, 1748.
32. Veith, M. *Angew. Chem. Int. Ed.* **1976**, *15*, 387.
33. Green, M. L. H.; James, J. T.; Chernega, A. N. *J. Chem. Soc., Dalton Trans.* **1997**, 1719.
34. Danopoulos, A. A.; Hay-Motherwell, R. S.; Wilkinson, G.; Sweet, T. K. N.; Hursthouse, M. B. *Polyhedron* **1997**, *16*, 1081.
35. Huynh, M. H. V.; Lee, D. G.; White, P. S.; Meyer, T. J. *Inorg. Chem.* **2001**, *40*, 3842.
36. Huynh, M. H. V.; El-Samanody, E. S.; Demadis, K. D.; White, P. S.; Meyer, T. J. *Inorg. Chem.* **2000**, *39*, 3075.

37. Coia, G. M.; Devenney, M.; White, P. S.; Meyer, T. J.; Wink, D. A. *Inorg. Chem.* **1997**, *36*, 2341.
38. Xia, A. B.; Sharp, P. R. *Inorg. Chem.* **2001**, *40*, 4016.
39. Ramamoorthy, V.; Wu, Z. D.; Yi, Y.; Sharp, P. R. *J. Am. Chem. Soc.* **1992**, *114*, 1526.
40. Noth, H.; Sachdev, H.; Schmidt, M.; Schwenk, H. *Chem. Ber.* **1995**, *128*, 105.
41. Roussel, P.; Boaretto, R.; Kingsley, A. J.; Alcock, N. W.; Scott, P. *J. Chem. Soc., Dalton Trans.* **2002**, 1423.
42. Nicholson, T.; Devries, N.; Davison, A.; Jones, A. G. *Inorg. Chem.* **1989**, *28*, 3813.
43. Rees, D. C.; Chan, M. K.; Kim, J. *Adv. Inorg. Chem.* **1993**, *40*, 89.
44. Eady, R. R. *Chem. Rev.* **1996**, *96*, 3013.
45. Malinak, S. M.; Demadis, K. D.; Coucouvanis, D. *J. Am. Chem. Soc.* **1995**, *117*, 3126.
46. Eady, R. R. *Adv. Inorg. Chem.* **1991**, *36*, 77.
47. Richards, R. L. *Coord. Chem. Rev.* **1996**, *154*, 83.
48. Hidai, M.; Mizobe, Y. *Chem. Rev.* **1995**, *95*, 1115.
49. Eady, R. R. *Polyhedron* **1989**, *8*, 1695.
50. Le Floch, C.; Henderson, R. A.; Hitchcock, P. B.; Hughes, D. L.; Janas, Z.; Richards, R. L.; Sobota, P.; Szafert, S. *J. Chem. Soc., Dalton Trans.* **1996**, 2755.
51. Preuss, F.; Noichl, H.; Kaub, J. *Z. Naturforsch* **1986**, *41B*, 1085.
52. Danopoulos, A. A.; Wilkinson, G.; Williams, D. J. *J. Chem. Soc., Dalton Trans.* **1994**, 907.
53. Mahy, J. P.; Battioni, P.; Mansuy, D.; Fisher, J.; Weiss, R.; Mispelter, J.; Morgensternbadarau, I.; Gans, P. *J. Am. Chem. Soc.* **1984**, *106*, 1699.
54. Kahlal, S.; Saillard, J. Y.; Hamon, J. R.; Manzur, C.; Carrillo, D. *New J. Chem.* **2001**, *25*, 231.
55. DuBois, D. L.; Hoffmann, R. *Nouv. J. Chim.* **1977**, *1*, 479.

56. Kahlal, S.; Saillard, J. Y.; Hamon, J. R.; Manzur, C.; Carrillo, D. *J. Chem. Soc., Dalton Trans.* **1998**, 1229.
57. Nicholson, T.; Kramer, D. J.; Davison, A.; Jones, A. G. *Inorg. Chim. Acta.* **2003**, 353, 177.
58. Nicholson, T.; Hirsch-Kuchma, M.; Davison, A.; Jones, A. G. *Inorg. Chim. Acta* **1998**, 271, 191.
59. Banerjee, S.; Odom, A. L. *Dalton Trans.* **2008**, 2005.
60. (a) COSMO V1.56, Software for the CCD Detector Systems for Determining Data Collection Parameters. Bruker Analytical X-ray Systems, Madison, WI (2006); (b) APEX2 V 1.2-0 Software for the CCD Detector System; Bruker Analytical X-ray Systems, Madison, WI (2006); (c) SAINT V 7.34 Software for the Integration of CCD Detector System Bruker Analytical X-ray Systems, Madison, WI (2001); (d) SADABS V2.10 Program for absorption corrections using Bruker-AXS CCD based on the method of Robert Blessing; Blessing, R.H. *Acta Cryst. A*51, 1995, 33-38; (e) SHELXTL 6.14 (PC-Version), Program library for Structure Solution and Molecular Graphics; Bruker Analytical X-ray Systems, Madison, WI (2000).

TITANIUM-CATALYZED ADDITIONS OF SUBSTITUTED HYDRAZINES TO
ALKYNES: CATALYST DESIGN, MECHANISTIC STUDIES, AND
APPLICATIONS IN HETEROCYCLE SYNTHESIS

VOLUME II

By

Sanjukta Banerjee

A DISSERTATION

Submitted to
Michigan State University
in partial fulfillment of the requirements
for the degree of

DOCTOR OF PHILOSOPHY

Chemistry

2008

APPENDIX A

Crystallographic information

Table A1.1 Crystal data of H₂enp (4)

Identification code	eyb011_0m	
Empirical formula	C ₁₄ H ₂₂ N ₄	
Formula weight	246.36	
Temperature	173(2) K	
Wavelength	0.71073 Å	
Crystal system	Triclinic	
Space group	P -1	
Unit cell dimensions	a = 8.5225(2) Å	alpha= 109.2960(10)°.
	b = 9.2895(2) Å	beta= 104.2810(10)°.
	c = 9.5622(2) Å	gamma = 93.0310(10)°.
Volume	684.91(3) Å ³	
Z	2	
Density (calculated)	1.195 Mg/m ³	
Absorption coefficient	0.074 mm ⁻¹	
F(000)	268	
Crystal size	0.23 × 0.20 × 0.18 mm ³	
Theta range for data collection	2.35 to 27.49°.	
Index ranges	-10 ≤ h ≤ 11, -12 ≤ k ≤ 12, -12 ≤ l ≤ 12	
Reflections collected	9850	

Independent reflections	3074 [R(int) = 0.0237]
Completeness to theta = 25.00°	99.8 %
Absorption correction	Semi-empirical from equivalents
Max. and min. transmission	0.9868 and 0.9833
Refinement method	Full-matrix least-squares on F ²
Data / restraints / parameters	3074 / 0 / 165
Goodness-of-fit on F ²	1.060
Final R indices [I > 2sigma(I)]	R1 = 0.0446, wR2 = 0.1155
R indices (all data)	R1 = 0.0545, wR2 = 0.1223
Largest diff. peak and hole	0.274 and -0.209 e.Å ⁻³

Table A1.2 Atomic coordinates ($\times 10^4$) and equivalent isotropic displacement parameters ($\text{\AA}^2 \times 10^3$) for H₂enp. U(eq) is defined as one third of the trace of the orthogonalized U^{ij} tensor

	x	y	z	U(eq)
N(1)	28(1)	2531(1)	5468(1)	27(1)
N(2)	3391(1)	3502(1)	5086(1)	21(1)
C(1)	-1417(2)	1539(2)	4869(2)	32(1)
C(2)	-2009(2)	1334(2)	3349(2)	31(1)
C(3)	-874(2)	2229(2)	2997(2)	28(1)
C(4)	375(2)	2964(2)	4327(2)	23(1)
C(5)	1847(2)	4074(2)	4607(2)	26(1)
C(6)	3536(2)	2092(2)	3887(2)	31(1)
C(7)	4826(2)	4699(2)	5615(1)	24(1)
N(3)	4296(1)	2663(1)	7863(1)	23(1)
N(4)	1139(1)	3479(1)	8872(1)	22(1)
C(8)	5483(2)	1730(2)	7740(2)	26(1)
C(9)	5963(2)	1424(2)	9074(2)	27(1)

C(10)	5026(2)	2203(2)	10043(2)	25(1)
C(11)	4006(2)	2965(1)	9273(1)	22(1)
C(12)	2850(2)	4032(2)	9800(2)	24(1)
C(13)	508(2)	2067(2)	9039(2)	33(1)
C(14)	93(2)	4694(2)	9178(1)	25(1)

Table A1.3 Bond lengths (Å) and angles (°) for H₂enp

N(1)-C(4)	1.3692(17)
N(1)-C(1)	1.3703(18)
N(1)-H(1)	0.8800
N(2)-C(6)	1.4624(17)
N(2)-C(5)	1.4704(16)
N(2)-C(7)	1.4721(16)
C(1)-C(2)	1.360(2)
C(1)-H(1A)	0.9500
C(2)-C(3)	1.414(2)
C(2)-H(2)	0.9500
C(3)-C(4)	1.3771(18)
C(3)-H(3)	0.9500
C(4)-C(5)	1.4916(18)
C(5)-H(5A)	0.9900
C(5)-H(5B)	0.9900
C(6)-H(6A)	0.9800
C(6)-H(6B)	0.9800
C(6)-H(6C)	0.9800
C(7)-C(7)#1	1.541(2)
C(7)-H(7A)	0.9900

C(7)-H(7B)	0.9900
N(3)-C(8)	1.3679(16)
N(3)-C(11)	1.3706(16)
N(3)-H(3A)	0.8800
N(4)-C(13)	1.4632(17)
N(4)-C(12)	1.4691(16)
N(4)-C(14)	1.4740(15)
C(8)-C(9)	1.3671(19)
C(8)-H(8)	0.9500
C(9)-C(10)	1.4158(19)
C(9)-H(9)	0.9500
C(10)-C(11)	1.3757(17)
C(10)-H(10)	0.9500
C(11)-C(12)	1.4920(17)
C(12)-H(12A)	0.9900
C(12)-H(12B)	0.9900
C(13)-H(13A)	0.9800
C(13)-H(13B)	0.9800
C(13)-H(13C)	0.9800
C(14)-C(14)#2	1.536(2)
C(14)-H(14A)	0.9900
C(14)-H(14B)	0.9900
C(4)-N(1)-C(1)	109.16(11)
C(4)-N(1)-H(1)	125.4
C(1)-N(1)-H(1)	125.4
C(6)-N(2)-C(5)	111.37(11)
C(6)-N(2)-C(7)	112.87(10)
C(5)-N(2)-C(7)	112.37(10)
C(2)-C(1)-N(1)	108.78(13)
C(2)-C(1)-H(1A)	125.6

N(1)-C(1)-H(1A)	125.6
C(1)-C(2)-C(3)	106.85(13)
C(1)-C(2)-H(2)	126.6
C(3)-C(2)-H(2)	126.6
C(4)-C(3)-C(2)	107.93(12)
C(4)-C(3)-H(3)	126.0
C(2)-C(3)-H(3)	126.0
N(1)-C(4)-C(3)	107.28(12)
N(1)-C(4)-C(5)	122.74(11)
C(3)-C(4)-C(5)	129.96(12)
N(2)-C(5)-C(4)	112.82(10)
N(2)-C(5)-H(5A)	109.0
C(4)-C(5)-H(5A)	109.0
N(2)-C(5)-H(5B)	109.0
C(4)-C(5)-H(5B)	109.0
H(5A)-C(5)-H(5B)	107.8
N(2)-C(6)-H(6A)	109.5
N(2)-C(6)-H(6B)	109.5
H(6A)-C(6)-H(6B)	109.5
N(2)-C(6)-H(6C)	109.5
H(6A)-C(6)-H(6C)	109.5
H(6B)-C(6)-H(6C)	109.5
N(2)-C(7)-C(7)#1	115.97(13)
N(2)-C(7)-H(7A)	108.3
C(7)#1-C(7)-H(7A)	108.3
N(2)-C(7)-H(7B)	108.3
C(7)#1-C(7)-H(7B)	108.3
H(7A)-C(7)-H(7B)	107.4
C(8)-N(3)-C(11)	109.47(11)
C(8)-N(3)-H(3A)	125.3
C(11)-N(3)-H(3A)	125.3

C(13)-N(4)-C(12)	111.37(10)
C(13)-N(4)-C(14)	112.96(10)
C(12)-N(4)-C(14)	112.06(10)
C(9)-C(8)-N(3)	108.46(12)
C(9)-C(8)-H(8)	125.8
N(3)-C(8)-H(8)	125.8
C(8)-C(9)-C(10)	106.86(12)
C(8)-C(9)-H(9)	126.6
C(10)-C(9)-H(9)	126.6
C(11)-C(10)-C(9)	107.94(12)
C(11)-C(10)-H(10)	126.0
C(9)-C(10)-H(10)	126.0
N(3)-C(11)-C(10)	107.27(11)
N(3)-C(11)-C(12)	122.52(11)
C(10)-C(11)-C(12)	130.08(12)
N(4)-C(12)-C(11)	113.38(10)
N(4)-C(12)-H(12A)	108.9
C(11)-C(12)-H(12A)	108.9
N(4)-C(12)-H(12B)	108.9
C(11)-C(12)-H(12B)	108.9
H(12A)-C(12)-H(12B)	107.7
N(4)-C(13)-H(13A)	109.5
N(4)-C(13)-H(13B)	109.5
H(13A)-C(13)-H(13B)	109.5
N(4)-C(13)-H(13C)	109.5
H(13A)-C(13)-H(13C)	109.5
H(13B)-C(13)-H(13C)	109.5
N(4)-C(14)-C(14)#2	116.12(13)
N(4)-C(14)-H(14A)	108.3
C(14)#2-C(14)-H(14A)	108.3
N(4)-C(14)-H(14B)	108.3

C(14)#2-C(14)-H(14B) 108.3

H(14A)-C(14)-H(14B) 107.4

Symmetry transformations used to generate equivalent atoms:

#1 -x+1,-y+1,-z+1 #2 -x,-y+1,-z+2

Table A1.4 Anisotropic displacement parameters ($\text{\AA}^2 \times 10^3$) for H₂enp. The anisotropic displacement factor exponent takes the form: $-2 \pi^2 [h^2 a^{*2} U^{11} + \dots + 2 h k a^* b^* U^{12}]$

	U ¹¹	U ²²	U ³³	U ²³	U ¹³	U ¹²
N(1)	21(1)	34(1)	24(1)	9(1)	6(1)	0(1)
N(2)	18(1)	22(1)	24(1)	8(1)	7(1)	1(1)
C(1)	24(1)	37(1)	37(1)	14(1)	13(1)	-2(1)
C(2)	23(1)	31(1)	33(1)	4(1)	7(1)	-2(1)
C(3)	25(1)	32(1)	25(1)	8(1)	8(1)	3(1)
C(4)	20(1)	24(1)	26(1)	9(1)	9(1)	5(1)
C(5)	22(1)	24(1)	34(1)	12(1)	9(1)	4(1)
C(6)	31(1)	25(1)	38(1)	7(1)	17(1)	4(1)
C(7)	21(1)	30(1)	21(1)	10(1)	4(1)	-3(1)
N(3)	21(1)	27(1)	26(1)	13(1)	9(1)	6(1)
N(4)	19(1)	23(1)	23(1)	7(1)	8(1)	6(1)
C(8)	21(1)	29(1)	32(1)	9(1)	13(1)	6(1)
C(9)	21(1)	27(1)	35(1)	12(1)	8(1)	6(1)
C(10)	23(1)	29(1)	26(1)	12(1)	7(1)	4(1)
C(11)	18(1)	23(1)	24(1)	6(1)	7(1)	2(1)
C(12)	20(1)	26(1)	25(1)	4(1)	7(1)	4(1)
C(13)	30(1)	28(1)	44(1)	10(1)	19(1)	5(1)
C(14)	25(1)	32(1)	23(1)	10(1)	10(1)	13(1)

Table A1.5 Hydrogen coordinates ($\times 10^4$) and isotropic displacement parameters ($\text{\AA}^2 \times 10^3$) for H₂enp

	x	y	z	U(eq)
H(1)	636	2841	6432	32
H(1A)	-1923	1072	5425	38
H(2)	-2995	708	2656	37
H(3)	-957	2309	2017	33
H(5A)	1805	4285	3650	31
H(5B)	1822	5059	5418	31
H(6A)	2697	1259	3757	46
H(6B)	4624	1802	4190	46
H(6C)	3386	2272	2912	46
H(7A)	5803	4281	6039	29
H(7B)	4675	5584	6471	29
H(3A)	3797	3015	7148	28
H(8)	5902	1358	6874	32
H(9)	6772	807	9306	33
H(10)	5090	2200	11048	30
H(12A)	2926	4176	10889	29
H(12B)	3188	5050	9759	29
H(13A)	689	2233	10137	49
H(13B)	1080	1225	8580	49
H(13C)	-667	1797	8513	49
H(14A)	-1011	4287	8446	30
H(14B)	543	5572	8955	30

Table A1.6 Torsion angles (°) for H₂enp

C(4)-N(1)-C(1)-C(2)	-0.24(16)
N(1)-C(1)-C(2)-C(3)	0.41(16)
C(1)-C(2)-C(3)-C(4)	-0.42(16)
C(1)-N(1)-C(4)-C(3)	-0.03(15)
C(1)-N(1)-C(4)-C(5)	178.37(12)
C(2)-C(3)-C(4)-N(1)	0.28(15)
C(2)-C(3)-C(4)-C(5)	-177.96(12)
C(6)-N(2)-C(5)-C(4)	62.08(14)
C(7)-N(2)-C(5)-C(4)	-170.17(10)
N(1)-C(4)-C(5)-N(2)	63.42(16)
C(3)-C(4)-C(5)-N(2)	-118.58(15)
C(6)-N(2)-C(7)-C(7)#1	61.98(18)
C(5)-N(2)-C(7)-C(7)#1	-64.97(18)
C(11)-N(3)-C(8)-C(9)	0.04(15)
N(3)-C(8)-C(9)-C(10)	0.10(15)
C(8)-C(9)-C(10)-C(11)	-0.20(15)
C(8)-N(3)-C(11)-C(10)	-0.17(15)
C(8)-N(3)-C(11)-C(12)	176.02(11)
C(9)-C(10)-C(11)-N(3)	0.23(15)
C(9)-C(10)-C(11)-C(12)	-175.57(13)
C(13)-N(4)-C(12)-C(11)	65.51(14)
C(14)-N(4)-C(12)-C(11)	-166.86(10)
N(3)-C(11)-C(12)-N(4)	65.26(16)
C(10)-C(11)-C(12)-N(4)	-119.50(15)
C(13)-N(4)-C(14)-C(14)#2	62.89(19)
C(12)-N(4)-C(14)-C(14)#2	-63.89(19)

Table A1.7 Hydrogen bonds (Å) angles (°) for H₂enp

D-H...A	d(D-H)	d(H...A)	d(D...A)	<(DHA)
N(1)-H(1)...N(4)	0.88	2.13	2.9606(15)	156.7
N(3)-H(3A)...N(2)	0.88	2.12	2.9450(15)	156.6

Table A2.1 Crystal data for Ti(bap)(NMe₂)₃ (**28**)

Identification code	sb11t
Empirical formula	C ₁₆ H ₃₆ N ₆ Ti
Formula weight	360.41
Temperature	446(2) K
Wavelength	0.71073 Å
Crystal system, space group	Monoclinic, P2(1)/c
Unit cell dimensions	a = 9.3023(11) Å alpha = 90° b = 11.1907(14) Å beta = 93.075(3)° c = 19.610(2) Å gamma = 90°
Volume	2038.4(4) Å ³
Z, Calculated density	4, 1.174 Mg/m ³
Absorption coefficient	0.429 mm ⁻¹
F(000)	784
Crystal size	0.32 × 0.68 × 0.71 mm
Theta range for data collection	2.08 to 23.28 deg.
Limiting indices	-10 ≤ h ≤ 10, -12 ≤ k ≤ 12, -21 ≤ l ≤ 21
Reflections collected / unique	17217 / 2937 [R(int) = 0.0782]
Completeness to theta = 23.28	99.9 %
Absorption correction	None
Refinement method	Full-matrix least-squares on F ²
Data / restraints / parameters	2937 / 0 / 208
Goodness-of-fit on F ²	1.049
Final R indices [I > 2σ(I)]	R1 = 0.0592, wR2 = 0.1566
R indices (all data)	R1 = 0.0894, wR2 = 0.1718
Largest diff. peak and hole	0.543 and -0.474 e.Å ⁻³

Table A2.2 Atomic coordinates ($\times 10^4$) and equivalent isotropic displacement parameters ($\text{\AA}^2 \times 10^3$) for $\text{Ti}(\text{bap})(\text{NMe}_2)_3$. $U(\text{eq})$ is defined as one third of the trace of the orthogonalized U_{ij} tensor

	x	y	z	$U(\text{eq})$
Ti	2808(1)	8439(1)	8492(1)	23(1)
N(1)	2428(4)	6737(3)	8030(2)	26(1)
C(32)	1536(7)	8458(6)	9865(3)	56(2)
C(11)	1968(5)	6683(4)	7352(2)	25(1)
N(11)	2325(4)	8824(4)	7363(2)	26(1)
N(4)	3007(4)	10153(4)	8674(2)	32(1)
N(2)	4745(4)	8088(4)	8808(2)	29(1)
N(14)	2153(4)	5233(4)	9445(2)	29(1)
C(14)	2714(5)	5581(4)	8231(2)	25(1)
C(141)	3269(5)	5291(5)	8942(2)	30(1)
N(3)	1393(4)	8229(4)	9142(2)	33(1)
C(113)	3762(5)	8843(5)	7073(3)	34(1)
C(112)	1599(6)	9984(5)	7204(3)	36(1)
C(22)	5461(6)	8570(5)	9424(3)	52(2)
C(111)	1465(5)	7831(4)	7041(2)	32(1)
C(13)	2464(5)	4824(5)	7686(3)	33(1)
C(42)	1845(6)	10916(5)	8875(3)	47(2)
C(142)	1286(6)	4171(5)	9336(3)	47(2)
C(41)	4254(6)	10880(5)	8538(3)	46(2)
C(143)	2839(7)	5214(6)	10128(3)	54(2)
C(12)	1980(5)	5530(5)	7120(3)	34(1)
C(31)	11(6)	7685(5)	8942(3)	47(2)
C(21)	5739(5)	7353(5)	8442(3)	33(1)

Table A2.3 Bond lengths (Å) and angles (°) for Ti(bap)(NMe₂)₃

Ti-N(3)	1.894(4)
Ti-N(2)	1.915(4)
Ti-N(4)	1.958(4)
Ti-N(1)	2.131(4)
Ti-N(11)	2.277(4)
N(1)-C(14)	1.374(6)
N(1)-C(11)	1.375(6)
C(32)-N(3)	1.440(7)
C(11)-C(12)	1.368(7)
C(11)-C(111)	1.487(7)
N(11)-C(113)	1.480(6)
N(11)-C(112)	1.488(6)
N(11)-C(111)	1.490(6)
N(4)-C(42)	1.448(7)
N(4)-C(41)	1.454(7)
N(2)-C(22)	1.452(6)
N(2)-C(21)	1.455(6)
N(14)-C(142)	1.445(6)
N(14)-C(143)	1.451(6)
N(14)-C(141)	1.471(6)
C(14)-C(13)	1.373(7)
C(14)-C(141)	1.497(7)
N(3)-C(31)	1.457(7)
C(13)-C(12)	1.415(7)
N(3)-Ti-N(2)	115.66(18)
N(3)-Ti-N(4)	93.52(17)
N(2)-Ti-N(4)	93.65(17)
N(3)-Ti-N(1)	94.01(16)

N(2)-Ti-N(1)	94.95(16)
N(4)-Ti-N(1)	164.81(16)
N(3)-Ti-N(11)	124.73(17)
N(2)-Ti-N(11)	119.08(16)
N(4)-Ti-N(11)	90.19(16)
N(1)-Ti-N(11)	74.68(14)
C(14)-N(1)-C(11)	106.3(4)
C(14)-N(1)-Ti	134.0(3)
C(11)-N(1)-Ti	119.1(3)
C(12)-C(11)-N(1)	110.8(4)
C(12)-C(11)-C(111)	133.3(4)
N(1)-C(11)-C(111)	115.6(4)
C(113)-N(11)-C(112)	108.4(4)
C(113)-N(11)-C(111)	108.9(4)
C(112)-N(11)-C(111)	109.5(4)
C(113)-N(11)-Ti	104.0(3)
C(112)-N(11)-Ti	115.6(3)
C(111)-N(11)-Ti	110.1(3)
C(42)-N(4)-C(41)	109.5(4)
C(42)-N(4)-Ti	124.2(3)
C(41)-N(4)-Ti	125.7(3)
C(22)-N(2)-C(21)	110.2(4)
C(22)-N(2)-Ti	125.1(3)
C(21)-N(2)-Ti	124.6(3)
C(142)-N(14)-C(143)	109.8(4)
C(142)-N(14)-C(141)	110.1(4)
C(143)-N(14)-C(141)	109.1(4)
C(13)-C(14)-N(1)	109.6(4)
C(13)-C(14)-C(141)	128.8(5)
N(1)-C(14)-C(141)	121.5(4)
N(14)-C(141)-C(14)	114.4(4)

C(32)-N(3)-C(31)	111.8(4)
C(32)-N(3)-Ti	127.6(4)
C(31)-N(3)-Ti	120.4(3)
C(11)-C(111)-N(11)	108.7(4)
C(14)-C(13)-C(12)	107.4(5)
C(11)-C(12)-C(13)	105.9(4)

Table A2.4 Anisotropic displacement parameters ($\text{\AA}^2 \times 10^3$) for $\text{Ti}(\text{bap})(\text{NMe}_2)_3$. The anisotropic displacement factor exponent takes the form: $-2 \pi^2 [h^2 a^{*2} U_{11} + \dots + 2 h k a^* b^* U_{12}]$

	U11	U22	U33	U23	U13	U12
Ti	24(1)	26(1)	21(1)	0(1)	3(1)	1(1)
N(1)	23(2)	31(3)	25(2)	1(2)	1(2)	-1(2)
C(32)	62(4)	67(4)	41(4)	-6(3)	21(3)	-3(4)
C(11)	21(3)	37(3)	18(3)	2(2)	1(2)	-2(2)
N(11)	24(2)	30(2)	25(2)	4(2)	1(2)	-1(2)
N(4)	32(2)	26(2)	36(2)	0(2)	6(2)	-2(2)
N(2)	27(2)	32(2)	26(2)	-4(2)	-3(2)	0(2)
N(14)	35(2)	27(2)	25(2)	5(2)	-3(2)	1(2)
C(14)	20(3)	28(3)	27(3)	0(2)	1(2)	0(2)
C(141)	25(3)	31(3)	34(3)	5(2)	-1(2)	1(2)
N(3)	34(3)	30(2)	35(3)	0(2)	11(2)	1(2)
C(113)	29(3)	43(3)	31(3)	6(2)	5(2)	1(2)
C(112)	36(3)	40(3)	32(3)	9(3)	1(2)	7(3)
C(22)	51(4)	52(4)	50(4)	-16(3)	-16(3)	7(3)
C(111)	28(3)	41(3)	26(3)	1(2)	-2(2)	-3(2)
C(13)	29(3)	32(3)	38(3)	-7(3)	7(2)	-1(2)

C(42)	51(4)	35(3)	54(4)	-4(3)	-1(3)	12(3)
C(142)	50(4)	44(4)	48(4)	3(3)	5(3)	-16(3)
C(41)	55(4)	38(3)	46(4)	2(3)	2(3)	-11(3)
C(143)	56(4)	73(5)	32(3)	5(3)	-2(3)	1(3)
C(12)	33(3)	43(3)	24(3)	-9(3)	4(2)	-5(3)
C(31)	34(3)	56(4)	51(4)	11(3)	13(3)	7(3)
C(21)	27(3)	40(3)	33(3)	4(3)	3(2)	3(2)

Table A2.5 Hydrogen coordinates ($\times 10^4$) and isotropic displacement parameters ($\text{\AA}^2 \times 10^3$) for $\text{Ti}(\text{bap})(\text{NMe}_2)_3$

	x	y	z	U(eq)
H(32A)	646	8272	10068	84
H(32B)	1765	9285	9941	84
H(32C)	2291	7969	10068	84
H(14A)	3762	4527	8936	36
H(14B)	971	5891	9089	36
H(11A)	3656	9003	6592	51
H(11B)	4222	8083	7146	51
H(11C)	4340	9458	7292	51
H(11D)	1440	10064	6719	54
H(11E)	2196	10628	7376	54
H(11F)	692	10007	7415	54
H(22A)	6426	8265	9471	78
H(22B)	4943	8338	9813	78
H(22C)	5488	9426	9395	78
H(11G)	452	7947	7115	38
H(11H)	1586	7818	6553	38

H(13A)	2590	4000	7688	39
H(42A)	2194	11718	8935	70
H(42B)	1492	10631	9296	70
H(42C)	1081	10904	8526	70
H(14C)	558	4145	9664	71
H(14D)	1888	3476	9387	71
H(14E)	838	4187	8883	71
H(41A)	4083	11691	8672	69
H(41B)	4417	10856	8059	69
H(41C)	5084	10575	8792	69
H(14F)	2115	5173	10458	81
H(14G)	3397	5929	10201	81
H(14H)	3457	4530	10176	81
H(12A)	1723	5265	6681	40
H(31A)	-572	7648	9331	70
H(31B)	165	6892	8774	70
H(31C)	-469	8157	8590	70
H(21A)	6645	7309	8699	50
H(21B)	5880	7701	8003	50
H(21C)	5347	6564	8382	50

Table A3.1 Crystal data for Ti(NNMe₂)(dap)(nacnac) (**36**)

Identification code	sb2t
Empirical formula	C ₂₂ H ₄₃ N ₇ Ti
Formula weight	453.53
Temperature	446(2) K
Wavelength	0.71073 Å
Crystal system, space group	Monoclinic, P2(1)/c
Unit cell dimensions	a = 9.1796(14) Å alpha = 90 deg. b = 19.161(3) Å beta = 102.598(3) deg. c = 15.043(2) Å gamma = 90 deg.
Volume	2582.3(7) Å ³
Z, Calculated density	4, 1.167 Mg/m ³
Absorption coefficient	0.353 mm ⁻¹
F(000)	984
Crystal size	0.42 × 0.45 × 0.54 mm
Theta range for data collection	1.75 to 23.33 deg.
Limiting indices	-10 ≤ h ≤ 10, -21 ≤ k ≤ 21, -16 ≤ l ≤ 16
Reflections collected / unique	22066 / 3737 [R(int) = 0.1467]
Completeness to theta = 23.33	99.7 %
Absorption correction	Empirical
Max. and min. transmission	0.2484 and 0.1016
Refinement method	Full-matrix least-squares on F ²
Data / restraints / parameters	3737 / 0 / 272
Goodness-of-fit on F ²	1.012
Final R indices [I > 2σ(I)]	R1 = 0.0436, wR2 = 0.1040
R indices (all data)	R1 = 0.0742, wR2 = 0.1300
Extinction coefficient	0.0199(18)
Largest diff. peak and hole	0.414 and -0.398 e. Å ⁻³

Table A3.2 Atomic coordinates ($\times 10^4$) and equivalent isotropic displacement parameters ($\text{\AA}^2 \times 10^3$) for Ti(NNMe₂)(dap)(nacnac). U(eq) is defined as one third of the trace of the orthogonalized U_{ij} tensor

	x	y	z	U(eq)
Ti	1167(1)	6109(1)	2069(1)	28(1)
N(1)	2126(3)	5174(1)	1708(2)	34(1)
N(2)	2461(3)	6550(1)	2859(2)	34(1)
N(3)	-37(3)	5533(1)	2834(2)	28(1)
N(4)	-799(3)	6638(1)	1609(2)	30(1)
N(11)	2128(3)	6396(1)	810(2)	35(1)
N(21)	3629(3)	6791(2)	3555(2)	46(1)
N(31)	190(3)	5362(1)	3798(2)	33(1)
C(1)	-4943(4)	4169(2)	3948(2)	54(1)
C(2)	-3660(4)	4044(2)	3488(2)	40(1)
C(3)	-3147(3)	4699(2)	3081(2)	31(1)
C(4)	-1852(3)	4551(2)	2624(2)	32(1)
C(5)	-1159(3)	5192(2)	2302(2)	28(1)
C(6)	-1758(3)	5459(2)	1420(2)	32(1)
C(7)	-1735(4)	6153(2)	1173(2)	34(1)
C(11)	1996(4)	4468(2)	1831(2)	38(1)
C(12)	2941(4)	4103(2)	1417(2)	44(1)
C(13)	3704(4)	4601(2)	998(2)	43(1)
C(14)	3180(3)	5241(2)	1187(2)	35(1)
C(15)	3513(4)	5970(2)	943(2)	41(1)
C(40)	-1380(4)	7375(2)	1557(2)	39(1)
C(41)	-177(4)	7825(2)	2134(3)	52(1)
C(42)	-2759(4)	7392(2)	1976(3)	54(1)
C(43)	-1777(5)	7647(2)	579(3)	61(1)
C(111)	1083(4)	6180(2)	-44(2)	47(1)
C(112)	2518(4)	7140(2)	736(3)	50(1)

C(211)	4977(4)	6364(2)	3606(3)	52(1)
C(212)	3912(4)	7525(2)	3475(3)	55(1)
C(311)	1708(4)	5106(2)	4120(2)	47(1)
C(312)	-41(4)	6007(2)	4266(2)	49(1)

Table A3.3 Bond lengths (Å) and angles (°) for Ti(NNMe₂)(dap)(nacnac)

Ti-N(2)	1.709(3)
Ti-N(4)	2.055(3)
Ti-N(3)	2.077(2)
Ti-N(1)	2.119(3)
Ti-N(11)	2.323(3)
Ti-C(7)	2.713(3)
N(1)-C(11)	1.373(4)
N(1)-C(14)	1.377(4)
N(2)-N(21)	1.403(4)
N(3)-C(5)	1.330(4)
N(3)-N(31)	1.457(3)
N(4)-C(7)	1.337(4)
N(4)-C(40)	1.504(4)
N(11)-C(112)	1.480(4)
N(11)-C(111)	1.485(4)
N(11)-C(15)	1.487(4)
N(21)-C(212)	1.440(4)
N(21)-C(211)	1.471(4)
N(31)-C(311)	1.457(4)
N(31)-C(312)	1.460(4)
C(1)-C(2)	1.510(4)

C(2)-C(3)	1.516(4)
C(3)-C(4)	1.524(4)
C(4)-C(5)	1.510(4)
C(5)-C(6)	1.418(4)
C(6)-C(7)	1.382(4)
C(11)-C(12)	1.366(4)
C(12)-C(13)	1.411(5)
C(13)-C(14)	1.370(4)
C(14)-C(15)	1.493(4)
C(40)-C(41)	1.516(5)
C(40)-C(43)	1.529(5)
C(40)-C(42)	1.533(5)
N(2)-Ti-N(4)	114.61(12)
N(2)-Ti-N(3)	104.51(11)
N(4)-Ti-N(3)	85.08(10)
N(2)-Ti-N(1)	109.38(11)
N(4)-Ti-N(1)	135.61(10)
N(3)-Ti-N(1)	89.65(10)
N(2)-Ti-N(11)	96.89(11)
N(4)-Ti-N(11)	94.02(10)
N(3)-Ti-N(11)	156.86(10)
N(1)-Ti-N(11)	74.83(10)
N(2)-Ti-C(7)	142.04(11)
N(4)-Ti-C(7)	28.53(9)
N(3)-Ti-C(7)	73.05(10)
N(1)-Ti-C(7)	108.48(10)
N(11)-Ti-C(7)	95.36(9)
C(11)-N(1)-C(14)	105.2(3)
C(11)-N(1)-Ti	138.1(2)
C(14)-N(1)-Ti	116.7(2)

N(21)-N(2)-Ti	169.6(2)
C(5)-N(3)-N(31)	114.3(2)
C(5)-N(3)-Ti	111.35(19)
N(31)-N(3)-Ti	133.86(19)
C(7)-N(4)-C(40)	116.4(3)
C(7)-N(4)-Ti	104.2(2)
C(40)-N(4)-Ti	139.1(2)
C(112)-N(11)-C(111)	109.0(3)
C(112)-N(11)-C(15)	108.9(3)
C(111)-N(11)-C(15)	109.6(2)
C(112)-N(11)-Ti	115.51(19)
C(111)-N(11)-Ti	110.55(19)
C(15)-N(11)-Ti	103.05(18)
N(2)-N(21)-C(212)	112.4(3)
N(2)-N(21)-C(211)	110.7(3)
C(212)-N(21)-C(211)	112.5(3)
N(3)-N(31)-C(311)	109.0(2)
N(3)-N(31)-C(312)	106.6(2)
C(311)-N(31)-C(312)	110.7(3)
C(1)-C(2)-C(3)	113.3(3)
C(2)-C(3)-C(4)	111.7(3)
C(5)-C(4)-C(3)	114.8(2)
N(3)-C(5)-C(6)	118.5(3)
N(3)-C(5)-C(4)	122.1(3)
C(6)-C(5)-C(4)	119.3(3)
C(7)-C(6)-C(5)	125.0(3)
N(4)-C(7)-C(6)	125.6(3)
N(4)-C(7)-Ti	47.24(15)
C(6)-C(7)-Ti	84.67(19)
C(12)-C(11)-N(1)	111.1(3)
C(11)-C(12)-C(13)	106.5(3)

C(14)-C(13)-C(12)	106.3(3)
C(13)-C(14)-N(1)	110.9(3)
C(13)-C(14)-C(15)	133.4(3)
N(1)-C(14)-C(15)	115.8(3)
N(11)-C(15)-C(14)	109.4(3)
N(4)-C(40)-C(41)	107.4(3)
N(4)-C(40)-C(43)	112.2(3)
C(41)-C(40)-C(43)	110.3(3)
N(4)-C(40)-C(42)	108.3(3)
C(41)-C(40)-C(42)	108.4(3)
C(43)-C(40)-C(42)	110.1(3)

Table A3.4 Anisotropic displacement parameters ($\text{\AA}^2 \times 10^3$) for Ti(NNMe₂)(dap)(nacnac). The anisotropic displacement factor exponent takes the form: $-2 \pi^2 [h^2 a^{*2} U^{11} + \dots + 2 h k a^* b^* U^{12}]$

	U11	U22	U33	U23	U13	U12
Ti	29(1)	31(1)	25(1)	-1(1)	7(1)	-1(1)
N(1)	34(2)	37(2)	32(2)	0(1)	7(1)	1(1)
N(2)	31(2)	36(2)	33(2)	-3(1)	6(1)	-5(1)
N(3)	29(2)	31(2)	23(2)	1(1)	4(1)	0(1)
N(4)	32(2)	29(2)	31(2)	2(1)	8(1)	-3(1)
N(11)	37(2)	40(2)	30(2)	-1(1)	12(1)	-2(1)
N(21)	40(2)	53(2)	43(2)	-9(2)	2(2)	-10(2)
N(31)	33(2)	46(2)	20(2)	4(1)	6(1)	2(1)
C(1)	44(2)	75(3)	44(2)	-4(2)	14(2)	-17(2)
C(2)	39(2)	43(2)	40(2)	-1(2)	10(2)	-7(2)
C(3)	29(2)	35(2)	28(2)	0(2)	1(2)	2(1)
C(4)	36(2)	28(2)	33(2)	-3(2)	7(2)	-1(2)

C(5)	28(2)	30(2)	28(2)	-4(2)	11(2)	3(1)
C(6)	37(2)	33(2)	23(2)	-4(2)	2(2)	-4(2)
C(7)	35(2)	41(2)	24(2)	5(2)	4(2)	1(2)
C(11)	45(2)	37(2)	31(2)	0(2)	5(2)	3(2)
C(12)	52(2)	40(2)	35(2)	-7(2)	-1(2)	12(2)
C(13)	35(2)	61(2)	30(2)	-9(2)	4(2)	13(2)
C(14)	27(2)	50(2)	29(2)	-6(2)	4(2)	2(2)
C(15)	37(2)	55(2)	34(2)	-6(2)	17(2)	-6(2)
C(40)	36(2)	29(2)	52(2)	7(2)	11(2)	3(2)
C(41)	47(2)	31(2)	81(3)	-9(2)	21(2)	-2(2)
C(42)	43(2)	41(2)	82(3)	2(2)	24(2)	2(2)
C(43)	65(3)	49(2)	68(3)	22(2)	12(2)	10(2)
C(111)	55(2)	57(2)	30(2)	1(2)	13(2)	-1(2)
C(112)	64(3)	45(2)	50(2)	2(2)	32(2)	-10(2)
C(211)	36(2)	68(3)	50(2)	0(2)	3(2)	-5(2)
C(212)	61(3)	49(2)	52(3)	-14(2)	6(2)	-14(2)
C(311)	37(2)	69(3)	31(2)	15(2)	2(2)	1(2)
C(312)	61(3)	56(2)	30(2)	-9(2)	15(2)	-7(2)

Table A3.5 Hydrogen coordinates ($\times 10^4$) and isotropic displacement parameters ($\text{\AA}^2 \times 10^3$) for Ti(NNMe₂)(dap)(nacnac)

	x	y	z	U(eq)
H(1A)	-5217	3737	4191	81
H(1B)	-5781	4350	3513	81
H(1C)	-4646	4500	4434	81
H(2A)	-3961	3701	3009	48
H(2B)	-2827	3851	3929	48

H(3A)	-2840	5043	3558	38
H(3B)	-3974	4893	2636	38
H(4A)	-1085	4301	3051	39
H(4B)	-2203	4248	2106	39
H(6A)	-2201	5143	972	38
H(7A)	-2431	6295	659	41
H(11A)	1350	4266	2154	46
H(12A)	3058	3621	1412	53
H(13A)	4421	4513	661	51
H(15A)	4274	6171	1425	49
H(15B)	3887	5969	388	49
H(41A)	696	7820	1880	78
H(41B)	70	7646	2744	78
H(41C)	-535	8295	2142	78
H(42A)	-2498	7221	2590	81
H(42B)	-3527	7104	1624	81
H(42C)	-3114	7863	1978	81
H(43A)	-907	7635	323	92
H(43B)	-2130	8119	578	92
H(43C)	-2543	7360	222	92
H(11B)	1496	6302	-557	70
H(11C)	144	6413	-90	70
H(11D)	934	5684	-36	70
H(11E)	2903	7208	198	76
H(11F)	3262	7273	1263	76
H(11G)	1643	7422	700	76
H(21A)	4735	5881	3659	78
H(21B)	5725	6501	4128	78
H(21C)	5352	6432	3064	78
H(21D)	3004	7781	3444	83
H(21E)	4274	7607	2931	83

H(21F)	4647	7676	3995	83
H(31A)	1839	4684	3804	70
H(31B)	1882	5015	4762	70
H(31C)	2403	5452	4006	70
H(31D)	-1046	6167	4046	73
H(31E)	645	6356	4152	73
H(31F)	125	5921	4909	73

Table A4.1 Crystal data for $\text{Ti}_2(\text{dap})_3(\text{NNMe}_2)_2(\text{NHNMe}_2)$ (37)

Identification code	sbfinal	
Empirical formula	$\text{C}_{28} \text{H}_{54} \text{Cl}_2 \text{N}_{12} \text{Ti}_2$	
Formula weight	725.53	
Temperature	173(2) K	
Wavelength	0.71073 Å	
Crystal system	Monoclinic	
Space group	P 21/n	
Unit cell dimensions	$a = 11.9144(3)$ Å	$a = 90^\circ$.
	$b = 9.9855(3)$ Å	$b = 93.951(2)^\circ$.
	$c = 30.2370(9)$ Å	$g = 90^\circ$.
Volume	$3588.78(18)$ Å ³	
Z	4	
Density (calculated)	1.343 Mg/m ³	
Absorption coefficient	0.632 mm^{-1}	
F(000)	1536	
Crystal size	$0.26 \times 0.18 \times 0.14 \text{ mm}^3$	
Theta range for data collection	1.80 to 25.39° .	
Index ranges	$-14 \leq h \leq 14$, $-9 \leq k \leq 12$, $-36 \leq l \leq 36$	
Reflections collected	42331	
Independent reflections	6579 [R(int) = 0.0376]	
Completeness to $\theta = 25.00^\circ$	100.0 %	
Absorption correction	Semi-empirical from equivalents	
Max. and min. transmission	0.9162 and 0.8530	
Refinement method	Full-matrix least-squares on F^2	
Data / restraints / parameters	6579 / 0 / 409	
Goodness-of-fit on F^2	1.031	
Final R indices [I > 2σ(I)]	R1 = 0.0334, wR2 = 0.0782	
R indices (all data)	R1 = 0.0449, wR2 = 0.0840	

Largest diff. peak and hole

0.508 and $-0.489 \text{ e.}\text{\AA}^{-3}$

Table A4.2 Atomic coordinates ($\times 10^4$) and equivalent isotropic displacement parameters ($\text{\AA}^2 \times 10^3$) for sbfinal. $U(\text{eq})$ is defined as one third of the trace of the orthogonalized U^{ij} tensor

	x	y	z	U(eq)
Ti(1)	10152(1)	2884(1)	1459(1)	17(1)
Ti(2)	8010(1)	1758(1)	1306(1)	17(1)
N(1)	11129(1)	1347(2)	1222(1)	22(1)
N(2)	11578(1)	2361(2)	2052(1)	24(1)
N(3)	10214(1)	4753(2)	1774(1)	21(1)
N(4)	11292(1)	4449(2)	1010(1)	26(1)
N(5)	9179(1)	1957(2)	1795(1)	18(1)
N(6)	8354(1)	1249(2)	2008(1)	21(1)
N(7)	9058(1)	2918(2)	993(1)	19(1)
N(8)	8192(1)	2771(2)	658(1)	22(1)
N(9)	6943(1)	3341(2)	1476(1)	22(1)
N(10)	6151(1)	884(2)	1242(1)	25(1)
N(11)	8472(1)	27(2)	1070(1)	23(1)
N(12)	8059(2)	-1217(2)	886(1)	27(1)
C(29)	11292(2)	842(2)	808(1)	30(1)
C(30)	12077(2)	-159(2)	836(1)	38(1)
C(31)	12433(2)	-301(2)	1289(1)	36(1)
C(32)	11836(2)	619(2)	1514(1)	25(1)
C(33)	11779(2)	908(2)	1993(1)	28(1)
C(34)	11216(2)	2607(3)	2503(1)	33(1)
C(35)	12647(2)	3083(2)	2011(1)	32(1)

C(36)	9647(2)	5248(2)	2120(1)	23(1)
C(37)	9972(2)	6536(2)	2220(1)	26(1)
C(38)	10789(2)	6879(2)	1922(1)	26(1)
C(39)	10919(2)	5779(2)	1661(1)	22(1)
C(40)	11724(2)	5527(2)	1314(1)	27(1)
C(41)	10494(2)	5066(2)	678(1)	36(1)
C(42)	12243(2)	3907(3)	774(1)	40(1)
C(43)	7881(2)	2013(2)	2368(1)	29(1)
C(44)	8745(2)	-88(2)	2162(1)	29(1)
C(45)	8561(2)	2056(2)	266(1)	32(1)
C(46)	7619(2)	4028(2)	514(1)	29(1)
C(47)	7136(2)	4689(2)	1540(1)	23(1)
C(48)	6144(2)	5362(2)	1566(1)	28(1)
C(49)	5281(2)	4393(2)	1520(1)	35(1)
C(50)	5795(2)	3182(2)	1468(1)	27(1)
C(51)	5379(2)	1781(2)	1471(1)	34(1)
C(52)	5811(2)	863(3)	763(1)	37(1)
C(53)	6016(2)	-478(2)	1425(1)	34(1)
C(54)	8429(2)	-1413(3)	440(1)	42(1)
C(55)	8490(2)	-2309(2)	1170(1)	42(1)
Cl(1)	4135(1)	7291(1)	631(1)	55(1)
Cl(2)	5747(1)	6659(1)	-19(1)	66(1)
C(56)	5460(2)	6622(3)	539(1)	52(1)

Table A4.3 Bond lengths (Å) and angles (°) for $\text{Ti}_2(\text{dap})_3(\text{NNMe}_2)_2(\text{NHNMe}_2)$

Ti(1)-N(5)	1.8425(15)
Ti(1)-N(7)	1.8516(16)
Ti(1)-N(1)	2.0833(16)

Ti(1)-N(3)	2.0936(17)
Ti(1)-N(2)	2.4399(17)
Ti(1)-N(4)	2.5259(17)
Ti(1)-Ti(2)	2.7971(5)
Ti(2)-N(11)	1.9631(17)
Ti(2)-N(5)	1.9707(16)
Ti(2)-N(7)	1.9888(16)
Ti(2)-N(9)	2.1150(17)
Ti(2)-N(6)	2.1937(17)
Ti(2)-N(8)	2.2286(17)
Ti(2)-N(10)	2.3768(17)
N(1)-C(29)	1.376(3)
N(1)-C(32)	1.382(3)
N(2)-C(35)	1.477(3)
N(2)-C(34)	1.480(3)
N(2)-C(33)	1.483(3)
N(3)-C(36)	1.376(2)
N(3)-C(39)	1.383(3)
N(4)-C(41)	1.472(3)
N(4)-C(42)	1.483(3)
N(4)-C(40)	1.484(3)
N(5)-N(6)	1.402(2)
N(6)-C(43)	1.475(3)
N(6)-C(44)	1.479(3)
N(7)-N(8)	1.404(2)
N(8)-C(45)	1.475(3)
N(8)-C(46)	1.480(3)
N(9)-C(50)	1.375(3)
N(9)-C(47)	1.377(3)
N(10)-C(52)	1.479(3)
N(10)-C(53)	1.481(3)

N(10)-C(51)	1.488(3)
N(11)-N(12)	1.434(2)
N(11)-H(11)	0.8800
N(12)-C(55)	1.458(3)
N(12)-C(54)	1.461(3)
C(29)-C(30)	1.367(3)
C(29)-H(29)	0.9500
C(30)-C(31)	1.414(3)
C(30)-H(30)	0.9500
C(31)-C(32)	1.371(3)
C(31)-H(31)	0.9500
C(32)-C(33)	1.485(3)
C(33)-H(33A)	0.9900
C(33)-H(33B)	0.9900
C(34)-H(34A)	0.9800
C(34)-H(34B)	0.9800
C(34)-H(34C)	0.9800
C(35)-H(35A)	0.9800
C(35)-H(35B)	0.9800
C(35)-H(35C)	0.9800
C(36)-C(37)	1.370(3)
C(36)-H(36)	0.9500
C(37)-C(38)	1.414(3)
C(37)-H(37)	0.9500
C(38)-C(39)	1.367(3)
C(38)-H(38)	0.9500
C(39)-C(40)	1.491(3)
C(40)-H(40A)	0.9900
C(40)-H(40B)	0.9900
C(41)-H(41A)	0.9800
C(41)-H(41B)	0.9800

C(41)-H(41C)	0.9800
C(42)-H(42A)	0.9800
C(42)-H(42B)	0.9800
C(42)-H(42C)	0.9800
C(43)-H(43A)	0.9800
C(43)-H(43B)	0.9800
C(43)-H(43C)	0.9800
C(44)-H(44A)	0.9800
C(44)-H(44B)	0.9800
C(44)-H(44C)	0.9800
C(45)-H(45A)	0.9800
C(45)-H(45B)	0.9800
C(45)-H(45C)	0.9800
C(46)-H(46A)	0.9800
C(46)-H(46B)	0.9800
C(46)-H(46C)	0.9800
C(47)-C(48)	1.367(3)
C(47)-H(47)	0.9500
C(48)-C(49)	1.412(3)
C(48)-H(48)	0.9500
C(49)-C(50)	1.369(3)
C(49)-H(49)	0.9500
C(50)-C(51)	1.485(3)
C(51)-H(51A)	0.9900
C(51)-H(51B)	0.9900
C(52)-H(52A)	0.9800
C(52)-H(52B)	0.9800
C(52)-H(52C)	0.9800
C(53)-H(53A)	0.9800
C(53)-H(53B)	0.9800
C(53)-H(53C)	0.9800

C(54)-H(54A)	0.9800
C(54)-H(54B)	0.9800
C(54)-H(54C)	0.9800
C(55)-H(55A)	0.9800
C(55)-H(55B)	0.9800
C(55)-H(55C)	0.9800
Cl(1)-C(56)	1.753(3)
Cl(2)-C(56)	1.744(3)
C(56)-H(56A)	0.9900
C(56)-H(56B)	0.9900
N(5)-Ti(1)-N(7)	89.57(7)
N(5)-Ti(1)-N(1)	101.95(7)
N(7)-Ti(1)-N(1)	97.65(7)
N(5)-Ti(1)-N(3)	101.58(7)
N(7)-Ti(1)-N(3)	109.32(7)
N(1)-Ti(1)-N(3)	144.05(7)
N(5)-Ti(1)-N(2)	85.40(6)
N(7)-Ti(1)-N(2)	168.66(7)
N(1)-Ti(1)-N(2)	73.56(6)
N(3)-Ti(1)-N(2)	81.69(6)
N(5)-Ti(1)-N(4)	171.46(7)
N(7)-Ti(1)-N(4)	87.51(6)
N(1)-Ti(1)-N(4)	86.40(6)
N(3)-Ti(1)-N(4)	71.91(6)
N(2)-Ti(1)-N(4)	98.85(6)
N(5)-Ti(1)-Ti(2)	44.63(5)
N(7)-Ti(1)-Ti(2)	45.21(5)
N(1)-Ti(1)-Ti(2)	99.91(5)
N(3)-Ti(1)-Ti(2)	115.92(5)
N(2)-Ti(1)-Ti(2)	128.07(4)

N(4)-Ti(1)-Ti(2)	132.68(4)
N(11)-Ti(2)-N(5)	99.22(7)
N(11)-Ti(2)-N(7)	98.03(7)
N(5)-Ti(2)-N(7)	82.18(6)
N(11)-Ti(2)-N(9)	159.23(7)
N(5)-Ti(2)-N(9)	98.45(7)
N(7)-Ti(2)-N(9)	95.09(7)
N(11)-Ti(2)-N(6)	96.24(7)
N(5)-Ti(2)-N(6)	38.89(6)
N(7)-Ti(2)-N(6)	120.88(6)
N(9)-Ti(2)-N(6)	90.71(6)
N(11)-Ti(2)-N(8)	91.96(7)
N(5)-Ti(2)-N(8)	120.53(6)
N(7)-Ti(2)-N(8)	38.36(6)
N(9)-Ti(2)-N(8)	88.38(6)
N(6)-Ti(2)-N(8)	158.89(6)
N(11)-Ti(2)-N(10)	86.00(6)
N(5)-Ti(2)-N(10)	134.74(6)
N(7)-Ti(2)-N(10)	141.99(7)
N(9)-Ti(2)-N(10)	73.80(6)
N(6)-Ti(2)-N(10)	95.95(6)
N(8)-Ti(2)-N(10)	104.02(6)
N(11)-Ti(2)-Ti(1)	97.98(5)
N(5)-Ti(2)-Ti(1)	41.06(4)
N(7)-Ti(2)-Ti(1)	41.36(5)
N(9)-Ti(2)-Ti(1)	102.49(5)
N(6)-Ti(2)-Ti(1)	79.95(4)
N(8)-Ti(2)-Ti(1)	79.66(4)
N(10)-Ti(2)-Ti(1)	174.53(4)
C(29)-N(1)-C(32)	105.65(17)
C(29)-N(1)-Ti(1)	134.38(15)

C(32)-N(1)-Ti(1)	119.94(13)
C(35)-N(2)-C(34)	107.65(17)
C(35)-N(2)-C(33)	108.67(16)
C(34)-N(2)-C(33)	109.38(17)
C(35)-N(2)-Ti(1)	113.32(13)
C(34)-N(2)-Ti(1)	114.22(12)
C(33)-N(2)-Ti(1)	103.42(12)
C(36)-N(3)-C(39)	105.00(16)
C(36)-N(3)-Ti(1)	131.49(13)
C(39)-N(3)-Ti(1)	123.49(13)
C(41)-N(4)-C(42)	107.55(17)
C(41)-N(4)-C(40)	107.41(17)
C(42)-N(4)-C(40)	108.62(16)
C(41)-N(4)-Ti(1)	106.26(12)
C(42)-N(4)-Ti(1)	119.41(14)
C(40)-N(4)-Ti(1)	107.05(11)
N(6)-N(5)-Ti(1)	173.49(14)
N(6)-N(5)-Ti(2)	79.18(10)
Ti(1)-N(5)-Ti(2)	94.31(7)
N(5)-N(6)-C(43)	113.17(15)
N(5)-N(6)-C(44)	112.61(15)
C(43)-N(6)-C(44)	111.24(16)
N(5)-N(6)-Ti(2)	61.93(9)
C(43)-N(6)-Ti(2)	122.69(13)
C(44)-N(6)-Ti(2)	123.25(13)
N(8)-N(7)-Ti(1)	172.38(13)
N(8)-N(7)-Ti(2)	80.10(10)
Ti(1)-N(7)-Ti(2)	93.43(7)
N(7)-N(8)-C(45)	112.64(16)
N(7)-N(8)-C(46)	115.17(16)
C(45)-N(8)-C(46)	109.38(16)

N(7)-N(8)-Ti(2)	61.53(9)
C(45)-N(8)-Ti(2)	122.51(13)
C(46)-N(8)-Ti(2)	124.97(13)
C(50)-N(9)-C(47)	105.79(17)
C(50)-N(9)-Ti(2)	121.57(14)
C(47)-N(9)-Ti(2)	131.81(13)
C(52)-N(10)-C(53)	108.88(17)
C(52)-N(10)-C(51)	109.14(18)
C(53)-N(10)-C(51)	107.03(16)
C(52)-N(10)-Ti(2)	105.96(13)
C(53)-N(10)-Ti(2)	115.58(13)
C(51)-N(10)-Ti(2)	110.12(12)
N(12)-N(11)-Ti(2)	143.72(13)
N(12)-N(11)-H(11)	108.1
Ti(2)-N(11)-H(11)	108.1
N(11)-N(12)-C(55)	108.79(17)
N(11)-N(12)-C(54)	110.88(17)
C(55)-N(12)-C(54)	109.06(19)
C(30)-C(29)-N(1)	110.6(2)
C(30)-C(29)-H(29)	124.7
N(1)-C(29)-H(29)	124.7
C(29)-C(30)-C(31)	106.9(2)
C(29)-C(30)-H(30)	126.6
C(31)-C(30)-H(30)	126.6
C(32)-C(31)-C(30)	106.4(2)
C(32)-C(31)-H(31)	126.8
C(30)-C(31)-H(31)	126.8
C(31)-C(32)-N(1)	110.50(19)
C(31)-C(32)-C(33)	132.5(2)
N(1)-C(32)-C(33)	116.96(17)
N(2)-C(33)-C(32)	108.97(17)

N(2)-C(33)-H(33A)	109.9
C(32)-C(33)-H(33A)	109.9
N(2)-C(33)-H(33B)	109.9
C(32)-C(33)-H(33B)	109.9
H(33A)-C(33)-H(33B)	108.3
N(2)-C(34)-H(34A)	109.5
N(2)-C(34)-H(34B)	109.5
H(34A)-C(34)-H(34B)	109.5
N(2)-C(34)-H(34C)	109.5
H(34A)-C(34)-H(34C)	109.5
H(34B)-C(34)-H(34C)	109.5
N(2)-C(35)-H(35A)	109.5
N(2)-C(35)-H(35B)	109.5
H(35A)-C(35)-H(35B)	109.5
N(2)-C(35)-H(35C)	109.5
H(35A)-C(35)-H(35C)	109.5
H(35B)-C(35)-H(35C)	109.5
C(37)-C(36)-N(3)	111.06(18)
C(37)-C(36)-H(36)	124.5
N(3)-C(36)-H(36)	124.5
C(36)-C(37)-C(38)	106.47(18)
C(36)-C(37)-H(37)	126.8
C(38)-C(37)-H(37)	126.8
C(39)-C(38)-C(37)	106.42(18)
C(39)-C(38)-H(38)	126.8
C(37)-C(38)-H(38)	126.8
C(38)-C(39)-N(3)	111.04(17)
C(38)-C(39)-C(40)	130.20(19)
N(3)-C(39)-C(40)	118.62(18)
N(4)-C(40)-C(39)	110.24(16)
N(4)-C(40)-H(40A)	109.6

C(39)-C(40)-H(40A)	109.6
N(4)-C(40)-H(40B)	109.6
C(39)-C(40)-H(40B)	109.6
H(40A)-C(40)-H(40B)	108.1
N(4)-C(41)-H(41A)	109.5
N(4)-C(41)-H(41B)	109.5
H(41A)-C(41)-H(41B)	109.5
N(4)-C(41)-H(41C)	109.5
H(41A)-C(41)-H(41C)	109.5
H(41B)-C(41)-H(41C)	109.5
N(4)-C(42)-H(42A)	109.5
N(4)-C(42)-H(42B)	109.5
H(42A)-C(42)-H(42B)	109.5
N(4)-C(42)-H(42C)	109.5
H(42A)-C(42)-H(42C)	109.5
H(42B)-C(42)-H(42C)	109.5
N(6)-C(43)-H(43A)	109.5
N(6)-C(43)-H(43B)	109.5
H(43A)-C(43)-H(43B)	109.5
N(6)-C(43)-H(43C)	109.5
H(43A)-C(43)-H(43C)	109.5
H(43B)-C(43)-H(43C)	109.5
N(6)-C(44)-H(44A)	109.5
N(6)-C(44)-H(44B)	109.5
H(44A)-C(44)-H(44B)	109.5
N(6)-C(44)-H(44C)	109.5
H(44A)-C(44)-H(44C)	109.5
H(44B)-C(44)-H(44C)	109.5
N(8)-C(45)-H(45A)	109.5
N(8)-C(45)-H(45B)	109.5
H(45A)-C(45)-H(45B)	109.5

N(8)-C(45)-H(45C)	109.5
H(45A)-C(45)-H(45C)	109.5
H(45B)-C(45)-H(45C)	109.5
N(8)-C(46)-H(46A)	109.5
N(8)-C(46)-H(46B)	109.5
H(46A)-C(46)-H(46B)	109.5
N(8)-C(46)-H(46C)	109.5
H(46A)-C(46)-H(46C)	109.5
H(46B)-C(46)-H(46C)	109.5
C(48)-C(47)-N(9)	110.60(19)
C(48)-C(47)-H(47)	124.7
N(9)-C(47)-H(47)	124.7
C(47)-C(48)-C(49)	106.50(19)
C(47)-C(48)-H(48)	126.7
C(49)-C(48)-H(48)	126.7
C(50)-C(49)-C(48)	106.72(19)
C(50)-C(49)-H(49)	126.6
C(48)-C(49)-H(49)	126.6
C(49)-C(50)-N(9)	110.39(19)
C(49)-C(50)-C(51)	132.77(19)
N(9)-C(50)-C(51)	116.12(18)
C(50)-C(51)-N(10)	110.29(17)
C(50)-C(51)-H(51A)	109.6
N(10)-C(51)-H(51A)	109.6
C(50)-C(51)-H(51B)	109.6
N(10)-C(51)-H(51B)	109.6
H(51A)-C(51)-H(51B)	108.1
N(10)-C(52)-H(52A)	109.5
N(10)-C(52)-H(52B)	109.5
H(52A)-C(52)-H(52B)	109.5
N(10)-C(52)-H(52C)	109.5

H(52A)-C(52)-H(52C)	109.5
H(52B)-C(52)-H(52C)	109.5
N(10)-C(53)-H(53A)	109.5
N(10)-C(53)-H(53B)	109.5
H(53A)-C(53)-H(53B)	109.5
N(10)-C(53)-H(53C)	109.5
H(53A)-C(53)-H(53C)	109.5
H(53B)-C(53)-H(53C)	109.5
N(12)-C(54)-H(54A)	109.5
N(12)-C(54)-H(54B)	109.5
H(54A)-C(54)-H(54B)	109.5
N(12)-C(54)-H(54C)	109.5
H(54A)-C(54)-H(54C)	109.5
H(54B)-C(54)-H(54C)	109.5
N(12)-C(55)-H(55A)	109.5
N(12)-C(55)-H(55B)	109.5
H(55A)-C(55)-H(55B)	109.5
N(12)-C(55)-H(55C)	109.5
H(55A)-C(55)-H(55C)	109.5
H(55B)-C(55)-H(55C)	109.5
Cl(2)-C(56)-Cl(1)	112.54(15)
Cl(2)-C(56)-H(56A)	109.1
Cl(1)-C(56)-H(56A)	109.1
Cl(2)-C(56)-H(56B)	109.1
Cl(1)-C(56)-H(56B)	109.1
H(56A)-C(56)-H(56B)	107.8

Table A4.4 Anisotropic displacement parameters ($\text{\AA}^2 \times 10^3$) for $\text{Ti}_2(\text{dap})_3(\text{NNMe}_2)_2(\text{NHNMe}_2)$ (37). The anisotropic displacement factor exponent takes the form: $-2 p^2 [h^2 a^* 2 U^{11} + \dots + 2 h k a^* b^* U^{12}]$

	U11	U22	U33	U23	U13	U12
Ti(1)	15(1)	18(1)	18(1)	0(1)	3(1)	0(1)
Ti(2)	17(1)	16(1)	19(1)	0(1)	2(1)	0(1)
N(1)	22(1)	22(1)	24(1)	-1(1)	3(1)	2(1)
N(2)	21(1)	28(1)	22(1)	-1(1)	1(1)	2(1)
N(3)	19(1)	22(1)	23(1)	-2(1)	4(1)	-2(1)
N(4)	25(1)	28(1)	24(1)	2(1)	8(1)	-1(1)
N(5)	19(1)	19(1)	17(1)	1(1)	4(1)	0(1)
N(6)	21(1)	20(1)	22(1)	3(1)	6(1)	-2(1)
N(7)	20(1)	20(1)	18(1)	1(1)	2(1)	0(1)
N(8)	24(1)	22(1)	19(1)	0(1)	-3(1)	1(1)
N(9)	19(1)	21(1)	26(1)	-1(1)	2(1)	0(1)
N(10)	21(1)	22(1)	32(1)	-3(1)	2(1)	-2(1)
N(11)	23(1)	20(1)	27(1)	-4(1)	1(1)	-1(1)
N(12)	31(1)	19(1)	32(1)	-4(1)	1(1)	1(1)
C(29)	31(1)	33(1)	26(1)	-6(1)	4(1)	4(1)
C(30)	37(1)	39(2)	39(1)	-14(1)	6(1)	11(1)
C(31)	30(1)	31(1)	47(2)	-3(1)	0(1)	12(1)
C(32)	20(1)	22(1)	34(1)	1(1)	2(1)	3(1)
C(33)	24(1)	28(1)	31(1)	4(1)	1(1)	6(1)
C(34)	30(1)	44(2)	25(1)	-3(1)	-3(1)	5(1)
C(35)	22(1)	37(1)	36(1)	1(1)	-4(1)	-4(1)
C(36)	18(1)	28(1)	24(1)	-2(1)	4(1)	1(1)
C(37)	24(1)	26(1)	26(1)	-7(1)	0(1)	2(1)
C(38)	27(1)	20(1)	32(1)	-2(1)	-2(1)	-5(1)
C(39)	20(1)	22(1)	25(1)	0(1)	1(1)	-2(1)

C(40)	24(1)	25(1)	32(1)	1(1)	6(1)	-5(1)
C(41)	43(1)	37(1)	27(1)	11(1)	5(1)	-10(1)
C(42)	40(1)	41(2)	41(1)	-7(1)	24(1)	-6(1)
C(43)	31(1)	33(1)	24(1)	0(1)	10(1)	1(1)
C(44)	35(1)	23(1)	29(1)	9(1)	3(1)	-1(1)
C(45)	44(1)	31(1)	20(1)	-2(1)	-1(1)	3(1)
C(46)	32(1)	26(1)	28(1)	6(1)	-4(1)	7(1)
C(47)	24(1)	22(1)	24(1)	-1(1)	-1(1)	-2(1)
C(48)	33(1)	20(1)	30(1)	-3(1)	2(1)	6(1)
C(49)	19(1)	36(1)	50(2)	-7(1)	4(1)	5(1)
C(50)	19(1)	28(1)	34(1)	-3(1)	3(1)	0(1)
C(51)	22(1)	30(1)	51(2)	-7(1)	10(1)	-3(1)
C(52)	29(1)	42(2)	39(1)	-1(1)	-8(1)	-5(1)
C(53)	28(1)	26(1)	49(2)	0(1)	6(1)	-7(1)
C(54)	54(2)	34(1)	39(1)	-16(1)	10(1)	-5(1)
C(55)	53(2)	22(1)	51(2)	-2(1)	-8(1)	2(1)
Cl(1)	35(1)	60(1)	72(1)	-20(1)	5(1)	10(1)
Cl(2)	54(1)	98(1)	46(1)	8(1)	9(1)	14(1)
C(56)	44(2)	74(2)	39(2)	-5(1)	-2(1)	26(2)

Table A4.5 Hydrogen coordinates ($\times 10^4$) and isotropic displacement parameters ($\text{\AA}^2 \times 10^3$) for $\text{Ti}_2(\text{dap})_3(\text{NNMe}_2)_2(\text{NHNMe}_2)$

	x	y	z	U(eq)
H(11)	9212	6	1081	28
H(29)	10912	1147	541	36
H(30)	12333	-663	596	46
H(31)	12979	-912	1413	43
H(33A)	11161	387	2113	34
H(33B)	12493	645	2157	34
H(34A)	10510	2130	2541	50
H(34B)	11102	3569	2545	50
H(34C)	11797	2284	2723	50
H(35A)	13212	2753	2236	48
H(35B)	12529	4043	2055	48
H(35C)	12911	2931	1716	48
H(36)	9103	4762	2270	28
H(37)	9700	7089	2445	31
H(38)	11173	7711	1906	32
H(40A)	11827	6358	1143	32
H(40B)	12464	5263	1456	32
H(41A)	9868	5463	826	53
H(41B)	10204	4381	467	53
H(41C)	10878	5765	518	53
H(42A)	12627	4643	632	59
H(42B)	11956	3268	547	59
H(42C)	12774	3453	986	59
H(43A)	8479	2219	2597	43
H(43B)	7297	1480	2498	43
H(43C)	7552	2849	2249	43

H(44A)	9159	-518	1931	44
H(44B)	8095	-641	2224	44
H(44C)	9241	8	2432	44
H(45A)	9053	2639	105	48
H(45B)	7902	1807	72	48
H(45C)	8974	1246	362	48
H(46A)	7409	4528	774	44
H(46B)	6942	3816	325	44
H(46C)	8128	4573	347	44
H(47)	7859	5094	1563	28
H(48)	6053	6298	1608	33
H(49)	4495	4550	1525	42
H(51A)	4616	1736	1320	41
H(51B)	5330	1479	1781	41
H(52A)	6332	298	609	56
H(52B)	5828	1777	645	56
H(52C)	5047	502	717	56
H(53A)	5220	-734	1394	51
H(53B)	6280	-486	1739	51
H(53C)	6459	-1115	1262	51
H(54A)	8077	-738	240	63
H(54B)	8209	-2309	334	63
H(54C)	9249	-1324	447	63
H(55A)	9314	-2285	1192	63
H(55B)	8233	-3166	1042	63
H(55C)	8213	-2209	1466	63
H(56A)	6046	7137	714	63
H(56B)	5495	5684	645	63

Table A4.6 Torsion angles (°) for $\text{Ti}_2(\text{dap})_3(\text{NNMe}_2)_2(\text{NHNMe}_2)$

N(5)-Ti(1)-Ti(2)-N(11)	-94.90(9)
N(7)-Ti(1)-Ti(2)-N(11)	93.10(9)
N(1)-Ti(1)-Ti(2)-N(11)	2.13(7)
N(3)-Ti(1)-Ti(2)-N(11)	-174.85(7)
N(2)-Ti(1)-Ti(2)-N(11)	-74.68(7)
N(4)-Ti(1)-Ti(2)-N(11)	96.39(7)
N(7)-Ti(1)-Ti(2)-N(5)	-172.00(10)
N(1)-Ti(1)-Ti(2)-N(5)	97.03(8)
N(3)-Ti(1)-Ti(2)-N(5)	-79.95(9)
N(2)-Ti(1)-Ti(2)-N(5)	20.22(9)
N(4)-Ti(1)-Ti(2)-N(5)	-168.71(9)
N(5)-Ti(1)-Ti(2)-N(7)	172.00(10)
N(1)-Ti(1)-Ti(2)-N(7)	-90.97(8)
N(3)-Ti(1)-Ti(2)-N(7)	92.06(9)
N(2)-Ti(1)-Ti(2)-N(7)	-167.78(9)
N(4)-Ti(1)-Ti(2)-N(7)	3.29(9)
N(5)-Ti(1)-Ti(2)-N(9)	88.56(8)
N(7)-Ti(1)-Ti(2)-N(9)	-83.45(8)
N(1)-Ti(1)-Ti(2)-N(9)	-174.42(7)
N(3)-Ti(1)-Ti(2)-N(9)	8.61(7)
N(2)-Ti(1)-Ti(2)-N(9)	108.78(7)
N(4)-Ti(1)-Ti(2)-N(9)	-80.15(7)
N(5)-Ti(1)-Ti(2)-N(6)	0.07(8)
N(7)-Ti(1)-Ti(2)-N(6)	-171.93(8)
N(1)-Ti(1)-Ti(2)-N(6)	97.10(6)
N(3)-Ti(1)-Ti(2)-N(6)	-79.88(7)
N(2)-Ti(1)-Ti(2)-N(6)	20.29(7)
N(4)-Ti(1)-Ti(2)-N(6)	-168.64(7)
N(5)-Ti(1)-Ti(2)-N(8)	174.56(8)

N(7)-Ti(1)-Ti(2)-N(8)	2.55(8)
N(1)-Ti(1)-Ti(2)-N(8)	-88.42(6)
N(3)-Ti(1)-Ti(2)-N(8)	94.61(7)
N(2)-Ti(1)-Ti(2)-N(8)	-165.22(7)
N(4)-Ti(1)-Ti(2)-N(8)	5.85(7)
N(5)-Ti(1)-Ti(2)-N(10)	41.7(5)
N(7)-Ti(1)-Ti(2)-N(10)	-130.3(5)
N(1)-Ti(1)-Ti(2)-N(10)	138.8(5)
N(3)-Ti(1)-Ti(2)-N(10)	-38.2(5)
N(2)-Ti(1)-Ti(2)-N(10)	62.0(5)
N(4)-Ti(1)-Ti(2)-N(10)	-127.0(5)
N(5)-Ti(1)-N(1)-C(29)	116.0(2)
N(7)-Ti(1)-N(1)-C(29)	24.8(2)
N(3)-Ti(1)-N(1)-C(29)	-114.1(2)
N(2)-Ti(1)-N(1)-C(29)	-162.5(2)
N(4)-Ti(1)-N(1)-C(29)	-62.2(2)
Ti(2)-Ti(1)-N(1)-C(29)	70.54(19)
N(5)-Ti(1)-N(1)-C(32)	-66.32(16)
N(7)-Ti(1)-N(1)-C(32)	-157.51(15)
N(3)-Ti(1)-N(1)-C(32)	63.58(19)
N(2)-Ti(1)-N(1)-C(32)	15.17(14)
N(4)-Ti(1)-N(1)-C(32)	115.49(15)
Ti(2)-Ti(1)-N(1)-C(32)	-111.78(14)
N(5)-Ti(1)-N(2)-C(35)	-170.20(14)
N(7)-Ti(1)-N(2)-C(35)	125.9(3)
N(1)-Ti(1)-N(2)-C(35)	85.89(14)
N(3)-Ti(1)-N(2)-C(35)	-67.76(14)
N(4)-Ti(1)-N(2)-C(35)	2.34(14)
Ti(2)-Ti(1)-N(2)-C(35)	175.71(12)
N(5)-Ti(1)-N(2)-C(34)	-46.43(15)
N(7)-Ti(1)-N(2)-C(34)	-110.3(3)

N(1)-Ti(1)-N(2)-C(34)	-150.34(16)
N(3)-Ti(1)-N(2)-C(34)	56.00(15)
N(4)-Ti(1)-N(2)-C(34)	126.11(15)
Ti(2)-Ti(1)-N(2)-C(34)	-60.53(16)
N(5)-Ti(1)-N(2)-C(33)	72.34(12)
N(7)-Ti(1)-N(2)-C(33)	8.4(4)
N(1)-Ti(1)-N(2)-C(33)	-31.57(12)
N(3)-Ti(1)-N(2)-C(33)	174.78(12)
N(4)-Ti(1)-N(2)-C(33)	-115.12(12)
Ti(2)-Ti(1)-N(2)-C(33)	58.25(13)
N(5)-Ti(1)-N(3)-C(36)	-3.95(19)
N(7)-Ti(1)-N(3)-C(36)	89.70(19)
N(1)-Ti(1)-N(3)-C(36)	-133.95(17)
N(2)-Ti(1)-N(3)-C(36)	-87.48(18)
N(4)-Ti(1)-N(3)-C(36)	170.32(19)
Ti(2)-Ti(1)-N(3)-C(36)	40.97(19)
N(5)-Ti(1)-N(3)-C(39)	174.59(15)
N(7)-Ti(1)-N(3)-C(39)	-91.76(16)
N(1)-Ti(1)-N(3)-C(39)	44.6(2)
N(2)-Ti(1)-N(3)-C(39)	91.06(16)
N(4)-Ti(1)-N(3)-C(39)	-11.13(15)
Ti(2)-Ti(1)-N(3)-C(39)	-140.49(14)
N(5)-Ti(1)-N(4)-C(41)	-50.5(5)
N(7)-Ti(1)-N(4)-C(41)	19.63(14)
N(1)-Ti(1)-N(4)-C(41)	117.45(14)
N(3)-Ti(1)-N(4)-C(41)	-91.63(14)
N(2)-Ti(1)-N(4)-C(41)	-169.82(13)
Ti(2)-Ti(1)-N(4)-C(41)	17.29(16)
N(5)-Ti(1)-N(4)-C(42)	-172.2(4)
N(7)-Ti(1)-N(4)-C(42)	-102.04(16)
N(1)-Ti(1)-N(4)-C(42)	-4.21(16)

N(3)-Ti(1)-N(4)-C(42)	146.71(17)
N(2)-Ti(1)-N(4)-C(42)	68.52(16)
Ti(2)-Ti(1)-N(4)-C(42)	-104.37(16)
N(5)-Ti(1)-N(4)-C(40)	64.1(5)
N(7)-Ti(1)-N(4)-C(40)	134.17(13)
N(1)-Ti(1)-N(4)-C(40)	-128.00(13)
N(3)-Ti(1)-N(4)-C(40)	22.92(12)
N(2)-Ti(1)-N(4)-C(40)	-55.27(13)
Ti(2)-Ti(1)-N(4)-C(40)	131.84(11)
N(7)-Ti(1)-N(5)-N(6)	4.7(12)
N(1)-Ti(1)-N(5)-N(6)	-93.0(12)
N(3)-Ti(1)-N(5)-N(6)	114.4(12)
N(2)-Ti(1)-N(5)-N(6)	-165.1(12)
N(4)-Ti(1)-N(5)-N(6)	74.7(13)
Ti(2)-Ti(1)-N(5)-N(6)	-1.0(11)
N(7)-Ti(1)-N(5)-Ti(2)	5.67(7)
N(1)-Ti(1)-N(5)-Ti(2)	-92.06(7)
N(3)-Ti(1)-N(5)-Ti(2)	115.31(7)
N(2)-Ti(1)-N(5)-Ti(2)	-164.16(7)
N(4)-Ti(1)-N(5)-Ti(2)	75.6(5)
N(11)-Ti(2)-N(5)-N(6)	-88.51(10)
N(7)-Ti(2)-N(5)-N(6)	174.57(10)
N(9)-Ti(2)-N(5)-N(6)	80.54(10)
N(8)-Ti(2)-N(5)-N(6)	173.67(9)
N(10)-Ti(2)-N(5)-N(6)	5.01(14)
Ti(1)-Ti(2)-N(5)-N(6)	179.89(13)
N(11)-Ti(2)-N(5)-Ti(1)	91.60(7)
N(7)-Ti(2)-N(5)-Ti(1)	-5.32(7)
N(9)-Ti(2)-N(5)-Ti(1)	-99.35(7)
N(6)-Ti(2)-N(5)-Ti(1)	-179.89(13)
N(8)-Ti(2)-N(5)-Ti(1)	-6.22(9)

N(10)-Ti(2)-N(5)-Ti(1)	-174.88(6)
Ti(1)-N(5)-N(6)-C(43)	-115.0(11)
Ti(2)-N(5)-N(6)-C(43)	-115.95(15)
Ti(1)-N(5)-N(6)-C(44)	117.8(11)
Ti(2)-N(5)-N(6)-C(44)	116.80(15)
Ti(1)-N(5)-N(6)-Ti(2)	1.0(11)
N(11)-Ti(2)-N(6)-N(5)	96.96(10)
N(7)-Ti(2)-N(6)-N(5)	-6.27(12)
N(9)-Ti(2)-N(6)-N(5)	-102.64(10)
N(8)-Ti(2)-N(6)-N(5)	-15.3(2)
N(10)-Ti(2)-N(6)-N(5)	-176.42(10)
Ti(1)-Ti(2)-N(6)-N(5)	-0.07(9)
N(11)-Ti(2)-N(6)-C(43)	-162.22(15)
N(5)-Ti(2)-N(6)-C(43)	100.82(18)
N(7)-Ti(2)-N(6)-C(43)	94.54(16)
N(9)-Ti(2)-N(6)-C(43)	-1.82(15)
N(8)-Ti(2)-N(6)-C(43)	85.5(2)
N(10)-Ti(2)-N(6)-C(43)	-75.60(15)
Ti(1)-Ti(2)-N(6)-C(43)	100.75(15)
N(11)-Ti(2)-N(6)-C(44)	-2.91(16)
N(5)-Ti(2)-N(6)-C(44)	-99.87(18)
N(7)-Ti(2)-N(6)-C(44)	-106.15(15)
N(9)-Ti(2)-N(6)-C(44)	157.49(15)
N(8)-Ti(2)-N(6)-C(44)	-115.2(2)
N(10)-Ti(2)-N(6)-C(44)	83.70(15)
Ti(1)-Ti(2)-N(6)-C(44)	-99.95(15)
N(5)-Ti(1)-N(7)-N(8)	-37.3(10)
N(1)-Ti(1)-N(7)-N(8)	64.7(10)
N(3)-Ti(1)-N(7)-N(8)	-139.4(10)
N(2)-Ti(1)-N(7)-N(8)	26.3(12)
N(4)-Ti(1)-N(7)-N(8)	150.8(10)

Ti(2)-Ti(1)-N(7)-N(8)	-31.7(9)
N(5)-Ti(1)-N(7)-Ti(2)	-5.61(7)
N(1)-Ti(1)-N(7)-Ti(2)	96.40(7)
N(3)-Ti(1)-N(7)-Ti(2)	-107.73(7)
N(2)-Ti(1)-N(7)-Ti(2)	57.9(3)
N(4)-Ti(1)-N(7)-Ti(2)	-177.58(7)
N(11)-Ti(2)-N(7)-N(8)	82.96(10)
N(5)-Ti(2)-N(7)-N(8)	-178.76(10)
N(9)-Ti(2)-N(7)-N(8)	-80.90(10)
N(6)-Ti(2)-N(7)-N(8)	-174.79(9)
N(10)-Ti(2)-N(7)-N(8)	-10.83(15)
Ti(1)-Ti(2)-N(7)-N(8)	175.95(13)
N(11)-Ti(2)-N(7)-Ti(1)	-92.99(7)
N(5)-Ti(2)-N(7)-Ti(1)	5.29(7)
N(9)-Ti(2)-N(7)-Ti(1)	103.15(7)
N(6)-Ti(2)-N(7)-Ti(1)	9.26(10)
N(8)-Ti(2)-N(7)-Ti(1)	-175.95(13)
N(10)-Ti(2)-N(7)-Ti(1)	173.22(7)
Ti(1)-N(7)-N(8)-C(45)	-83.7(10)
Ti(2)-N(7)-N(8)-C(45)	-115.87(15)
Ti(1)-N(7)-N(8)-C(46)	149.9(9)
Ti(2)-N(7)-N(8)-C(46)	117.74(15)
Ti(1)-N(7)-N(8)-Ti(2)	32.1(10)
N(11)-Ti(2)-N(8)-N(7)	-100.48(10)
N(5)-Ti(2)-N(8)-N(7)	1.43(12)
N(9)-Ti(2)-N(8)-N(7)	100.29(10)
N(6)-Ti(2)-N(8)-N(7)	12.5(2)
N(10)-Ti(2)-N(8)-N(7)	173.15(10)
Ti(1)-Ti(2)-N(8)-N(7)	-2.72(9)
N(11)-Ti(2)-N(8)-C(45)	-0.47(16)
N(5)-Ti(2)-N(8)-C(45)	101.44(16)

N(7)-Ti(2)-N(8)-C(45)	100.01(18)
N(9)-Ti(2)-N(8)-C(45)	-159.70(16)
N(6)-Ti(2)-N(8)-C(45)	112.5(2)
N(10)-Ti(2)-N(8)-C(45)	-86.84(16)
Ti(1)-Ti(2)-N(8)-C(45)	97.29(15)
N(11)-Ti(2)-N(8)-C(46)	157.33(16)
N(5)-Ti(2)-N(8)-C(46)	-100.76(16)
N(7)-Ti(2)-N(8)-C(46)	-102.19(19)
N(9)-Ti(2)-N(8)-C(46)	-1.90(16)
N(6)-Ti(2)-N(8)-C(46)	-89.7(2)
N(10)-Ti(2)-N(8)-C(46)	70.96(16)
Ti(1)-Ti(2)-N(8)-C(46)	-104.91(16)
N(11)-Ti(2)-N(9)-C(50)	12.8(3)
N(5)-Ti(2)-N(9)-C(50)	-135.31(16)
N(7)-Ti(2)-N(9)-C(50)	141.87(16)
N(6)-Ti(2)-N(9)-C(50)	-97.04(16)
N(8)-Ti(2)-N(9)-C(50)	104.06(16)
N(10)-Ti(2)-N(9)-C(50)	-1.05(15)
Ti(1)-Ti(2)-N(9)-C(50)	-176.90(15)
N(11)-Ti(2)-N(9)-C(47)	-155.18(19)
N(5)-Ti(2)-N(9)-C(47)	56.72(19)
N(7)-Ti(2)-N(9)-C(47)	-26.10(19)
N(6)-Ti(2)-N(9)-C(47)	94.99(18)
N(8)-Ti(2)-N(9)-C(47)	-63.92(18)
N(10)-Ti(2)-N(9)-C(47)	-169.02(19)
Ti(1)-Ti(2)-N(9)-C(47)	15.12(19)
N(11)-Ti(2)-N(10)-C(52)	-72.76(14)
N(5)-Ti(2)-N(10)-C(52)	-171.79(13)
N(7)-Ti(2)-N(10)-C(52)	25.16(18)
N(9)-Ti(2)-N(10)-C(52)	102.36(14)
N(6)-Ti(2)-N(10)-C(52)	-168.63(14)

N(8)-Ti(2)-N(10)-C(52)	18.26(14)
Ti(1)-Ti(2)-N(10)-C(52)	150.2(4)
N(11)-Ti(2)-N(10)-C(53)	47.91(15)
N(5)-Ti(2)-N(10)-C(53)	-51.12(17)
N(7)-Ti(2)-N(10)-C(53)	145.83(14)
N(9)-Ti(2)-N(10)-C(53)	-136.97(15)
N(6)-Ti(2)-N(10)-C(53)	-47.96(15)
N(8)-Ti(2)-N(10)-C(53)	138.93(14)
Ti(1)-Ti(2)-N(10)-C(53)	-89.1(5)
N(11)-Ti(2)-N(10)-C(51)	169.33(15)
N(5)-Ti(2)-N(10)-C(51)	70.30(17)
N(7)-Ti(2)-N(10)-C(51)	-92.75(17)
N(9)-Ti(2)-N(10)-C(51)	-15.55(14)
N(6)-Ti(2)-N(10)-C(51)	73.46(15)
N(8)-Ti(2)-N(10)-C(51)	-99.65(15)
Ti(1)-Ti(2)-N(10)-C(51)	32.3(6)
N(5)-Ti(2)-N(11)-N(12)	141.2(2)
N(7)-Ti(2)-N(11)-N(12)	-135.5(2)
N(9)-Ti(2)-N(11)-N(12)	-6.8(4)
N(6)-Ti(2)-N(11)-N(12)	102.0(2)
N(8)-Ti(2)-N(11)-N(12)	-97.4(2)
N(10)-Ti(2)-N(11)-N(12)	6.5(2)
Ti(1)-Ti(2)-N(11)-N(12)	-177.3(2)
Ti(2)-N(11)-N(12)-C(55)	-120.2(2)
Ti(2)-N(11)-N(12)-C(54)	119.9(2)
C(32)-N(1)-C(29)-C(30)	-0.5(2)
Ti(1)-N(1)-C(29)-C(30)	177.46(16)
N(1)-C(29)-C(30)-C(31)	0.0(3)
C(29)-C(30)-C(31)-C(32)	0.5(3)
C(30)-C(31)-C(32)-N(1)	-0.8(3)
C(30)-C(31)-C(32)-C(33)	175.9(2)

C(29)-N(1)-C(32)-C(31)	0.8(2)
Ti(1)-N(1)-C(32)-C(31)	-177.49(15)
C(29)-N(1)-C(32)-C(33)	-176.46(18)
Ti(1)-N(1)-C(32)-C(33)	5.3(2)
C(35)-N(2)-C(33)-C(32)	-77.9(2)
C(34)-N(2)-C(33)-C(32)	164.87(17)
Ti(1)-N(2)-C(33)-C(32)	42.80(17)
C(31)-C(32)-C(33)-N(2)	147.5(2)
N(1)-C(32)-C(33)-N(2)	-36.0(2)
C(39)-N(3)-C(36)-C(37)	0.5(2)
Ti(1)-N(3)-C(36)-C(37)	179.25(14)
N(3)-C(36)-C(37)-C(38)	-0.1(2)
C(36)-C(37)-C(38)-C(39)	-0.4(2)
C(37)-C(38)-C(39)-N(3)	0.8(2)
C(37)-C(38)-C(39)-C(40)	-175.0(2)
C(36)-N(3)-C(39)-C(38)	-0.8(2)
Ti(1)-N(3)-C(39)-C(38)	-179.66(14)
C(36)-N(3)-C(39)-C(40)	175.50(18)
Ti(1)-N(3)-C(39)-C(40)	-3.4(3)
C(41)-N(4)-C(40)-C(39)	83.0(2)
C(42)-N(4)-C(40)-C(39)	-160.95(18)
Ti(1)-N(4)-C(40)-C(39)	-30.76(19)
C(38)-C(39)-C(40)-N(4)	-158.8(2)
N(3)-C(39)-C(40)-N(4)	25.7(3)
C(50)-N(9)-C(47)-C(48)	-0.6(2)
Ti(2)-N(9)-C(47)-C(48)	168.80(14)
N(9)-C(47)-C(48)-C(49)	0.4(2)
C(47)-C(48)-C(49)-C(50)	-0.1(3)
C(48)-C(49)-C(50)-N(9)	-0.3(3)
C(48)-C(49)-C(50)-C(51)	169.3(2)
C(47)-N(9)-C(50)-C(49)	0.5(2)

Ti(2)-N(9)-C(50)-C(49)	-170.18(15)
C(47)-N(9)-C(50)-C(51)	-170.99(19)
Ti(2)-N(9)-C(50)-C(51)	18.3(3)
C(49)-C(50)-C(51)-N(10)	159.6(2)
N(9)-C(50)-C(51)-N(10)	-31.2(3)
C(52)-N(10)-C(51)-C(50)	-87.5(2)
C(53)-N(10)-C(51)-C(50)	154.82(19)
Ti(2)-N(10)-C(51)-C(50)	28.4(2)

Table A5.1 Crystal data for 3-mesitylpyrrole (**43**)

Identification code	sb1076
Empirical formula	C ₁₃ H ₁₅ N
Formula weight	185.26
Temperature	173(2) K
Wavelength	0.71073 Å
Crystal system	Orthorhombic
Space group	P b c a
Unit cell dimensions	a = 10.4998(18) Å α = 90° b = 10.8656(17) Å β = 90° c = 17.915(3) Å γ = 90°
Volume	2043.9(6) Å ³
Z	8
Density (calculated)	1.204 Mg/m ³
Absorption coefficient	0.070 mm ⁻¹
F(000)	800
Crystal size	0.37 × 0.34 × 0.23 mm ³
Theta range for data collection	2.27 to 27.49°.
Index ranges	-13 ≤ h ≤ 13, -13 ≤ k ≤ 13, -21 ≤ l ≤ 21
Reflections collected	20550
Independent reflections	2284 [R(int) = 0.0253]
Completeness to theta = 25.00°	99.4 %
Absorption correction	Semi-empirical from equivalents
Max. and min. transmission	0.9839 and 0.9750
Refinement method	Full-matrix least-squares on F ²
Data / restraints / parameters	2284 / 0 / 130
Goodness-of-fit on F ²	1.056
Final R indices [I > 2σ(I)]	R1 = 0.0462, wR2 = 0.1306
R indices (all data)	R1 = 0.0520, wR2 = 0.1366
Largest diff. peak and hole	0.327 and -0.336 e.Å ⁻³

Table A5.2 Atomic coordinates ($\times 10^4$) and equivalent isotropic displacement parameters ($\text{\AA}^2 \times 10^3$) for 3-mesitylpyrrole. U(eq) is defined as one third of the trace of the orthogonalized U_{ij} tensor

	x	y	z	U(eq)
N(1)	6987(1)	415(1)	1433(1)	30(1)
C(1)	7831(1)	-260(1)	1026(1)	28(1)
C(2)	8902(1)	436(1)	926(1)	25(1)
C(3)	8708(1)	1593(1)	1288(1)	22(1)
C(4)	7508(1)	1539(1)	1598(1)	27(1)
C(5)	9639(1)	2626(1)	1309(1)	21(1)
C(6)	10160(1)	3077(1)	640(1)	23(1)
C(7)	11104(1)	3984(1)	665(1)	26(1)
C(8)	11533(1)	4482(1)	1331(1)	26(1)
C(9)	10970(1)	4069(1)	1992(1)	24(1)
C(10)	10033(1)	3153(1)	1992(1)	21(1)
C(11)	9726(1)	2631(1)	-117(1)	33(1)
C(12)	12593(1)	5424(1)	1339(1)	34(1)
C(13)	9481(1)	2744(1)	2728(1)	28(1)

Table A5.3 Bond lengths (Å) and angles (°) for 3-mesitylpyrrole

N(1)-C(1)	1.3623(18)
N(1)-C(4)	1.3694(17)
C(1)-C(2)	1.3672(17)
C(2)-C(3)	1.4292(17)
C(3)-C(4)	1.3775(17)
C(3)-C(5)	1.4885(16)
C(5)-C(6)	1.4068(17)
C(5)-C(10)	1.4121(17)
C(6)-C(7)	1.3990(17)
C(6)-C(11)	1.5095(18)
C(7)-C(8)	1.3852(19)
C(8)-C(9)	1.3973(18)
C(8)-C(12)	1.5121(18)
C(9)-C(10)	1.3998(17)
C(10)-C(13)	1.5082(17)
C(1)-N(1)-C(4)	109.60(11)
N(1)-C(1)-C(2)	107.87(11)
C(1)-C(2)-C(3)	108.07(11)
C(4)-C(3)-C(2)	105.96(11)
C(4)-C(3)-C(5)	128.49(11)
C(2)-C(3)-C(5)	125.54(11)
N(1)-C(4)-C(3)	108.50(12)
C(6)-C(5)-C(10)	118.91(11)
C(6)-C(5)-C(3)	119.73(11)
C(10)-C(5)-C(3)	121.35(10)
C(7)-C(6)-C(5)	119.55(11)
C(7)-C(6)-C(11)	117.95(11)
C(5)-C(6)-C(11)	122.50(11)

C(8)-C(7)-C(6)	122.26(12)
C(7)-C(8)-C(9)	117.82(12)
C(7)-C(8)-C(12)	120.84(12)
C(9)-C(8)-C(12)	121.33(12)
C(8)-C(9)-C(10)	121.73(12)
C(9)-C(10)-C(5)	119.62(11)
C(9)-C(10)-C(13)	118.67(11)
C(5)-C(10)-C(13)	121.71(11)

Table A5.4 Anisotropic displacement parameters ($\text{\AA}^2 \times 10^3$) for 3-mesitylpyrrole. The displacement factor exponent takes the form: $-2 \pi^2 [h^2 a^{*2} U_{11} + \dots + 2 h k a^* b^* U_{12}]$

	U ₁₁	U ₂₂	U ₃₃	U ₂₃	U ₁₃	U ₁₂
N(1)	21(1)	29(1)	40(1)	7(1)	-1(1)	-6(1)
C(1)	30(1)	21(1)	31(1)	3(1)	-7(1)	-3(1)
C(2)	25(1)	22(1)	28(1)	0(1)	-2(1)	0(1)
C(3)	21(1)	19(1)	25(1)	3(1)	-2(1)	1(1)
C(4)	23(1)	24(1)	36(1)	2(1)	2(1)	0(1)
C(5)	18(1)	18(1)	26(1)	1(1)	0(1)	2(1)
C(6)	24(1)	19(1)	26(1)	-1(1)	2(1)	1(1)
C(7)	27(1)	24(1)	28(1)	3(1)	7(1)	-1(1)
C(8)	20(1)	21(1)	37(1)	0(1)	2(1)	0(1)
C(9)	21(1)	23(1)	27(1)	-3(1)	-3(1)	1(1)
C(10)	18(1)	20(1)	25(1)	1(1)	1(1)	3(1)
C(11)	45(1)	29(1)	24(1)	-1(1)	2(1)	-6(1)
C(12)	27(1)	32(1)	44(1)	-2(1)	4(1)	-8(1)
C(13)	26(1)	33(1)	24(1)	2(1)	0(1)	-2(1)

Table A5.5 Hydrogen coordinates ($\times 10^4$) and isotropic displacement parameters ($\text{\AA}^2 \times 10^3$) for 3-mesitylpyrrole

	x	y	z	U(eq)
H(1)	6224	168	1570	36
H(1A)	7699	-1071	844	33
H(2)	9645	194	661	30
H(4)	7110	2173	1878	33
H(7)	11463	4268	210	32
H(9)	11230	4420	2453	29
H(11A)	9862	3281	-488	49
H(11B)	8819	2423	-97	49
H(11C)	10217	1900	-258	49
H(12A)	13404	5013	1445	52
H(12B)	12422	6039	1727	52
H(12C)	12641	5830	852	52
H(13A)	9964	3119	3138	42
H(13B)	9532	1846	2767	42
H(13C)	8588	3002	2760	42

Table A5.6 Torsion angles (°) for 3-mesitylpyrrole

C(4)-N(1)-C(1)-C(2)	-0.21(15)
N(1)-C(1)-C(2)-C(3)	0.04(15)
C(1)-C(2)-C(3)-C(4)	0.14(14)
C(1)-C(2)-C(3)-C(5)	-179.56(11)
C(1)-N(1)-C(4)-C(3)	0.31(15)
C(2)-C(3)-C(4)-N(1)	-0.27(14)
C(5)-C(3)-C(4)-N(1)	179.42(11)
C(4)-C(3)-C(5)-C(6)	-126.61(14)
C(2)-C(3)-C(5)-C(6)	53.02(17)
C(4)-C(3)-C(5)-C(10)	54.67(18)
C(2)-C(3)-C(5)-C(10)	-125.70(13)
C(10)-C(5)-C(6)-C(7)	3.51(17)
C(3)-C(5)-C(6)-C(7)	-175.24(11)
C(10)-C(5)-C(6)-C(11)	-175.61(11)
C(3)-C(5)-C(6)-C(11)	5.64(18)
C(5)-C(6)-C(7)-C(8)	-1.43(19)
C(11)-C(6)-C(7)-C(8)	177.73(12)
C(6)-C(7)-C(8)-C(9)	-1.41(19)
C(6)-C(7)-C(8)-C(12)	177.47(12)
C(7)-C(8)-C(9)-C(10)	2.17(18)
C(12)-C(8)-C(9)-C(10)	-176.70(12)
C(8)-C(9)-C(10)-C(5)	-0.08(18)
C(8)-C(9)-C(10)-C(13)	179.27(11)
C(6)-C(5)-C(10)-C(9)	-2.78(17)
C(3)-C(5)-C(10)-C(9)	175.96(10)
C(6)-C(5)-C(10)-C(13)	177.89(11)
C(3)-C(5)-C(10)-C(13)	-3.38(17)

Table A6.1 Crystal data for $\text{Ti}(\text{dap}^{3\text{-mes}})_2(\text{NMe}_2)_2$ (**45**)

Identification code	sbfinal	
Empirical formula	$\text{C}_{36.5} \text{H}_{55} \text{Cl} \text{N}_6 \text{Ti}$	
Formula weight	661.22	
Temperature	173(2) K	
Wavelength	0.71073 Å	
Crystal system	Monoclinic	
Space group	P 21/n	
Unit cell dimensions	$a = 12.8140(4)$ Å	$\alpha = 90^\circ$
	$b = 18.4577(7)$ Å	$\beta = 105.887(2)^\circ$
	$c = 16.0983(6)$ Å	$\gamma = 90^\circ$
Volume	3662.1(2) Å ³	
Z	4	
Density (calculated)	1.199 Mg/m ³	
Absorption coefficient	0.340 mm ⁻¹	
F(000)	1420	
Crystal size	0.41 × 0.23 × 0.22 mm ³	
Theta range for data collection	2.12 to 25.38°.	
Index ranges	-15 ≤ h ≤ 15, -22 ≤ k ≤ 22, -19 ≤ l ≤ 19	
Reflections collected	46233	
Independent reflections	6730 [R(int) = 0.0301]	
Completeness to theta = 25.00°	100.0 %	
Absorption correction	Semi-empirical from equivalents	
Max. and min. transmission	0.9290 and 0.8719	
Refinement method	Full-matrix least-squares on F ²	
Data / restraints / parameters	6730 / 0 / 420	
Goodness-of-fit on F ²	1.032	
Final R indices [I > 2σ(I)]	R1 = 0.0393, wR2 = 0.1005	
R indices (all data)	R1 = 0.0473, wR2 = 0.1063	

Largest diff. peak and hole

0.686 and $-0.746 \text{ e.}\text{\AA}^{-3}$ **Table A6.2** Atomic coordinates ($\times 10^4$) and equivalent isotropic displacement parameters ($\text{\AA}^2 \times 10^3$) for $\text{Ti}(\text{dap}^{3\text{-mes}})_2(\text{NMe}_2)_2$. $U(\text{eq})$ is defined as one third of the trace of the orthogonalized U^{ij} tensor

	x	y	z	$U(\text{eq})$
Ti(1)	2071(1)	10456(1)	3218(1)	22(1)
N(1)	3101(1)	9706(1)	2923(1)	24(1)
N(2)	1799(1)	10462(1)	1588(1)	28(1)
N(3)	784(1)	9707(1)	2941(1)	26(1)
N(4)	476(1)	11079(1)	3392(1)	29(1)
N(5)	2497(1)	10222(1)	4418(1)	26(1)
N(6)	2776(1)	11374(1)	3244(1)	29(1)
C(1)	3915(1)	9307(1)	3463(1)	25(1)
C(2)	4307(1)	8788(1)	3015(1)	24(1)
C(3)	3702(1)	8877(1)	2134(1)	26(1)
C(4)	2978(1)	9429(1)	2108(1)	25(1)
C(5)	2061(2)	9711(1)	1392(1)	28(1)
C(6)	2607(2)	10950(1)	1384(1)	39(1)
C(7)	719(2)	10646(1)	1021(1)	43(1)
C(8)	5153(1)	8245(1)	3401(1)	24(1)
C(9)	5041(1)	7802(1)	4085(1)	26(1)
C(10)	5872(2)	7322(1)	4477(1)	29(1)
C(11)	6810(2)	7256(1)	4209(1)	29(1)
C(12)	6901(2)	7685(1)	3523(1)	28(1)
C(13)	6096(1)	8170(1)	3114(1)	25(1)
C(14)	6256(2)	8612(1)	2373(1)	34(1)
C(15)	4036(2)	7820(1)	4401(1)	33(1)
C(16)	7685(2)	6724(1)	4631(1)	43(1)
C(17)	703(2)	8988(1)	2682(1)	27(1)
C(18)	-142(2)	8651(1)	2894(1)	28(1)

C(19)	-615(2)	9183(1)	3318(1)	33(1)
C(20)	-29(2)	9806(1)	3337(1)	28(1)
C(21)	-28(2)	10506(1)	3799(1)	31(1)
C(22)	-329(2)	11309(1)	2591(1)	41(1)
C(23)	703(2)	11704(1)	3992(2)	42(1)
C(24)	-492(1)	7884(1)	2725(1)	28(1)
C(25)	-1225(2)	7687(1)	1935(1)	29(1)
C(26)	-1577(2)	6970(1)	1801(1)	33(1)
C(27)	-1215(2)	6441(1)	2425(1)	34(1)
C(28)	-479(2)	6643(1)	3198(1)	32(1)
C(29)	-113(2)	7352(1)	3359(1)	30(1)
C(30)	-1620(2)	8243(1)	1234(1)	38(1)
C(31)	-1568(2)	5661(1)	2270(2)	49(1)
C(32)	692(2)	7539(1)	4210(1)	42(1)
C(33)	3966(2)	11332(1)	3588(1)	38(1)
C(34)	2491(2)	12111(1)	2953(2)	41(1)
C(35)	2318(2)	9507(1)	4744(1)	34(1)
C(36)	3067(2)	10680(1)	5142(1)	37(1)
CI(1S)	1075(1)	5300(1)	5394(1)	91(1)
C(1S)	276(5)	4747(3)	4637(4)	62(2)

Table A6.3 Bond lengths (Å) and angles (°) for $\text{Ti}(\text{dap}^{3\text{-mes}})_2(\text{NMe}_2)_2$

Ti(1)-N(5)	1.9076(15)
Ti(1)-N(6)	1.9156(16)
Ti(1)-N(1)	2.0548(15)
Ti(1)-N(3)	2.1035(15)
Ti(1)-N(4)	2.4276(15)
Ti(1)-N(2)	2.5510(16)
N(1)-C(1)	1.375(2)
N(1)-C(4)	1.377(2)
N(2)-C(7)	1.474(3)
N(2)-C(6)	1.477(3)
N(2)-C(5)	1.480(2)
N(3)-C(20)	1.375(2)
N(3)-C(17)	1.387(2)
N(4)-C(22)	1.476(3)
N(4)-C(21)	1.483(2)
N(4)-C(23)	1.483(3)
N(5)-C(35)	1.462(2)
N(5)-C(36)	1.463(2)
N(6)-C(34)	1.454(3)
N(6)-C(33)	1.474(3)
C(1)-C(2)	1.375(2)
C(1)-H(1)	0.9500
C(2)-C(3)	1.428(2)
C(2)-C(8)	1.482(2)
C(3)-C(4)	1.371(3)
C(3)-H(3)	0.9500
C(4)-C(5)	1.496(3)
C(5)-H(5A)	0.9900
C(5)-H(5B)	0.9900

C(6)-H(6A)	0.9800
C(6)-H(6B)	0.9800
C(6)-H(6C)	0.9800
C(7)-H(7A)	0.9800
C(7)-H(7B)	0.9800
C(7)-H(7C)	0.9800
C(8)-C(9)	1.411(3)
C(8)-C(13)	1.414(2)
C(9)-C(10)	1.396(3)
C(9)-C(15)	1.508(3)
C(10)-C(11)	1.388(3)
C(10)-H(10)	0.9500
C(11)-C(12)	1.390(3)
C(11)-C(16)	1.506(3)
C(12)-C(13)	1.388(3)
C(12)-H(12)	0.9500
C(13)-C(14)	1.505(3)
C(14)-H(14A)	0.9800
C(14)-H(14B)	0.9800
C(14)-H(14C)	0.9800
C(15)-H(15A)	0.9800
C(15)-H(15B)	0.9800
C(15)-H(15C)	0.9800
C(16)-H(16A)	0.9800
C(16)-H(16B)	0.9800
C(16)-H(16C)	0.9800
C(17)-C(18)	1.370(3)
C(17)-H(17)	0.9500
C(18)-C(19)	1.422(3)
C(18)-C(24)	1.489(3)
C(19)-C(20)	1.370(3)

C(19)-H(19)	0.9500
C(20)-C(21)	1.490(3)
C(21)-H(21A)	0.9900
C(21)-H(21B)	0.9900
C(22)-H(22A)	0.9800
C(22)-H(22B)	0.9800
C(22)-H(22C)	0.9800
C(23)-H(23A)	0.9800
C(23)-H(23B)	0.9800
C(23)-H(23C)	0.9800
C(24)-C(29)	1.402(3)
C(24)-C(25)	1.406(3)
C(25)-C(26)	1.396(3)
C(25)-C(30)	1.507(3)
C(26)-C(27)	1.385(3)
C(26)-H(26)	0.9500
C(27)-C(28)	1.391(3)
C(27)-C(31)	1.509(3)
C(28)-C(29)	1.391(3)
C(28)-H(28)	0.9500
C(29)-C(32)	1.512(3)
C(30)-H(30A)	0.9800
C(30)-H(30B)	0.9800
C(30)-H(30C)	0.9800
C(31)-H(31A)	0.9800
C(31)-H(31B)	0.9800
C(31)-H(31C)	0.9800
C(32)-H(32A)	0.9800
C(32)-H(32B)	0.9800
C(32)-H(32C)	0.9800
C(33)-H(33A)	0.9800

C(33)-H(33B)	0.9800
C(33)-H(33C)	0.9800
C(34)-H(34A)	0.9800
C(34)-H(34B)	0.9800
C(34)-H(34C)	0.9800
C(35)-H(35A)	0.9800
C(35)-H(35B)	0.9800
C(35)-H(35C)	0.9800
C(36)-H(36A)	0.9800
C(36)-H(36B)	0.9800
C(36)-H(36C)	0.9800
Cl(1S)-C(1S)	1.701(6)
Cl(1S)-C(1S)#1	1.721(6)
C(1S)-Cl(1S)#1	1.721(6)
C(1S)-C(1S)#1	1.787(10)
C(1S)-H(1SA)	0.9601
C(1S)-H(1SB)	0.9600
N(5)-Ti(1)-N(6)	100.08(7)
N(5)-Ti(1)-N(1)	93.33(6)
N(6)-Ti(1)-N(1)	105.75(6)
N(5)-Ti(1)-N(3)	93.26(6)
N(6)-Ti(1)-N(3)	157.45(7)
N(1)-Ti(1)-N(3)	91.41(6)
N(5)-Ti(1)-N(4)	90.41(6)
N(6)-Ti(1)-N(4)	89.15(6)
N(1)-Ti(1)-N(4)	163.71(6)
N(3)-Ti(1)-N(4)	72.54(6)
N(5)-Ti(1)-N(2)	164.48(6)
N(6)-Ti(1)-N(2)	87.11(6)
N(1)-Ti(1)-N(2)	71.39(5)

N(3)-Ti(1)-N(2)	84.61(6)
N(4)-Ti(1)-N(2)	103.53(5)
C(1)-N(1)-C(4)	105.84(14)
C(1)-N(1)-Ti(1)	129.70(12)
C(4)-N(1)-Ti(1)	123.84(12)
C(7)-N(2)-C(6)	108.57(16)
C(7)-N(2)-C(5)	108.25(15)
C(6)-N(2)-C(5)	108.06(15)
C(7)-N(2)-Ti(1)	118.63(12)
C(6)-N(2)-Ti(1)	108.93(11)
C(5)-N(2)-Ti(1)	103.92(10)
C(20)-N(3)-C(17)	105.26(15)
C(20)-N(3)-Ti(1)	117.63(12)
C(17)-N(3)-Ti(1)	133.06(12)
C(22)-N(4)-C(21)	107.87(16)
C(22)-N(4)-C(23)	108.09(16)
C(21)-N(4)-C(23)	107.36(15)
C(22)-N(4)-Ti(1)	116.47(12)
C(21)-N(4)-Ti(1)	101.26(11)
C(23)-N(4)-Ti(1)	115.02(12)
C(35)-N(5)-C(36)	109.23(15)
C(35)-N(5)-Ti(1)	122.53(12)
C(36)-N(5)-Ti(1)	128.21(13)
C(34)-N(6)-C(33)	108.25(16)
C(34)-N(6)-Ti(1)	138.26(14)
C(33)-N(6)-Ti(1)	113.23(13)
N(1)-C(1)-C(2)	111.39(15)
N(1)-C(1)-H(1)	124.3
C(2)-C(1)-H(1)	124.3
C(1)-C(2)-C(3)	105.32(16)
C(1)-C(2)-C(8)	125.56(16)

C(3)-C(2)-C(8)	129.09(16)
C(4)-C(3)-C(2)	107.15(15)
C(4)-C(3)-H(3)	126.4
C(2)-C(3)-H(3)	126.4
C(3)-C(4)-N(1)	110.29(16)
C(3)-C(4)-C(5)	131.58(16)
N(1)-C(4)-C(5)	117.83(15)
N(2)-C(5)-C(4)	109.69(15)
N(2)-C(5)-H(5A)	109.7
C(4)-C(5)-H(5A)	109.7
N(2)-C(5)-H(5B)	109.7
C(4)-C(5)-H(5B)	109.7
H(5A)-C(5)-H(5B)	108.2
N(2)-C(6)-H(6A)	109.5
N(2)-C(6)-H(6B)	109.5
H(6A)-C(6)-H(6B)	109.5
N(2)-C(6)-H(6C)	109.5
H(6A)-C(6)-H(6C)	109.5
H(6B)-C(6)-H(6C)	109.5
N(2)-C(7)-H(7A)	109.5
N(2)-C(7)-H(7B)	109.5
H(7A)-C(7)-H(7B)	109.5
N(2)-C(7)-H(7C)	109.5
H(7A)-C(7)-H(7C)	109.5
H(7B)-C(7)-H(7C)	109.5
C(9)-C(8)-C(13)	118.50(16)
C(9)-C(8)-C(2)	119.99(16)
C(13)-C(8)-C(2)	121.49(16)
C(10)-C(9)-C(8)	119.50(16)
C(10)-C(9)-C(15)	118.53(17)
C(8)-C(9)-C(15)	121.97(17)

C(11)-C(10)-C(9)	122.25(17)
C(11)-C(10)-H(10)	118.9
C(9)-C(10)-H(10)	118.9
C(10)-C(11)-C(12)	117.71(17)
C(10)-C(11)-C(16)	121.27(18)
C(12)-C(11)-C(16)	121.00(18)
C(13)-C(12)-C(11)	122.07(17)
C(13)-C(12)-H(12)	119.0
C(11)-C(12)-H(12)	119.0
C(12)-C(13)-C(8)	119.93(17)
C(12)-C(13)-C(14)	118.76(16)
C(8)-C(13)-C(14)	121.30(16)
C(13)-C(14)-H(14A)	109.5
C(13)-C(14)-H(14B)	109.5
H(14A)-C(14)-H(14B)	109.5
C(13)-C(14)-H(14C)	109.5
H(14A)-C(14)-H(14C)	109.5
H(14B)-C(14)-H(14C)	109.5
C(9)-C(15)-H(15A)	109.5
C(9)-C(15)-H(15B)	109.5
H(15A)-C(15)-H(15B)	109.5
C(9)-C(15)-H(15C)	109.5
H(15A)-C(15)-H(15C)	109.5
H(15B)-C(15)-H(15C)	109.5
C(11)-C(16)-H(16A)	109.5
C(11)-C(16)-H(16B)	109.5
H(16A)-C(16)-H(16B)	109.5
C(11)-C(16)-H(16C)	109.5
H(16A)-C(16)-H(16C)	109.5
H(16B)-C(16)-H(16C)	109.5
C(18)-C(17)-N(3)	110.98(16)

C(18)-C(17)-H(17)	124.5
N(3)-C(17)-H(17)	124.5
C(17)-C(18)-C(19)	106.08(17)
C(17)-C(18)-C(24)	127.20(17)
C(19)-C(18)-C(24)	126.71(16)
C(20)-C(19)-C(18)	106.69(16)
C(20)-C(19)-H(19)	126.7
C(18)-C(19)-H(19)	126.7
C(19)-C(20)-N(3)	110.97(16)
C(19)-C(20)-C(21)	131.64(17)
N(3)-C(20)-C(21)	116.76(16)
N(4)-C(21)-C(20)	109.74(15)
N(4)-C(21)-H(21A)	109.7
C(20)-C(21)-H(21A)	109.7
N(4)-C(21)-H(21B)	109.7
C(20)-C(21)-H(21B)	109.7
H(21A)-C(21)-H(21B)	108.2
N(4)-C(22)-H(22A)	109.5
N(4)-C(22)-H(22B)	109.5
H(22A)-C(22)-H(22B)	109.5
N(4)-C(22)-H(22C)	109.5
H(22A)-C(22)-H(22C)	109.5
H(22B)-C(22)-H(22C)	109.5
N(4)-C(23)-H(23A)	109.5
N(4)-C(23)-H(23B)	109.5
H(23A)-C(23)-H(23B)	109.5
N(4)-C(23)-H(23C)	109.5
H(23A)-C(23)-H(23C)	109.5
H(23B)-C(23)-H(23C)	109.5
C(29)-C(24)-C(25)	119.33(17)
C(29)-C(24)-C(18)	120.42(17)

C(25)-C(24)-C(18)	120.23(17)
C(26)-C(25)-C(24)	119.45(18)
C(26)-C(25)-C(30)	120.14(18)
C(24)-C(25)-C(30)	120.40(18)
C(27)-C(26)-C(25)	121.77(18)
C(27)-C(26)-H(26)	119.1
C(25)-C(26)-H(26)	119.1
C(26)-C(27)-C(28)	118.02(18)
C(26)-C(27)-C(31)	121.79(19)
C(28)-C(27)-C(31)	120.16(19)
C(27)-C(28)-C(29)	122.03(19)
C(27)-C(28)-H(28)	119.0
C(29)-C(28)-H(28)	119.0
C(28)-C(29)-C(24)	119.39(18)
C(28)-C(29)-C(32)	119.71(18)
C(24)-C(29)-C(32)	120.90(18)
C(25)-C(30)-H(30A)	109.5
C(25)-C(30)-H(30B)	109.5
H(30A)-C(30)-H(30B)	109.5
C(25)-C(30)-H(30C)	109.5
H(30A)-C(30)-H(30C)	109.5
H(30B)-C(30)-H(30C)	109.5
C(27)-C(31)-H(31A)	109.5
C(27)-C(31)-H(31B)	109.5
H(31A)-C(31)-H(31B)	109.5
C(27)-C(31)-H(31C)	109.5
H(31A)-C(31)-H(31C)	109.5
H(31B)-C(31)-H(31C)	109.5
C(29)-C(32)-H(32A)	109.5
C(29)-C(32)-H(32B)	109.5
H(32A)-C(32)-H(32B)	109.5

C(29)-C(32)-H(32C)	109.5
H(32A)-C(32)-H(32C)	109.5
H(32B)-C(32)-H(32C)	109.5
N(6)-C(33)-H(33A)	109.5
N(6)-C(33)-H(33B)	109.5
H(33A)-C(33)-H(33B)	109.5
N(6)-C(33)-H(33C)	109.5
H(33A)-C(33)-H(33C)	109.5
H(33B)-C(33)-H(33C)	109.5
N(6)-C(34)-H(34A)	109.5
N(6)-C(34)-H(34B)	109.5
H(34A)-C(34)-H(34B)	109.5
N(6)-C(34)-H(34C)	109.5
H(34A)-C(34)-H(34C)	109.5
H(34B)-C(34)-H(34C)	109.5
N(5)-C(35)-H(35A)	109.5
N(5)-C(35)-H(35B)	109.5
H(35A)-C(35)-H(35B)	109.5
N(5)-C(35)-H(35C)	109.5
H(35A)-C(35)-H(35C)	109.5
H(35B)-C(35)-H(35C)	109.5
N(5)-C(36)-H(36A)	109.5
N(5)-C(36)-H(36B)	109.5
H(36A)-C(36)-H(36B)	109.5
N(5)-C(36)-H(36C)	109.5
H(36A)-C(36)-H(36C)	109.5
H(36B)-C(36)-H(36C)	109.5
C(1S)-Cl(1S)-C(1S)#1	62.9(3)
Cl(1S)-C(1S)-Cl(1S)#1	117.1(3)
Cl(1S)-C(1S)-C(1S)#1	59.1(3)
Cl(1S)#1-C(1S)-C(1S)#1	58.0(3)

Cl(1S)-C(1S)-H(1SA)	108.0
Cl(1S)#1-C(1S)-H(1SA)	108.0
C(1S)#1-C(1S)-H(1SA)	126.4
Cl(1S)-C(1S)-H(1SB)	108.0
Cl(1S)#1-C(1S)-H(1SB)	108.0
C(1S)#1-C(1S)-H(1SB)	126.4
H(1SA)-C(1S)-H(1SB)	107.3

Table A6.4 Anisotropic displacement parameters ($\text{\AA}^2 \times 10^3$) for $\text{Ti}(\text{dap}^{3\text{-mes}})_2(\text{NMe}_2)_2$. The anisotropic displacement factor exponent takes the form: $-2 \pi^2 [h^2 a^{*2} U_{11} + \dots + 2 h k a^* b^* U_{12}]$

	U11	U22	U33	U23	U13	U12
Ti(1)	22(1)	22(1)	23(1)	-2(1)	7(1)	0(1)
N(1)	24(1)	26(1)	22(1)	-3(1)	6(1)	1(1)
N(2)	31(1)	26(1)	27(1)	1(1)	7(1)	4(1)
N(3)	25(1)	27(1)	28(1)	-2(1)	9(1)	-1(1)
N(4)	31(1)	25(1)	33(1)	-2(1)	11(1)	3(1)
N(5)	27(1)	28(1)	25(1)	-3(1)	8(1)	0(1)
N(6)	31(1)	26(1)	31(1)	-3(1)	11(1)	-1(1)
C(1)	23(1)	29(1)	22(1)	-1(1)	5(1)	1(1)
C(2)	24(1)	24(1)	25(1)	-2(1)	8(1)	-2(1)
C(3)	29(1)	26(1)	24(1)	-3(1)	9(1)	1(1)
C(4)	27(1)	25(1)	23(1)	-2(1)	8(1)	-1(1)
C(5)	32(1)	29(1)	23(1)	-2(1)	6(1)	2(1)
C(6)	55(1)	32(1)	34(1)	2(1)	20(1)	-5(1)
C(7)	42(1)	48(1)	34(1)	2(1)	3(1)	17(1)
C(8)	25(1)	23(1)	24(1)	-5(1)	5(1)	-1(1)
C(9)	28(1)	26(1)	24(1)	-4(1)	7(1)	-2(1)

C(10)	37(1)	26(1)	24(1)	1(1)	7(1)	-1(1)
C(11)	30(1)	26(1)	28(1)	-4(1)	3(1)	2(1)
C(12)	25(1)	28(1)	31(1)	-5(1)	8(1)	2(1)
C(13)	27(1)	23(1)	26(1)	-4(1)	7(1)	-2(1)
C(14)	33(1)	35(1)	39(1)	7(1)	17(1)	4(1)
C(15)	35(1)	35(1)	33(1)	3(1)	14(1)	-1(1)
C(16)	45(1)	42(1)	39(1)	6(1)	7(1)	13(1)
C(17)	27(1)	28(1)	27(1)	-4(1)	9(1)	-1(1)
C(18)	26(1)	31(1)	27(1)	-1(1)	7(1)	-3(1)
C(19)	28(1)	37(1)	38(1)	-2(1)	15(1)	-2(1)
C(20)	24(1)	31(1)	30(1)	-2(1)	10(1)	1(1)
C(21)	29(1)	32(1)	35(1)	-1(1)	14(1)	3(1)
C(22)	38(1)	40(1)	44(1)	8(1)	10(1)	11(1)
C(23)	48(1)	30(1)	52(1)	-10(1)	24(1)	2(1)
C(24)	25(1)	30(1)	32(1)	-3(1)	13(1)	-3(1)
C(25)	27(1)	33(1)	30(1)	-2(1)	12(1)	0(1)
C(26)	31(1)	36(1)	32(1)	-7(1)	8(1)	-3(1)
C(27)	34(1)	31(1)	41(1)	-5(1)	16(1)	-3(1)
C(28)	32(1)	33(1)	34(1)	4(1)	14(1)	1(1)
C(29)	26(1)	35(1)	30(1)	-2(1)	10(1)	-1(1)
C(30)	42(1)	40(1)	31(1)	0(1)	9(1)	0(1)
C(31)	61(2)	33(1)	51(1)	-5(1)	12(1)	-10(1)
C(32)	42(1)	46(1)	34(1)	0(1)	2(1)	-2(1)
C(33)	32(1)	39(1)	44(1)	-9(1)	13(1)	-9(1)
C(34)	50(1)	28(1)	49(1)	-2(1)	18(1)	-4(1)
C(35)	39(1)	35(1)	28(1)	4(1)	10(1)	1(1)
C(36)	40(1)	41(1)	27(1)	-8(1)	5(1)	-3(1)
Cl(1S)	102(1)	106(1)	72(1)	-8(1)	35(1)	-24(1)
C(1S)	86(4)	51(3)	57(3)	8(3)	35(3)	25(3)

Table A6.5 Hydrogen coordinates ($\times 10^4$) and isotropic displacement parameters ($\text{\AA}^2 \times 10^3$) for $\text{Ti}(\text{dap}^{3\text{-mes}})_2(\text{NMe}_2)_2$

	x	y	z	U(eq)
H(1)	4174	9381	4069	30
H(3)	3785	8604	1656	31
H(5A)	2268	9702	842	34
H(5B)	1416	9398	1324	34
H(6A)	2586	10898	774	58
H(6B)	3333	10825	1746	58
H(6C)	2439	11453	1498	58
H(7A)	547	11150	1120	65
H(7B)	173	10325	1150	65
H(7C)	719	10584	416	65
H(10)	5794	7031	4943	35
H(12)	7534	7645	3327	33
H(14A)	7034	8673	2437	51
H(14B)	5918	9089	2371	51
H(14C)	5919	8363	1828	51
H(15A)	3953	7354	4667	50
H(15B)	3399	7910	3912	50
H(15C)	4103	8208	4828	50
H(16A)	7573	6559	5178	64
H(16B)	8396	6959	4741	64
H(16C)	7658	6308	4248	64
H(17)	1171	8759	2395	32
H(19)	-1219	9118	3545	40
H(21A)	-782	10645	3776	37
H(21B)	384	10451	4413	37
H(22A)	-559	10889	2213	61
H(22B)	-4	11672	2294	61

H(22C)	-961	11520	2735	61
H(23A)	963	12113	3715	62
H(23B)	1259	11569	4520	62
H(23C)	37	11844	4138	62
H(26)	-2077	6841	1269	40
H(28)	-219	6285	3630	39
H(30A)	-1024	8378	991	57
H(30B)	-1875	8674	1476	57
H(30C)	-2218	8039	777	57
H(31A)	-957	5367	2207	73
H(31B)	-2167	5626	1741	73
H(31C)	-1808	5482	2760	73
H(32A)	761	7129	4608	63
H(32B)	436	7966	4459	63
H(32C)	1400	7644	4114	63
H(33A)	4306	11441	3127	57
H(33B)	4172	10842	3809	57
H(33C)	4209	11683	4058	57
H(34A)	2629	12435	3453	62
H(34B)	1721	12132	2635	62
H(34C)	2932	12263	2573	62
H(35A)	3008	9313	5100	51
H(35B)	2022	9180	4257	51
H(35C)	1803	9547	5093	51
H(36A)	2648	10704	5567	55
H(36B)	3151	11169	4931	55
H(36C)	3784	10474	5413	55
H(1SA)	573	4267	4728	74
H(1SB)	324	4903	4080	74

Table A6.6 Torsion angles (°) for $\text{Ti}(\text{dap}^{3\text{-mes}})_2(\text{NMe}_2)_2$

N(5)-Ti(1)-N(1)-C(1)	-10.30(16)
N(6)-Ti(1)-N(1)-C(1)	91.16(16)
N(3)-Ti(1)-N(1)-C(1)	-103.65(16)
N(4)-Ti(1)-N(1)-C(1)	-113.3(2)
N(2)-Ti(1)-N(1)-C(1)	172.51(17)
N(5)-Ti(1)-N(1)-C(4)	159.28(14)
N(6)-Ti(1)-N(1)-C(4)	-99.26(14)
N(3)-Ti(1)-N(1)-C(4)	65.93(14)
N(4)-Ti(1)-N(1)-C(4)	56.3(3)
N(2)-Ti(1)-N(1)-C(4)	-17.91(13)
N(5)-Ti(1)-N(2)-C(7)	139.2(2)
N(6)-Ti(1)-N(2)-C(7)	-102.60(15)
N(1)-Ti(1)-N(2)-C(7)	149.71(16)
N(3)-Ti(1)-N(2)-C(7)	56.40(15)
N(4)-Ti(1)-N(2)-C(7)	-14.17(15)
N(5)-Ti(1)-N(2)-C(6)	-96.0(2)
N(6)-Ti(1)-N(2)-C(6)	22.21(13)
N(1)-Ti(1)-N(2)-C(6)	-85.48(13)
N(3)-Ti(1)-N(2)-C(6)	-178.79(13)
N(4)-Ti(1)-N(2)-C(6)	110.64(12)
N(5)-Ti(1)-N(2)-C(5)	19.0(3)
N(6)-Ti(1)-N(2)-C(5)	137.21(12)
N(1)-Ti(1)-N(2)-C(5)	29.53(11)
N(3)-Ti(1)-N(2)-C(5)	-63.79(11)
N(4)-Ti(1)-N(2)-C(5)	-134.36(11)
N(5)-Ti(1)-N(3)-C(20)	61.48(14)
N(6)-Ti(1)-N(3)-C(20)	-65.0(2)
N(1)-Ti(1)-N(3)-C(20)	154.90(14)
N(4)-Ti(1)-N(3)-C(20)	-27.92(13)

N(2)-Ti(1)-N(3)-C(20)	-133.94(14)
N(5)-Ti(1)-N(3)-C(17)	-92.12(17)
N(6)-Ti(1)-N(3)-C(17)	141.41(18)
N(1)-Ti(1)-N(3)-C(17)	1.30(17)
N(4)-Ti(1)-N(3)-C(17)	178.48(18)
N(2)-Ti(1)-N(3)-C(17)	72.46(16)
N(5)-Ti(1)-N(4)-C(22)	-170.97(14)
N(6)-Ti(1)-N(4)-C(22)	88.95(14)
N(1)-Ti(1)-N(4)-C(22)	-67.6(3)
N(3)-Ti(1)-N(4)-C(22)	-77.68(14)
N(2)-Ti(1)-N(4)-C(22)	2.13(15)
N(5)-Ti(1)-N(4)-C(21)	-54.30(12)
N(6)-Ti(1)-N(4)-C(21)	-154.38(12)
N(1)-Ti(1)-N(4)-C(21)	49.1(3)
N(3)-Ti(1)-N(4)-C(21)	38.99(11)
N(2)-Ti(1)-N(4)-C(21)	118.80(11)
N(5)-Ti(1)-N(4)-C(23)	61.07(14)
N(6)-Ti(1)-N(4)-C(23)	-39.01(14)
N(1)-Ti(1)-N(4)-C(23)	164.47(19)
N(3)-Ti(1)-N(4)-C(23)	154.36(15)
N(2)-Ti(1)-N(4)-C(23)	-125.83(13)
N(6)-Ti(1)-N(5)-C(35)	-169.64(14)
N(1)-Ti(1)-N(5)-C(35)	-62.99(14)
N(3)-Ti(1)-N(5)-C(35)	28.61(15)
N(4)-Ti(1)-N(5)-C(35)	101.15(14)
N(2)-Ti(1)-N(5)-C(35)	-53.0(3)
N(6)-Ti(1)-N(5)-C(36)	7.80(17)
N(1)-Ti(1)-N(5)-C(36)	114.45(16)
N(3)-Ti(1)-N(5)-C(36)	-153.95(16)
N(4)-Ti(1)-N(5)-C(36)	-81.41(16)
N(2)-Ti(1)-N(5)-C(36)	124.5(2)

N(5)-Ti(1)-N(6)-C(34)	-126.0(2)
N(1)-Ti(1)-N(6)-C(34)	137.63(19)
N(3)-Ti(1)-N(6)-C(34)	-0.6(3)
N(4)-Ti(1)-N(6)-C(34)	-35.7(2)
N(2)-Ti(1)-N(6)-C(34)	67.9(2)
N(5)-Ti(1)-N(6)-C(33)	60.82(14)
N(1)-Ti(1)-N(6)-C(33)	-35.59(14)
N(3)-Ti(1)-N(6)-C(33)	-173.82(15)
N(4)-Ti(1)-N(6)-C(33)	151.08(13)
N(2)-Ti(1)-N(6)-C(33)	-105.33(13)
C(4)-N(1)-C(1)-C(2)	-0.1(2)
Ti(1)-N(1)-C(1)-C(2)	170.92(12)
N(1)-C(1)-C(2)-C(3)	0.7(2)
N(1)-C(1)-C(2)-C(8)	-177.35(16)
C(1)-C(2)-C(3)-C(4)	-1.0(2)
C(8)-C(2)-C(3)-C(4)	176.92(17)
C(2)-C(3)-C(4)-N(1)	1.0(2)
C(2)-C(3)-C(4)-C(5)	-172.42(19)
C(1)-N(1)-C(4)-C(3)	-0.6(2)
Ti(1)-N(1)-C(4)-C(3)	-172.28(12)
C(1)-N(1)-C(4)-C(5)	173.87(16)
Ti(1)-N(1)-C(4)-C(5)	2.2(2)
C(7)-N(2)-C(5)-C(4)	-163.63(16)
C(6)-N(2)-C(5)-C(4)	78.96(18)
Ti(1)-N(2)-C(5)-C(4)	-36.66(16)
C(3)-C(4)-C(5)-N(2)	-158.93(19)
N(1)-C(4)-C(5)-N(2)	28.0(2)
C(1)-C(2)-C(8)-C(9)	52.9(3)
C(3)-C(2)-C(8)-C(9)	-124.7(2)
C(1)-C(2)-C(8)-C(13)	-125.7(2)
C(3)-C(2)-C(8)-C(13)	56.7(3)

C(13)-C(8)-C(9)-C(10)	2.2(3)
C(2)-C(8)-C(9)-C(10)	-176.33(16)
C(13)-C(8)-C(9)-C(15)	-176.77(17)
C(2)-C(8)-C(9)-C(15)	4.7(3)
C(8)-C(9)-C(10)-C(11)	-1.0(3)
C(15)-C(9)-C(10)-C(11)	178.08(17)
C(9)-C(10)-C(11)-C(12)	-0.4(3)
C(9)-C(10)-C(11)-C(16)	-178.80(18)
C(10)-C(11)-C(12)-C(13)	0.4(3)
C(16)-C(11)-C(12)-C(13)	178.85(18)
C(11)-C(12)-C(13)-C(8)	0.9(3)
C(11)-C(12)-C(13)-C(14)	-179.74(17)
C(9)-C(8)-C(13)-C(12)	-2.2(3)
C(2)-C(8)-C(13)-C(12)	176.34(16)
C(9)-C(8)-C(13)-C(14)	178.44(17)
C(2)-C(8)-C(13)-C(14)	-3.0(3)
C(20)-N(3)-C(17)-C(18)	1.0(2)
Ti(1)-N(3)-C(17)-C(18)	156.88(14)
N(3)-C(17)-C(18)-C(19)	-0.6(2)
N(3)-C(17)-C(18)-C(24)	180.00(17)
C(17)-C(18)-C(19)-C(20)	0.0(2)
C(24)-C(18)-C(19)-C(20)	179.41(18)
C(18)-C(19)-C(20)-N(3)	0.6(2)
C(18)-C(19)-C(20)-C(21)	-169.8(2)
C(17)-N(3)-C(20)-C(19)	-0.9(2)
Ti(1)-N(3)-C(20)-C(19)	-161.27(13)
C(17)-N(3)-C(20)-C(21)	171.00(16)
Ti(1)-N(3)-C(20)-C(21)	10.7(2)
C(22)-N(4)-C(21)-C(20)	77.42(19)
C(23)-N(4)-C(21)-C(20)	-166.31(16)
Ti(1)-N(4)-C(21)-C(20)	-45.38(16)

C(19)-C(20)-C(21)-N(4)	-161.7(2)
N(3)-C(20)-C(21)-N(4)	28.4(2)
C(17)-C(18)-C(24)-C(29)	94.3(2)
C(19)-C(18)-C(24)-C(29)	-84.9(2)
C(17)-C(18)-C(24)-C(25)	-87.1(2)
C(19)-C(18)-C(24)-C(25)	93.7(2)
C(29)-C(24)-C(25)-C(26)	1.0(3)
C(18)-C(24)-C(25)-C(26)	-177.52(17)
C(29)-C(24)-C(25)-C(30)	-178.21(17)
C(18)-C(24)-C(25)-C(30)	3.2(3)
C(24)-C(25)-C(26)-C(27)	-0.5(3)
C(30)-C(25)-C(26)-C(27)	178.72(18)
C(25)-C(26)-C(27)-C(28)	-0.2(3)
C(25)-C(26)-C(27)-C(31)	-178.08(19)
C(26)-C(27)-C(28)-C(29)	0.5(3)
C(31)-C(27)-C(28)-C(29)	178.39(19)
C(27)-C(28)-C(29)-C(24)	0.0(3)
C(27)-C(28)-C(29)-C(32)	-179.70(18)
C(25)-C(24)-C(29)-C(28)	-0.8(3)
C(18)-C(24)-C(29)-C(28)	177.79(17)
C(25)-C(24)-C(29)-C(32)	178.91(18)
C(18)-C(24)-C(29)-C(32)	-2.5(3)
C(1S)#1-Cl(1S)-C(1S)-Cl(1S)#1	0.0

Table A7.1 Crystal data for V(NNMe₂)(TIP)(dmpe)(I) (**49**)

Identification code	odomsb920_0m	
Empirical formula	C ₂₁ H ₃₁ I N ₃ O P ₂ S V	
Formula weight	613.33	
Temperature	173(2) K	
Wavelength	0.71073 Å	
Crystal system	Orthorhombic	
Space group	Pbca	
Unit cell dimensions	a = 10.8685(2) Å	a = 90°.
	b = 18.3385(3) Å	b = 90°.
	c = 26.2108(5) Å	g = 90°.
Volume	5224.13(16) Å ³	
Z	8	
Density (calculated)	1.560 Mg/m ³	
Absorption coefficient	1.782 mm ⁻¹	
F(000)	2464	
Crystal size	0.28 × 0.12 × 0.10 mm ³	
Theta range for data collection	2.22 to 27.90°.	
Index ranges	-12 ≤ h ≤ 14, -24 ≤ k ≤ 24, -31 ≤ l ≤ 33	
Reflections collected	67170	
Independent reflections	6199 [R(int) = 0.0556]	
Completeness to theta = 25.00°	100.0 %	
Absorption correction	None	
Refinement method	Full-matrix least-squares on F ²	
Data / restraints / parameters	6199 / 0 / 277	
Goodness-of-fit on F ²	1.019	
Final R indices [I > 2σ(I)]	R1 = 0.0325, wR2 = 0.0627	
R indices (all data)	R1 = 0.0566, wR2 = 0.0701	
Largest diff. peak and hole	0.689 and -0.471 e.Å ⁻³	

Table A7.2 Atomic coordinates ($\times 10^4$) and equivalent isotropic displacement parameters ($\text{\AA}^2 \times 10^3$) for V(NNMe₂)(TIP)(dmpe)(I). U(eq) is defined as one third of the trace of the orthogonalized U_{ij} tensor

	x	y	z	U(eq)
V(1)	7765(1)	4141(1)	3509(1)	22(1)
S(1)	8030(1)	5259(1)	3094(1)	29(1)
P(1)	7387(1)	4955(1)	4262(1)	29(1)
P(2)	7751(1)	3304(1)	4266(1)	29(1)
O(1)	8064(2)	3256(1)	3147(1)	26(1)
N(1)	6231(2)	4125(1)	3388(1)	25(1)
N(2)	5130(2)	4083(1)	3203(1)	36(1)
N(3)	9749(2)	4223(1)	3497(1)	23(1)
C(1)	9483(2)	5494(1)	3342(1)	26(1)
C(2)	9885(3)	6216(1)	3371(1)	33(1)
C(3)	10986(3)	6381(2)	3606(1)	37(1)
C(4)	11702(3)	5833(2)	3814(1)	33(1)
C(5)	11327(2)	5111(1)	3782(1)	28(1)
C(6)	10222(2)	4945(1)	3544(1)	24(1)
C(7)	10530(2)	3710(1)	3392(1)	25(1)
C(8)	10208(2)	2978(1)	3250(1)	24(1)
C(9)	11147(3)	2458(1)	3188(1)	33(1)
C(10)	10898(3)	1769(1)	3015(1)	35(1)
C(11)	9693(3)	1584(1)	2891(1)	32(1)
C(12)	8754(3)	2080(1)	2941(1)	29(1)
C(13)	8990(2)	2786(1)	3121(1)	24(1)
C(14)	4677(3)	3368(2)	3052(1)	51(1)
C(15)	4278(3)	4683(2)	3263(2)	54(1)
C(16)	6605(4)	4428(2)	4757(1)	57(1)
C(17)	7287(4)	3746(2)	4857(1)	65(1)
C(18)	6357(3)	5716(2)	4177(1)	57(1)

C(19)	8688(3)	5351(2)	4581(1)	49(1)
C(20)	6690(3)	2558(2)	4189(1)	43(1)
C(21)	9183(3)	2858(2)	4440(1)	52(1)
I(1)	1920(1)	8379(1)	4394(1)	36(1)

Table A7.3 Bond lengths (Å) and angles (°) for V(NNMe₂)(TIP)(dmpe)(I)

V(1)-N(1)	1.698(2)
V(1)-O(1)	1.9081(17)
V(1)-N(3)	2.162(2)
V(1)-S(1)	2.3383(8)
V(1)-P(2)	2.5079(8)
V(1)-P(1)	2.5078(8)
S(1)-C(1)	1.761(3)
P(1)-C(19)	1.796(3)
P(1)-C(18)	1.803(3)
P(1)-C(16)	1.827(3)
P(2)-C(20)	1.801(3)
P(2)-C(21)	1.817(3)
P(2)-C(17)	1.820(3)
O(1)-C(13)	1.328(3)
N(1)-N(2)	1.293(3)
N(2)-C(15)	1.447(4)
N(2)-C(14)	1.455(4)
N(3)-C(7)	1.298(3)
N(3)-C(6)	1.425(3)
C(1)-C(6)	1.393(4)
C(1)-C(2)	1.396(4)
C(2)-C(3)	1.380(4)

C(2)-H(2)	0.9300
C(3)-C(4)	1.382(4)
C(3)-H(3)	0.9300
C(4)-C(5)	1.389(4)
C(4)-H(4)	0.9300
C(5)-C(6)	1.387(4)
C(5)-H(5)	0.9300
C(7)-C(8)	1.437(3)
C(7)-H(7)	0.9300
C(8)-C(9)	1.405(3)
C(8)-C(13)	1.411(4)
C(9)-C(10)	1.370(4)
C(9)-H(9)	0.9300
C(10)-C(11)	1.392(4)
C(10)-H(10)	0.9300
C(11)-C(12)	1.373(4)
C(11)-H(11)	0.9300
C(12)-C(13)	1.402(4)
C(12)-H(12)	0.9300
C(14)-H(14A)	0.9600
C(14)-H(14B)	0.9600
C(14)-H(14C)	0.9600
C(15)-H(15A)	0.9600
C(15)-H(15B)	0.9600
C(15)-H(15C)	0.9600
C(16)-C(17)	1.477(5)
C(16)-H(16A)	0.9700
C(16)-H(16B)	0.9700
C(17)-H(17A)	0.9700
C(17)-H(17B)	0.9700
C(18)-H(18A)	0.9600

C(18)-H(18B)	0.9600
C(18)-H(18C)	0.9600
C(19)-H(19A)	0.9600
C(19)-H(19B)	0.9600
C(19)-H(19C)	0.9600
C(20)-H(20A)	0.9600
C(20)-H(20B)	0.9600
C(20)-H(20C)	0.9600
C(21)-H(21A)	0.9600
C(21)-H(21B)	0.9600
C(21)-H(21C)	0.9600
N(1)-V(1)-O(1)	93.40(9)
N(1)-V(1)-N(3)	167.99(9)
O(1)-V(1)-N(3)	83.22(8)
N(1)-V(1)-S(1)	92.79(8)
O(1)-V(1)-S(1)	119.53(6)
N(3)-V(1)-S(1)	79.03(6)
N(1)-V(1)-P(2)	97.55(8)
O(1)-V(1)-P(2)	82.74(6)
N(3)-V(1)-P(2)	93.46(6)
S(1)-V(1)-P(2)	154.89(3)
N(1)-V(1)-P(1)	89.81(8)
O(1)-V(1)-P(1)	157.76(6)
N(3)-V(1)-P(1)	97.69(6)
S(1)-V(1)-P(1)	82.23(3)
P(2)-V(1)-P(1)	75.02(3)
C(1)-S(1)-V(1)	98.82(9)
C(19)-P(1)-C(18)	103.56(17)
C(19)-P(1)-C(16)	104.47(18)
C(18)-P(1)-C(16)	102.08(18)

C(19)-P(1)-V(1)	118.51(11)
C(18)-P(1)-V(1)	117.69(11)
C(16)-P(1)-V(1)	108.62(11)
C(20)-P(2)-C(21)	103.56(16)
C(20)-P(2)-C(17)	104.85(17)
C(21)-P(2)-C(17)	102.90(19)
C(20)-P(2)-V(1)	112.39(11)
C(21)-P(2)-V(1)	117.99(10)
C(17)-P(2)-V(1)	113.73(11)
C(13)-O(1)-V(1)	135.01(16)
N(2)-N(1)-V(1)	168.5(2)
N(1)-N(2)-C(15)	120.3(2)
N(1)-N(2)-C(14)	118.0(2)
C(15)-N(2)-C(14)	119.9(2)
C(7)-N(3)-C(6)	117.1(2)
C(7)-N(3)-V(1)	127.25(17)
C(6)-N(3)-V(1)	115.05(16)
C(6)-C(1)-C(2)	119.0(2)
C(6)-C(1)-S(1)	118.70(19)
C(2)-C(1)-S(1)	122.2(2)
C(3)-C(2)-C(1)	120.3(3)
C(3)-C(2)-H(2)	119.9
C(1)-C(2)-H(2)	119.9
C(2)-C(3)-C(4)	120.3(3)
C(2)-C(3)-H(3)	119.9
C(4)-C(3)-H(3)	119.9
C(3)-C(4)-C(5)	120.3(3)
C(3)-C(4)-H(4)	119.8
C(5)-C(4)-H(4)	119.8
C(6)-C(5)-C(4)	119.4(3)
C(6)-C(5)-H(5)	120.3

C(4)-C(5)-H(5)	120.3
C(5)-C(6)-C(1)	120.8(2)
C(5)-C(6)-N(3)	123.7(2)
C(1)-C(6)-N(3)	115.5(2)
N(3)-C(7)-C(8)	125.0(2)
N(3)-C(7)-H(7)	117.5
C(8)-C(7)-H(7)	117.5
C(9)-C(8)-C(13)	119.0(2)
C(9)-C(8)-C(7)	119.1(2)
C(13)-C(8)-C(7)	121.6(2)
C(10)-C(9)-C(8)	121.4(3)
C(10)-C(9)-H(9)	119.3
C(8)-C(9)-H(9)	119.3
C(9)-C(10)-C(11)	119.2(3)
C(9)-C(10)-H(10)	120.4
C(11)-C(10)-H(10)	120.4
C(12)-C(11)-C(10)	121.0(3)
C(12)-C(11)-H(11)	119.5
C(10)-C(11)-H(11)	119.5
C(11)-C(12)-C(13)	120.5(3)
C(11)-C(12)-H(12)	119.7
C(13)-C(12)-H(12)	119.7
O(1)-C(13)-C(12)	118.6(2)
O(1)-C(13)-C(8)	122.5(2)
C(12)-C(13)-C(8)	118.9(2)
N(2)-C(14)-H(14A)	109.5
N(2)-C(14)-H(14B)	109.5
H(14A)-C(14)-H(14B)	109.5
N(2)-C(14)-H(14C)	109.5
H(14A)-C(14)-H(14C)	109.5
H(14B)-C(14)-H(14C)	109.5

N(2)-C(15)-H(15A)	109.5
N(2)-C(15)-H(15B)	109.5
H(15A)-C(15)-H(15B)	109.5
N(2)-C(15)-H(15C)	109.5
H(15A)-C(15)-H(15C)	109.5
H(15B)-C(15)-H(15C)	109.5
C(17)-C(16)-P(1)	110.0(2)
C(17)-C(16)-H(16A)	109.7
P(1)-C(16)-H(16A)	109.7
C(17)-C(16)-H(16B)	109.7
P(1)-C(16)-H(16B)	109.7
H(16A)-C(16)-H(16B)	108.2
C(16)-C(17)-P(2)	111.4(2)
C(16)-C(17)-H(17A)	109.4
P(2)-C(17)-H(17A)	109.4
C(16)-C(17)-H(17B)	109.4
P(2)-C(17)-H(17B)	109.4
H(17A)-C(17)-H(17B)	108.0
P(1)-C(18)-H(18A)	109.5
P(1)-C(18)-H(18B)	109.5
H(18A)-C(18)-H(18B)	109.5
P(1)-C(18)-H(18C)	109.5
H(18A)-C(18)-H(18C)	109.5
H(18B)-C(18)-H(18C)	109.5
P(1)-C(19)-H(19A)	109.5
P(1)-C(19)-H(19B)	109.5
H(19A)-C(19)-H(19B)	109.5
P(1)-C(19)-H(19C)	109.5
H(19A)-C(19)-H(19C)	109.5
H(19B)-C(19)-H(19C)	109.5
P(2)-C(20)-H(20A)	109.5

P(2)-C(20)-H(20B)	109.5
H(20A)-C(20)-H(20B)	109.5
P(2)-C(20)-H(20C)	109.5
H(20A)-C(20)-H(20C)	109.5
H(20B)-C(20)-H(20C)	109.5
P(2)-C(21)-H(21A)	109.5
P(2)-C(21)-H(21B)	109.5
H(21A)-C(21)-H(21B)	109.5
P(2)-C(21)-H(21C)	109.5
H(21A)-C(21)-H(21C)	109.5
H(21B)-C(21)-H(21C)	109.5

Table A7.4 Anisotropic displacement parameters ($\text{\AA}^2 \times 10^3$) for $V(\text{NNMe}_2)(\text{TIP})(\text{dmpe})(\text{I})$. The anisotropic displacement factor exponent takes the form: $-2 \pi^2 [h^2 a^{*2} U_{11} + \dots + 2 h k a^* b^* U_{12}]$

	U ₁₁	U ₂₂	U ₃₃	U ₂₃	U ₁₃	U ₁₂
V(1)	19(1)	24(1)	23(1)	0(1)	1(1)	1(1)
S(1)	26(1)	29(1)	33(1)	7(1)	0(1)	4(1)
P(1)	31(1)	29(1)	27(1)	-2(1)	4(1)	4(1)
P(2)	36(1)	27(1)	25(1)	2(1)	1(1)	-5(1)
O(1)	21(1)	29(1)	28(1)	-4(1)	0(1)	2(1)
N(1)	23(1)	29(1)	23(1)	1(1)	1(1)	1(1)
N(2)	19(1)	44(2)	44(2)	-3(1)	-5(1)	-1(1)
N(3)	22(1)	23(1)	25(1)	1(1)	0(1)	0(1)
C(1)	25(1)	29(1)	24(1)	1(1)	7(1)	1(1)
C(2)	39(2)	24(1)	35(2)	3(1)	7(1)	3(1)
C(3)	45(2)	24(1)	41(2)	-2(1)	9(2)	-9(1)
C(4)	29(2)	36(2)	35(2)	-4(1)	1(1)	-6(1)

C(5)	25(2)	28(1)	32(2)	-1(1)	5(1)	0(1)
C(6)	25(1)	22(1)	26(2)	-2(1)	5(1)	-2(1)
C(7)	21(1)	28(1)	26(2)	1(1)	-3(1)	0(1)
C(8)	23(1)	23(1)	27(2)	0(1)	-1(1)	1(1)
C(9)	26(2)	29(1)	42(2)	2(1)	-1(1)	4(1)
C(10)	39(2)	25(2)	40(2)	-1(1)	1(1)	9(1)
C(11)	42(2)	23(1)	31(2)	-2(1)	4(1)	-2(1)
C(12)	31(2)	30(2)	25(2)	-2(1)	3(1)	-5(1)
C(13)	26(1)	26(1)	20(1)	2(1)	2(1)	1(1)
C(14)	44(2)	67(2)	41(2)	-22(2)	0(2)	-19(2)
C(15)	31(2)	55(2)	76(3)	23(2)	-12(2)	7(2)
C(16)	74(3)	49(2)	47(2)	-7(2)	32(2)	-5(2)
C(17)	130(4)	35(2)	30(2)	0(2)	27(2)	-2(2)
C(18)	63(2)	57(2)	50(2)	-21(2)	-11(2)	31(2)
C(19)	37(2)	74(2)	37(2)	-21(2)	0(2)	0(2)
C(20)	42(2)	35(2)	51(2)	5(2)	0(2)	-8(1)
C(21)	40(2)	70(2)	46(2)	34(2)	-6(2)	-7(2)
I(1)	41(1)	40(1)	28(1)	3(1)	0(1)	-11(1)

Table A7.5 Hydrogen coordinates ($\times 10^4$) and isotropic displacement parameters ($\text{\AA}^2 \times 10^3$) for V(NNMe₂)(TIP)(dmpe)(I)

	x	y	z	U(eq)
H(2)	9410	6587	3230	39
H(3)	11247	6863	3626	44
H(4)	12438	5949	3975	40
H(5)	11812	4742	3919	34
H(7)	11363	3824	3410	30

H(9)	11953	2584	3267	39
H(10)	11528	1429	2980	42
H(11)	9521	1117	2772	38
H(12)	7955	1946	2854	35
H(14A)	5348	3080	2924	76
H(14B)	4068	3423	2790	76
H(14C)	4317	3129	3341	76
H(15A)	3815	4618	3572	81
H(15B)	3726	4695	2977	81
H(15C)	4727	5133	3280	81
H(16A)	6554	4713	5068	68
H(16B)	5775	4313	4647	68
H(17A)	6772	3416	5052	78
H(17B)	8012	3854	5059	78
H(18A)	6279	5977	4492	85
H(18B)	5564	5540	4072	85
H(18C)	6679	6036	3919	85
H(19A)	9032	5729	4372	74
H(19B)	9298	4981	4640	74
H(19C)	8430	5553	4901	74
H(20A)	6735	2244	4481	64
H(20B)	6900	2286	3888	64
H(20C)	5869	2745	4156	64
H(21A)	9072	2596	4754	78
H(21B)	9816	3218	4483	78
H(21C)	9418	2524	4176	78

Table A7.6 Torsion angles (°) for V(NNMe₂)(TIP)(dmpe)(I)

N(1)-V(1)-S(1)-C(1)	163.52(11)
O(1)-V(1)-S(1)-C(1)	-100.99(11)
N(3)-V(1)-S(1)-C(1)	-25.34(11)
P(2)-V(1)-S(1)-C(1)	49.06(12)
P(1)-V(1)-S(1)-C(1)	74.10(9)
N(1)-V(1)-P(1)-C(19)	-171.61(16)
O(1)-V(1)-P(1)-C(19)	89.9(2)
N(3)-V(1)-P(1)-C(19)	-1.02(15)
S(1)-V(1)-P(1)-C(19)	-78.77(14)
P(2)-V(1)-P(1)-C(19)	90.52(14)
N(1)-V(1)-P(1)-C(18)	-45.71(17)
O(1)-V(1)-P(1)-C(18)	-144.2(2)
N(3)-V(1)-P(1)-C(18)	124.87(16)
S(1)-V(1)-P(1)-C(18)	47.13(15)
P(2)-V(1)-P(1)-C(18)	-143.58(16)
N(1)-V(1)-P(1)-C(16)	69.51(16)
O(1)-V(1)-P(1)-C(16)	-29.0(2)
N(3)-V(1)-P(1)-C(16)	-119.90(15)
S(1)-V(1)-P(1)-C(16)	162.35(14)
P(2)-V(1)-P(1)-C(16)	-28.36(14)
N(1)-V(1)-P(2)-C(20)	38.93(14)
O(1)-V(1)-P(2)-C(20)	-53.56(13)
N(3)-V(1)-P(2)-C(20)	-136.27(13)
S(1)-V(1)-P(2)-C(20)	152.41(13)
P(1)-V(1)-P(2)-C(20)	126.69(12)
N(1)-V(1)-P(2)-C(21)	159.34(16)
O(1)-V(1)-P(2)-C(21)	66.85(15)
N(3)-V(1)-P(2)-C(21)	-15.86(15)
S(1)-V(1)-P(2)-C(21)	-87.18(16)

P(1)-V(1)-P(2)-C(21)	-112.90(14)
N(1)-V(1)-P(2)-C(17)	-80.01(18)
O(1)-V(1)-P(2)-C(17)	-172.49(18)
N(3)-V(1)-P(2)-C(17)	104.80(18)
S(1)-V(1)-P(2)-C(17)	33.48(19)
P(1)-V(1)-P(2)-C(17)	7.76(17)
N(1)-V(1)-O(1)-C(13)	-165.1(2)
N(3)-V(1)-O(1)-C(13)	26.5(2)
S(1)-V(1)-O(1)-C(13)	99.8(2)
P(2)-V(1)-O(1)-C(13)	-67.9(2)
P(1)-V(1)-O(1)-C(13)	-67.3(3)
O(1)-V(1)-N(1)-N(2)	-45.9(10)
N(3)-V(1)-N(1)-N(2)	27.3(13)
S(1)-V(1)-N(1)-N(2)	74.0(10)
P(2)-V(1)-N(1)-N(2)	-129.0(10)
P(1)-V(1)-N(1)-N(2)	156.2(10)
V(1)-N(1)-N(2)-C(15)	-125.5(9)
V(1)-N(1)-N(2)-C(14)	69.5(11)
N(1)-V(1)-N(3)-C(7)	-89.4(5)
O(1)-V(1)-N(3)-C(7)	-15.1(2)
S(1)-V(1)-N(3)-C(7)	-137.0(2)
P(2)-V(1)-N(3)-C(7)	67.1(2)
P(1)-V(1)-N(3)-C(7)	142.5(2)
N(1)-V(1)-N(3)-C(6)	81.6(5)
O(1)-V(1)-N(3)-C(6)	155.85(18)
S(1)-V(1)-N(3)-C(6)	33.94(16)
P(2)-V(1)-N(3)-C(6)	-121.89(17)
P(1)-V(1)-N(3)-C(6)	-46.56(17)
V(1)-S(1)-C(1)-C(6)	20.3(2)
V(1)-S(1)-C(1)-C(2)	-155.8(2)
C(6)-C(1)-C(2)-C(3)	-1.5(4)

S(1)-C(1)-C(2)-C(3)	174.6(2)
C(1)-C(2)-C(3)-C(4)	0.3(4)
C(2)-C(3)-C(4)-C(5)	0.7(4)
C(3)-C(4)-C(5)-C(6)	-0.5(4)
C(4)-C(5)-C(6)-C(1)	-0.7(4)
C(4)-C(5)-C(6)-N(3)	-179.1(2)
C(2)-C(1)-C(6)-C(5)	1.7(4)
S(1)-C(1)-C(6)-C(5)	-174.5(2)
C(2)-C(1)-C(6)-N(3)	-179.7(2)
S(1)-C(1)-C(6)-N(3)	4.1(3)
C(7)-N(3)-C(6)-C(5)	-40.4(4)
V(1)-N(3)-C(6)-C(5)	147.7(2)
C(7)-N(3)-C(6)-C(1)	141.1(2)
V(1)-N(3)-C(6)-C(1)	-30.8(3)
C(6)-N(3)-C(7)-C(8)	-169.3(2)
V(1)-N(3)-C(7)-C(8)	1.5(4)
N(3)-C(7)-C(8)-C(9)	-174.6(3)
N(3)-C(7)-C(8)-C(13)	11.7(4)
C(13)-C(8)-C(9)-C(10)	-1.0(4)
C(7)-C(8)-C(9)-C(10)	-174.9(3)
C(8)-C(9)-C(10)-C(11)	0.8(4)
C(9)-C(10)-C(11)-C(12)	-0.1(4)
C(10)-C(11)-C(12)-C(13)	-0.3(4)
V(1)-O(1)-C(13)-C(12)	160.11(19)
V(1)-O(1)-C(13)-C(8)	-22.5(4)
C(11)-C(12)-C(13)-O(1)	177.7(2)
C(11)-C(12)-C(13)-C(8)	0.2(4)
C(9)-C(8)-C(13)-O(1)	-176.9(2)
C(7)-C(8)-C(13)-O(1)	-3.2(4)
C(9)-C(8)-C(13)-C(12)	0.5(4)
C(7)-C(8)-C(13)-C(12)	174.2(2)

C(19)-P(1)-C(16)-C(17)	-75.9(3)
C(18)-P(1)-C(16)-C(17)	176.4(3)
V(1)-P(1)-C(16)-C(17)	51.5(3)
P(1)-C(16)-C(17)-P(2)	-44.8(4)
C(20)-P(2)-C(17)-C(16)	-103.4(3)
C(21)-P(2)-C(17)-C(16)	148.6(3)
V(1)-P(2)-C(17)-C(16)	19.8(3)

APPENDIX B

Kinetic reaction plots

Figure B1.1 Kinetic plot for Run 1 with 10% $\text{Ti}(\text{dap})_2(\text{NMe}_2)_2$ (1).

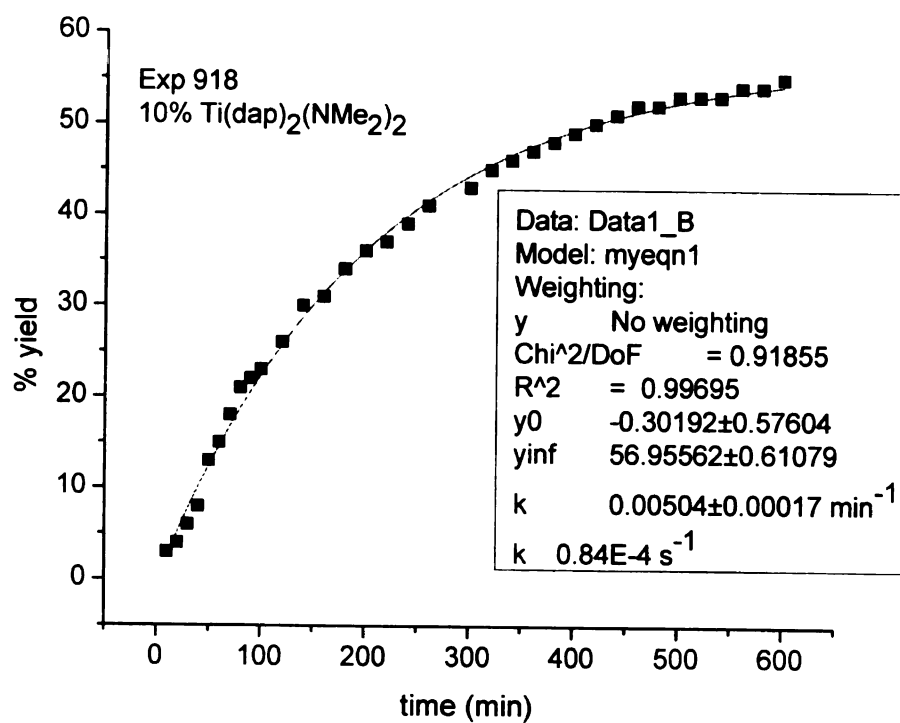


Figure B1.2 Kinetic plot for Run 2 with 10% Ti(dap)₂(NMe₂)₂ (1).

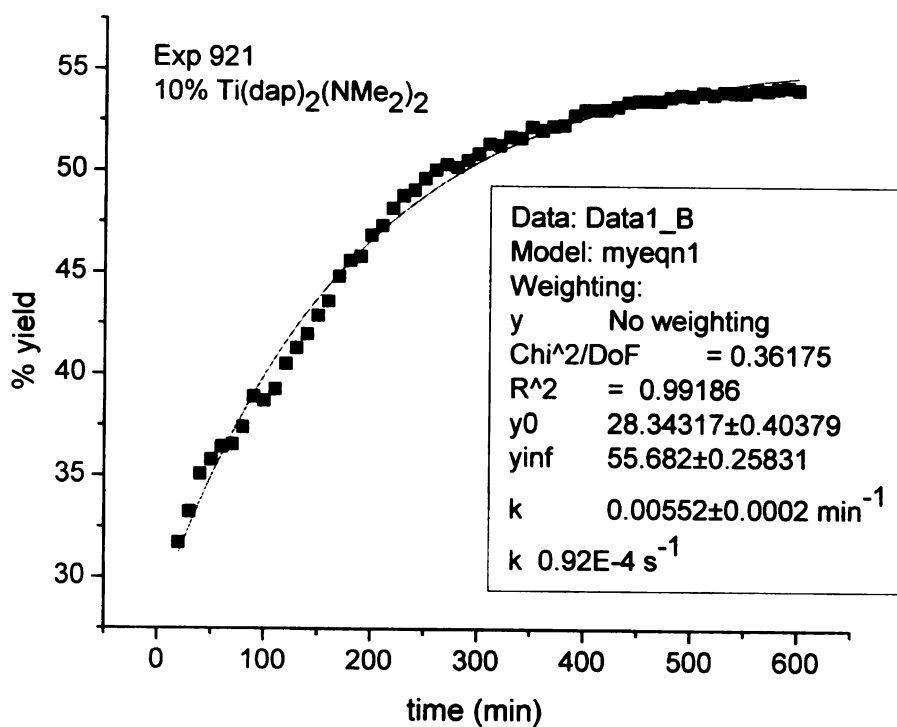


Figure B1.3 Kinetic plot for Run 3 with 10% Ti(dap)₂(NMe₂)₂ (1).

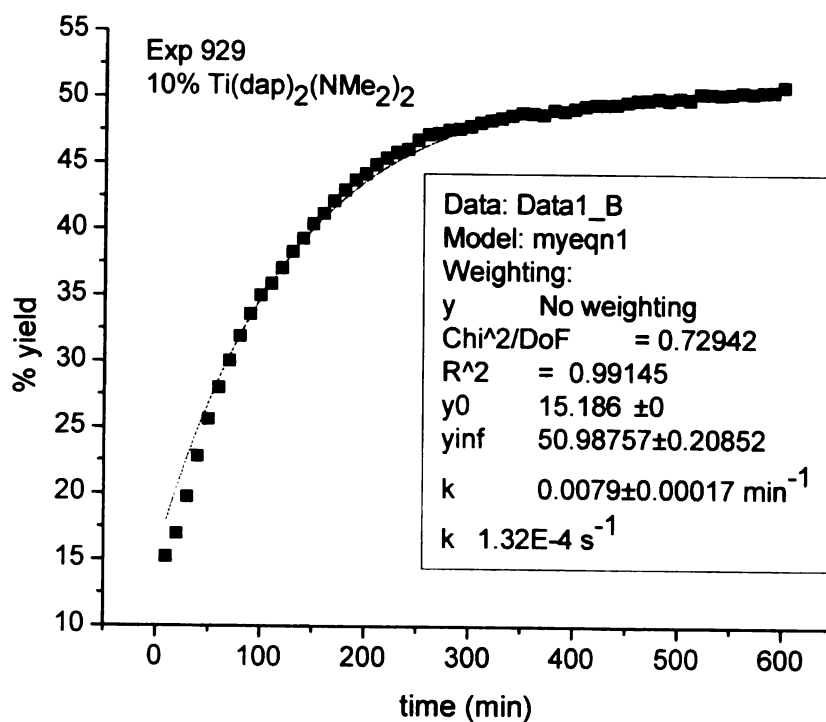


Figure B2.1 Kinetic plot for run 1 with 10% 36.

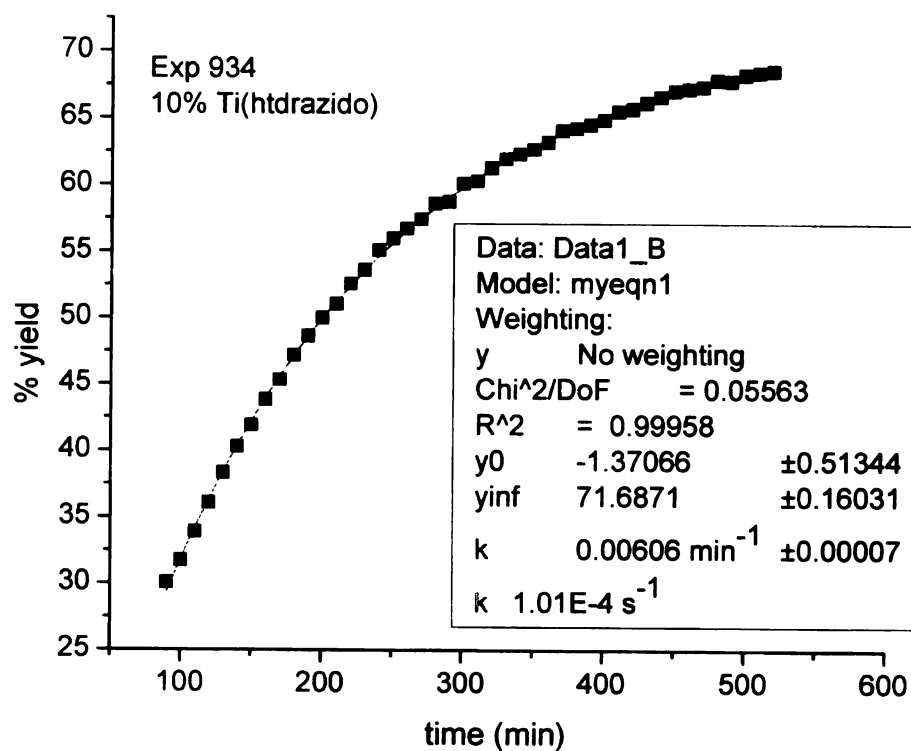


Figure B2.2 Kinetic plot for run 2 with 36.

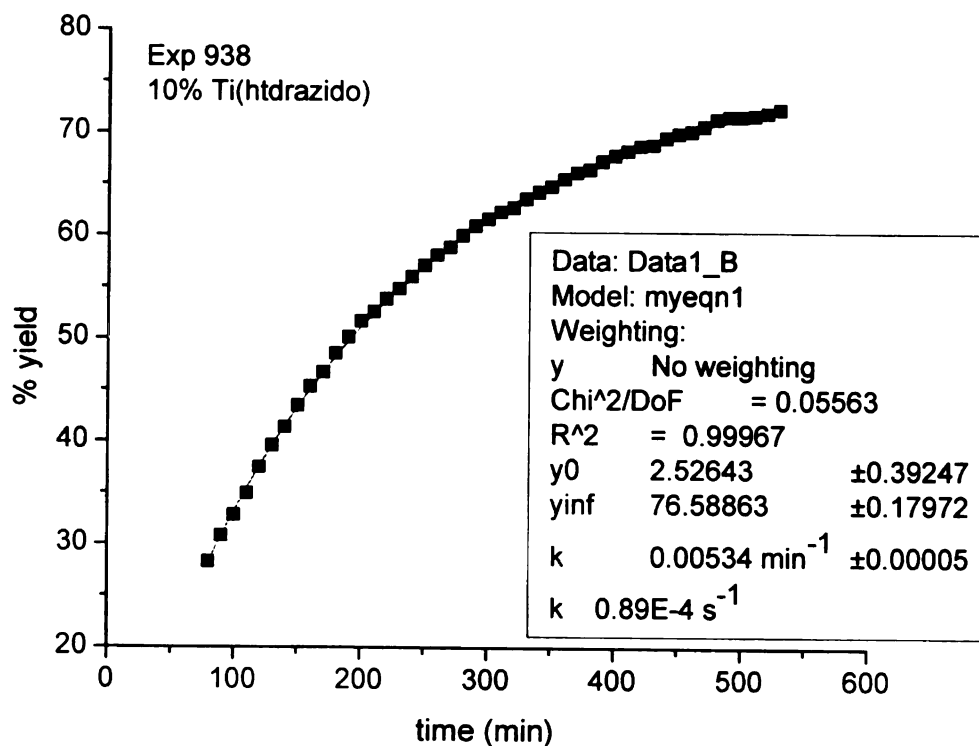


Figure B2.3 Kinetic plot for run 3 with 10% 36.

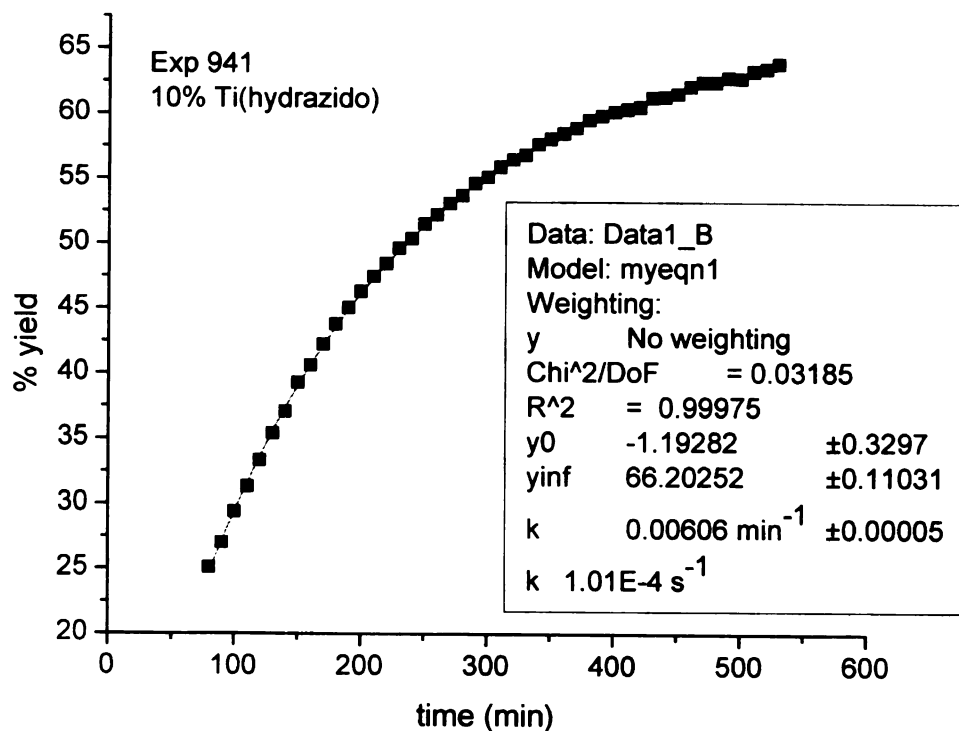


Figure B3.1 Kinetic plot for run 1 with 36 + 10 Me₂NNH₂ reaction.

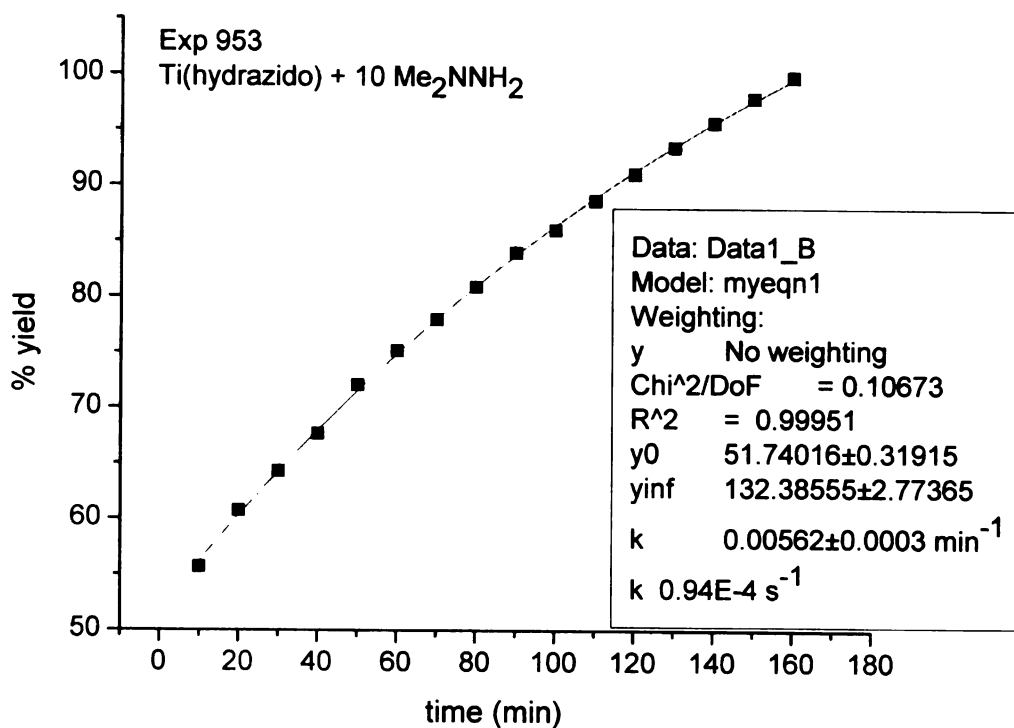


Figure B3.2 Kinetic plot for run 2 with $36 + 10 \text{ Me}_2\text{NNH}_2$ reaction.

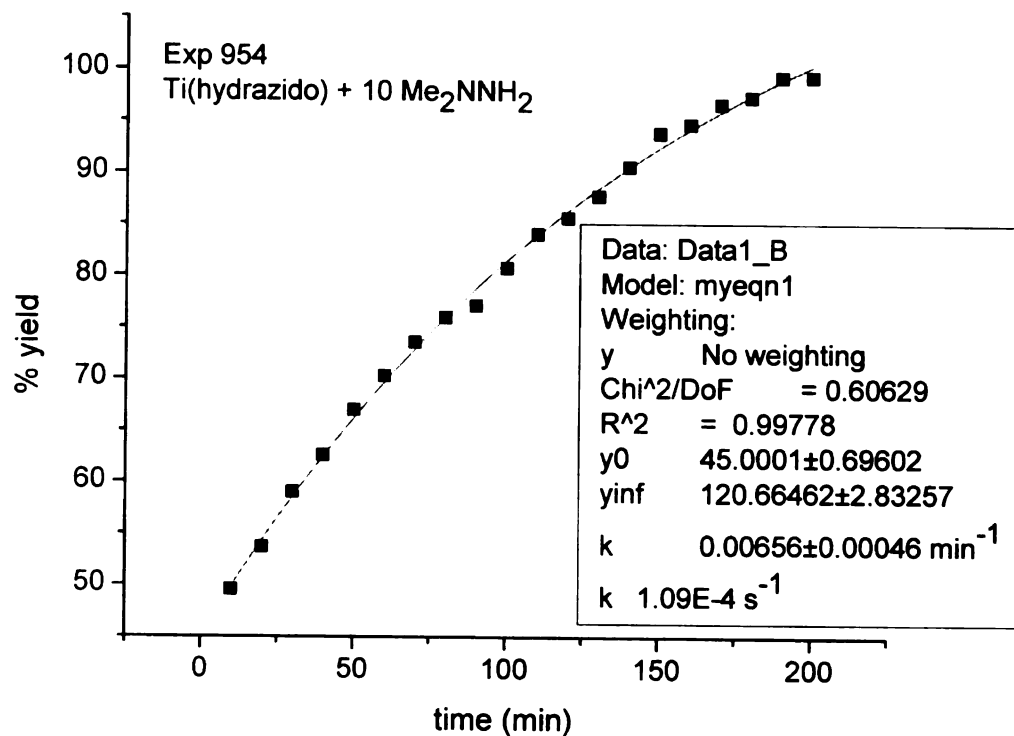


Figure B3.3 Kinetic plot for run 3 with $36 + 10 \text{ Me}_2\text{NNH}_2$ reaction.

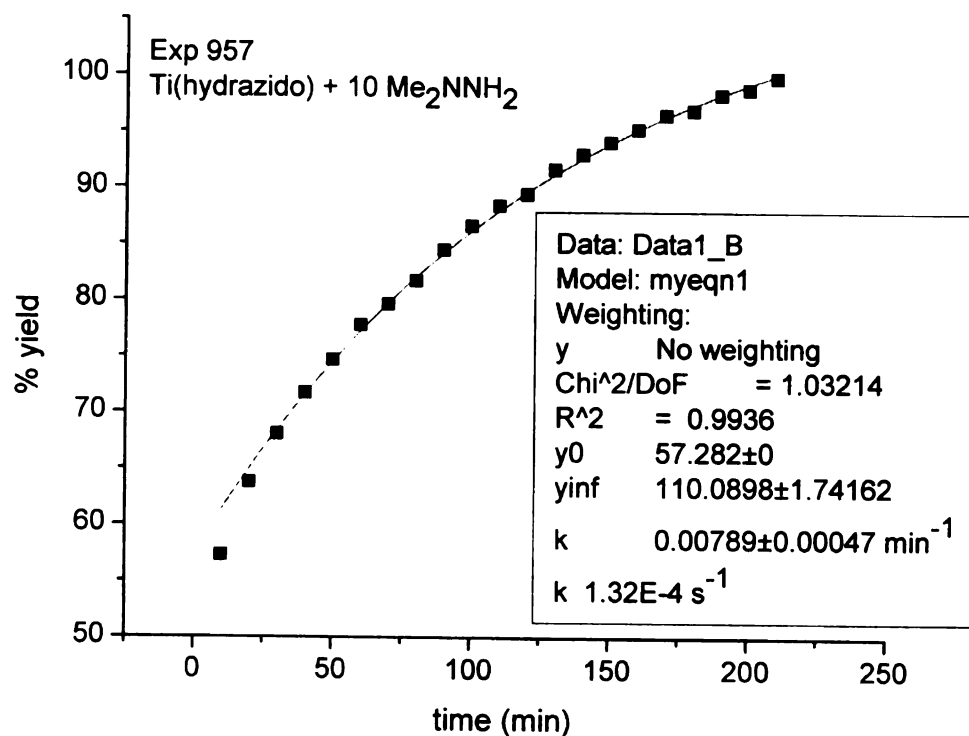


Figure B4.1 Kinetic plot for run 1 with 36 + 10% Hdap reaction.

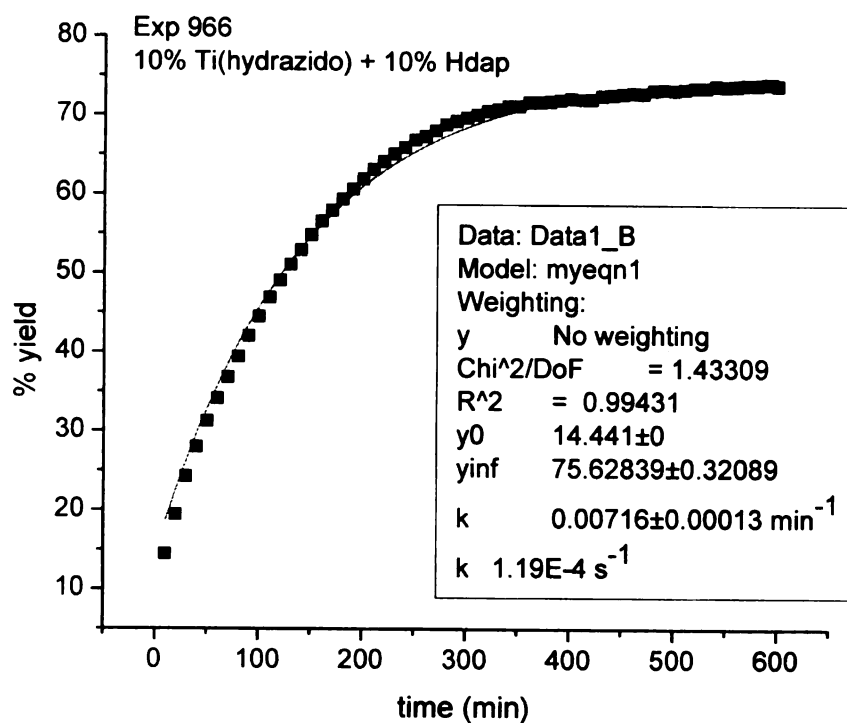


Figure B4.2 Kinetic plot for run 2 with 10% 36 + 10% Hdap reaction.

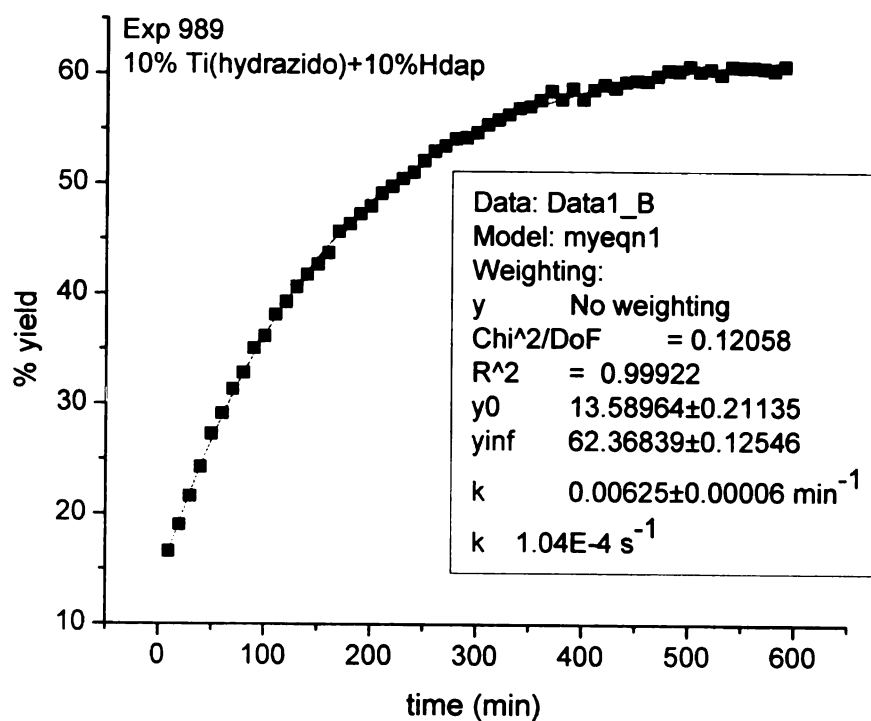


Figure B4.3 Kinetic plot for run 3 with 10% 36 + 10% Hdap reaction.

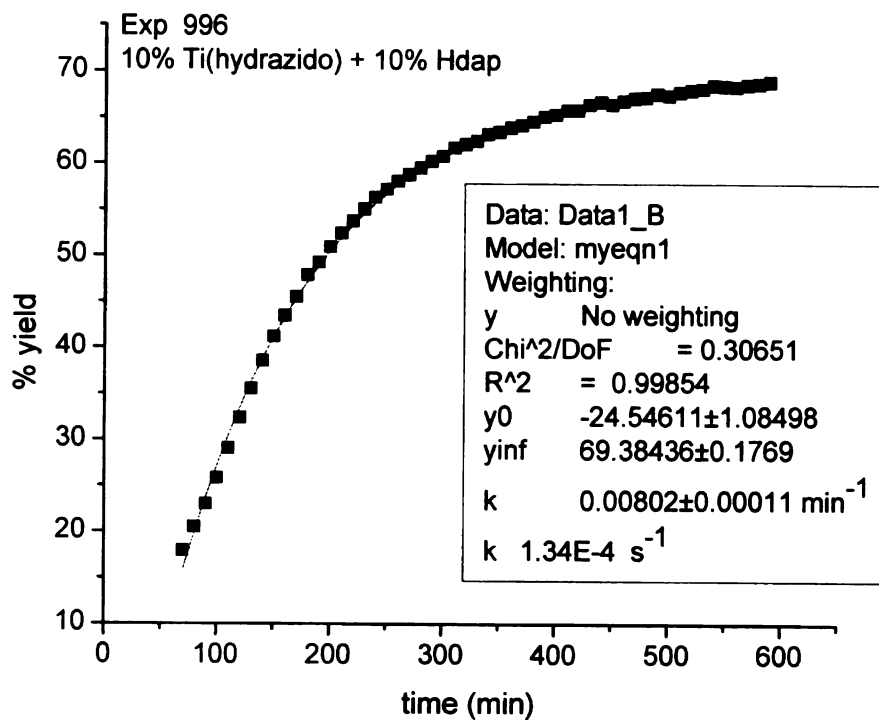


Figure B5.1 Kinetic plot for run 1 with 10% 37.

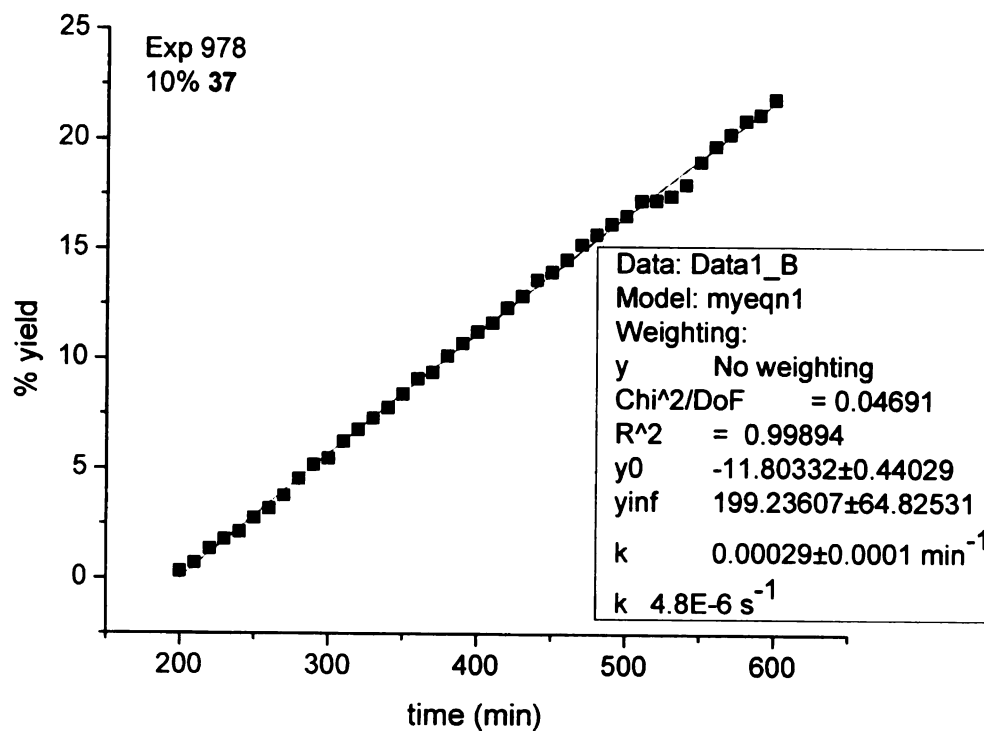


Figure B6.1 Kinetic plot with 15% $\text{Ti}(\text{dap})_2(\text{NMe}_2)_2$.

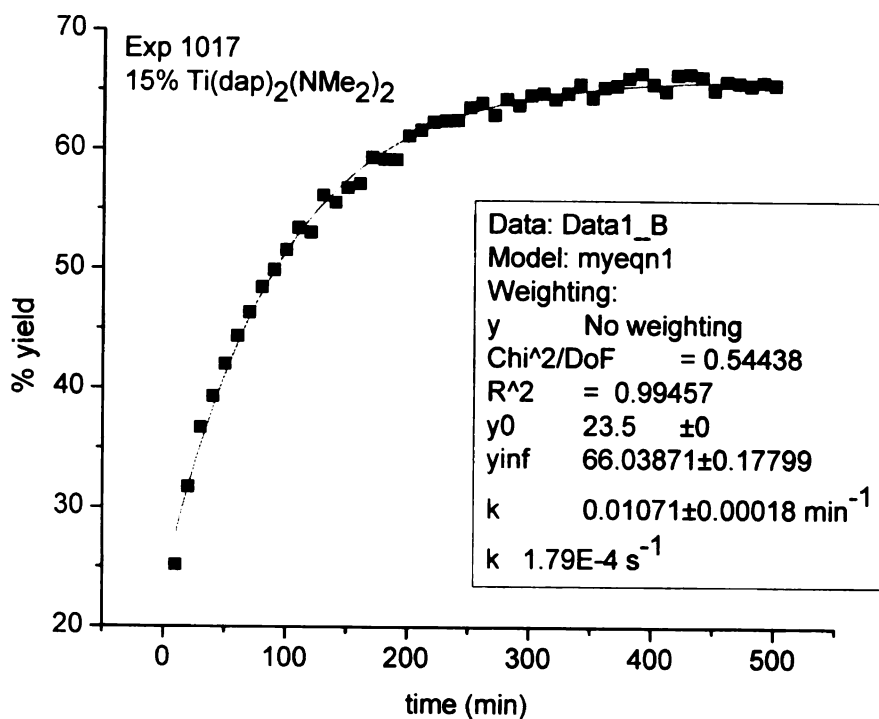


Figure B6.2 Kinetic plot with 5% $\text{Ti}(\text{dap})_2(\text{NMe}_2)_2$.

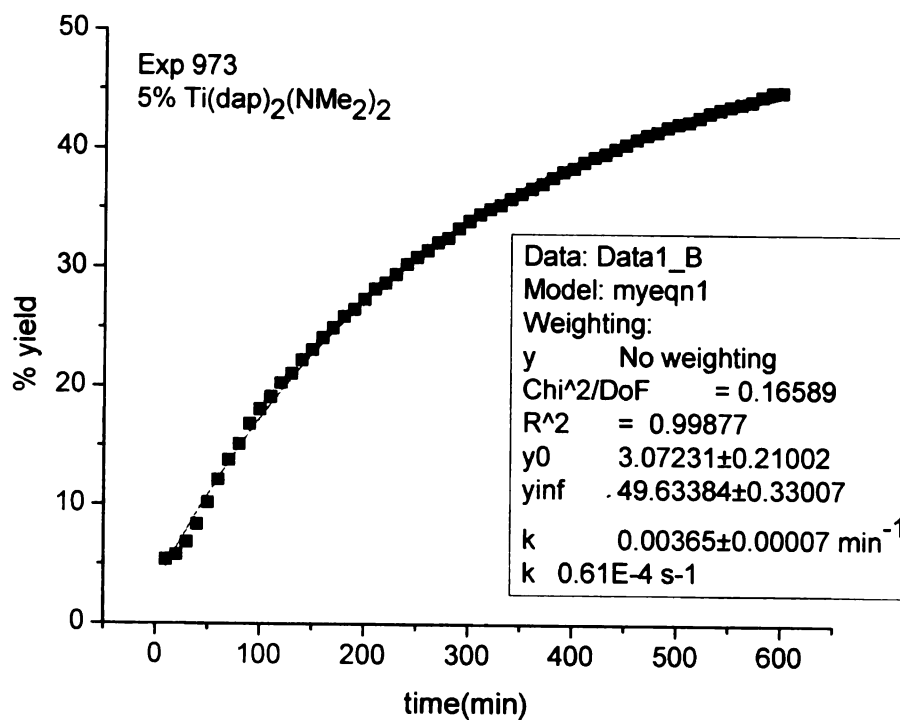
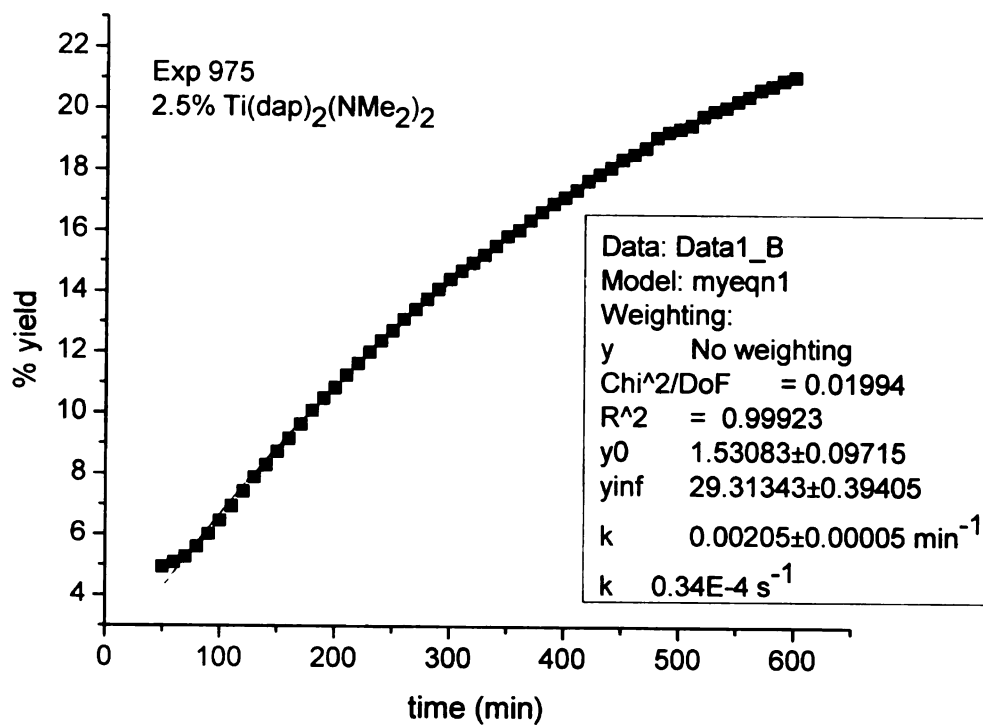


Figure B6.3 Kinetic plot with 2.5% $\text{Ti}(\text{dap})_2(\text{NMe}_2)_2$.



APPENDIX C

Figure C.1 ^1H and ^{13}C NMR spectra of compound 2.

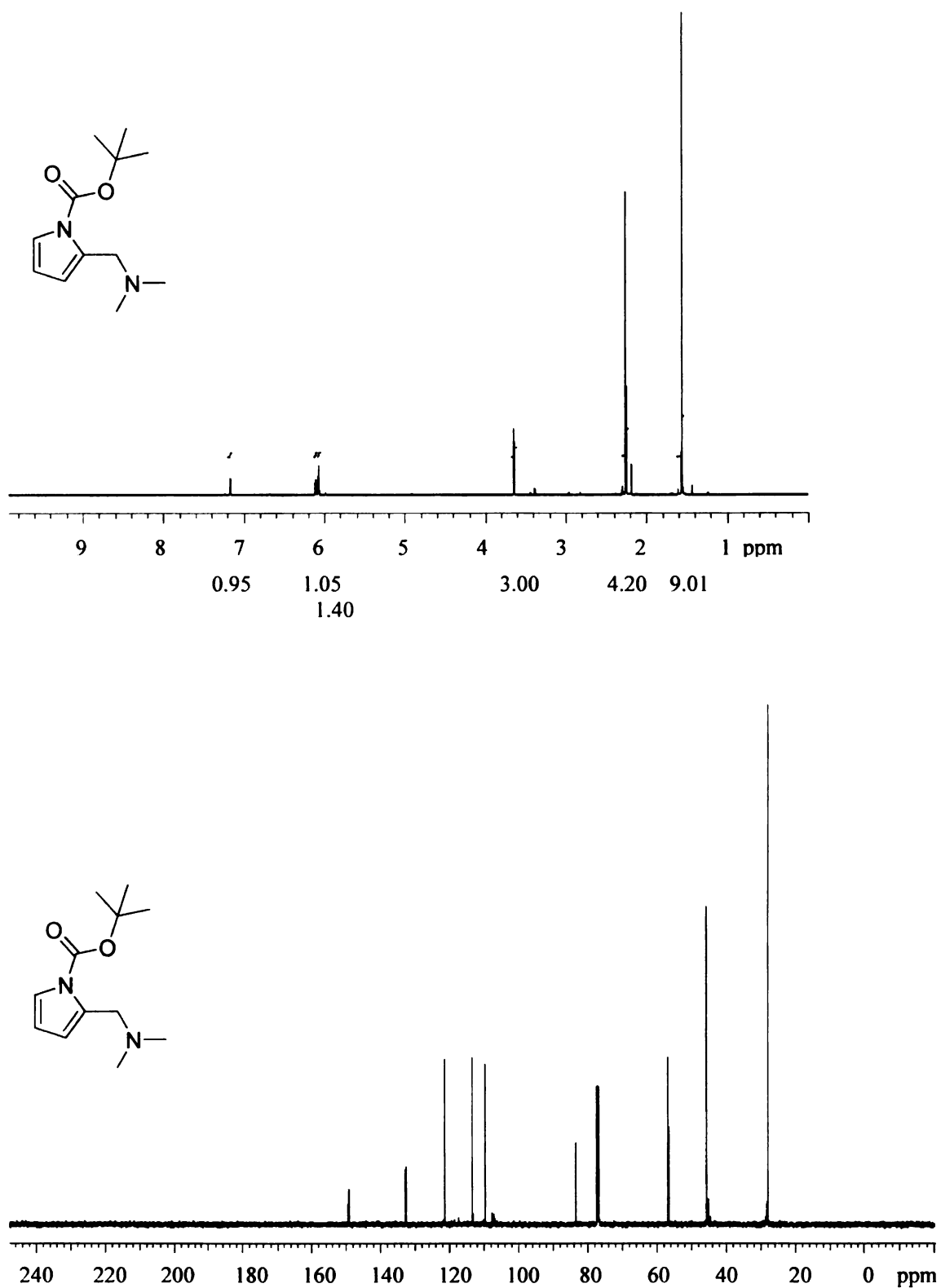


Figure C.2 ^1H and ^{13}C NMR spectra of compound 4.

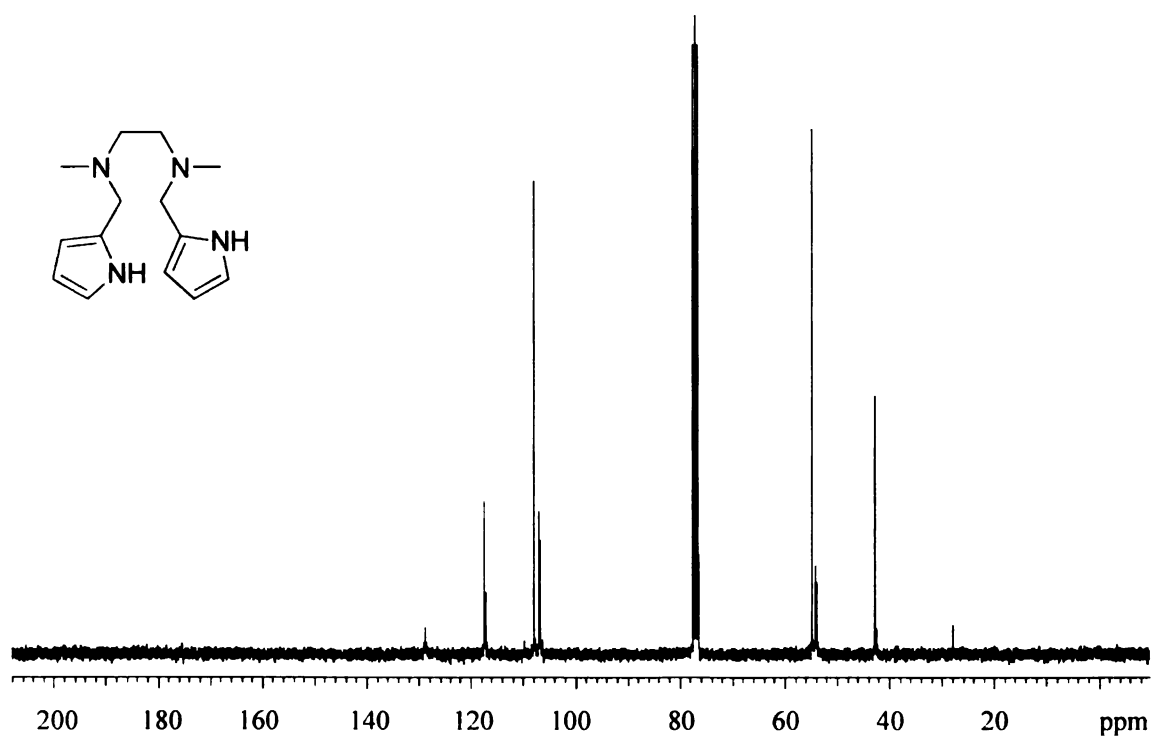
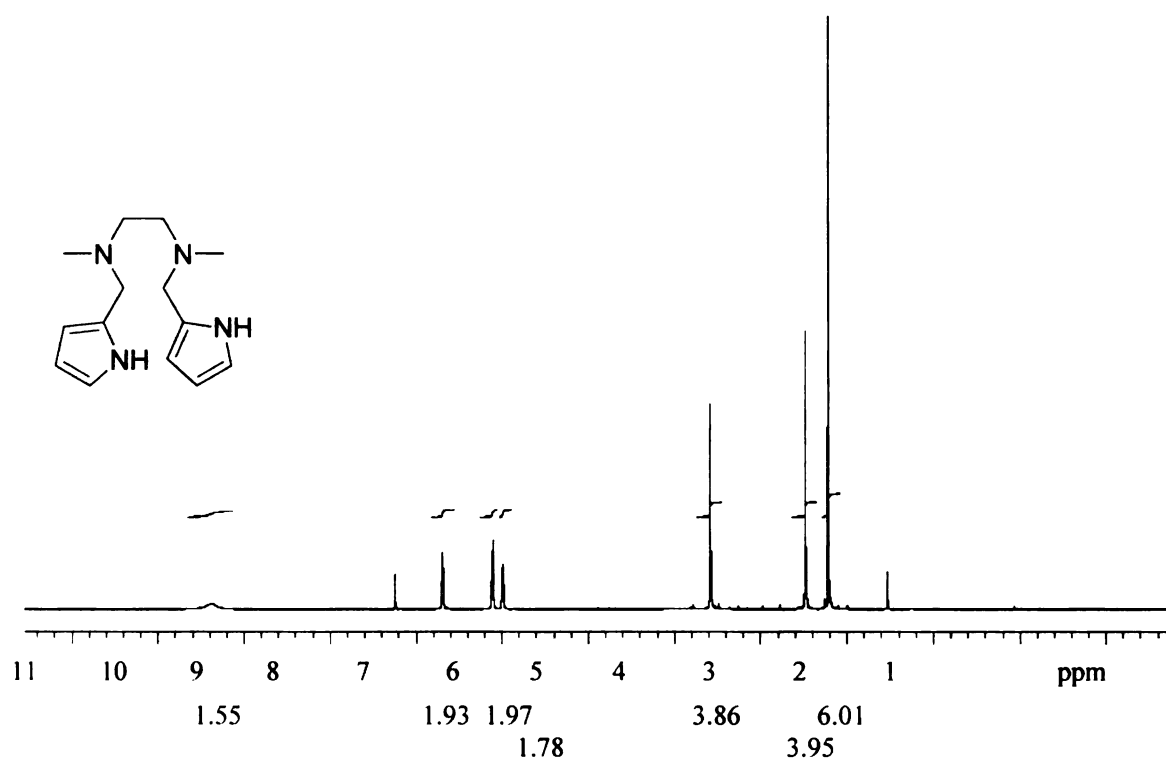


Figure C.3 ^1H and ^{13}C NMR spectra of compound 5.

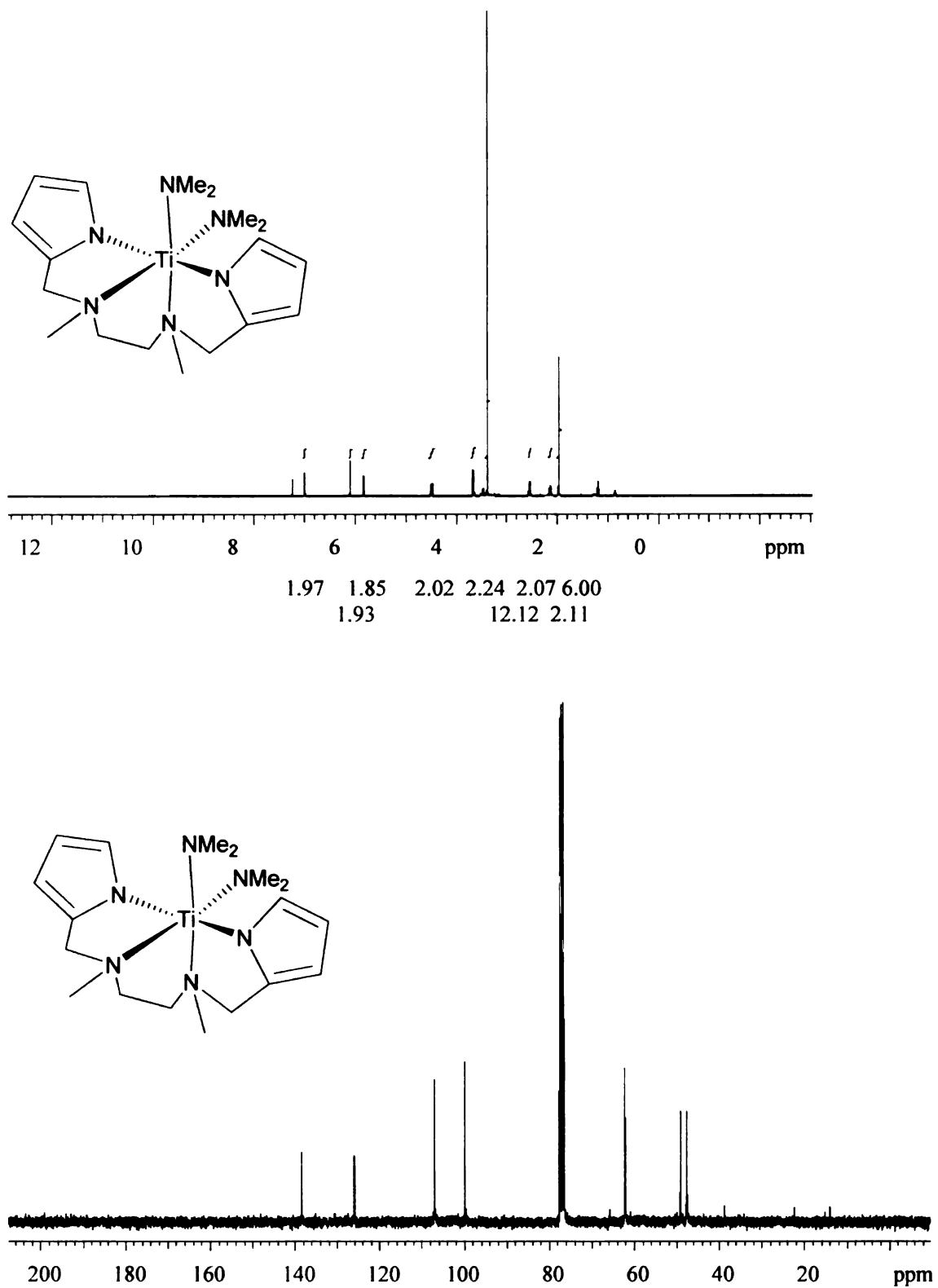


Figure C.4 ^1H and ^{13}C Ctra of compound 7.

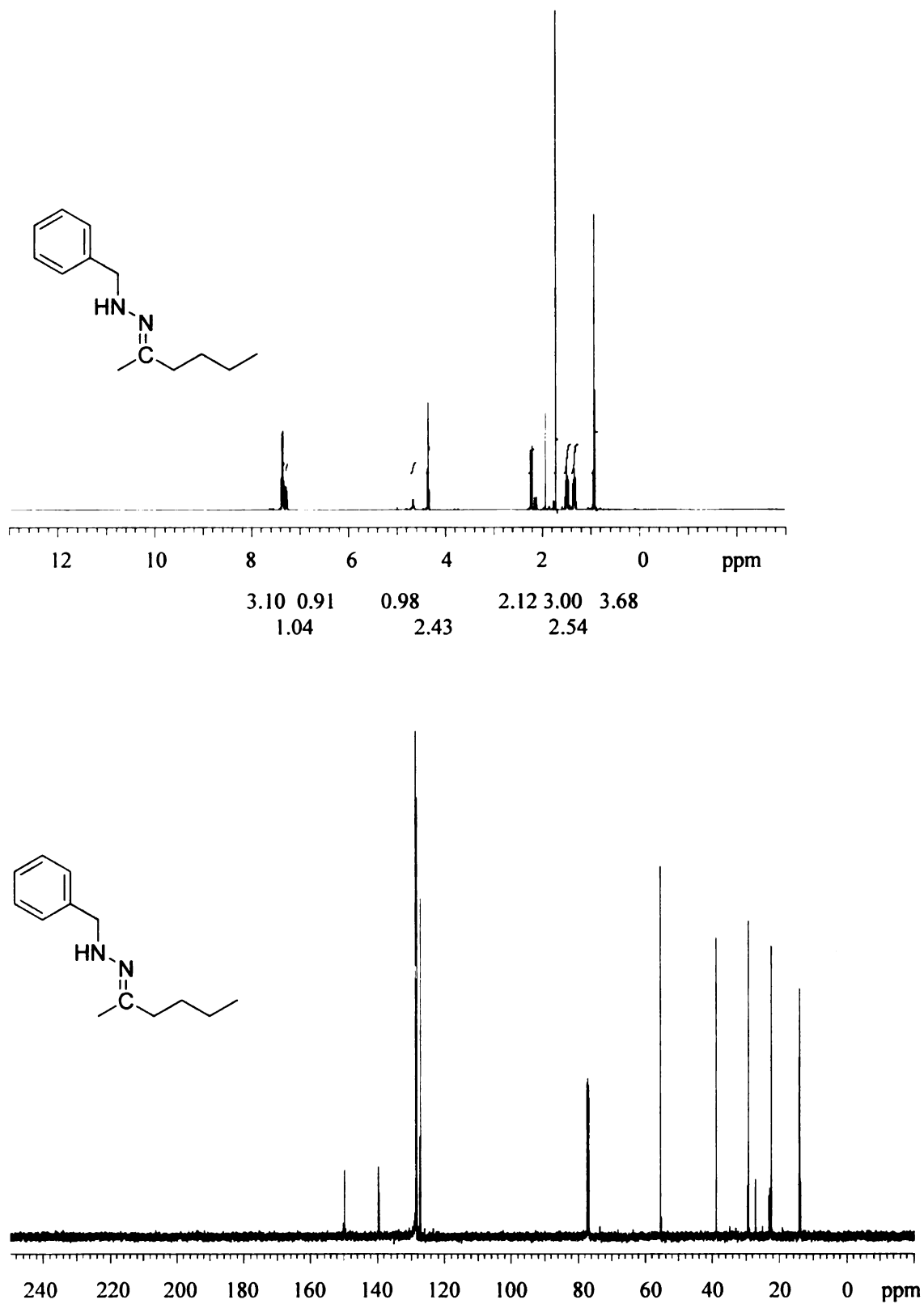


Figure C.5 ^1H and ^{13}C NMR spectral data of compound **13** and **14**.

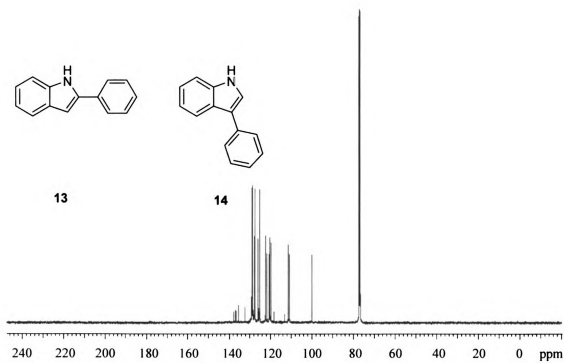
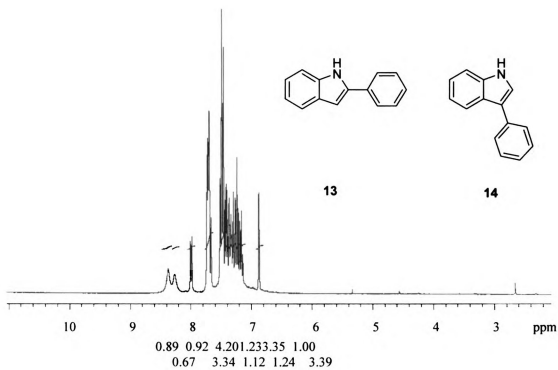


Figure C.6 ^1H and ^{13}C NMR spectral data of compound 15.

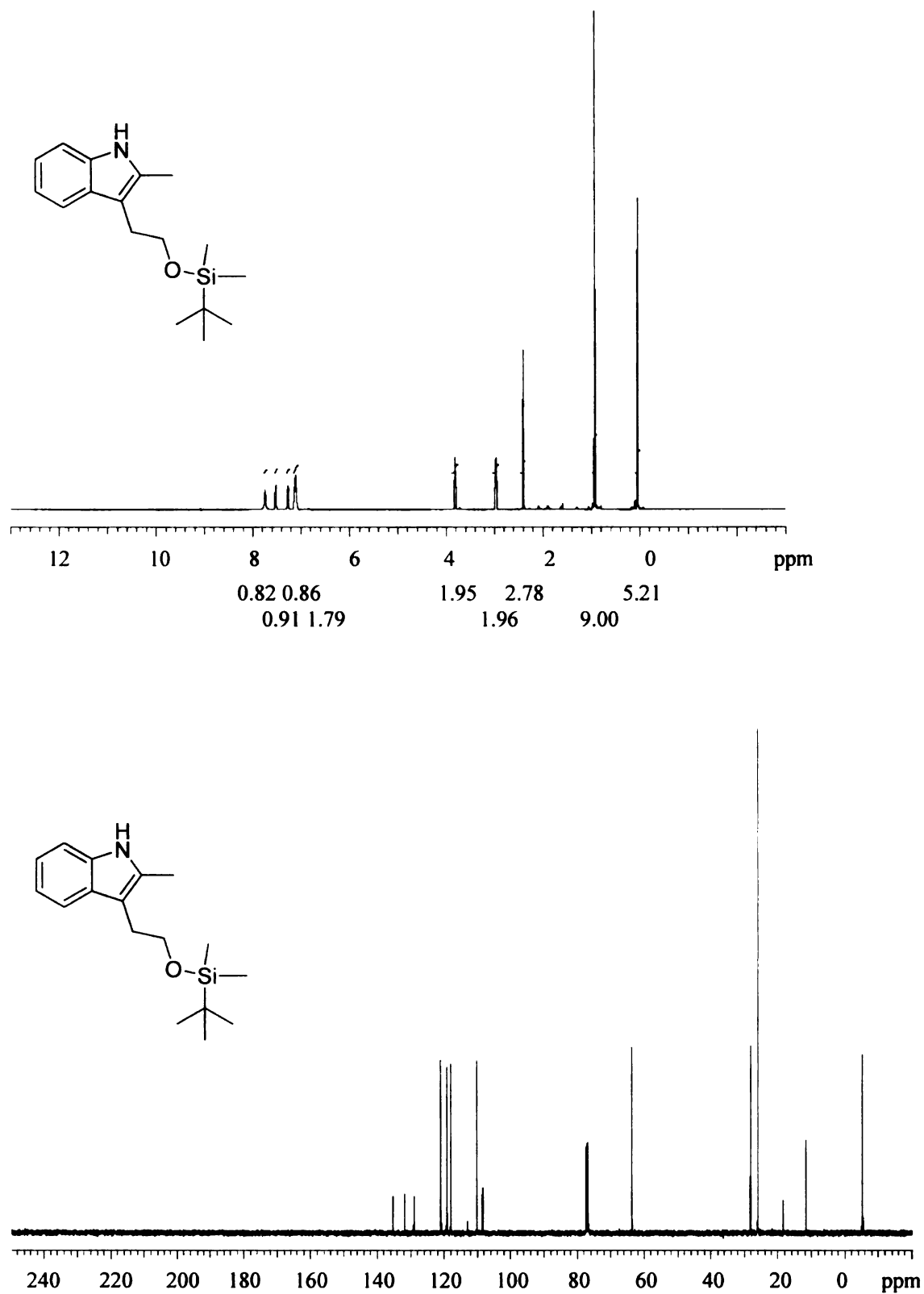


Figure C.7 ^1H and ^{13}C NMR spectral data of compound 17.

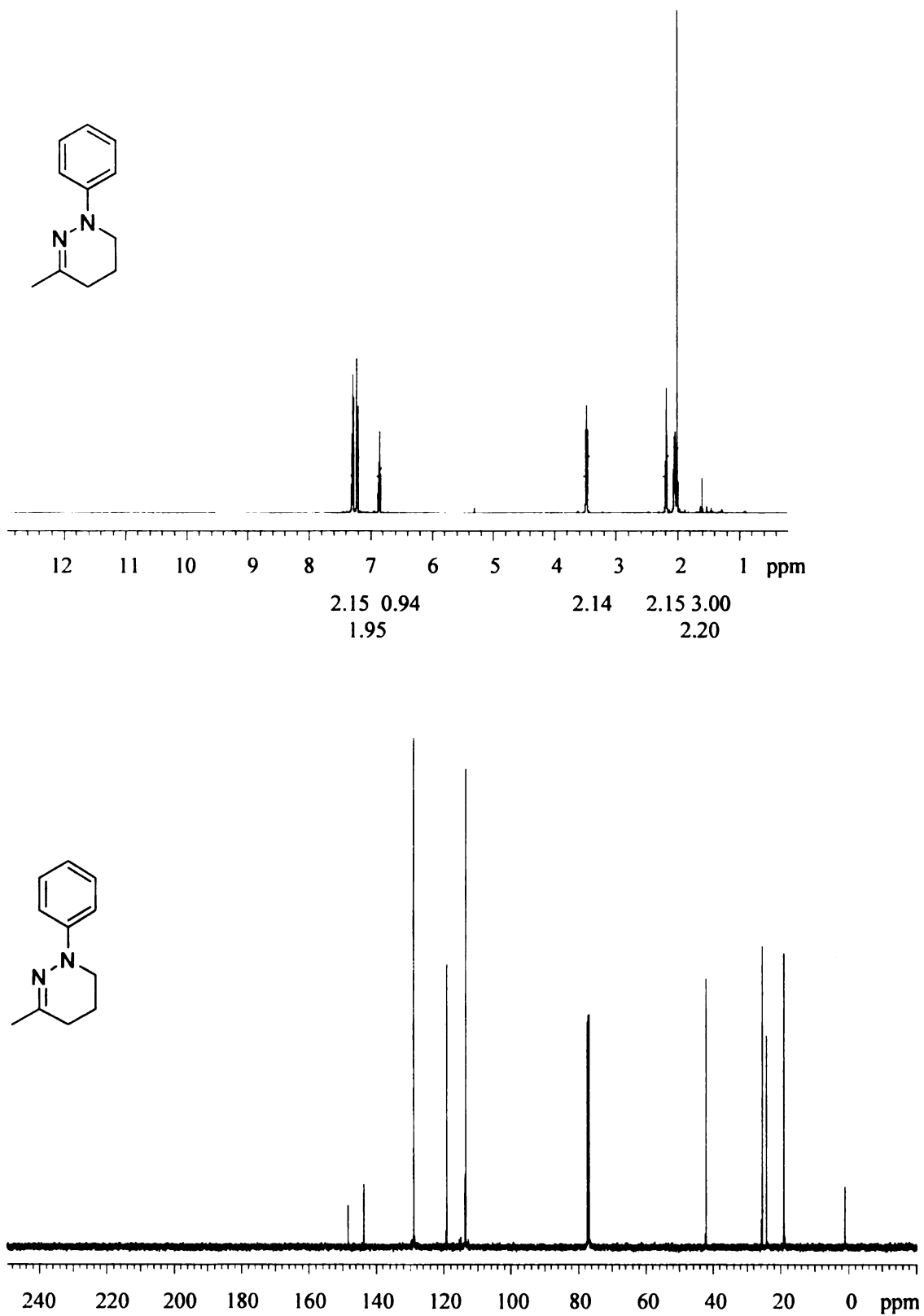


Figure C.8 ^1H and ^{13}C NMR spectra of compound **20**.

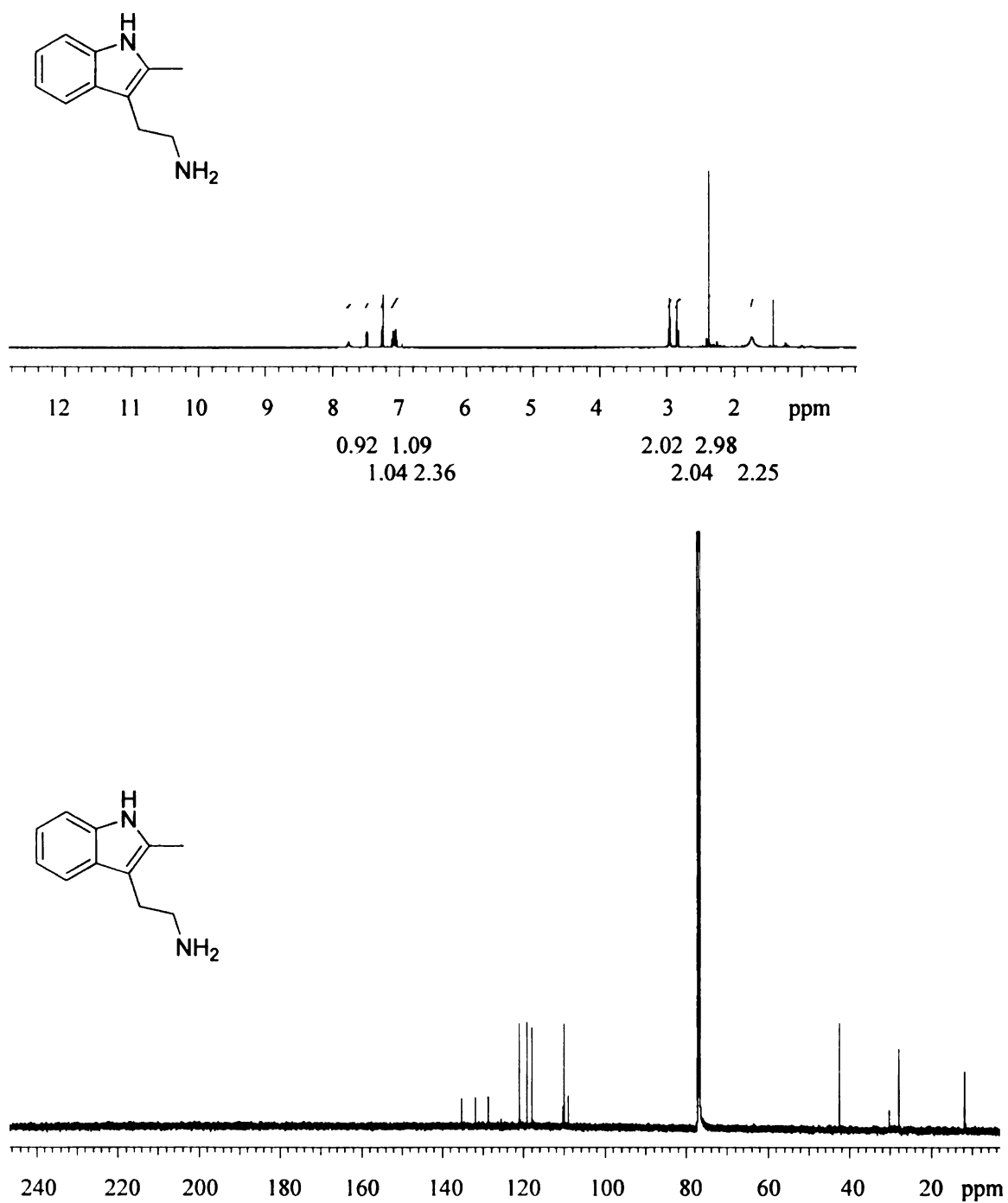


Figure C.9 ^1H and ^{13}C NMR spectra of compound **21**.

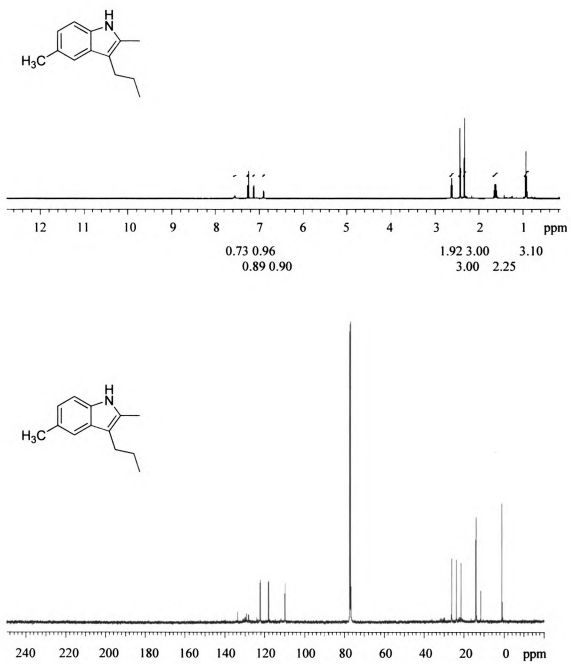


Figure C.10 ^1H and ^{13}C NMR spectra of compound 24.

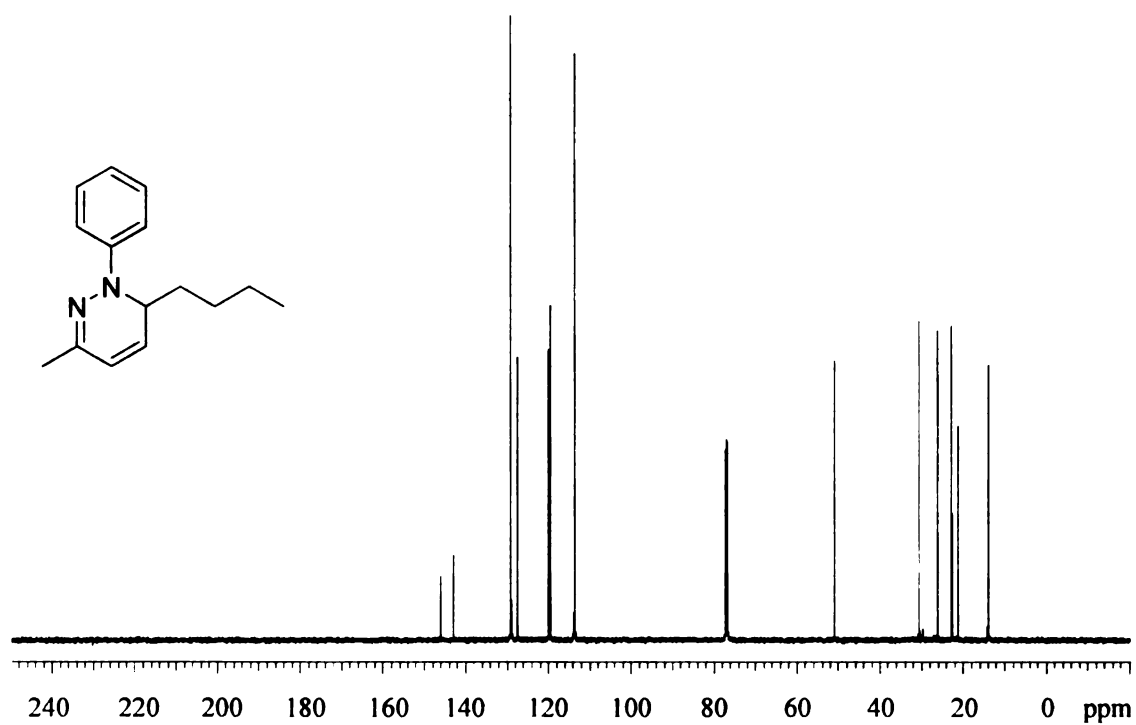
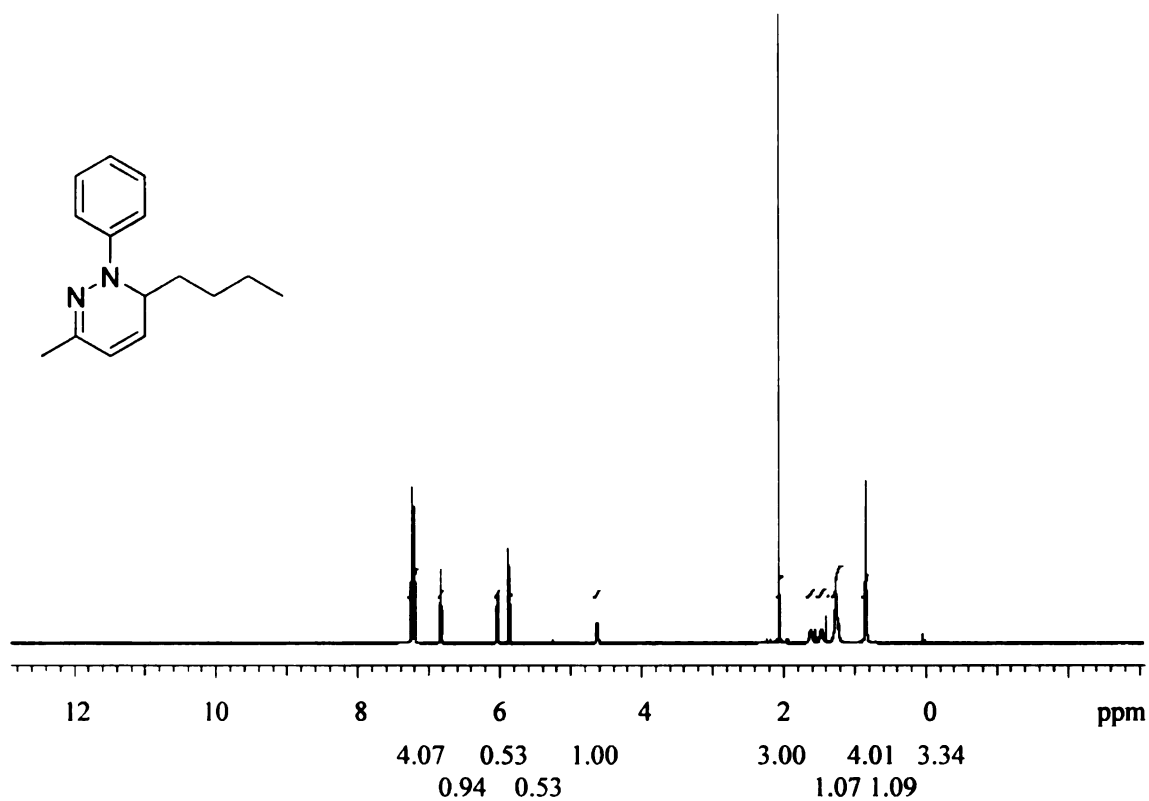


Figure C.11 ^1H and ^{13}C NMR spectra of compound **25**.

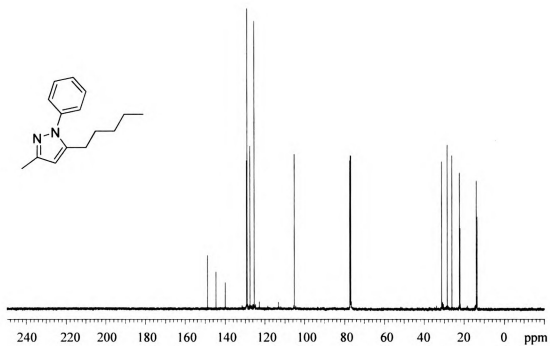
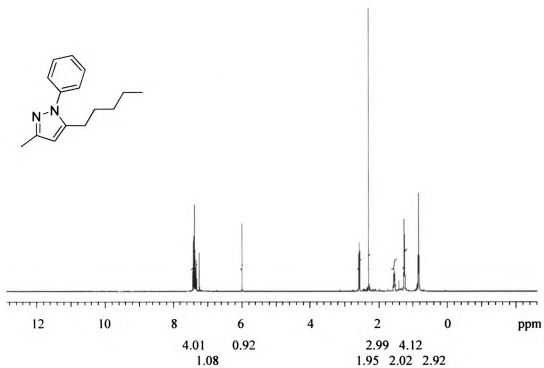


Figure C.12 ^1H and ^{13}C NMR spectra of compound 35.

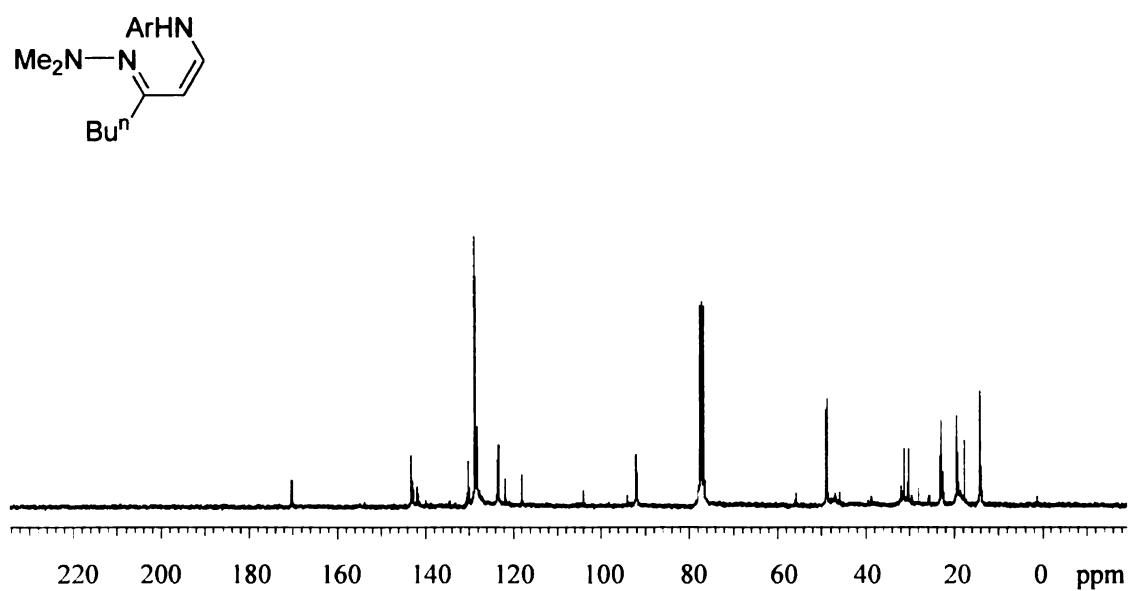
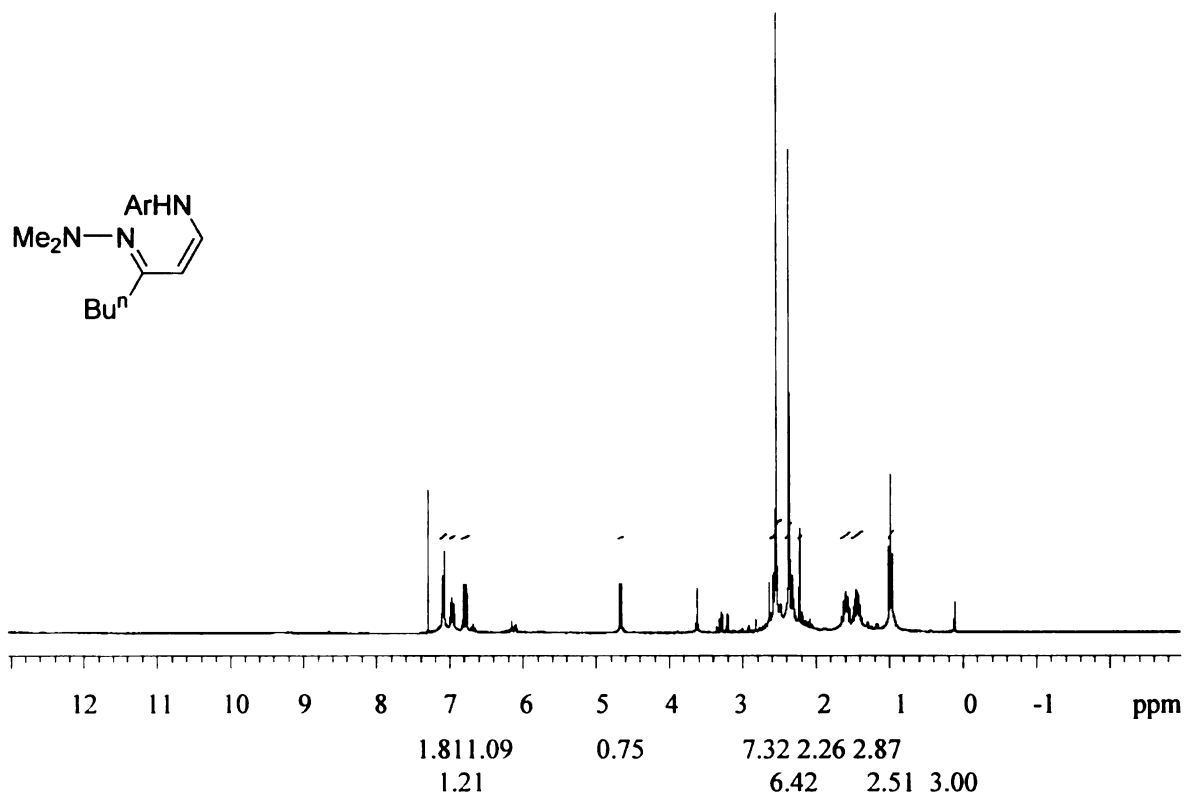


Figure C.13 ^1H and ^{13}C NMR spectra of compound **38**.

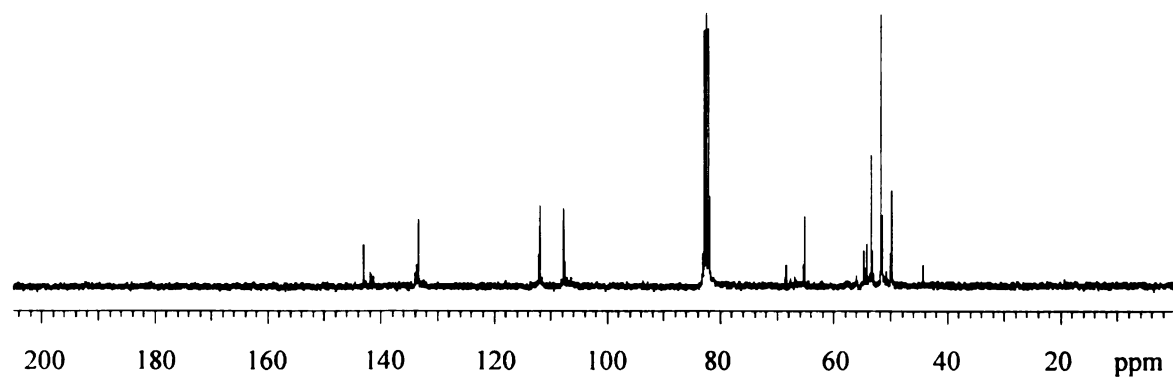
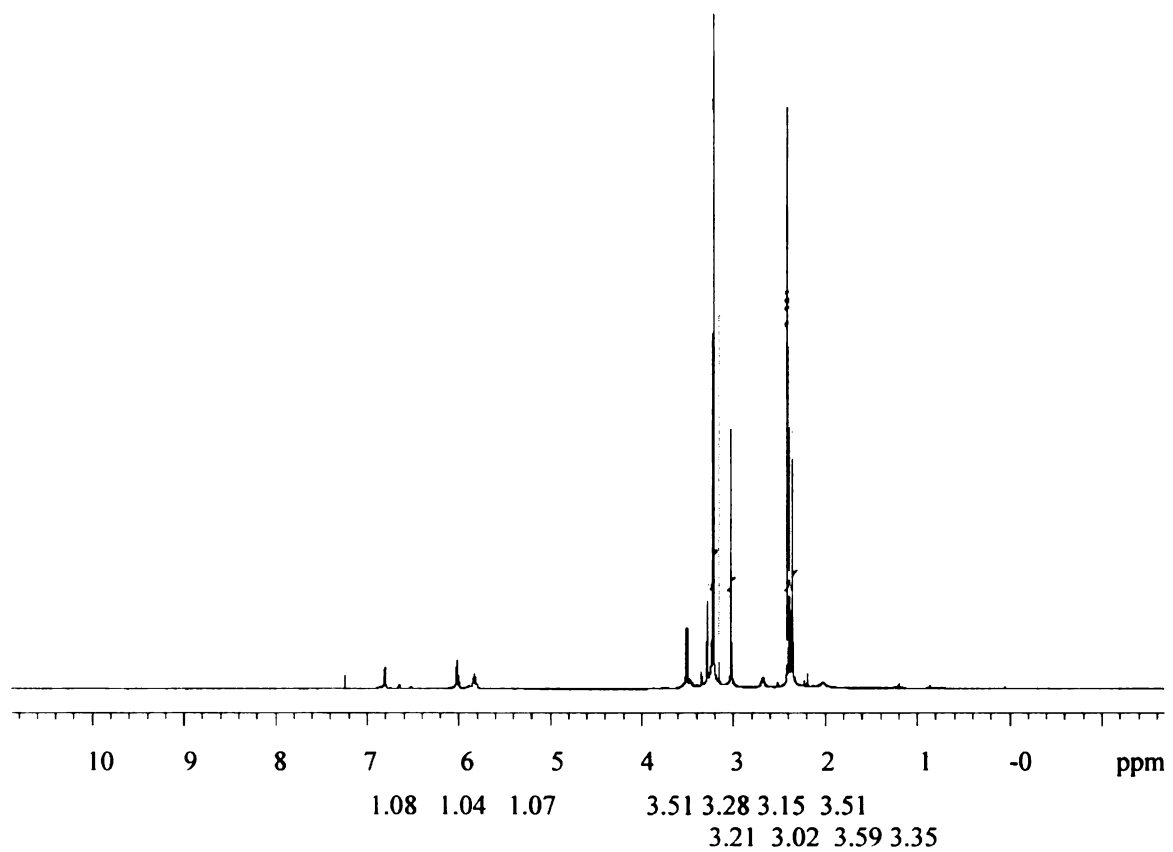


Figure C.14 ^1H and ^{13}C NMR spectra of compound 39.

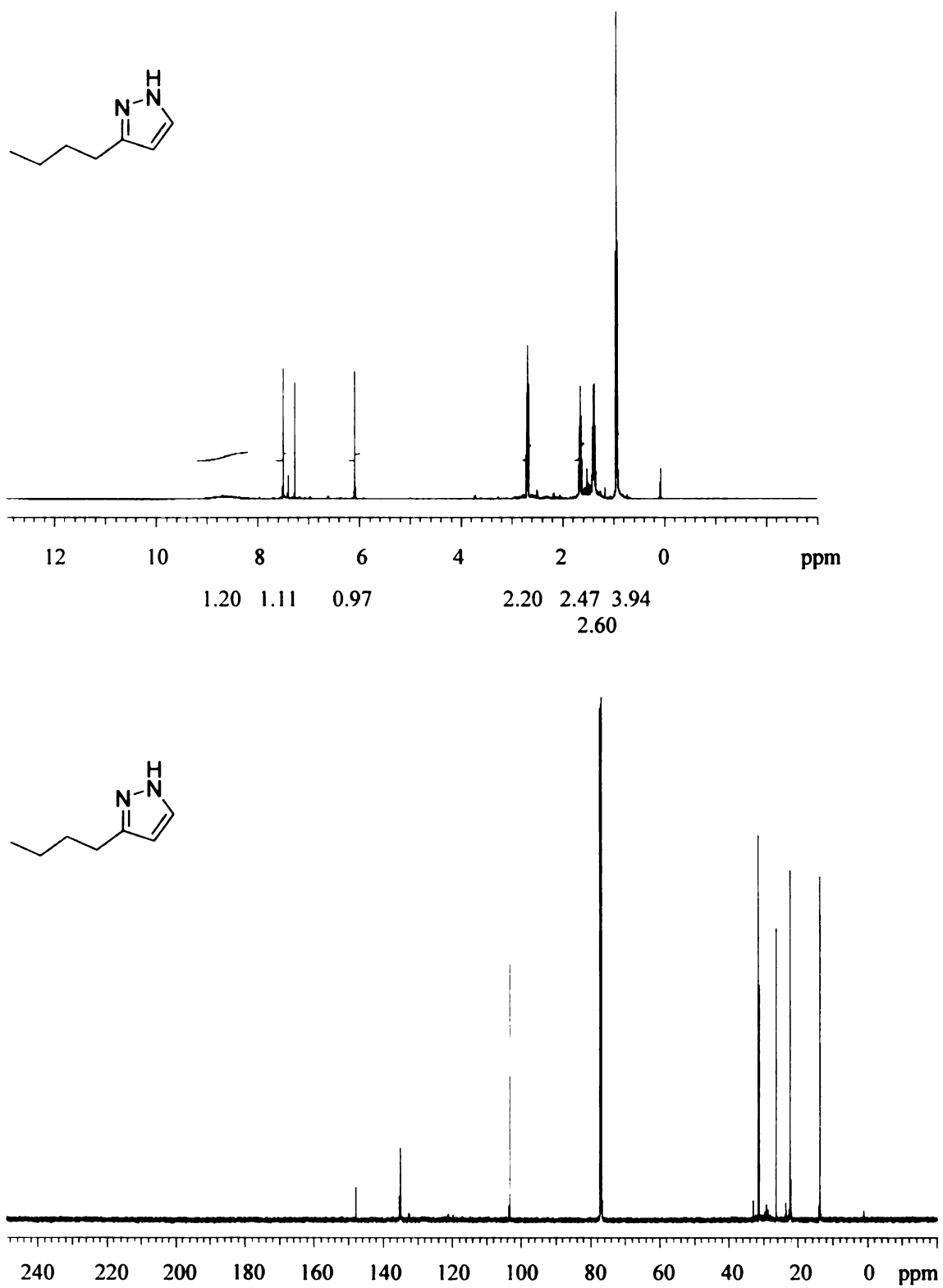


Figure C.15 ^1H and ^{13}C NMR spectra of compound 40.

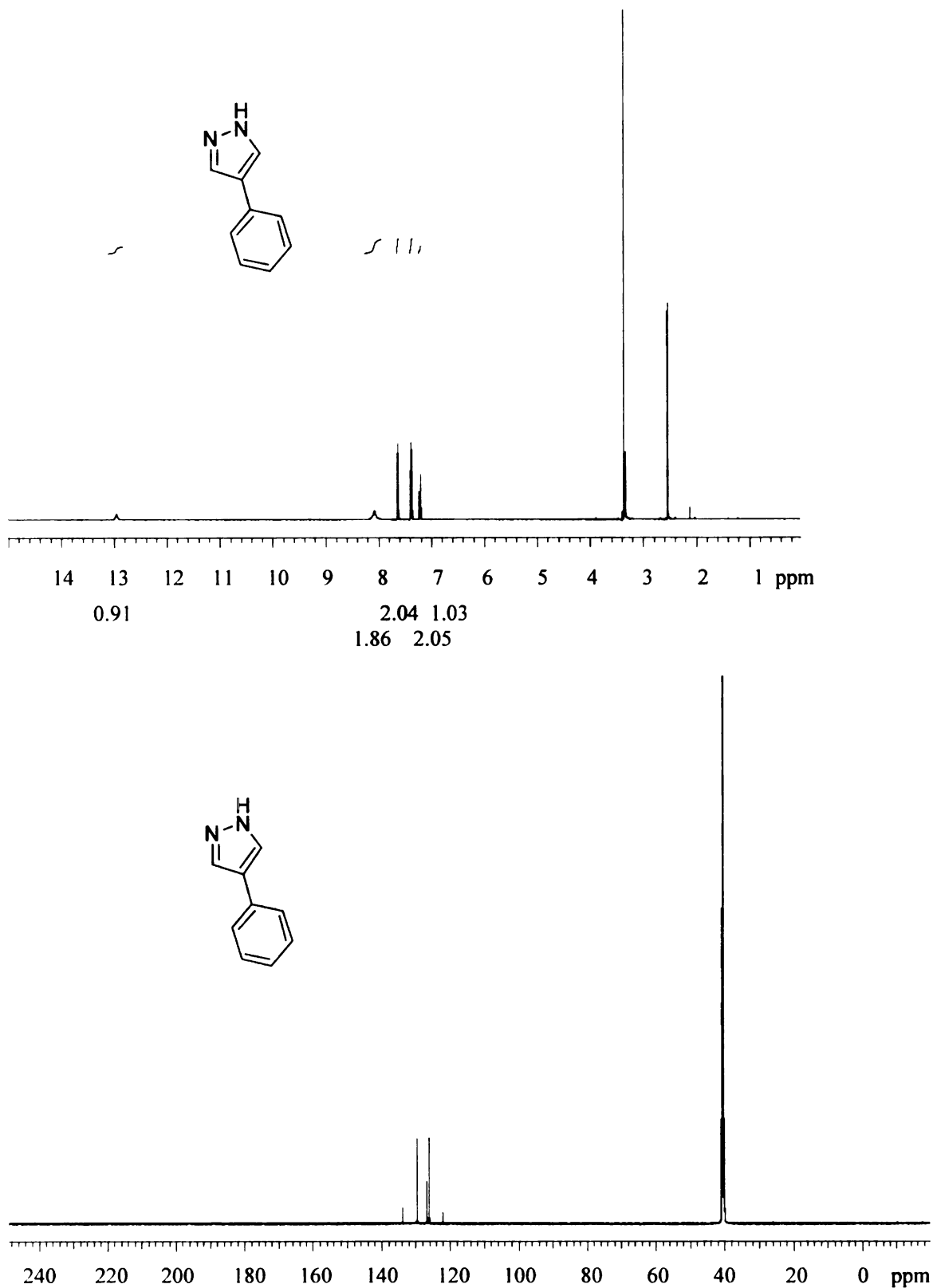


Figure C.16 ^1H and ^{13}C NMR spectra of compound 41.

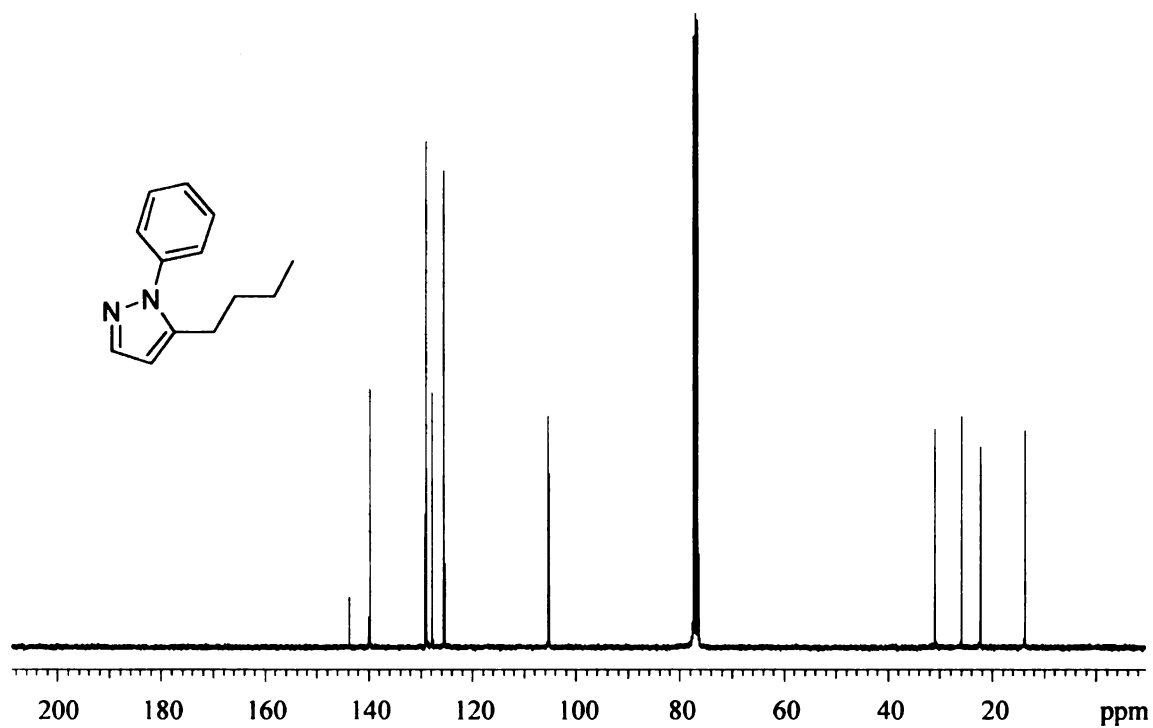
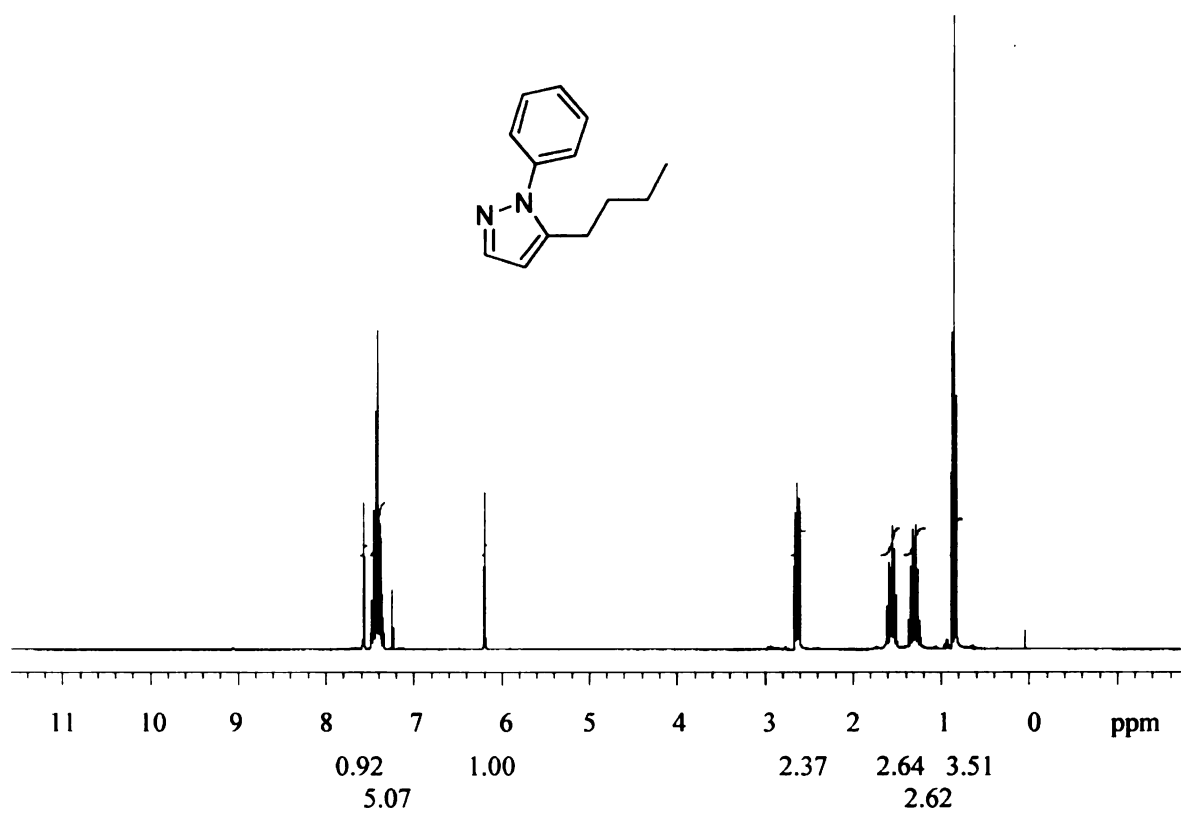


Figure C.17 ^1H and ^{13}C NMR spectra of compound 42.

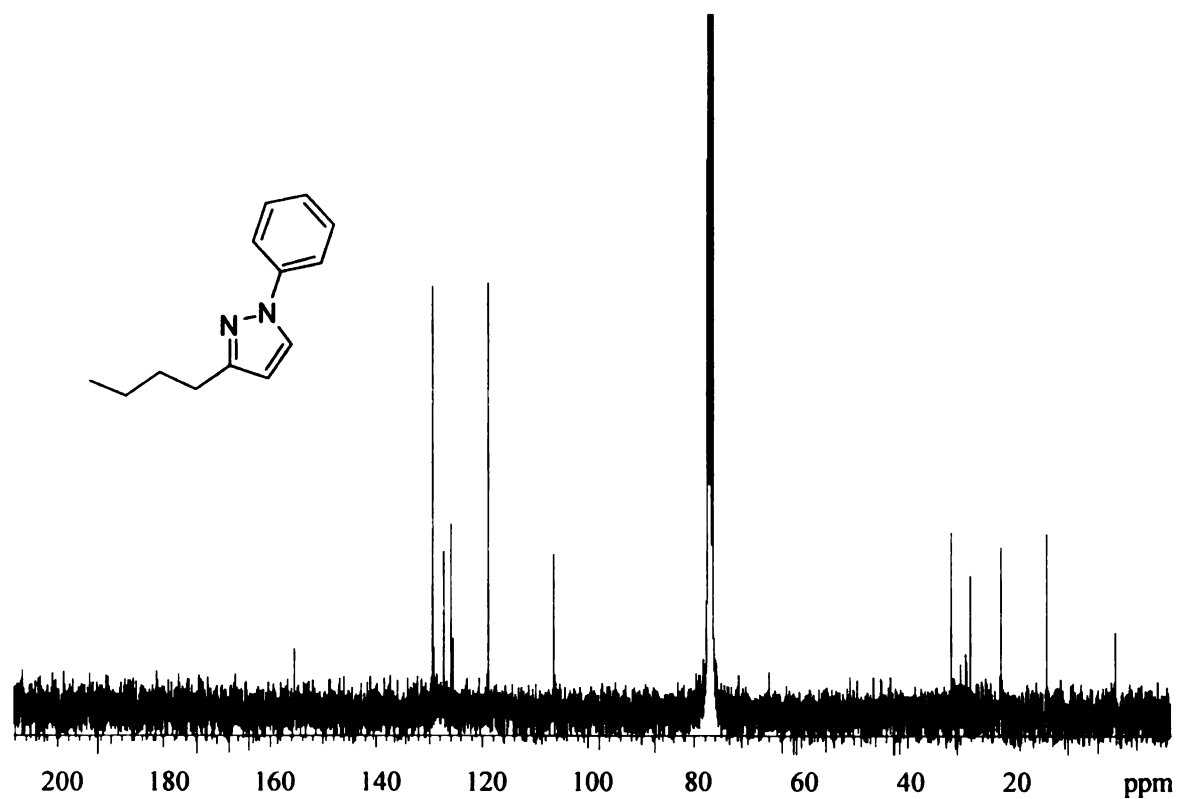
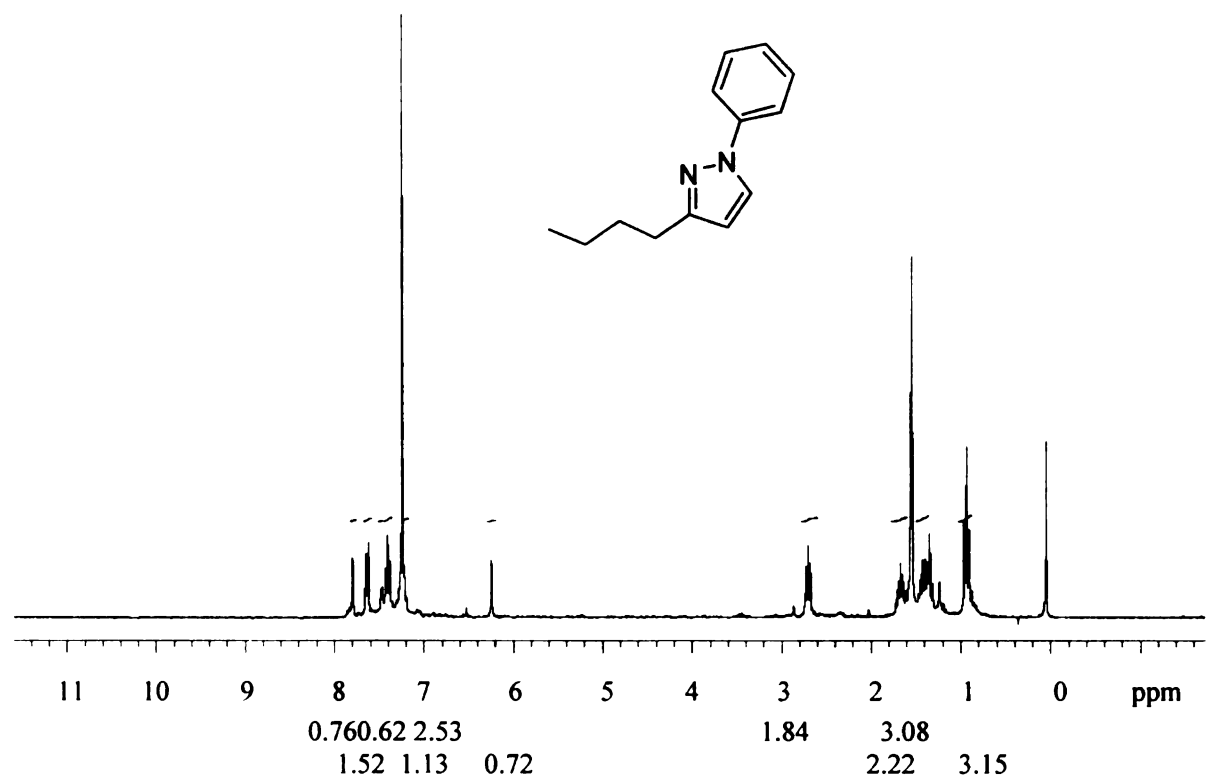


Figure C.18 ^1H and ^{13}C NMR spectra of compound 44.

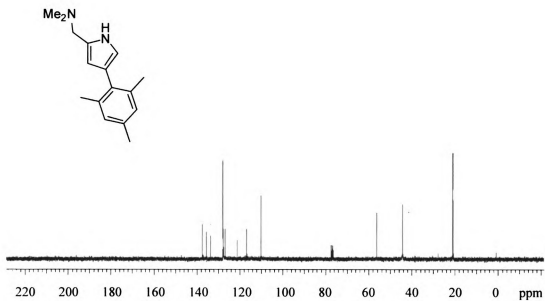
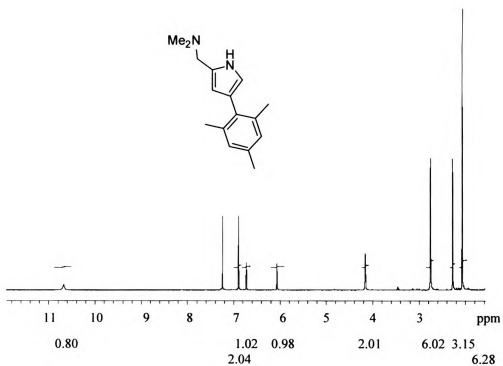


Figure C.19 ^1H and ^{13}C NMR spectra of compound 45.

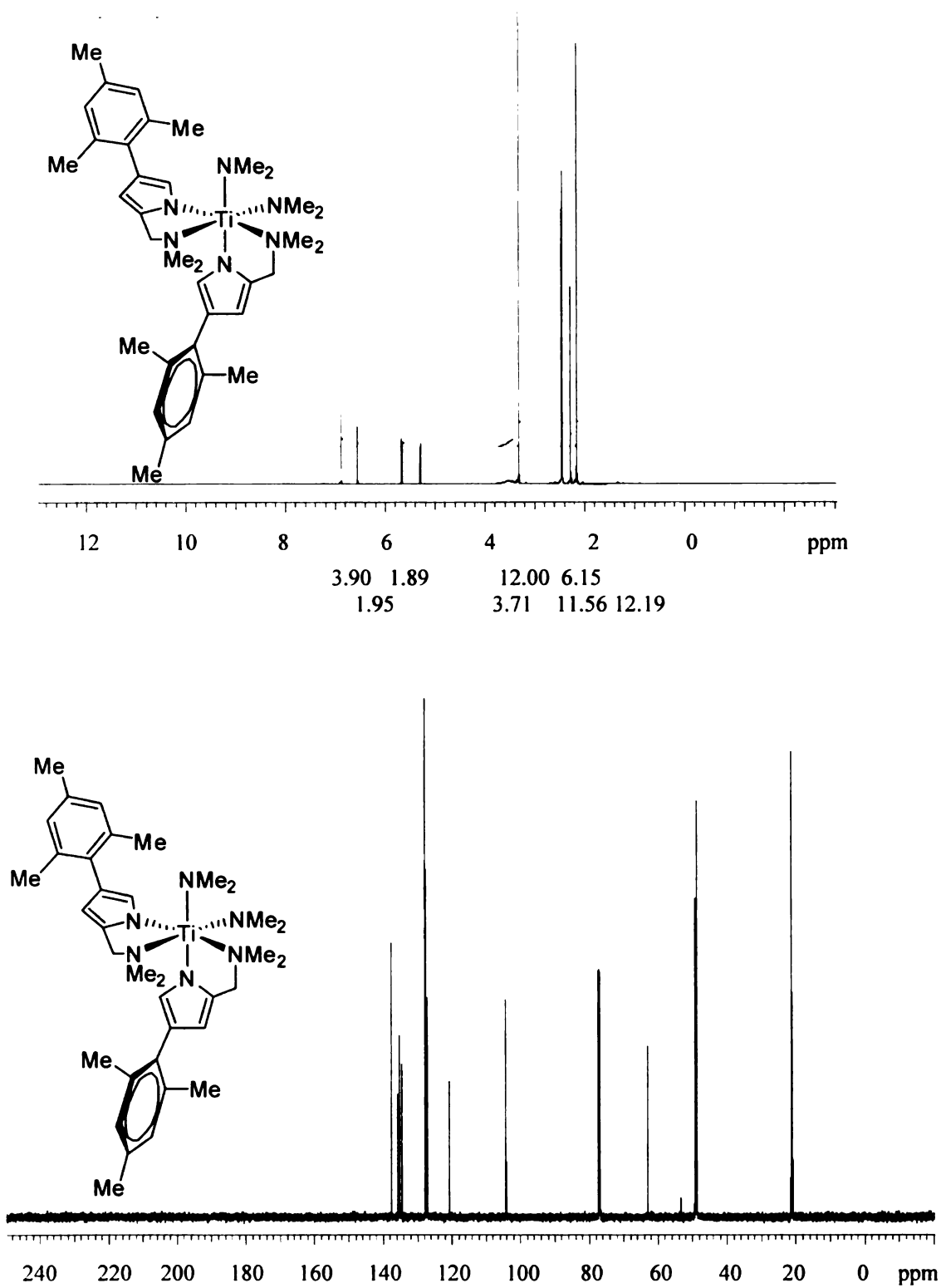
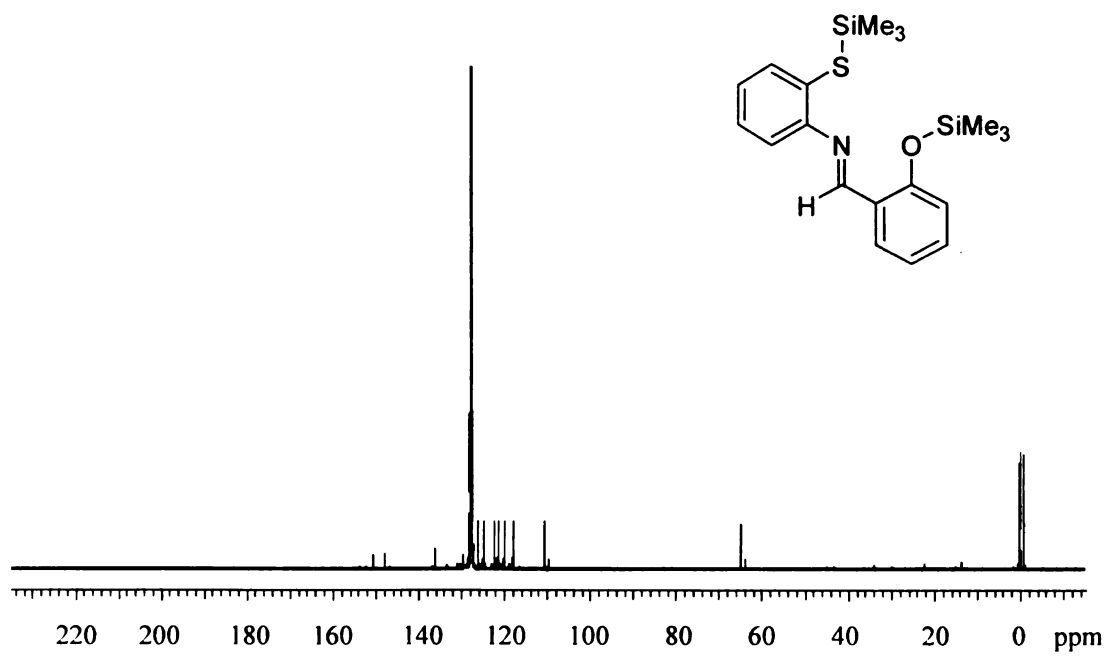
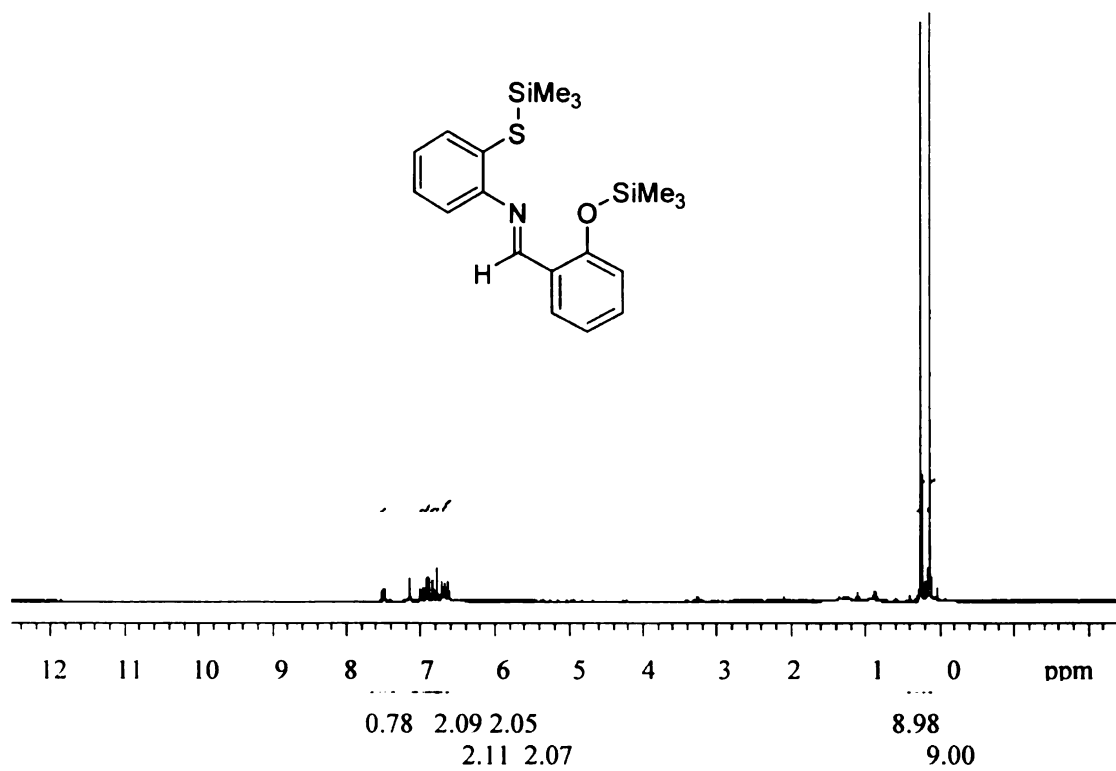


Figure C.20 ^1H and ^{13}C NMR spectra of compound 46.



MICHIGAN STATE UNIVERSITY LIBRARIES



3 1293 03062 4799